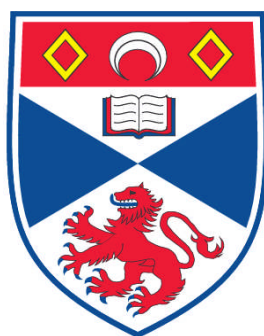# STEREOSPECIFIC DEHYDROXYFLUORINATION AND THE SYNTHESIS OF TRIFLUORO D-HEXOSE SUGAR ANALOGUES

Stefano Bresciani

A Thesis Submitted for the Degree of PhD
at the
University of St. Andrews

2011

Stereospecific dehydroxyfluorination and the synthesis of trifluoro D-hexose sugar analogues
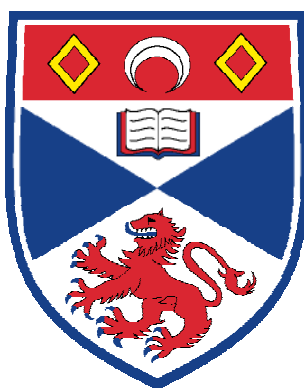
University
of
St Andrews

A thesis presented for the degree of Doctor of Philosophy to the School of Chemistry University of St Andrews

Stefano Bresciani

September 2010

1. Candidate's declarations:

I, Stefano Bresciani, hereby certify that this thesis, which is approximately 36000 words in length, has been written by me, that it is the record of work carried out by me and that it has not been submitted in any previous application for a higher degree.

I was admitted as a research student in March 2007 and as a candidate for the degree of Doctor of Philosophy in March 2007; the higher study for which this is a record was carried out in the University of St Andrews between 2007 and 2010.

Date ……..................signature of candidate ....………

2. Supervisor's declaration:

I hereby certify that the candidate has fulfilled the conditions of the Resolution and Regulations appropriate for the degree of Doctor of Philosophy in the University of St Andrews and that the candidate is qualified to submit this thesis in application for that degree.

Date ….................… signature of supervisor ………..

3. Permission for electronic publication:

In submitting this thesis to the University of St Andrews I understand that I am giving permission for it to be made available for use in accordance with the regulations of the University Library for the time being in force, subject to any copyright vested in the work not being affected thereby. I also understand that the title and the abstract will be published, and that a copy of the work may be made and supplied to any bona fide library or research worker, that my thesis will be electronically accessible for personal or research use unless exempt by award of an embargo as requested below, and that the library has the right to migrate my thesis into new electronic forms as required to ensure continued access to the thesis. I have obtained any third-party copyright permissions that may be required in order to allow such access and migration, or have requested the appropriate embargo below.

The following is an agreed request by candidate and supervisor regarding the electronic publication of this thesis: access to printed copy and electronic publication of thesis through the University of St Andrews.

Date ……........signature of candidate …..................signature of supervisor …....…...............…

Acknowledgements

I wish to express my thanks to all the people who contributed to help me complete this thesis. In particular, I would like to thank Professor David O'Hagan for his continual guidance and advice during the PhD. I am also very grateful for the funds provided by the University of St Andrews and EPSRC.

I would like to acknowledge the technical support staff and collaborators of the school of chemistry for the excellent quality of their work. Particularly, I would like to thank Prof. Alexandra M. Z. Slawin, Dr Tomas Lebl and Mrs Melanjia Smith for X-ray and NMR analyses, and Mrs Caroline Horsburgh and Mr Peter J. Pogorzelec for mass spectroscopic and gas chromatography analyses.

I wish to thank all my colleagues and friends in St Andrews, particularly the members of the DOH group, past and present. A special thank goes to Jason Chan, Dr Vicente Del Amo, Federico Medda and Dr Michael Corr for their help and friendship.

Finally, I dedicate this thesis to the people who mean the most to me, my parents Lucia and Alberto and my brother Giorgio for their endless support and patience, and my girlfriend Sarah for her love and care.

Table of contents

Chapter 5:   Experimental section:

Abbreviations

α	alpha
atm.	atmosphere
Å	angstrom
ATP	adenosine-5'-triphosphate
Boc	*t*-butoxycarbonyl
(*n*-Bu$_3$PMeF)	methyl *tri-n*-butylfluorophosphorane
bp	boiling point
br	broad
β	beta
cat.	catalytic
CI	chemical ionisation
Cbz	carboxybenzyl
COSY	correlation spectroscopy
Δ	delta
DCC	*N,N'*-dicyclohexylcarbodiimide
DMAP	4-dimethylaminopyridine
DAST	diethylaminosulfur trifluoride
DMF	dimethylformamide
de	diastereomeric excess
DFT	density functional theory
Deoxofluor^{TM}	[*bis*(2-methoxyethyl)amino]sulfur trifluoride
dr	diastereomeric ratio
ee	enantiomeric excess
EI	electron impact
EPSRC	engineering and physical sciences research council
EXSY	exchange spectroscopy
Fluolead^{TM}	4-*tert*-butyl-2,6-dimethylphenylsulfur trifluoride
FA	formamide
GC-MS	gas chromatography-mass spectrometry
Glut1	Human Facilitative Glucose Transporter
FID	flame ionization detector

HMBC	heteronuclear multiple bond correlation
HOMO	highest occupied molecular orbital
Hz	hertz
IPF	internal perfluoroalkylidene fragment
J	coupling constant
k_{ef}	efflux rate constant
LUMO	lowest unoccupied molecular orbital
MFA	*N*-methylformamide
m-CPBA	*meta*-chloroperoxybenzoic acid
MW	microwave
m	multiplet
molec.	molecular
μ	mu
m/z	molecular mass to charge ratio
(*R*)-MPTA	(*R*)-*α*-methoxy-*α*-trifluoromethylphenylacetic acid
min	minute
mp	melting point
NMDA	*N*-methyl-D-aspartate
NFSI	*N*-fluorobenzenesulfonimide
NOESY	nuclear overhauser effect correlation spectrosopy
NMR	nuclear magnetic resonance
NOE	nuclear overhauser effect
no.	number
n_D	refractive index
ppm	parts per million
PE	polyethylene
PBSF	perfluorobutansulfonyl fluoride
π	pi
rpm	rotation per minute
IR	infrared spectroscopy
RT	room temperature
Red-Al®	sodium *bis*(2-methoxyethoxy)aluminium hydride
SIM	selective ion monitoring
σ	sigma

Ts	tosyl
t.l.c	thin layer chromatography
TFEDMA	1,1,2,2-tetrafluoro-*N*-*N*-dimethylethylamine
THF	tetrahydrofuran
TBAF	tetra butylammonium fluoride
TBATF	tetrabutylammonium dihydrogen trifluoride
temp.	temperature
TMS	trimethylsilyl
w/v	weight to volume

Abstract

This thesis describes stereospecific fluorination reactions, and addresses the synthesis of fluorosugars. In **Chapter 1**, the influence of fluorine on the physical properties of organic molecules, as well as its stereoelectronic effects, are introduced. Furthermore, an overview of nucleophilic and electrophilic fluorination reactions is given. **Chapter 2** describes the dehydroxyfluorination of allylic alcohol diastereoisomers **155a** and **155b**, which can proceed either by direct or allylic fluorination. The regio- and stereo- selectivities were also assessed. **Chapter 3** outline the synthesis of the novel trifluoro D-glucose analogue **193** and trifluoro D-altrose analogue **216**.

OH   OH

F   F

193   216
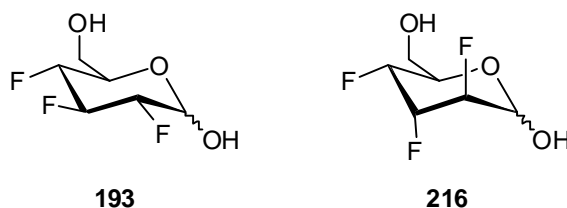
The transport of these hexose analogues across the red blood cell membranes was then explored, to investigate the influence of polarity versus hydrogen bonding ability in carbohydrate-protein interactions. **Chapter 4** describes the development and optimisation of Bio's methodology, to promote stereospecific dehydroxyfluorination of benzylic alcohols (*R*)-**213** and (*R*)-**227** by addition of TMS-amine additives **226** and **229**. And finally **Chapter 5** reports the experimental procedures as well as the characterisation and the crystallographic data of the molecules prepared in this thesis.

Chapter 1: Fluorine in organic chemistry

1.1) Organofluorine chemistry:

Organofluorine research actively contributes to progress in a broad range of technologies including applications in medicinal chemistry,[1] in soft materials chemistry[2] and in the development of agrochemical products.[3] Fluorine is introduced into organic molecules to modulate their molecular properties, most often by the substitution of hydrogen and/or oxygen by fluorine. To do this, a broad range of new fluorination reagents and novel synthetic methodologies have been developed.[2] Today organofluorine research still receives significant attention from both the academic and industrial scientific communities, and the study of newly generated fluorinated analogues is an important aspect of chemistry research.

1.2) The effect of fluorine on the physical properties of organic molecules:

1.2.1) Electronic effects:

Some of the important effects which arise from the introduction of fluorine into organic molecules can be rationalised by the principles of molecular orbital theory. For instance the replacement of hydrogen by a fluorine atom in organic molecules generates HOMO (highest occupied molecular orbital) and LUMO (lowest unoccupied molecular orbital) energy levels both of which are lower in energy than the analogous hydrocarbon.[4] A low HOMO indicates that the valence electrons ($2s$ and $2p$) are more tightly held to the nucleus. As a result, the electronic polarisability of the fluorinated analogue is reduced. Electronic polarisability can be assessed by determining the refractive index (n_D), a value which is lower in fluorinated

compounds compared to their non-fluorinated analogues. The limited electronic polarisability of fluorinated analogues weakens the van der Waals forces,[4] which is the basis of many characteristic properties of fluorinated molecules.

1.2.2) Boiling point:

Generally the boiling point of structurally related compounds depends upon their molecular weight, the higher the molecular weight, the higher the boiling point. However, this is not always true for halogenated organic compounds. Fluorination decreases the electronic polarisability of organic molecules and consequently reduces the van der Waals interactions which may result in lower boiling points, and as stated above, lower refractive indices. For instance, a linear correlation is found between the refractive indices and the boiling points.[5]

1.2.3) Miscibility:

The definition of "fluorous" was described by D. P. Curran in 2002.[6] "Fluorous" refers to highly fluorinated sp^3-hybridized moieties such as perfluoroalkanes, and perfluorotrialkylamine compounds. "Fluorophilic" is used to describe molecules that show an affinity for fluorous media, whereas "fluorophobic" are molecules that do not (e.g. hydrocarbons).[6] In this regard, the polarity, as well as the electronic polarisability, plays a central role. In fact, perfluorinated organic compounds are neither soluble in organic solvents, nor in water. The fluorinated analogues, deficient in electronic polarisability, are unable to make sufficient van der Waals interactions with neighboring organic solvent molecules, making them insoluble in organic media.[4] In addition, fluorinated analogues cannot establish

adequate hydrogen bonding with surrounding water molecules and they form weak van der Waals forces with each other while isolated from water molecules.[4]

1.2.4) Lipophilicity:

The partition coefficient, log D, is the conventional parameter for measuring the effect of fluorine substitution on lipophilicity. Log D is defined as the logarithmic coefficient of a compound's distribution between octanol and water at a given pH, typically 7.4.[7] Fluorine substitution has multiple effects upon lipophilicity, and no simple rules exist to predict these effects. A study by H. -J. Böhm[8] examined the effects of fluorine substitution, by replacing a hydrogen atom with fluorine in a series of 293 pairs of structurally related molecules.

For each molecule the log D was determined and the difference between each pair of fluorinated and non-fluorinated analogues was calculated. The graph in Figure 1.1 illustrates a Gaussian distribution with a maximum around 160 (number of observations) which corresponds to a log D difference a little higher than zero. This study also demonstrates that, on average, the replacement of a hydrogen atom by fluorine enhances the lipophilicity by approximately 0.25 log units. Log D values below zero indicate that fluorine substitution can also decrease lipophilicity. In these instances, an oxygen atom is always located near the fluorine (Figure 1.2).
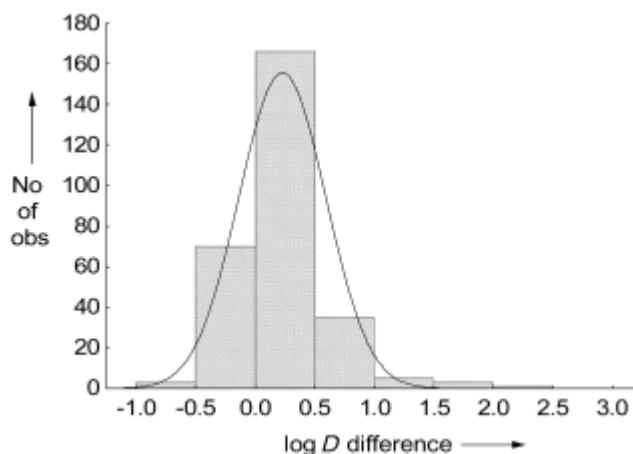
Figure 1.1. Log *D* variation observed after substitution of a hydrogen atom by fluorine.[8] H. -J. Böhm, D. Banner, S. Bendels, M. Kansy, B. Kuhn, K. Müller, U. Obst-Sander, M. Stahl, *ChemBioChem,* 2004, **5**, 637-643. Copyright Wiley-VCH Verlag GmbH & Co. KGaA. Reproduced with permission.
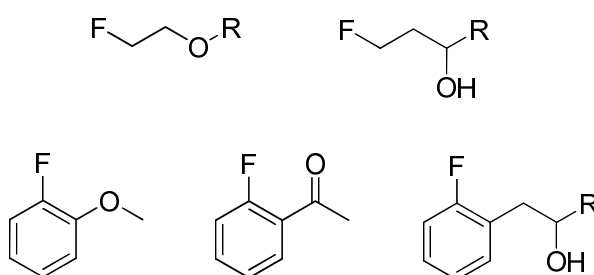
Figure 1.2. Examples of compounds for which a fluorine substituent decreases log *D*.[8]

Conformational analyses and *ab initio* quantum-chemical calculations of these molecules revealed that the positioning of the fluorine close to an oxygen atom increases the polarity of the molecule. This might favour the formation of stronger hydrogen bonding with the surrounding water molecules. In contrast, most cases reporting a positive Δ log *D* are characterised by the presence of one or more basic nitrogens, whose basicity is reduced by the fluorine electron-withdrawing effect.

1.3) Electronic effects:

1.3.1) Acidity:

Fluorine is the most electronegative element (3.98 on the Pauling scale) in the Periodic Table.[9] This makes the C-F bond extremely polar with a characteristic dipole moment (μ) of approximately 1.4 D. The introduction of fluorine into a molecule can have a significant effect on the acidity of the molecule.[10] For instance the pK_a of a series of organic acids is reported in Table 1.1.[10] The pK_a decreases after fluorine introduction due to the inductive effect. Fluorination also decreases the basicity (pK_b) of organic bases as shown in Table 1.2.[10]

Acid (H)	pK_a	Acid (F)	pK_a
CH_3COOH	4.76	CF_3COOH	0.52
C_6H_5COOH	4.21	C_6F_5COOH	1.75
CH_3CH_2OH	15.9	CF_3CH_2OH	12.4
$(CH_3)_2CHOH$	16.1	$(CF_3)_2CHOH$	9.3
$(CH_3)_3COH$	19.0	$(CF_3)_3COH$	5.4
C_6H_5OH	10.0	C_6F_5OH	5.5

Table 1.1. Acidities (pK_a) of organic acids in comparison with their fluorinated analogues.[10]

Base (H)	pK_b	Base (F)	pK_b
$CH_3CH_2NH_2$	3.3	$CF_3CH_2NH_2$	8.1
$C_6H_5NH_2$	9.4	$C_6F_5NH_2$	14.36

Table 1.2. Basicities (pK_b) of organic bases in comparison with their fluorinated analogues.[10]

Fluorine also alters the reactivity of charged intermediates. For instance, fluorine can influence the stability of fluorinated carbocations.[11] α-Fluoro substitution of a carbocation stabilises the positive charge by the mesomeric effect, but destabilises the positive charge by the inductive effect as shown in Figure 1.3.[2] In general, a single fluorine atom will increase the stability of a carbocation. β-Fluoro substitution destabilises a carbocation by the inductive effect (Figure 1.3). α-Fluoro substitution of carbanions destabilises the negative charge by an n-π interaction, whereas β-fluoro substitution stabilises the charge by the inductive effect and by negative hyperconjugation (Figure 1.4).
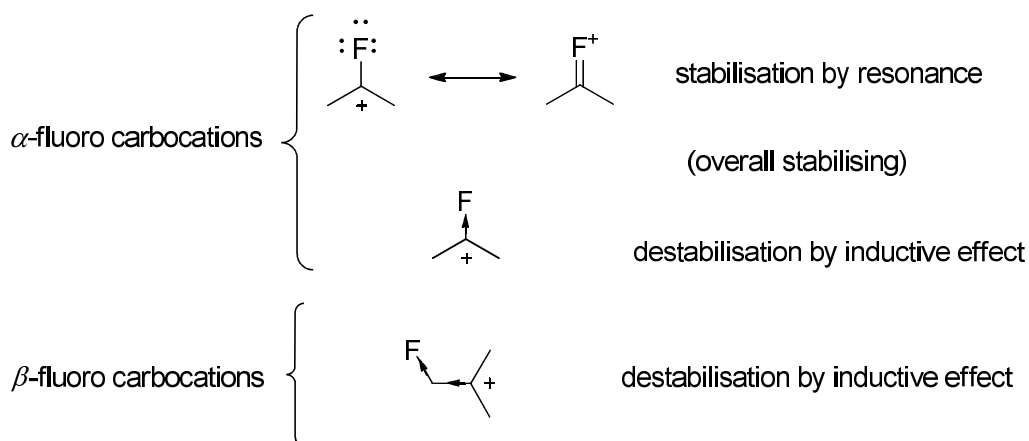
Figure 1.3. Influence of fluorine on carbocation stability.[2]
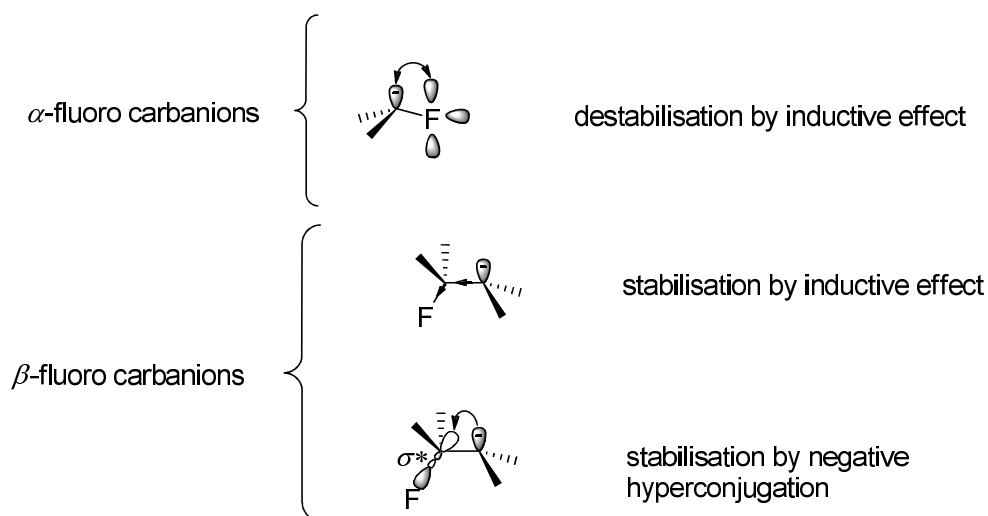
Figure 1.4. Influence of fluorine on carbanion stability.[2]

6

1.3.2) Bond energy and bond length:

As fluorine is the most electronegative atom, the C-F bond is the strongest bond in organic chemistry (105.4 kcal/mol), making it extremely stable.[12] This property confers thermal and oxidative stability to fluorinated compounds. The length of the C-F bond determines the strength of the C-F bond, highlighted by the sequence of substituted methanes in Table 1.3.[12]

Molecule	C–F bond length (Å)	C–F bond strength (kcal/mol)
CH_3F	1.39	107
CH_2F_2	1.36	109.6
CHF_3	1.33	114.6
CF_4	1.32	116

Table 1.3. C-F bond length and C-F bond strength in substituted methanes.[12]

1.4) Stereoelectronic effects in organofluorine molecules:

1.4.1) The size of fluorine and steric effects:

An important property of fluorine is its small size, with a van der Waals radius of 1.47 Å, just slightly bigger than that of hydrogen (1.20 Å).[13] Thus, the replacement of hydrogen by fluorine is the most conservative, in regards to steric effects, but the most dramatic with respect to alteration of electronic properties. As the carbon-fluorine bond length (1.39 Å) is close to that of carbon–oxygen (1.43 Å),[13] the replacement of oxygen for fluorine in organic molecules is the most neutral change in terms of both steric and electronic effects.

1.4.2) Anomeric effect involving n-$\sigma^*_{C\text{-}F}$ interactions:

The $\sigma^*_{C\text{-}F}$ antibonding orbital, similar to the $\sigma^*_{C\text{-}O}$ orbital, can take part in anomeric stabilisation. A well established example is the "anomeric effect" in carbohydrates.[14] When an electron-withdrawing atom X such as fluorine (or oxygen), is introduced at the anomeric position the axial orientation is favoured over the equatorial orientation, as shown in Figure 1.5.[15] This stabilisation (X = F, 2.8-2.9 kcal/mol)[15] takes place involving a favourable n-σ^* interaction between the lone pair n on the oxygen and $\sigma^*_{C\text{-}X}$.

X = O
X = F
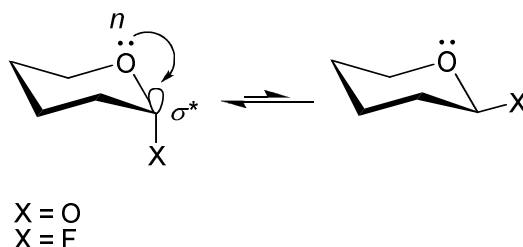
Figure 1.5. Stabilising n-σ^* interaction favouring the electronegative substituent in the axial position.[15]

1.4.3) Organic fluorine as a hydrogen bond acceptor:

Hydrogen bonding plays a fundamental role in nature, shaping the three-dimensional structures of important macromolecules such as proteins and sugars. It is also involved in numerous molecular recognition processes. Although inorganic fluoride can behave as a strong hydrogen bond acceptor,[16] the role of organic fluorine in hydrogen bond interactions is still debatable.[4] Firstly, fluorine can behave only as a hydrogen bond acceptor. Moreover, the hydrogen-bond acceptor ability of organic fluorine is very weak; in fact the low energy of the HOMO (lone pair) orbital level in organic fluorine makes significant interactions with proton donors unlikely. An authentic hydrogen bond should involve orbital interactions, with

the construction of a bond path and exchange of the proton.[4] In this sense, hydrogen bonds are classified as strong (bond energy = 15-30 kcal/mol), medium (4-15 kcal/mol) and weak (<4 kcal/mol).[17] While strong and medium hydrogen bonds have mainly covalent characteristics, the weak hydrogen bond is principally an electrostatic interaction between the proton and the negative charge on the heteroatom.[4] These weak hydrogen bonds include O-H···F-C, N-H···F-C and C-H···F-C interactions, which are best described as a charge-dipole interactions between the δ^+ charge of the hydrogen and the lone pair of electrons of the fluorine.[18] The intensity of such interactions is mainly dependant upon the chemical surroundings. Organic fluorine can also stabilise some molecular conformations by intramolecular hydrogen bonding. A well-known example is the intramolecular hydrogen bonding in β-fluorinated alcohols (see section 1.4.4.2). Experimental observations of fluorine hydrogen bond interactions, are quite rare, and up until now, only one measurement of H-F spin-spin coupling by ^{19}F NMR and ^{1}H NMR has been recorded, found in compound **1** shown in Figure 1.6.[19]

1

$J_{\text{H-F}}$ = 6.6 Hz
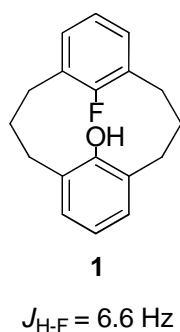
Figure 1.6. ^{1}H NMR of **1** shows spin-spin coupling between the phenol proton and the organic fluorine.[19]

An important example of intramolecular hydrogen bond in pharmaceutical chemistry is observed in the two isomers of 2-fluoro **2** and 6-fluoronorepinephrine **3** (Figure 1.7).[20] In

these examples, fluorine stabilises two different conformations by intramolecular hydrogen

bonding with the aliphatic hydroxyl group, and this results in different biological activities.
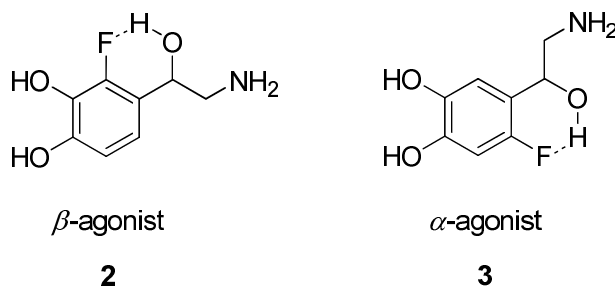
Figure 1.7. Stabilisation of two different conformations of **2** and **3** by intramolecular hydrogen bonds with

organic fluorine.[20]

The C-H···F-C interaction is weak and essentially electrostatic in nature. The interaction is

involved in crystal packing. For instance, the crystal packing of fluorobenzenes in contrast to

the corresponding chloro-, bromo- and iodo- analogues, seems to be stabilised by C-H···F-C

interactions, rather than F-F contacts as shown in Figure 1.8.[21]
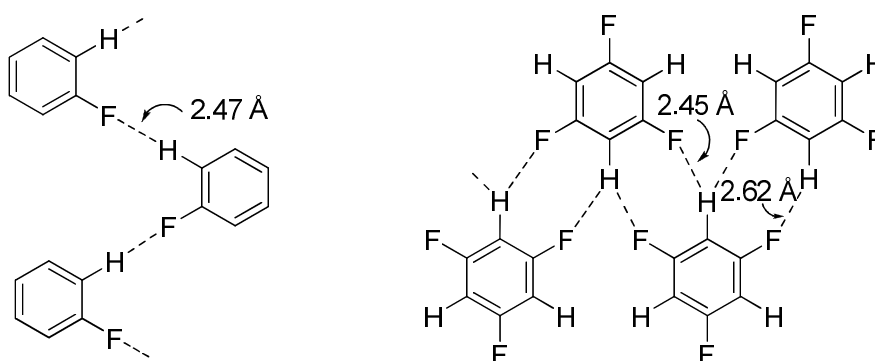
Figure 1.8. C-H···F-C electrostatic interactions rather than F-F interactions occur in fluorobenzenes.[21]

The hydrogen bond distances involved are long and in the region of 2.47-2.65 Å, thus it

would be expected that the interactions are very weak. However, throughout a crystal lattice

they contribute significantly to overall stabilisation.

1.4.4) Effect of fluorine on molecular conformation:

1.4.4.1) Fluorine gauche effect:

The *gauche* effect was first described by Wolfe as "*a tendency to adopt that structure which has the maximum number of gauche interactions between the adjacent electron pairs and/or polar bond*".[22] For example, when two fluorines are placed vicinal to each other in a hydrocarbon motif, a *gauche* rather than an *anti* conformation is preferred. The well-known example is 1,2-difluoroethane, where the *gauche* conformer **4a** is more stable than the *anti* conformer **4b** by around 0.8 kcal/mol (Figure 1.9).[12]

4a *gauche*　　　　**4b** *anti*
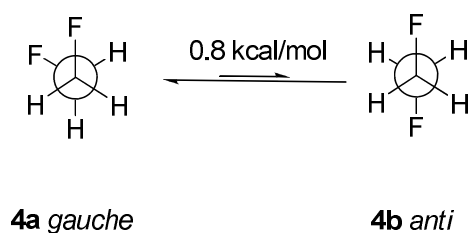
Figure 1.9. The *gauche* conformer **4a** is lower in energy than the *anti* conformer **4b** in 1,2-difluoroethane.[12]

Currently there are two main explanations for the *gauche* effect: the "hyperconjugative stabilisation" theory proposed by P. Rablen[23] and the "bent-bond" theory suggested by K. B. Wiberg.[24] The hyperconjugation model in 1,2-difluoroethane argues a stabilising interaction between the σ_{C-H} orbital (HOMO) and the vicinal σ^{*}_{C-F} orbital (LUMO) as shown in Figure 1.10.
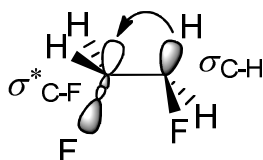
Figure 1.10. Representation of hyperconjugative stabilisation in 1,2-difluoroethane, $\sigma_{C-H} \rightarrow \sigma^*_{C-F.}$[23]

The σ_{C-H} orbital is a better electron donor than the σ_{C-F} orbital, and the σ^*_{C-F} orbital is a better electron acceptor than the σ^*_{C-H} orbital. Only the *gauche* conformer possesses the correct geometry between the σ_{C-H} orbital and the σ^*_{C-F} orbital (antiperiplanar) to allow this stabilising interaction. Conversely, no hyperconjugation can take place in the *anti* conformer. Wibergs "bent-bond" theory[24] was proposed to explain the energy difference between the *gauche* and the *anti* conformer in 1,2-difluoroethane. This theory suggests that due to the strong electronegativity of the fluorine atom, overlap between the sp^3 orbitals along the C-C bond is reduced as a result of the C-C bond bending towards the fluorine (Figure 1.11). However, in the *anti* conformer the C-C orbitals are bent in opposite directions and consequently there is poor overlap, whereas in the *gauche* conformer the orbitals are bent in the same direction resulting in a better overlap.

4a *gauche*   **4b** *anti*
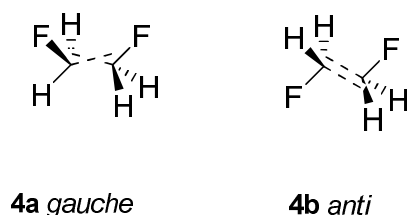
Figure 1.11. 1,2–Difluoroethane, bond overlap in the *anti* conformer **4b** and *gauche* conformer **4a**.[24]

Wiberg also used charge density difference maps[24,25] to explain the higher stability of the *cis* isomer **5a** over the *trans* isomer **5b** (by 1 kcal/mol) in 1,2 difluoroethene. The electron density maps (Figure 1.12) show that the σ bond electron density is higher in the region of

fluorine due to its high electronegativity. Electron density maps revealed a stronger overlap of the C-C orbitals in the *cis* isomer due to the C-C bond bending towards the fluorines, and a poorer overlap in the *trans* conformer as the C-C bond is bent in the opposite direction.
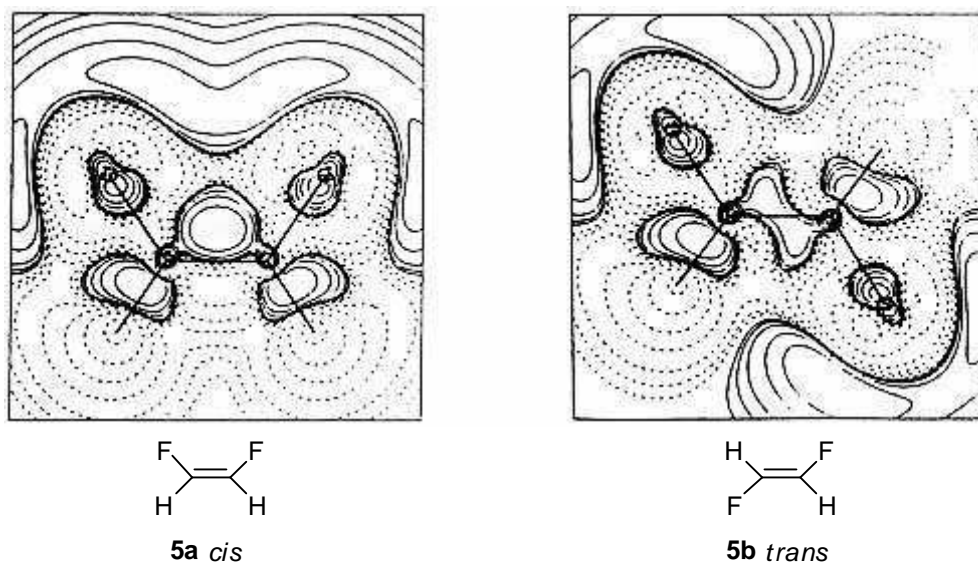
Figure 1.12. Wiberg electron density maps of the σ bonds of *cis*-1,2-difluoroethene **5a** (left) and *trans*-1,2-difluoroethene **5b** (right).[24] Reprinted with permission of K. B. Wiberg, *Acc. Chem. Res.*, 1996, **29**, 229-234. Copyright 1996 American Chemical Society.

1.4.4.2) An electrostatic gauche effect:

A preferential *gauche* conformation is favoured over an *anti* conformation in β-fluoroalcohols.[26,27] 2-Fluoroethanol has been explored by Density Functional Theory (DFT). Calculations were performed to assess the conformational relationship between the C-F and the C-O bond. It was found that the *gauche* conformer **6a** is stabilised by 2.0 kcal/mol over the *anti* conformer **6b** as shown in Figure 1.13. However, this stabilisation is mostly due to an intramolecular O-H⋯F hydrogen bond and not a stereoelectronic effect. In fact, the *gauche* structure **7a**, which is deficient in intramolecular hydrogen bond, is stabilised over the *anti*

conformer **7b** by only 0.1 kcal/mol. Therefore the *gauche* preference in 2-fluoroethanol is almost entirely due to intramolecular O-H···F hydrogen bonding.
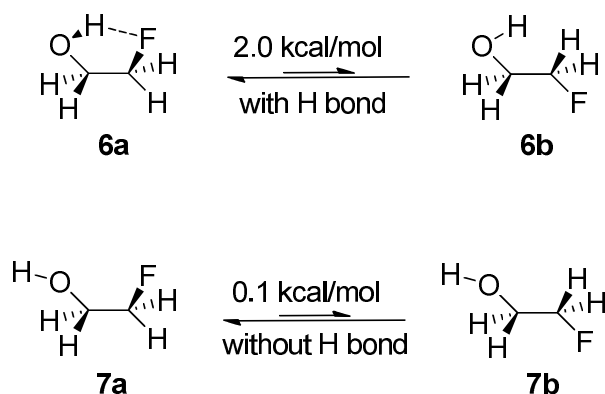
Figure 1.13. Calculated conformations for 2-fluoroethanol.[26, 27]

The same type of studies have also been performed in molecules where the hydroxyl group is protonated as shown in Figure 1.14. The positive charge on the oxygen increases the polarisation of the C-O bond which should result in a stronger stereoelectronic effect. In this case the *gauche* conformer **8a** which takes account of hydrogen bonding, is lower in energy than its *anti* structure **8b** by 7.2 kcal/mol. The calculated *gauche* structure **9a** which lacks an intramolecular hydrogen bond, is stabilised over its *anti* conformer **9b** by 4.4 kcal/mol which is almost four times the stereoelectronic *gauche* stabilisation in 1,2-difluoroethane. It was concluded that the stabilisation due to intramolecular hydrogen bond is around 2.6 kcal/mol which is similar to that found for the non-protonated fluoroalcohols.[26,27]
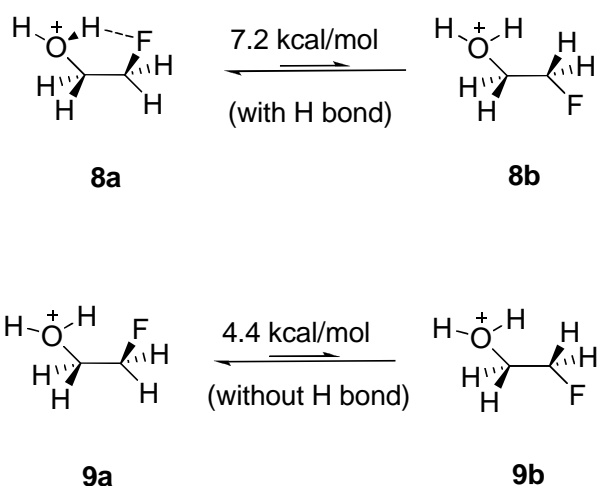
Figure 1.14. Calculated energy difference in different conformations in protonated 2-fluoroethanol.[26, 27]

D. Y. Buissonneaud *et al.*[28] carried out density functional theory (DFT) calculations[28] to examine the relative energies of the *gauche* and *anti* conformers of β-substituted α-fluoroethanes (F-CH$_2$CH$_2$-X), where substituent X can be F (**4**), NH$_3^+$ (**10**), OCOH (**11**), NO$_2$ (**12**), NHCHO (**13**), N$_3$ (**14**), NCO (**15**), CH=NH (**16**), NCS (**17**), CH=C=CH$_2$ (**18**), CH$_3$ (**19**), CH=CH$_2$ (**20**), NC (**21**), CN (**22**) and CHO (**23**) and CCH (**24**). *Gauche* preferences for 1,2-difluoroethane (**4**) are attributable to hyperconjugative interactions ($\sigma_{C-H} \rightarrow \sigma^*_{C-F}$) and for β-fluoroethylammonium (**10**) they are caused by a charge-dipole interaction.[29] For the remaining compounds, preferences for *gauche* or *anti* conformers were established by analysing hyperconjugative, steric and electrostatic contributions. To achieve this, full rotational energy profiles were obtained by progressive rotation around the FC-CX bond. For compounds **11**, **12**, **13**, **14** and **15**, the *gauche* conformer is favoured over the *anti*. For instance, the *gauche* conformation in **15** is adopted as a result of an electrostatic interaction between the electropositive carbon (in substituent NCO) and F, as well as hyperconjugative $\sigma_{C-H} \rightarrow \sigma^*_{C-N}$ interaction (Figure 1.15).[28] Furthermore, the most stable *gauche* conformation is the one with the C-F bond and isocyanate group co-aligned, a result of repulsion between the lone pair of electrons of the nitrogen and F.
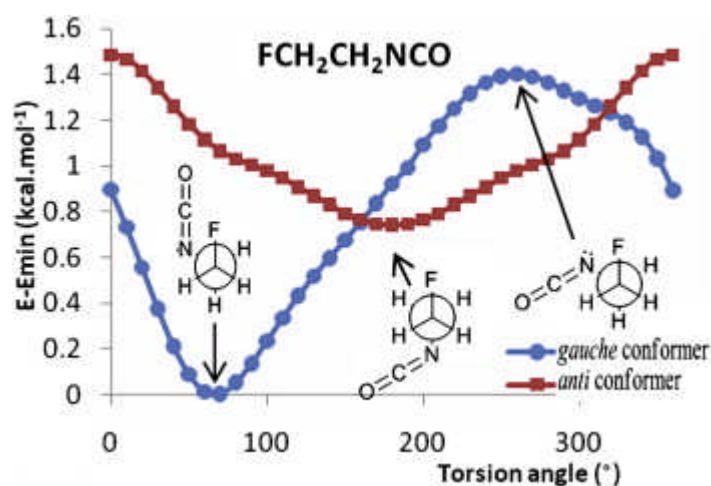
Figure 1.15. Rotational energy profiles of *gauche* and *anti* conformers of **15**.[28] Reprinted from D. Y. Buissonneaud, T. V. Mourik, D. O. Hagan, *Tetrahedron*, 2010, **66**, 2196-2202., Copyright 2010, with permission from Elsevier.

The preference to adopt a *gauche* conformation in compounds **16-20** is weak. For instance the hyperconjugative interaction ($\sigma_{C\text{-}H} \rightarrow \sigma^*_{C\text{-}X}$) in **17** (X = NCS) is weaker compared to **15** (X = NCO), as the C-N bond in the isothiocyanate group is less polarised. Compounds **21** (X = NC), **22** (X = CN), **23** (X = CHO) and **24** (X = CCH) prefer to adopt an *anti* conformation. For instance an *anti* conformation in **23** is preferred because of a stabilising antiparallel dipolar C=O$^{\delta-}$····$^{\delta+}$HFC$^{\delta-}$ interaction. In **24**, a repulsion between the *sp* hybridised C≡CH substituent and *p* orbitals of the fluorine disfavours the *gauche* conformation (Figure 1.16).[28]
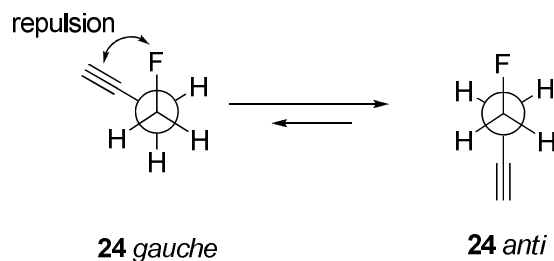
Figure 1.16. The *anti* conformer is lower in energy than the *gauche* conformer in **24**.[28]

1.4.4.3) 1,3-Fluorine-fluorine repulsion:

Sun *et al.*[30] carried out *ab initio* calculations to examine the energy of different conformations of 1,3-difluoropropane. Four different conformations named CG, AG, AA and G'G' were explored, and the conformational energy was found to increase in the order GG < AG < AA < GG' as shown in Figure 1.17.

GG	GA	AA	GG'
0.0 kcal/mol	1.16 kcal/mol	2.41 kcal/mol	3.33 kcal/mol
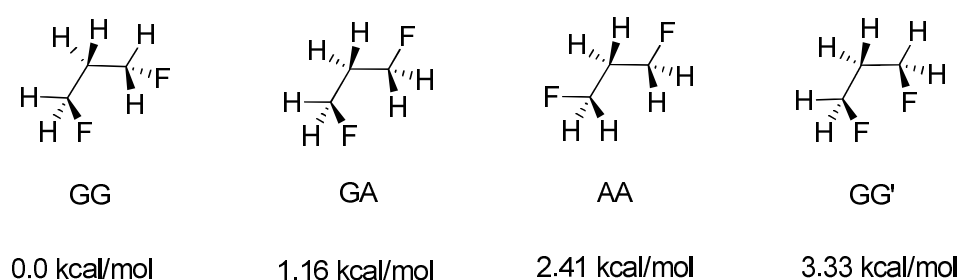
Figure 1.17. Energy of different conformations of 1,3-difluoropropane.[30]

Two $\sigma_{C-H}/\sigma^*_{C-F}$ stabilising interactions occur in the GG conformer, whereas in GA and AA there are one and no $\sigma_{C-H}/\sigma^*_{C-F}$ interactions respectively. Although the GG' conformer has two $\sigma_{C-H}/\sigma^*_{C-F}$ interactions, it is the less stable. Sun *et al.*,[30] suggested that a 1,3-repulsive difluoro interaction, calculated at 3.33 kcal/mol destabilises the GG' conformation. This repulsive interaction was also observed in multivicinal hexafluoroalkanes synthesised by L. Hunter[31] shown in Figure 1.18. The 1,3-repulsive difluoro interaction induces a helical arrangement of the C-F bonds in the all *syn* compound **25**, but not in the *syn-anti-syn-anti-syn* compound **26** where a zigzag conformation is favoured (Figure 1.19) .
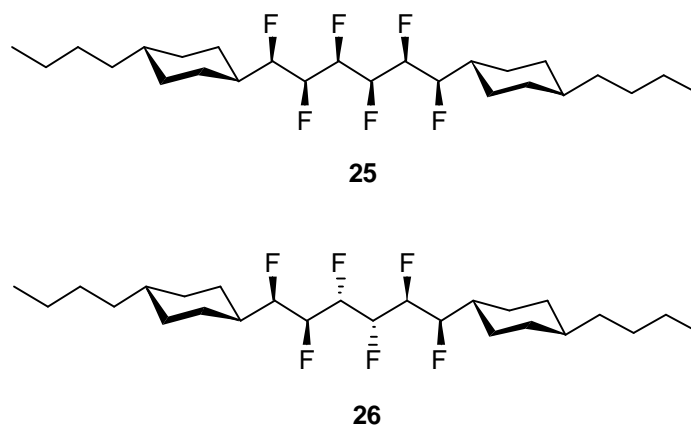
Figure 1.18. All *syn* compound **25** and *syn-anti-syn-anti-syn* compound **26**.[31]
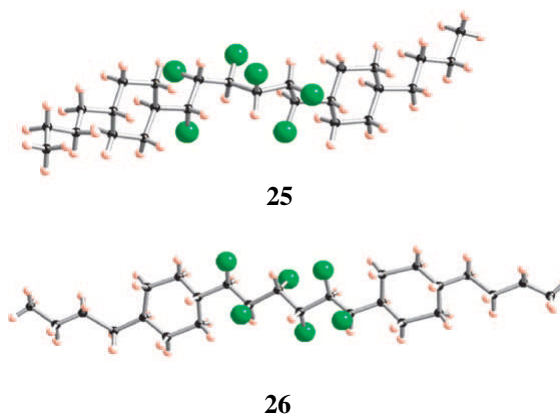
Figure 1.19. X-ray structures of **25** and **26**.[31] L. Hunter, P. Kirsch, A, M. Z. Slawin, D. O'Hagan, *Angew. Chem. Int. Ed.*, 2009, **48**, 5457-5460. Copyright Wiley-VCH Verlag GmbH & Co. KGaA. Reproduced with permission.

1.5) Synthesis of organofluorine compounds:

1.5.1) Monofluorination:

In recent years, there has been significant progress in the development of synthetic methodologies for the selective fluorination of organic molecules. Although this is a very

broad topic, the most established monofluorination methods are reviewed and are classified below as nucleophilic and electrophilic fluorination methods.[2]

1.5.1.1) Nucleophilic fluorination:

Amongst the selective direct fluorination methodologies, the preparation of mono-fluorinated compounds by nucleophilic fluorination plays a central role, particularly in industrial chemistry, for the preparation of fine chemicals.[2] The main problem associated with nucleophilic fluorination is the poor nucleophilicity of fluoride. In fact, fluoride ion is an excellent hydrogen-bond acceptor as it is the smallest anion with the highest negative charge density and lowest polarisability. Therefore, the use of protic solvents, which are of course hydrogen bond donors, is not useful, as fluoride is strongly solvated. Fluoride is a much better nucleophile in polar aprotic solvents such as dimethylformamide (DMF) and acetonitrile (CH_3CN). There are several sources of fluoride suitable for nucleophilic fluorination reactions.

Popular choices involve metallic fluorides such as potassium fluoride (KF), sodium fluoride (NaF), cesium fluoride (CsF), silver fluoride (AgF) as well as ammonium fluorides such as tetrabutylammonium fluoride (TBAF) and tetrabutylammonium dihydrogen trifluoride (TBATF).[32] For these reagents, the nucleophilicity of fluoride is affected by the reaction conditions, predominantly by interaction with the solvent and the positively charged metal. Use of ammonium fluorides, like TBAF and TBATF (Figure 1.20), provides an effective way of increasing the nucleophilicity of fluoride. These reagents decrease fluoride interactions with metal ions due to the presence of large lipophilic cations. As a result, the nucleophilicity of the fluoride is enhanced.[33]
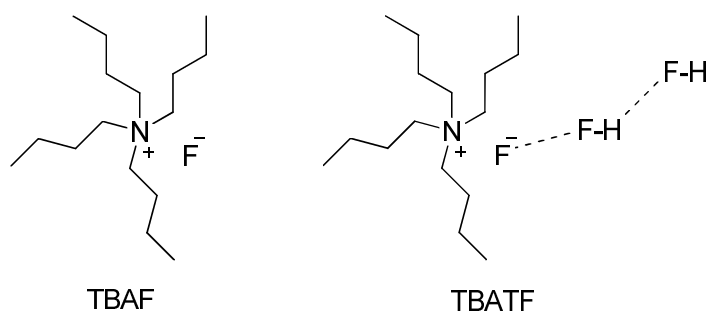
Figure 1.20. Molecular structures of TBAF and TBATF.[32]

Furthermore, crown ethers have been used to increase the nucleophilicity of fluoride, as they bind the metal cations.[33] The poor nucleophilicity of fluoride is not the only issue associated with nucleophilic fluorination reactions. A further problem is that the fluoride ion is also a strong base, which can result in deprotonation and therefore elimination before, during or after the fluorination step. For instance, an elimination reaction occurs during the dehydroxyfluorination of alcohol **27** with diethylaminosulfur trifluoride (DAST), due to the presence of fluoride ions (Scheme 1.1).[41] This becomes an issue, particularly when the desired process involves a nucleophilic S_N2 reaction.[34]
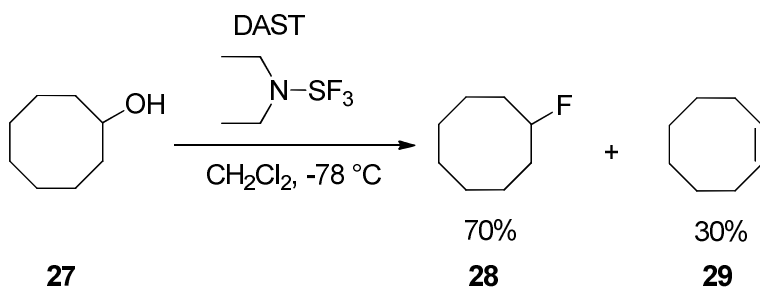
Scheme 1.1. DAST-mediated dehydroxyfluorination of **29**.[41]

Fluoride is a poor leaving group (order of nucleofugicity $I^- > Br^- > Cl^- > F^-$) in aliphatic nucleophilic substitution reactions as the C-F bond is very strong. The Finkelstein exchange reaction used for the synthesis of alkyl fluorides[35] takes advantage of the limited

nucleofugicity of fluoride and the lower boiling point of fluoroaliphatic molecules. In this

reaction an alkyl tosylate **30** is reacted with KF with heating, and the resultant alkyl fluoride

31 is isolated by distillation during the course of the reaction (Scheme 1.2).

$$R-OTs \xrightarrow[\text{120 °C}]{\text{KF, (HOCH}_2\text{CH}_2)_2\text{O}} R-F$$

30   **31** 60-80%
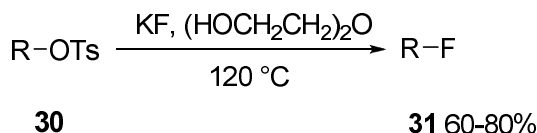
Scheme 1.2. Finkelstein exchange of tosylates **30** by fluoride.[35]

Hydrogen fluoride (HF) is no longer used as a source of fluoride ions due to its corrosive

nature and high toxicity. Reagents that are both safer and easier to handle have been prepared

by combining HF with amines. The first amine-hydrogen fluoride reagent prepared was

pyridinium poly(hydrogen fluoride) known as Olah's Reagent.[36] It is a complex composed by

70% HF and 30% pyridine, which can etch glass similar to anhydrous HF. It was found that

the nucleophilicity of the fluoride could be improved by increasing the percentage of the

amine. This resulted in the preparation of the more neutral $Et_3N\cdot 3HF$,[37] which does not etch

glass. These types of reagent normally require an activated substrate. For instance, Olah's

reagent was successfully used for the introduction of fluorine at the anomeric position in the

synthesis of **33** as shown in Scheme 1.3.[38] The reaction proceeded *via* a stabilised

oxocarbenium ion as shown in Scheme 1.4.[38]
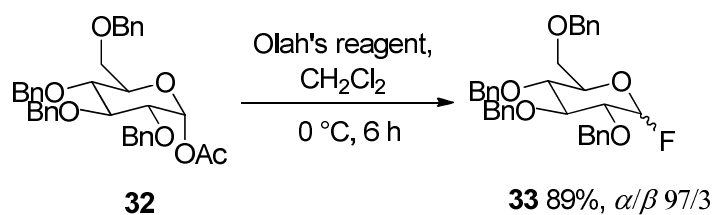
Scheme 1.3. Preparation of **33** using Olah's reagent.[38]
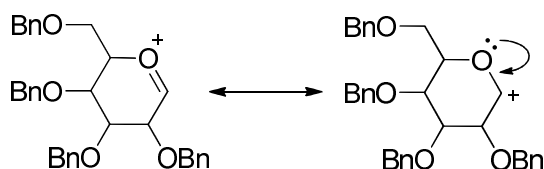
Scheme 1.4. Stabilised oxocarbenium ion formed in the synthesis of **33**.[38]

Amongst the nucleophilic fluorination methodologies, the dehydroxyfluorination of alcohols, where a hydroxyl group is converted to fluorine, plays an important role. This can be achieved either by a two-step activation-fluorination procedure or by a direct dehydroxyfluorination.[34] In the first case, initially the OH group is activated by forming a good leaving group, such as triflate or a mesylate, which is isolated and followed by direct displacement with fluoride. An example of this type of synthesis is shown in Scheme 1.5. The triflate derivative **35** is isolated and then reacted with TBAF to generate the enantiopure vicinal difluoride **36**.[39]
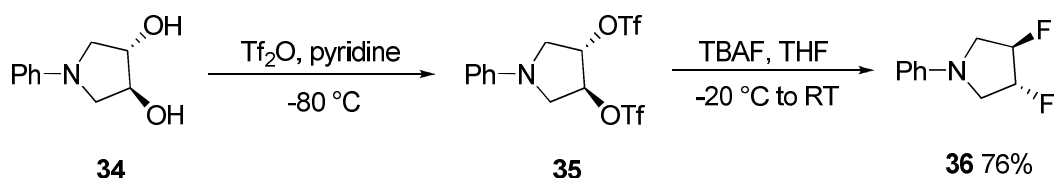
Scheme 1.5. Preparation of the activated diol **35** and subsequent nucleophilic fluorination.[39]

In the second case, the substitution of OH for F is achieved in a one-step procedure. One of the first reagents used for this type of reaction was sulfur tetrafluoride (SF_4).[40] As shown in Scheme 1.6, alcohol **37** is converted to unstable intermediate **38** and then immediate fluoride displacement generates alkyl fluoride **39**, HF and sulfonyl fluoride.[2]
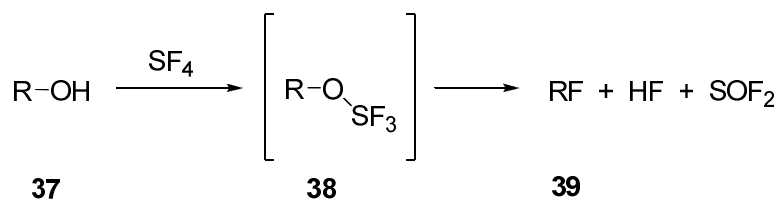
Scheme 1.6. Dehydroxyfluorination of **37** using SF_4.[2]

SF_4 is a very toxic gas, thus not easy to handle. Therefore, analogues have been prepared by replacing one fluorine atom with a dialkylamino group (Scheme 1.7), eg. DuPont generated diethylaminosulfur trifluoride (DAST), which is a more user friendly form of SF_4 that became commercially available in the 1980's.[41]
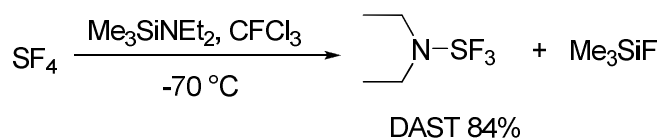
Scheme 1.7. Preparation of DAST.[41]

The mechanism of action of DAST is similar to that for SF_4. The hydroxyl group of alcohol **40** is transformed into a good leaving group by nucleophilic attack of the oxygen to the sulfur of DAST, to generate the unstable intermediate **41**. This is followed by displacement by fluoride to generate **42** (Scheme 1.8).[42]
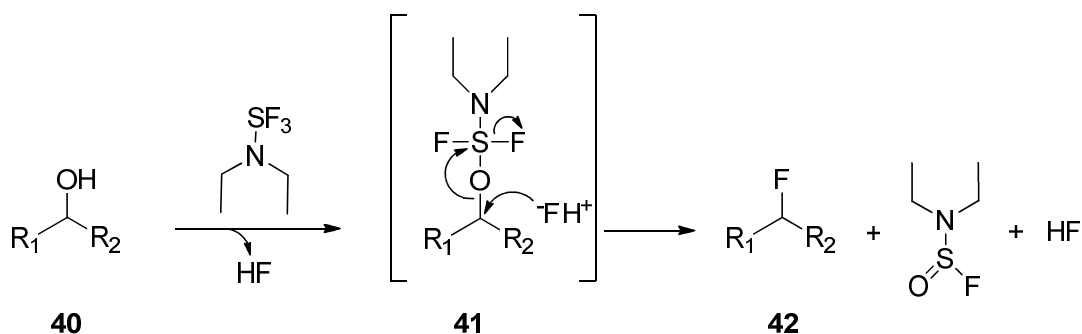
Scheme 1.8. Mechanism of a DAST-mediated dehydroxyfluorination reaction.[42]

Dehydroxyfluorination of *n*-octanol **43** with DAST generated the corresponding fluoride **44** (Scheme 1.9).[41]
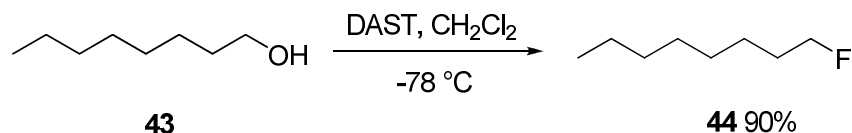
Scheme 1.9. Dehydroxyfluorination of *n*-octanol **43** using DAST.[41]

However, DAST is less reactive than SF_4 due to the inductive effect and steric hindrance of the dialkylamino moiety. For instance, dehydroxyfluorination of ribose derivative **45**, as shown in Scheme 1.10, failed using DAST although use of the two-step activation-fluorination method with Tf_2O and TBAF was successful.[43]
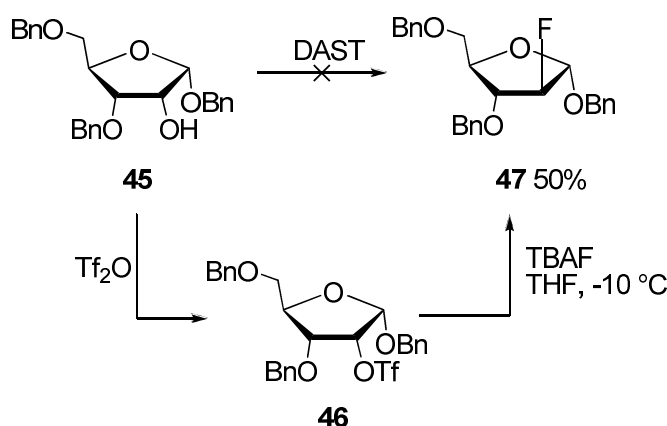
Scheme 1.10. Unsuccessful dehydroxyfluorination of **45** using DAST, and successful two-step activation-fluorination generating product **47**.[43]

A kinetic resolution using a chiral amine to generate DAST analogue (*S*)-2-(methoxymethyl)pyrrolidin-1-ylsulfur trifluoride **49** has been reported (Scheme 1.11),[44] however, this was not very successful and gave a product **50** in only 8% ee along with 2-octene **51**.
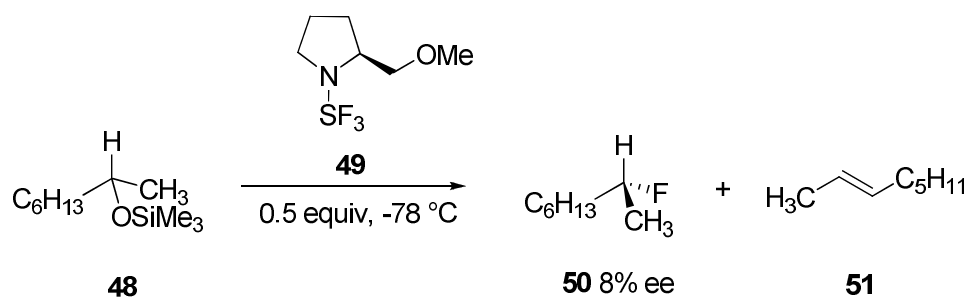
Scheme 1.11. A poor kinetic resolution using the chiral DAST analogue **49**.[44]

Heating of DAST above 50 °C can lead to violent explosions, particularly on a larger scale, as the sulfur-nitrogen bond is not stable. The reagent [*bis*(2-methoxyethyl)amino]sulfur trifluoride (Deoxofluor[TM]) has emerged[45] as a second generation DAST reagent (Figure 1.21) that is proving to have widespread utility, as it is more thermally stable and less hazardous than DAST for large scale conversions. This stability is attributed to the coordination between the ether oxygen and sulfur.[46] Other reagents such as Ishikawa's reagent ($F_3CCHFCF_2NEt_2$)[47] and Yarovenko's reagent ($ClCHFCF_2NEt_2$)[48] (Figure 1.21) have been explored in dehydroxyfluorination reactions, but have not been widely used. Most recently, 1,1,2,2-tetrafluoro-*N*-*N*-dimethylethylamine (TFEDMA)[49] (Figure 1.21) was introduced as a commercially available reagent; the scope and limitations of this reagent are still emerging. A new fluorinating reagent developed in 2008, with high stability and ease of handling, 4-*tert*-butyl-2,6-dimethylphenylsulfur trifluoride (FLUOLEAD[TM]),[50] is also an alternative to current fluorinating reagents (Figure 1.21).

Figure 1.21. Dehydroxyfluorination reagents Deoxofluor[TM], TFEDMA, Ishikawa's and Yarovenko's reagents, and Fluolead[TM] [45-49]

Nucleophilic fluorination is also an important methodology for epoxide ring opening for the preparation of fluorohydrins, important building blocks in organofluorine chemistry.[51] Although many reagents and reaction conditions have been developed,[51] the nucleophilic ring opening of epoxides very often requires harsh reaction conditions and long reaction times due to the poor nucleophilicity of fluoride and its potential to behave as a strong base.[34] Ring opening can occur *via* S_N2 or S_N1 mechanisms. The most frequently used nucleophilic reagents for the ring opening of epoxides are KF, CsF, potassium hydrogen fluoride (KHF$_2$), TBAF, TBATF, tetrafluorosilane (SiF$_4$) , boron trifluoride etherate (BF$_3$·OEt$_2$) as well as a combination of HF-amine adducts, such as triethylamine trihydrofluoride (Et$_3$N·3HF) and Olah's reagent (Py·9HF).[51]

The influence of the type of fluoride source using amine/HF adducts on the regioselectivity of ring opening, particularly of terminal epoxides, was investigated by G. Haufe *et al.*,[51] with ethyl 10,11-epoxyundecanoate **52** as the model substrate (Scheme 1.12). Use of pyridine/HF mixtures in ring opening of **52** (Scheme 1.12, Table 1.4) with a lower level of HF altered the product distribution towards the fluorination at the primary position generating **54**.[51] A similar study was performed by ring opening of **52** with Et$_3$N·3HF (Scheme 1.12, Table 1.5) and different equivalents of a second amine, as shown in Table 1.5. It is clear that increasing the level of amine increased the product distribution in favour of fluorination at the primary

position generating **54** (Table 1.5). A 45:55 mixture of **53:54** was obtained using neat Et$_3$N·3HF.
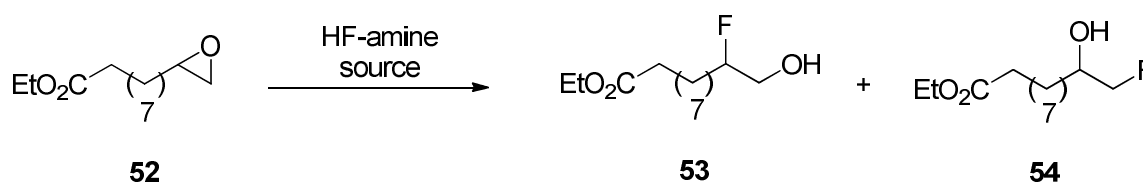
Scheme 1.12. Product ratios of fluorohydrins **53** and **54** formed in ring opening of **52** with different types of fluoride source.[51]

Entry	HF (wt.%)	Product ratio (53:54)	Conversion GC (%)	Combined isolated yield (%)
1	65	92:8	>99	83
2	60	83:17	>99	79
3	50	74:26	>99	74
4	40	55:45	5	ND[a]
5	30	50:50	2	ND[a]

Table 1.4. Product ratios of fluorohydrins **53** and **54** formed in ring opening of **52** with different pyridine/HF mixtures in CH$_2$Cl$_2$ at RT.[51]

[a] Not determined.

Entry	Amine	Et$_3$N·3HF (neat)/second amine ratio	Product ratio (53:54)	Conversion (by GC, %)	Combined isolated yield (%)
1	none	-	45:55	>99	77
2	C$_6$H$_5$CH$_2$NH$_2$	1:1.5	25:75	ND	<2
3	(c-C$_6$H$_{11}$)$_2$NH	1:1	20:80	96	23
4	i-Pr$_2$NH	1:1.2	18:82	97	23
5	Et$_3$N	1:2	24:76	82	44
6	i-Pr$_2$Et$_3$N	1:1	25:75	98	54

Table 1.5. Effect of added amines on product ratios of fluorohydrins **53** and **54** formed in ring opening of **52** with neat Et$_3$N·3HF, heating at 100 °C for 36 h.[51]

Potassium hydrogen difluoride (KHF_2) is a good nucleophilic source of fluoride. A comparison between the epoxide ring opening of **55** using Py·9HF and the more neutral KHF_2 in the presence of a crown ether is summarised in Scheme 1.13,[51] and shows that KHF_2, as opposed to Py·9HF, favours fluorination at the primary position over the secondary position.

Py·9HF	>99	:	traces
KHF_2	10		90
55	**56**		**57**
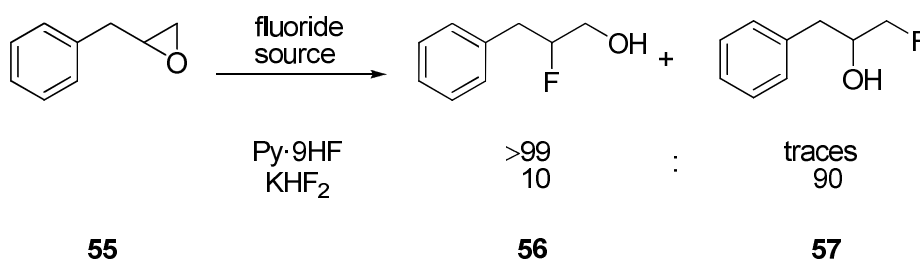
Scheme 1.13. Ring opening of **55** with Py·9HF and KHF_2.[51]

It is concluded that acidic complexes like pyridine/HF mixtures favour a S_N1 process, as the first step is the protonation of the oxygen, followed by fluoride attack at the most stable carbocationic centre (secondary position) as shown in Scheme 1.14, (a).[52,53] Conversely, the S_N2 mechanism is favoured by more neutral reagents such as $Et_3N·3HF$ and KHF_2, as the ring opening occurs *via* attack at the less hindered position (primary position) of the epoxide as shown in Scheme 1.14 (b).[54] In fact, Py·9HF prepared by Olah in 1978[55] is a 70:30 mixture of hydrogen fluoride and pyridine (in molar ratio 9:1 favouring the HF), therefore it is more acidic than $Et_3N·3HF$ which has a molar ratio of HF to amine of around 3:1.

Scheme 1.14. (a) Representation of (a) an S_N1 mechanism[52,53] and (b) an S_N2 mechanism[54] occurring at the epoxide opening with fluoride ion.

The regio- and stereo- selective outcome is not only influenced by the type of fluoride source, but also the nature of substituents present on the epoxide. The reaction pathway is controlled by the presence of electron-donating or electron-withdrawing groups on the epoxide ring. For instance the presence of phthalimide (electron-withdrawing) at the β position to the epoxide ring in compound **58** (Scheme 1.15) strongly destabilises the formation of a carbocationic intermediate at the secondary position,[51] thus fluoride ion attack, when using Py·9HF, occurs preferentially at the primary position over the secondary position, generating **60** and **59** in a 85:15 ratio.[51] The presence of electron-withdrawing groups at the *β* position to the epoxide ring in compound **61** such as 4- and 5- nitroimidazoles again disfavours formation of a carbocationic intermediate at the secondary carbon, which further promotes fluoride ion attack at the primary position favouring the formation of **63** over **62** (Scheme 1.15).[51]
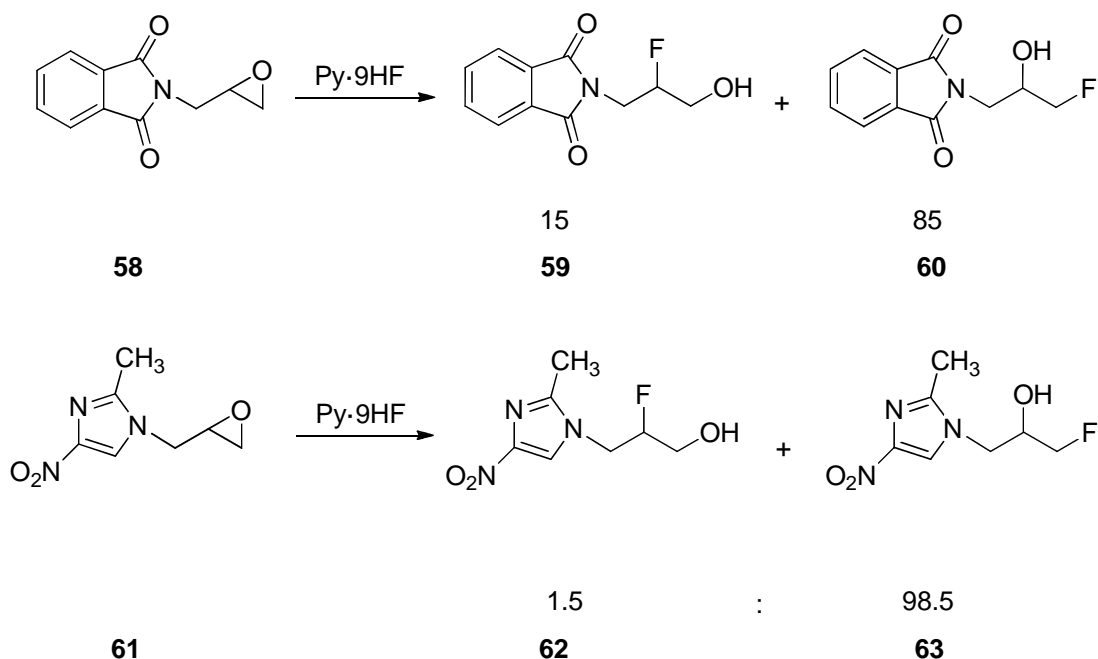
Scheme 1.15. Epoxide opening reactions of **58** and **61** with Py·HF.[51]

The combination of TBATF and a catalytic amount of KHF_2 under solid-liquid phase transfer catalysis has been used by Landini *et al.*[56] for the ring opening of enantiopure (+)-(2*R*)-

[(triphenylmethoxy)methyl]oxirane **64** (Scheme 1.16). The reaction generated (*R*)-**65** as the major product. TBATF can also be used alone as shown in Scheme 1.17, and generated fluorohydrin **67** with good regioselectivity (25:1) after reaction with **66**.[57] TBAF in THF was used for epoxide ring opening of **68** as shown in Scheme 1.18.[58] Sharpless *et al.* demonstrated that TBAF was also suitable for ring opening of cyclic sulfates.[59] This strategy was used by Hunter *et al.* as a method for the stereospecific opening of **70** (Scheme 1.19) to generate fluorohydrin **71**.[60]
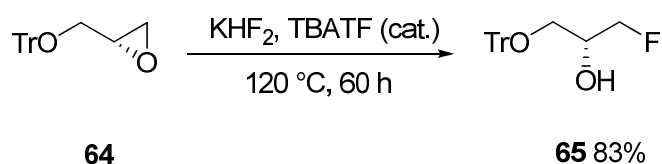
Scheme 1.16. Epoxide opening of **64** with TBATF and a catalytic amount of KHF_2.[56]
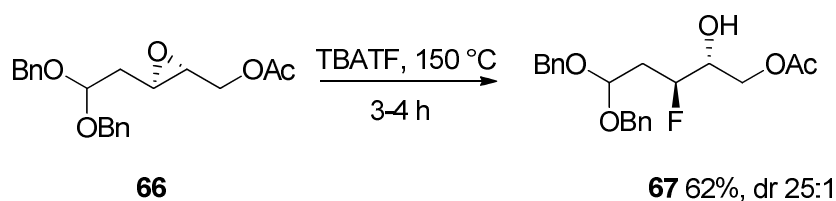
Scheme 1.17. Epoxide opening of **66** with TBATF.[57]
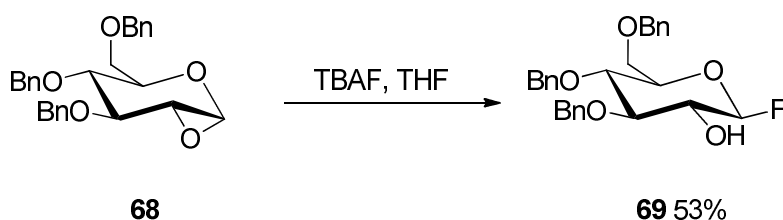
Scheme 1.18. Epoxide opening of **68** with TBAF.[58]
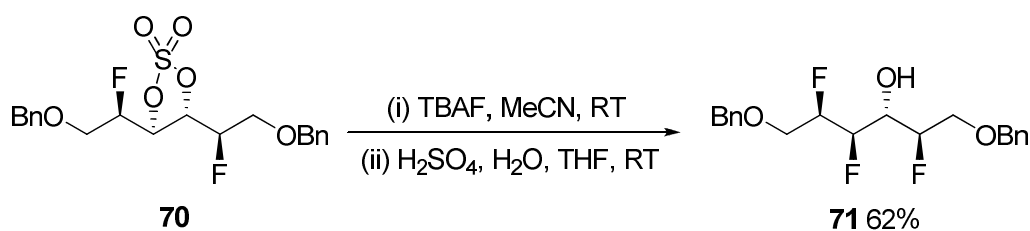
Scheme 1.19. Ring opening of cyclic sulfate **70** and subsequent hydrolysis to **71**.[60]

Other approaches have been explored to develop new methods for the preparation of enantiopure fluorohydrins. Haufe *et al.*[61,62] explored the catalytic enantioselective nucleophilic ring opening of *meso* and racemic epoxides using a Jacobsen's (salen) complex. This involved using the (*S,S*)-(+)-(salen)chromium chloride complex **72** as a catalyst (Figure 1.22) in association with a nucleophilic source of fluorine. For instance, when cyclohexene oxide **73** was reacted with 1 equivalent of TBATF, 20 mol% of catalyst **72** and 20 mol% of AgF in Et$_2$O at RT for 140 h, the product (*R,R*)-(-)-2-fluorocyclohexanol **74** was generated in 67% ee and 42% yield along with the side-product chlorohydrin **75** (Scheme 1.20).
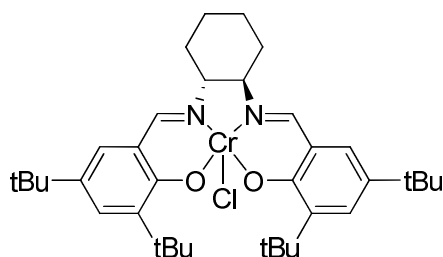
Figure 1.22. Jacobsen's enantiopure (salen)chromium chloride complex **72**.[62]
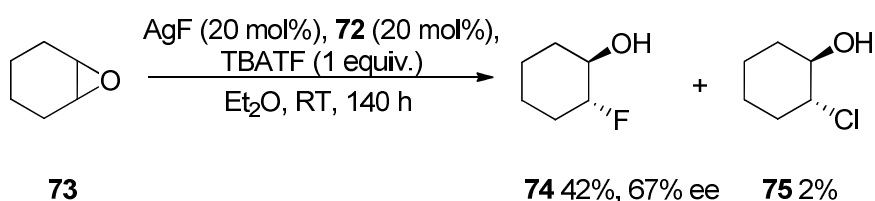
Scheme 1.20. Catalytic enantioselective nucleophilic ring opening of *meso* **73**.[62]

Reaction of racemic styrene oxide **76** with 1.5 equivalents of AgF and 50 mol% of catalyst **72** at 50 °C for 5 h in CH$_3$CN generated the fluorohydrin **77** in 74% ee and 43% yield (Scheme 1.21).
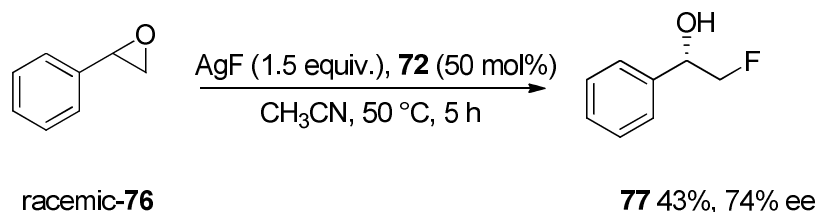
Scheme 1.21. Catalytic enantioselective nucleophilic ring opening of racemic-**76**.[62]

1.5.1.2) Electrophilic fluorination:

Electrophilic fluorination involves reagents containing an "F$^+$" equivalent, which is then attacked by a nucleophile. As a result, the "F$^+$" is transferred to the reactant. Despite elemental fluorine (F$_2$) being a highly toxic and aggressive reagent due to the low F-F bond energy (36.6 kcal/mol), it has been used as an electrophilic fluorinating reagent. A successful example of the use of elemental fluorine as an electrophilic is found in the synthesis of 5-fluorouracil **80** by reaction of **78** with dilute F$_2$ in an inert gas such as N$_2$. This reaction is still used in industry to produce **80** which is an important chemotherapeutic reagent (Scheme 1.22).[63]
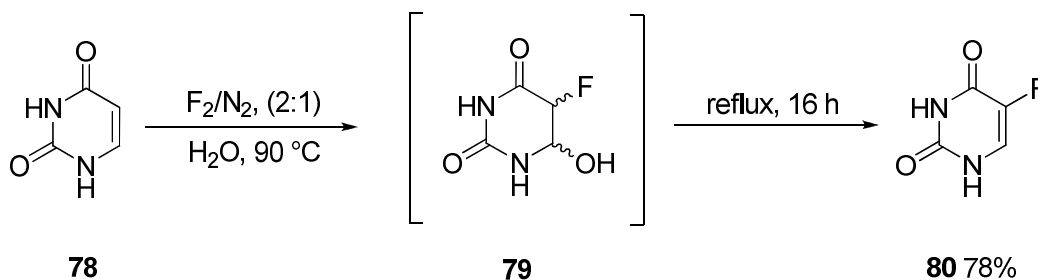
Scheme 1.22. Industrial preparation of 5-fluorouracil **80**.[61] Scheme adapted from P. D. Schuman *et al.*[63]

However, the difficulty in handling F_2 and sometimes its lack of selectivity led to the introduction of more refined reagents. Hypofluorites, also called "OF" reagents, are characterised by the activation of fluorine by oxygen. Examples of this class are CH_3COOF,[64] CF_3COOF[65] and CF_3OF.[66] However, many of these reagents are strong oxidising agents and suffer from a lack of selectivity which lead to unwanted side-products.[67] Significant progress came with the synthesis of less reactive N-F reagents. The fluorinating strength of this type of reagent is decreased compared to the "OF" reagents, as the N-F bond is stronger than the O-F bond, and this decreases the electrophilicity of the fluorine, enabling more controlled fluorinations to be performed. Also, the strength of the N-F bond can be further modulated by the introduction of electron-donating or withdrawing substituents on the nitrogen. Important reagents of this class are Selectfluor[TM] and *N*-fluorosulfonamides. Selectfluor[TM] (Figure 1.23) is a very stable and versatile electrophilic fluorinating reagent that was developed by Banks *et al.*[68,69] in 1988.
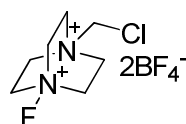
Figure 1.23. Electrophilic fluorination reagent Selectfluor.[68,69]

The utility of the *N*-fluorosulfonamides as electrophilic reagents for the fluorination of carbanions was first demonstrated by Barnette.[70] An important reagent of this category is the *N*-fluorobenzenesulfonimide (NFSI) shown in Figure 1.24.
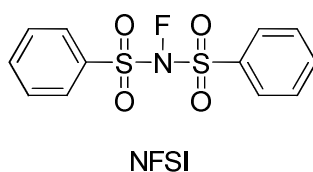
NFSI

Figure 1.24. Electrophilic fluorination reagent NFSI .[70]

Stereoselective preparation of *α*-fluorinated carbonyl compounds by asymmetric fluorination[71] emerged as a result of the extensive development of electrophilic reagents. The first example of an enantioselective fluorination reaction was reported by Differding and Lang[72] in 1988 by the use of the *N*-fluorocamphorsultams **81** and **82** (Figure 1.25).

81 R = H
82 R = CH_3

Figure 1.25. Electrophilic fluorination reagents *N*-fluorocamphorsultams **81** and **82**.[72]

Enantioselective electrophilic fluorination using *N*-fluoro quaternary ammonium salts of cinchona alkaloids was developed by Cahard[73] and Shibata[74] in parallel in 2000. This followed the pioneering work of Banks *et al.*,[75] who reported the quantitative conversion of Selectfluor^TM and quinuiclidine **83** to *N*-fluoro quinuclidine **84** (Scheme 1.23).
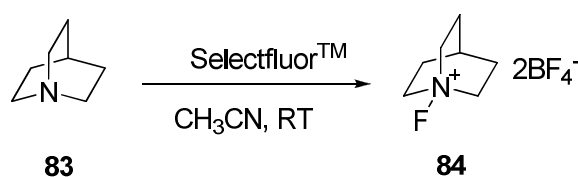
Scheme 1.23. Preparation of *N*-fluoro quinuclidine **84**.[75]

For instance, Cahard *et al.*[73] synthesised the *N*-fluoro quaternary ammonium salt of cinchona alkaloid **86** by a transfer fluorination reaction between Selectfluor^TM and cinchonidine **85** (Scheme 1.24). Cinchona alkaloid **86** was then used for the fluorination of the sodium enolate of 2-methyl-1-tetralone **87** to generate **88** in 80% yield and 56% ee. (Scheme 1.25).
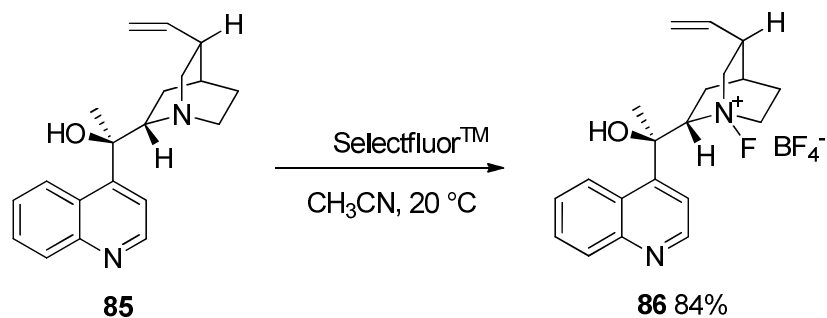
Scheme 1.24. Preparation of the *N*-fluoro quaternary ammonium salt of cinchona alkaloid **86**.[73]
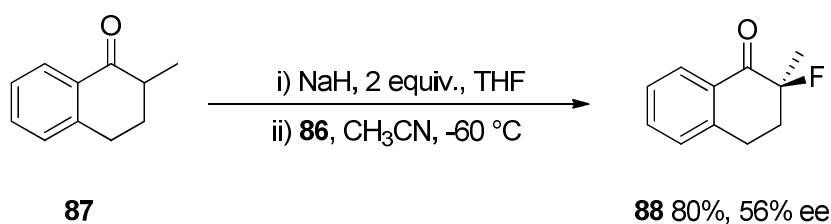
Scheme 1.25. Electrophilic fluorination of the sodium enolate of **87**.[73]

Togni and Hintermann in 2000[76] reported the first catalytic enantioselective electrophilic fluorination of a *β*-ketoester by the use of chiral titanium-based Lewis acids catalysts. This finding followed observations that substoichiometric amounts of a Lewis acid might catalyse the enolisation reaction.[77] After extended screening, the best results were found with Selectfluor[TM] and a titanium taddolate complex (*R*)-**89** or (*R*)-**90** (Figure 1.26), an example is reported in Scheme 1.26.

Ar = 1-naphthyl

(*R*)-**89**   (*R*)-**90**
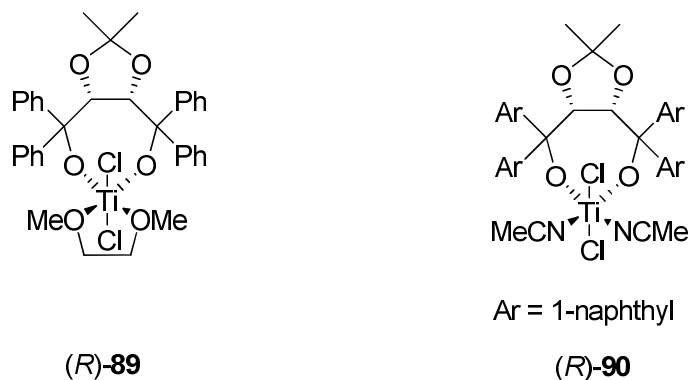
Figure 1.26. Chiral titanium-based Lewis acids catalysts (*R*)-**89** and (*R*)-**90**.[76]
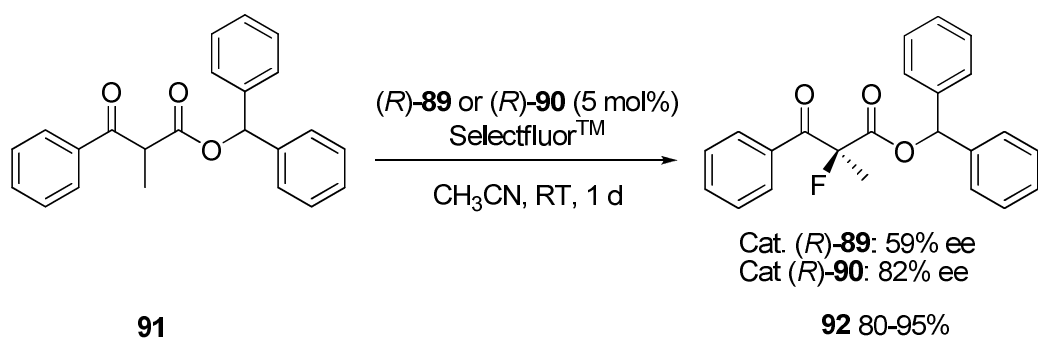
Scheme 1.26. Enantioselective electrophilic fluorination of **91** by the use of chiral catalysts (*R*)-**89** and (*R*)-**90**.[76]

Another important result in this context was reported in 2005 by Shibata *et al.*,[78] who demonstrated that chiral Ni^{II} or Zn^{II} complexes of the ligand phenyl-*bis*(oxazoline) (*R,R*)-**93** (Figure 1.27) can catalyse the enantioselective asymmetric fluorination of *β*-ketoesters with NFSI to generate products with excellent enantioselectivities. For instance, treatment of the non symmetrical malonate ester **94** as shown in Scheme 1.27 generated the *α*-fluoro-*β*-ketoester **95** in good yields (up to 95%) and very good enantiopurities (up to 99% ee).[78]
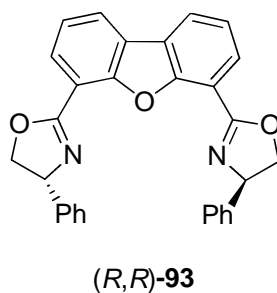
Figure 1.27. Ligand phenyl-*bis*(oxazoline) (*R,R*)-**93**.[78]
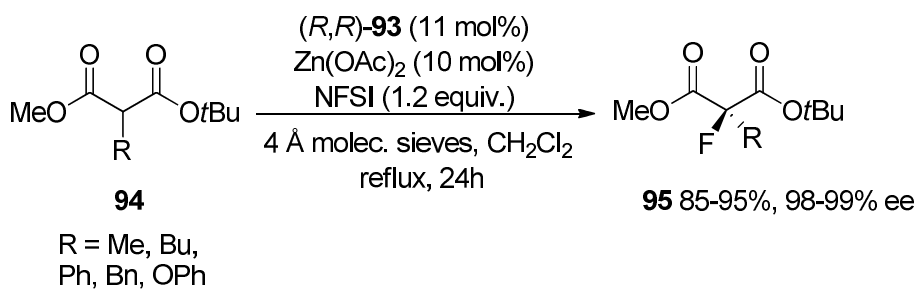
Scheme 1.27. Catalyitic asymmetric fluorination of nonsymmetrical malonate esters **94**.[78]

1.6) Polar hydrophobicity:

1.6.1) The "hydrophobic effect" of fluorinated compounds:

As previously discussed (see section 1.2.3), perfluorinated compounds and their analogous hydrocarbons are hydrophobic, thus are not miscible in water.[79] The exact nature of the hydrophobic interactions is still debatable.[80] However, the hydrophobic effect is an important aspect to take into consideration when a fluorinated molecule is biologically active. The entropy of the binding of a hydrophobic substrate such as a hydrocarbon or a fluorocarbon to a physiological receptor, due to liberation of water by desolvation, is high and positive. Thus, the hydrophobic effect is exploited for the synthesis of more potent enzyme inhibitors.[81] For instance Whitesides *et al.*,[82] synthesised inhibitors of carbonic anhydrase (Figure 1.28), and reported that the binding was directly proportional to their hydrophobic surface. However higher affinities were observed for the fluorocarbons, due to the larger hydrophobic surface areas compared to the hydrocarbon analogues.

1.6.2) Fluorosugars and polar hydrophobicity:

The C-F bond can take part in electrostatic (dipole-dipole or point-dipole) interactions, which are weakened in the presence of polar heteroatom solvents.[83] However, the C-F bond cannot take part in dipole-induced dipole, ion-induced dipole and dispersion interactions, due to its low polarisability.[83] Various studies[84] have reported that favourable dipolar C-F⋯M interactions, where M is a metal cation, occur in preorganised systems such as macrocyclic fluorinated ligands. The synergy between hydrophobic effects, and the ability of the C-F bond to interact with dipoles or positive ions, is named "polar hydrophobicity",[83] and has

been largely exploited in protein-ligand interactions. In this respect, the replacement of hydrophilic groups (OH) by polar hydrophobic groups (CF_2) in a sugar is thought to be a general strategy to enhance its binding to a physiological receptor.[85]

1.7) Aims and objectives:

This chapter introduced the concept of fluorine in organic molecules, and methods to introduce fluorine. This thesis now describes research addressing studies on dehydroxyfluorination reactions, and appropriate reagents, and describes the synthesis of two trifluoro D-hexose sugar analogues.

Chapter 2 explores allylic fluorination as a key aspect of the trifluoro D-hexose sugar analogue syntheses, and Chapter 3 then describes the syntheses of the final sugars and their transmembrane transport studies using red blood cells. Chapter 4 investigates the methodology for promoting S_N2 rather than S_N1 reactions processes in dehydroxyfluorination, in order to mediate highly stereospecific fluorination reactions.

References Chapter 1

[1] S. Purser, P. R. Moore, S. Swallow, V. Gouverneur, *Chem. Soc. Rev*., 2008, **37**, 320-330.

[2] P. Kirsch, "*Modern fluoroorganic chemistry: Synthesis, reactivity, applications*", Wiley VCH: Weinheim, 2004.

[3] P. Jeschke, *ChemBioChem*, 2004, **5**, 570-589.

[4] K. Uneyama, "*Organofluorine chemistry*", Blackwell Publishing, 2006.

[5] M. Naritomi, H. Murofushi, N. Nakashima, *Bull. Chem. Soc. Jpn*., 2004, **77**, 2121-2127.

[6] J. A. Gladysz, D. P. Curran, *Tetrahedron,* 2002, **58**, 3823-3825.

[7] A. Leo, C. Hansch, D. Elkins, *Chem. Rev*., 1971, **71**, 525-616.

[8] H. -J. Böhm, D. Banner, S. Bendels, M. Kansy, B. Kuhn, K. Müller, U. Obst-Sander, M. Stahl, *ChemBioChem,* 2004, **5**, 637-643.

[9] L. Pauling, "*The Nature of the Chemical Bond and the Structure of Molecules and Crystals: An Introduction to Modern Structural Chemistry*", Cornell University Press, Ithaca, NY, 1939.

[10] B. E. Smart, *J. Fluorine. Chem*., 2001, **109**, 3-11.

[11] C. G. Krespan, V. A. Petrov, *Chem. Rev*., 1996, **96**, 3269-3301.

[12] D. O'Hagan, *Chem. Soc. Rev*., 2008, **37**, 308-319.

[13] J. –A. Ma, D. Cahard, *Chem. Rev*., 2004, **104**, 6119-6146.

[14] A. J. Kirby, "*The Anomeric Effect and Related Stereoelectronic Effects at Oxygen*", Springer, Berlin, 1983.

[15] D. O'Hagan, H. S. Rzepa, *Chem. Commun*., 1997, 645-652.

[16] J. H. Clark, D. M. Goodall, M. S. White, *Tetrahedron Lett.,* 1983, **24**, 1097-1100.

[17] (a) G. A. Jeffery, 1997, "*An introduction to Hydrogen Bond*", Oxford University Press, Oxford, 1997; (b) S. Scheiner, 1997, "*Hydrogen Bond: A theoretical Perspective*", Oxford

University Press, Oxford, 1997; (c) G. R. Desiraju, T. Steiner, *"The Weak Hydrogen Bond in Structural Chemistry and Biology"*, IUCr/Oxford Sci Publ, Oxford, 1997.

[18] A. M. Sum, D. C. Lankin, K. Hardcastle, J. P. Snyder, *Chem.-Eur. J.*, 2005, **11**, 1579-1591.

[19] H. Takemura, M. Kotoku, M. Yasukate, M., T. Shinmyozu, *Eur. J. Org. Chem.*, 2004, **9**, 2019-2024.

[20] D. Cantacuzene, K. L. Kirk, D. H. McCulloh, C. R. Crevelins, *Science*, 1979, **204**, 1217-1219.

[21] (a) V. R. Thallady, H. C. Weiss, D. Blaser, R. Boese, A. Nangia, G. R. Desiraju, *J. Am. Chem. Soc.*, 1998, **120**, 8702-8710; (b) G. R. Desiraju, G. R., *Acc. Chem. Res.*, 2002, **35**, 565-573.

[22] P. Deslongchamps, *"Stereoelectronic effecs in organic chemistry"*, ed. P. Press Oxford, 1983.

[23] P. R. Rablen, R. W. Hoffmann, D. A. Hrovat, W. T. Borden*, J. Chem. Soc., Perkin Trans. 2.*, 1999, 1719-1726.

[24] K. B. Wiberg, *Acc. Chem. Res.*, 1996, **29**, 229-234.

[25] K. B. Wiberg, M. A. Murcko, K. E. Laidig, P. J. MacDougall, *J. Phys. Chem.*, 1990, **94**, 6956-6959.

[26] C. R. S. Briggs, M. J. Allen, D. O'Hagan, D. J. Tozer, A. M. Z. Slawin, A. E. Goeta, J. A. K. Howard, *Org. Biomol. Chem.*, 2004, **2**, 732-740.

[27] D. A. Dixon, B. E. Smart, *J. Phys. Chem.*, 1991, **95**, 1609-1612.

[28] D. Y. Buissonneaud, T. V. Mourik, D. O. Hagan, *Tetrahedron*, 2010, **66**, 2196-2202.

[29] (a) N. E. J. Gooseman, D. O'Hagan, M. J. G. Peach, A. M. Z. Slawin, D. J. Tozer, R. J. Young, *Angew. Chem. Int. Ed.*, 2007, **46**, 5904-5908; (b) N. E. J. Gooseman, D. O'Hagan, A. M. Z. Slawin, A. M. Teale, D. J. Tozer, R. J. Young, *Chem. Commun.*, 2006, **30**, 3190-3192.

[30] D. Wu, A. Tian, H. Sun, *J. Phys. Chem.*, 1998, **102**, 9901-9905.

[31] L. Hunter, P. Kirsch, A, M. Z. Slawin, D. O'Hagan, *Angew. Chem. Int. Ed*., 2009, **48**, 5457-5460.

[32] J. Cousseau, P. Albert, *Bull. Soc. Chim. Fr*., 1986, 910-915.

[33] U. Langa, A. Senning, *Chem. Ber*., 1991, **124**, 1879-1880.

[34] V. A. Soloshonok, "*Enantiocontrolled synthesis of fluoro-organic compounds*", Wiley, 1999.

[35] *"Organikum"*, 21st ed., Wiley, 2001.

[36] (a) G. A. Olah, M. Nojima, I. Kerekes, *Synthesis*, 1973, 779-780; (b) G. A. Olah, M. Nojima, I. Kerekes, *Synthesis*, 1973, 780-783; (c) G. A. Olah, J. T. Welsh, Y. D. Vankar, M. Nojima, I. Kerekes, J. A. Olah, *J. Org. Chem*., 1979, **44**, 3872-3881.

[37] (a) R. Franz, *J. Fluorine Chem*., 1980, **15**, 423-434; (b) M. A. McClinton, *Aldrichimica Acta*, 1995, **28**, 31-35.

[38] (a) M. Hayashi, S. Hashimoto, R. Noyori, *Chem. Lett*., 1984, 1747-1750; (b) M, Palme, A. Vasella, *Helv. Chim. Acta*, 1995, **78**, 959-969.

[39] C. M. Marson, R. C. Melling, *Chem. Commun*., 1998, 1223-1224.

[40] C. –L. J. Wang, *Org. React.*, 1985, **34**, 319-400.

[41] W. J. Middleton, *J. Org. Chem*., 1975, **40**, 574-578.

[42] (a) K. L. Kirk, *Org. Process. Res. Dev*., 2008, **12**, 305-321; (b) S. T. Purrington, B. S. Kagen, T. B. Patrick, *Chem. Rev*., 1986, **86**, 997-1018.

[43] T. -L. Su, R. S. Klein, J. J. Fox, *J. Org. Chem*., 1982, **47**, 1506-1509.

[44] G. L. Hann, P. Sampson, *J. Chem. Soc., Chem. Commun*., 1989, 1650-1651.

[45] S. Lal, G. P. Pez, R. J. Pesaresi, F. M. Prozonic, H. Cheng, *J. Org. Chem*., 1999, **64**, 7048-7054.

[46] R. P. Singh, J. M. Shreeve, *Synthesis*, 2002, 2561-2578.

[47] A. Takaoka, H. Iwakiri, N. Ishikawa, *Bull. Chem. Soc. Jpn*., 1979, **52**, 3377-3380.

[48] N. N. Yarovenko, M. A, Raksha, V. N. Shemanina, A. S. Vasileva, *Zh. Obshch. Khim.*, 1957, **27**, 2246.

[49] V. A. Petrov, S. Swearingen, W. Hong, W. C. Petersen, *J. Fluorine Chem.*, 2001, **109**, 25-31.

[50] (a) T. Umemoto, Y. Xu, *US patent* 7,265,247 (IM&T Research Inc.) Feb 2008 (b) T. Umemoto, R. P. Singh, *US patent* 20080039660 (IM&T Research Inc.) Feb 2008 (c). S. Bresciani, *J. Fluorine Chem.*, 2009, **130**, 537-543.

[51] G. Haufe, *J. Fluorine. Chem.*, 2004, **125**, 875-894.

[52] C. Bonini, G. Righi, *Synthesis*, 1994, 225-238.

[53] R. Skupin, G. Haufe, *J. Fluorine Chem.*, 1998, **92**, 157-165.

[54] U. Sulser, J. Widmer, H. Goeth, *Helv. Chim. Acta*, 1977, **60**, 1676-1690.

[55] G. A. Olah, D. Meidar, *Isr. J. Chem.*, 1978, **17**, 148-149.

[56] D. Landini, D. Albanese, M. Penso, *Tetrahedron*, 1992, **48**, 4163-4170.

[57] D. M. Gordon, S. J. Danishefsky, *Carbohydr. Res.*, 1990, **206**, 361.

[58] R. D. Chambers, S. J. Mullins, A. J. Roche, J. F. S. Vaughan, *Chem. Commun.*, 1995, 841-842.

[59] Y. Gao, Y, K. B. Sharpless, *J. Am. Chem. Soc.*, 1988, **110**, 7538-7539.

[60] L. Hunter, D. O'Hagan, A. M. Z. Slawin, *J. Am. Chem. Soc.*, 2006, **128**, 16422-16423.

[61] S. Bruns, G. Haufe. *J. Fluorine Chem.*, 2000, **104**, 247-254.

[62] G. Haufe, S. Bruns, *Adv. Synth. Catal.*, 2002, **344**, 165-171.

[63] P. D. Schuman, P. Tarrant, D. A. Warner, G. Westmoreland, *US patent* 3954758, 1971.

[64] D. Hebel, O. Lerman, S. Rozen, *J. Fluorine Chem.*, 1985, **30**, 141-146.

[65] (a) Appelman, M. H. Mendelsohn, H. Kim, *J. Am. Chem. Soc.*, 1985, **107**, 6515-6518; (b) S. Rozen, Y. Menahem, *J. Fluorine Chem.*, 1980, **16**, 19-31.

[66] (a) D. H. R. Barton, L. S. Godinho, R. H. Hesse, M. M. Pechet, *Chem. Commun.*, 1968, 804-806; (b) D. H. R. Barton, L. J. Danks, A. K. Ganguly, R. H. Hesse, G. Tarzia, M. M. Pechet, *Chem. Commun.*, 1969, 227-228.

[67] S. T. Purrington, B. S. Kagen, *Chem. Rev.*, 1986, **86**, 997-1018.

[68] R. E. Banks, R. A. D. Boisson, W. D. Morton, E. Tsiliopoulos, *J. Chem. Soc., Perkin Trans. 1*, 1996, 2069-2076.

[69] R. E. Banks, M. K. Besheesh, S. N. Mohialdin-Khaffaf, I. Sharif, *J. Chem. Soc., Perkin Trans. 1*, 1996, 2069-2076.

[70] W. E. Barnette, *J. Am. Chem. Soc.*, 1984, **106**, 452-454.

[71] V. A. Brunet, D. O'Hagan, *Angew. Chem. Int. Ed.*, 2008, **47**, 1179-1182.

[72] E. Differding, R. W. Lang, *Tetrahedron Lett.*, 1988, **29**, 6087-6090.

[73] D. Cahard, C. Audouard, J. C. Plaquevent, N. Roques, *Org. Lett.*, 2000, **2,** 3699-3701.

[74] N. Shibata, E. Suzuky, Y. Takeuchi, *J. Am. Chem. Soc.*, 2000, **122**, 10728-10729.

[75] M. Abdul-Ghani, R. E. Banks, M. K. Beshees, I. Sharif, R. G. Syvret, *J. Fluorine Chem.*, 1995, **73**, 255-257.

[76] L. Hintermann, A. Togni, *Angew. Chem. Int. Ed.*, 2000, **39**, 4359-4362.

[77] D. A. Evans, S. G. Nelson, *J. Am. Chem. Soc.*, 1997, **119**, 6452-6453.

[78] N. Shibata, J. Kohno, K. Takay, T. Ishimaru, S. Nakamura, T. Toru, S. Kanemasa, *Angew. Chem. Int. Ed.*, 2005, **44**, 4204-4207.

[79] (a) K. A. Dill, *Biochemistry*, 1990, **29**, 7133-7155; (b) P. L. Privalov, S. J. Jill, *Adv. Protein Chem.*, 1988, **39**, 191-234; (c) A. Ben-Naim, "*Hydrophobic Interactions*", Plenum, 1980; (d) L. R. Pratt, *Annu. Rev. Phys. Chem.*, 1985, **36**, 433-449; (e) C. Tanford, "*The hydrophobic Effect*", Wiley, 1980.

[80] G. Graziano, G. Barone, *J. Am. Chem. Soc.*, 1996, **118**, 1831-1835.

[81] E. A. Meyer, R. K. Castellano, F. Diederich, *Angew. Chem. Int. Ed.*, 2003, **115**, 1244-1287.

[82] J. Gao, Q. Shuang, G. M. Whitesides, *J. Med. Chem.*, 1995, **38**, 2292-2301.

[83] J. C. Biffinger, H. W. Kim, S. G. DiMagno, *ChemBioChem*, 2004, **5**, 622-627.

[84] (a) R. J. Kulawiec, R. H. Crabtree, *Coord. Chem. Rev.*, 1990, **99**, 89-115; (b) H. Plenio, R. Diodone, *Angew. Chem. Int. Ed. Engl.*, 1994, **33**, 2175-2177; (c) H. Plenio, R. Diodone, *J. Am. Chem. Soc.*, 1996, **118**, 356-367; (d) H. Plenio, *Chem. Rev.*, 1997, **97**, 3363-3384; (e) H. –J. Buschmann, J. Hermann, M. Kaupp, H. Plenio, *Chem. Eur. J.*, 1999, **5**, 2566-2572.

[85] H. W. Kim, P. Rossi, R. K. Shoemaker, S. G. DiMagno, *J. Am. Chem. Soc.*, 1998, **120**, 9082-9083.

Chapter 2: Synthesis of allylic fluorides by dehydroxyfluorination of allylic alcohols with a range of reagents

2.1) Introduction:

2.1.1) The importance of the allylic fluoride motif:

Allylic fluorides are a key functional group. They are found in fluorinated analogues of important biological molecules and they can be subject to various synthetic transformations.[1] For instance an allylic fluoride motif is contained in the fluorinated Vitamin D analogue Ro 26-9228 **96**, which was developed by Hoffmann-La Roche, and found to be more pharmacologically active than the natural analogue calcitriol **97** (Figure 2.1).[2,3]
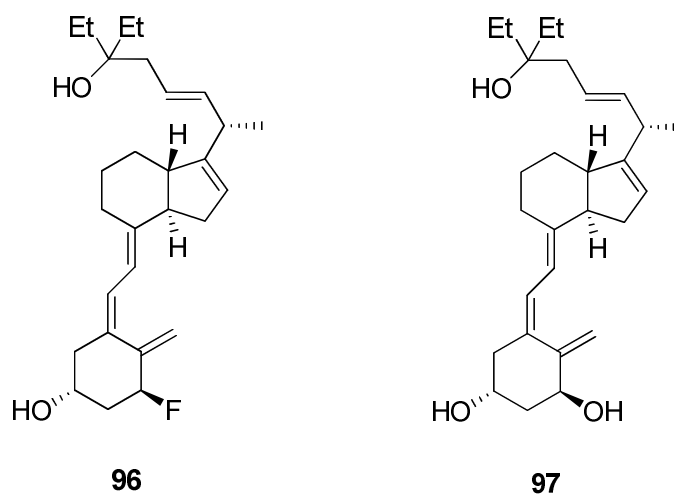
Figure 2.1. Ro 26-9228 **96** and calcitriol **97**.[2,3]

The analogues prostacyclin, 7-F-PGI$_2$ **98** and 5-F-PGI$_2$ **99** (Figure 2.2) are allylic fluorides which have been developed to increase the metabolic stability of the parent prostacyclin PGI$_2$ **100**.[4]
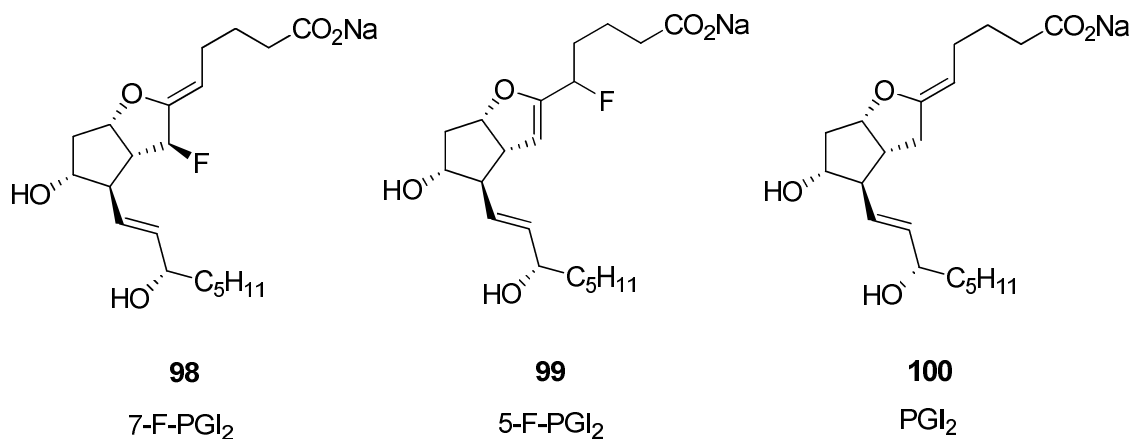
Figure 2.2. Allylic fluorides 7-F-PGI$_2$ **98**, 5-F-PGI$_2$ **99** and PGI$_2$ **100**.[4]

An allylic fluoride motif is present in the fluorinated fatty acid **101**, prepared by Yamamoto *et al.*,[5] to increase the antidiabetic effect of the natural analogue fatty acid docosahexaenoic acid **102** (DHA) (Figure 2.3).
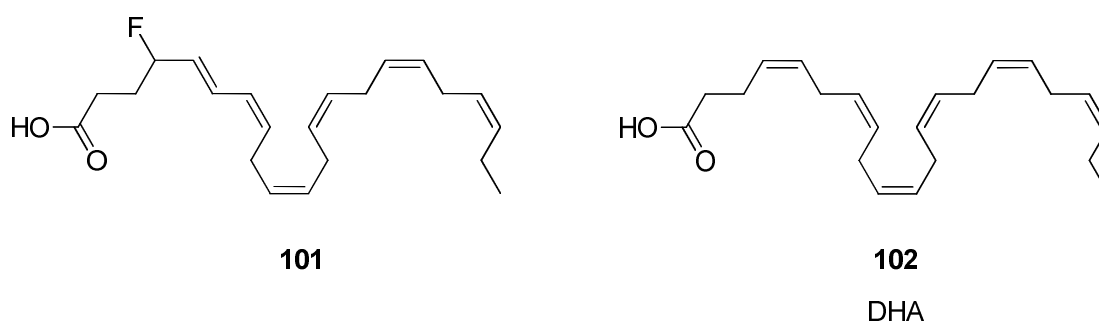
Figure 2.3. The fluorinated fatty acid **101** and docosahexaenoic acid (DHA) **102**.[5]

The anti-asthmatic and anti-dermatosis fluticasone propionate **103** also contains an allylic fluoride motif (Figure 2.4).[6]
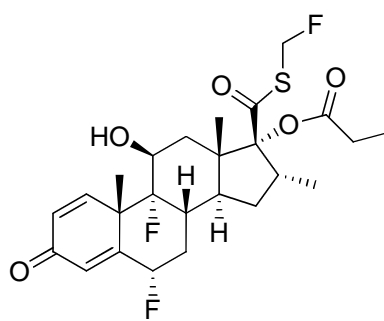
103

Figure 2.4. The anti-asthmatic and anti-dermatosis, fluticasone propionate **103**.[6]

Allylic fluoride motifs, either racemic or enantiomerically enriched, are attractive building blocks in organofluorine chemistry.[1] For example Grée *et al.*[7] reported the epoxidation of allylic fluoride **104** using *m*-CPBA (Scheme 2.1), whereby the fluoro-epoxides **105** and **106** are generated as a 1:1 diastereomeric mixture. Conversely the *m*-CPBA epoxidation of the analogous non fluorinated allylic alcohol of **104** proceeds with high diastereoselectivity,[8] demonstrating the importance of hydrogen bonding to achieve high selectivity in these type of reactions.
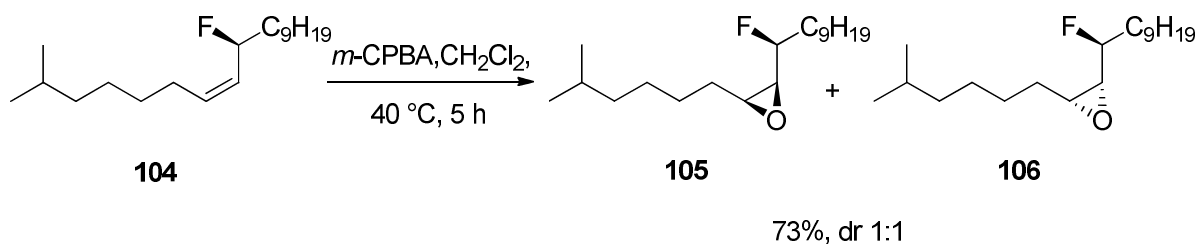
Scheme 2.1. Epoxidation of the allylic fluoride **104** using *m*-CPBA.[7]

Dollé *et al.*[9] documented the predominant substitution of the tosyl group on allylic fluoride **107** by nucleophilic attack by **108** (Scheme 2.2) clearly because the tosyl group is more polarisable than fluorine.
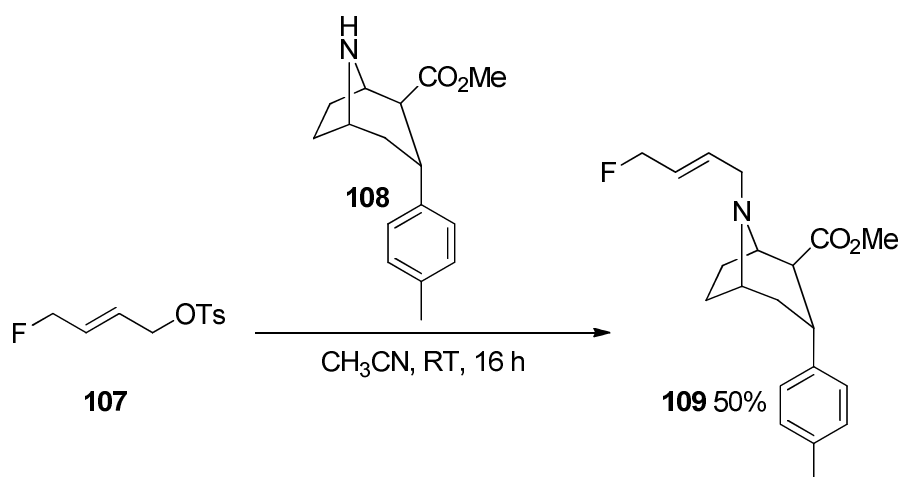
Scheme 2.2 Nucleophilic substitution of the tosyl group on the allylic fluoride **107**.[9]

Davis *et al.*[10] demonstrated that diol **111** is generated as a single diastereoisomer after Sharpless dihydroxylation of allylic fluoride **110** using AD-mix-*β* (Scheme 2.3).

Scheme 2.3 Sharpless dihydroxylation of **110** to generate **111**.[10]

Matsuda *et al.*[11] described the dihydroxylation of allylic fluoride **112** by the use of potassium permanganate (KMnO₄) to generate the corresponding diol (Scheme 2.4), followed by oxidative cleavage with sodium metaperiodate (NaIO₄) to furnish aldehyde **113**.
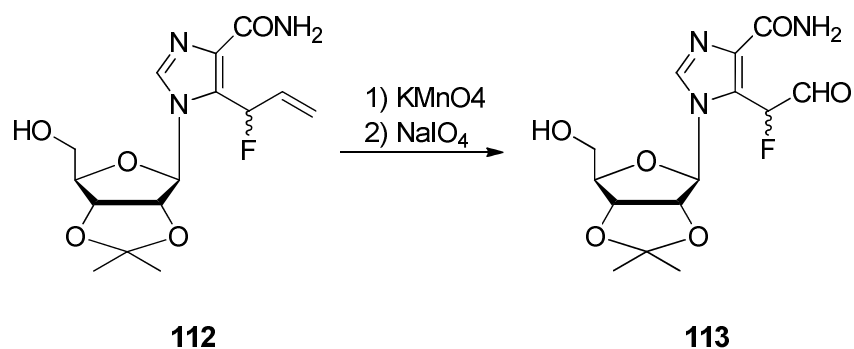
Scheme 2.4 Dihydroxylation and oxidative cleavage of **112** to generate aldehyde **113**.[11]

Hunter *et al.*[12] reported the self-metathesis reaction of the enantiomerically enriched allylic fluoride **114** (Scheme 2.5). This reaction generated a statistical 8:4:1 mixture of (*S,S*), (*R,R*) and (*R,S*) stereoisomers. The major isomer (*S,S*) **115** (98% ee) was isolated by column chromatography in 69% yield.

114
9:1 mixture favouring (*S*)

115 69%, 98% ee
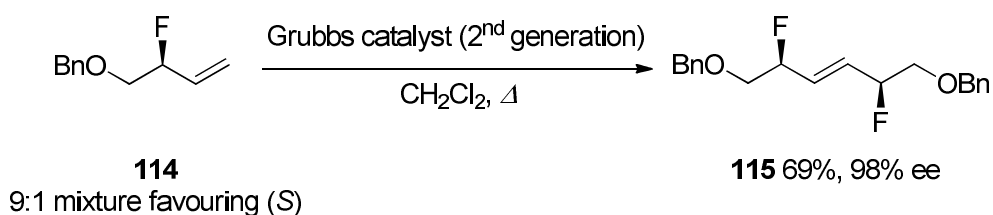
Scheme 2.5. Self-metathesis reaction of allylic fluoride **114**.[12]

2.1.2) Regio- and stereo- selective dehydroxyfluorination of allylic alcohols:

Dehydroxyfluorination of an enantiomerically pure allylic alcohol to an enantiomerically pure allylic fluorine product is attractive. However reaction of allylic alcohols with dehydroxyfluorination reagents such as diethylaminosulfur trifluoride (DAST) can progress by S_N2, S_N2', S_Ni' or S_N1 reaction courses,[1] and as a result a poor level of regio- and stereo-selectivity is frequently observed (Scheme 2.6).
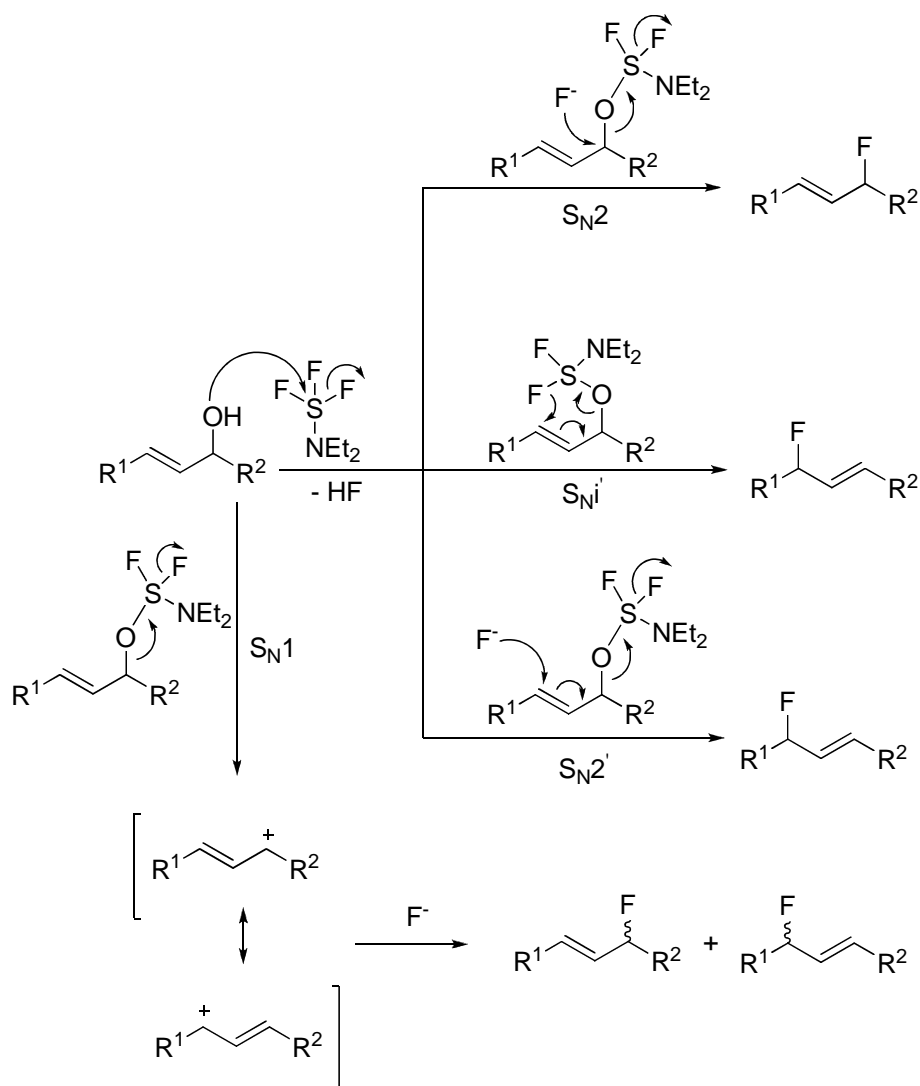
Scheme 2.6 Possible mechanisms in the dehydroxyfluorination of allylic alcohols mediated by DAST.[1]

The first allylic shift observed using DAST as a dehydroxyfluorination reagent was reported by Middleton[13] (Scheme 2.7), whereby dehydroxyfluorination of crotyl alcohol **116** in diglyme gave a mixture of **117** and **118** in a 28:72 ratio. Changing the solvent to the more apolar isooctane only had a small influence on the outcome (ratio 36:64).
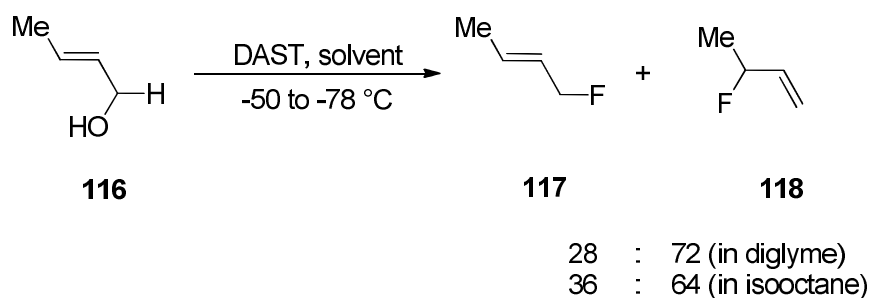
Scheme 2.7. Fluorination of allylic alcohol **116** using DAST reported by Middleton.[13]

The ratio of products of direct versus allylic fluorination is extremely substrate dependent. A detailed study on this subject has been carried out by A. Grée *et al.*[14] They repeated the experiment shown in Scheme 2.7 using CH_2Cl_2 as a solvent, whereby dehydroxyfluorination of **116** generated **117** and **118** in 1:3 ratio (Scheme 2.8), a regioselective outcome very similar to Middleton's result. Furthermore when the hydrogen α to the OH was replaced by an isopropyl group (compound **119**) (Scheme 2.8), the ratio of the direct (compound **120**) versus allylic fluorination (compound **121**) increased from 1:3 to 2:3, thus alkyl groups had a modest effect on the regioselective outcome.
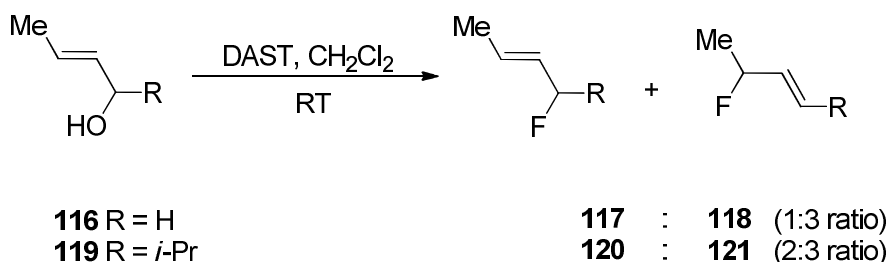
Scheme 2.8. Dehydroxyfluorination of **116** and **119** using DAST in CH_2Cl_2.[14]

The regioselectivity changes dramatically when R is a phenyl group. For instance dehydroxyfluorination of **122** with DAST gave exclusively the most conjugated product **124**, and the same product is generated entirely from **123** (Scheme 2.9).[14]
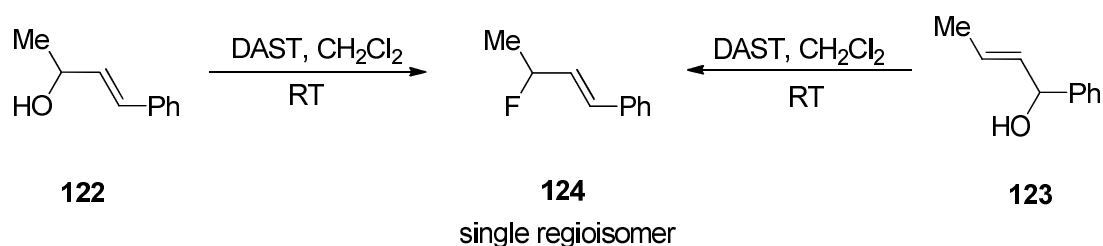
Scheme 2.9. Dehydroxyfluorination of **122** and **123** using DAST generated **124**, exclusively.[14]

However the formation of the most conjugated system is not always favoured. For instance dehydroxyfluorination of allylic alcohol **125** (Scheme 2.10) using DAST gave preferably the least conjugated secondary fluoride **126** over the more conjugated primary fluoride **127**.[14] In general the formation of secondary fluorides is preferred over primary fluorides, and this generally overcomes the formation of the most conjugated product,[14] with the exception of allylic alcohols conjugated with electron-withdrawing groups. For instance the DAST-mediated dehydroxyfluorination (Scheme 2.11) of **128** (R = Me) gave mainly the secondary fluoride **129** over the primary fluoride **130** (9:1 ratio), however dehydroxyfluorination of **131** (R = CO$_2$Me) using DAST (Scheme 2.11) generated a 1:4 ratio of primary fluoride **133** versus secondary fluoride **132**.[14]
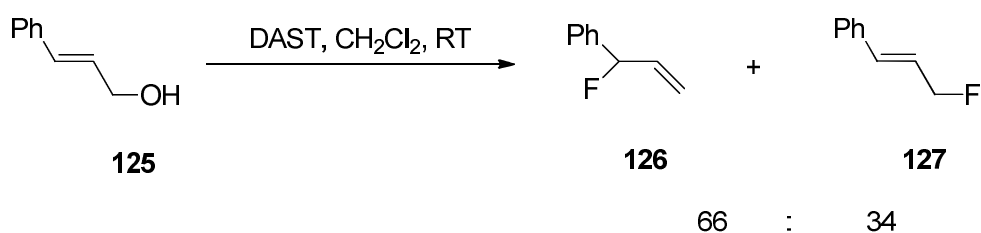
Scheme 2.10. Dehydroxyfluorination of **125** using DAST gave preferably **126** over **127**.[14]

Scheme 2.11. Dehydroxyfluorination of **128** and **131** using DAST.[14]

De Jonghe *et al.*[15] reported that dehydroxyfluorination of *N*-Boc-protected sphinghosine using DAST occurred with modest regio- and stereo- selectivity. For instance treatment of **134** with DAST at -78 °C gave allylic fluorides **135** and **136** and oxazolidinone **137** (Scheme 2.12). Treatment of *N*-acyl-protected allylic alcohol **138** generated allylic fluorides **139** and **140** as well as oxazoline **141** (Scheme 2.13). Both of the products generated by direct substitution of OH by F (**135** and **139**) were formed in favour of the *threo* diastereoisomer, however no preference was shown for products **136** and **140** generated by allylic transposition.

Scheme 2.12 Dehydroxyfluorination of **134** reported by De Jonghe *et al.*[15]
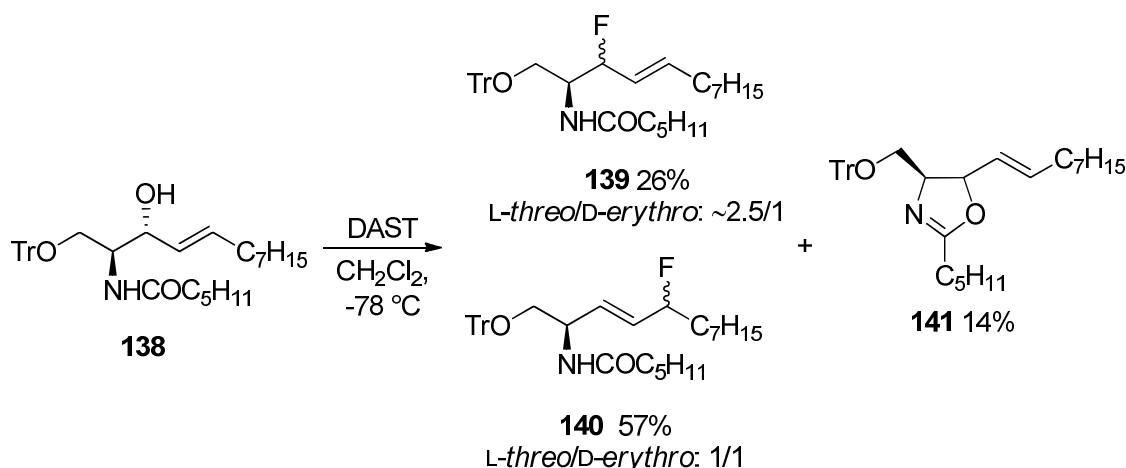
Scheme 2.13 Dehydroxyfluorination of **138** reported by De Jonghe *et al.*[15]

To date, only a few examples of the dehydroxyfluorination of allylic alcohols using reagents other than DAST have been reported. For instance, Middleton[13] reported a similar level of allylic transposition in comparison to that using DAST (Scheme 2.7), when **116** (Scheme 2.14) was subjected to reaction with Deoxofluor™.
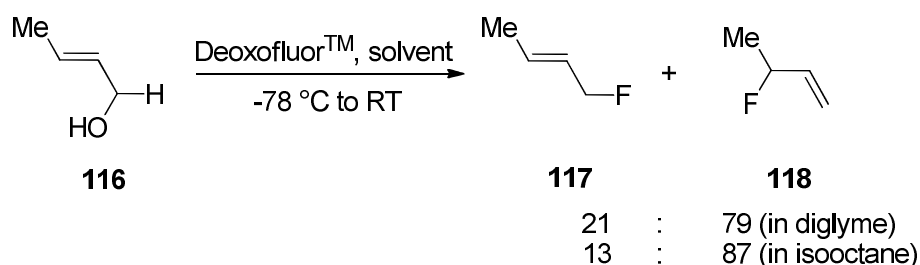
Scheme 2.14 Dehydroxyfluorination of **116** using Deoxofluor™ reported by Middleton.[13]

Reaction of **145** with Yarovenko's reagent (Scheme 2.15) generated a 1:4 mixture of regioisomers, **146** and **147** (**a** and **b**). The product **146**, generated by direct substitution by fluoride, was isolated as a single stereoisomer by column chromatography, and was assumed to be generated through an S$_N$2 reaction mechanism. The mixture **147** (**a** and **b**), generated by allylic substitution by fluoride, was isolated as a 1:1 diastereomeric mixture.[16]
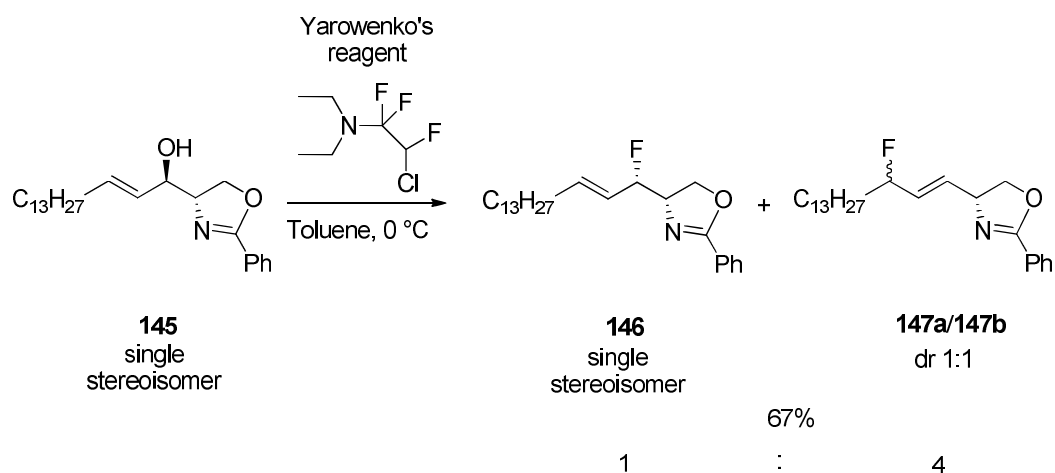
Scheme 2.15. Dehydroxyfluorination of **145** using Yarovenko's reagent.[16]

Dollé *et al.*[17] reported the preparation of **149** by fluorination of the tosylate **148** with TBAF (Scheme 2.16). Monosubstitution of the tosyl group by fluoride generated **149** in 30% yield.
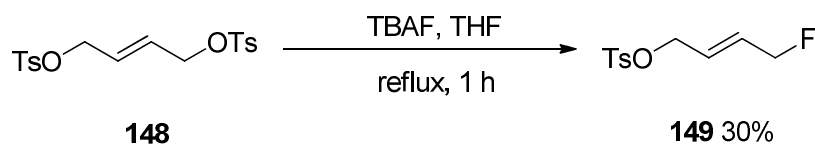
Scheme 2.16. Fluorination of the tosylate **148** by treatment with TBAF.[17]

2.2) Aims and objectives:

For the synthetic programme aimed at the synthesis of trifluorosugars, presented later in this thesis (Chapter 3), we required to fluorinate the diastereoisomers of allylic alcohol **155** (**a** and **b**) for conversion to **156** (**a** and **b**) as illustrated in Scheme 2.17. However fluorination can proceed either by direct substitution of OH for F to give **156**, or by an allylic substitution reaction to generate product **157**. Furthermore for each reaction course there are two stereochemical outcomes, thus diastereoisomers **155a** and **155b** can potentially generate a mixture of four products, **156a/156b**, and/or **157a/157b** (Scheme 2.17). However the

outcomes of the regio- and stereo- selectivity of fluorination of **155a** and **155b** may be influenced depending on the fluorination reagent used. In order to enhance direct substitution over allylic substitution, fluorination of **155a/155b** was screened with various reagents including DAST, Deoxofluor[TM], TFEDMA, Fluolead[TM] and perfluorobutansulfonyl fluoride (PBSF) in combination with Et$_3$N·3HF (Figure 2.5).[18]
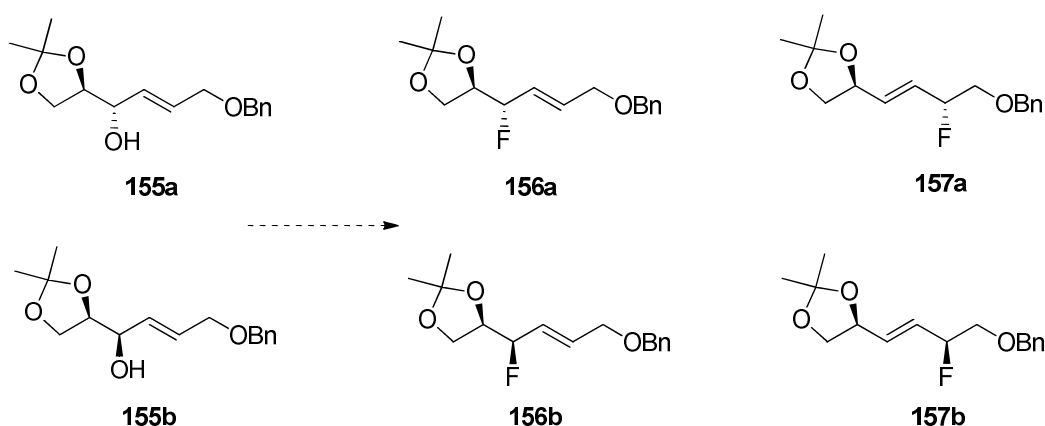
Scheme 2.17. Diastereoisomers **155a** and **155b** can generate four different isomeric products, as a result of dehydroxyfluorination progressing either by direct or allylic fluorination.
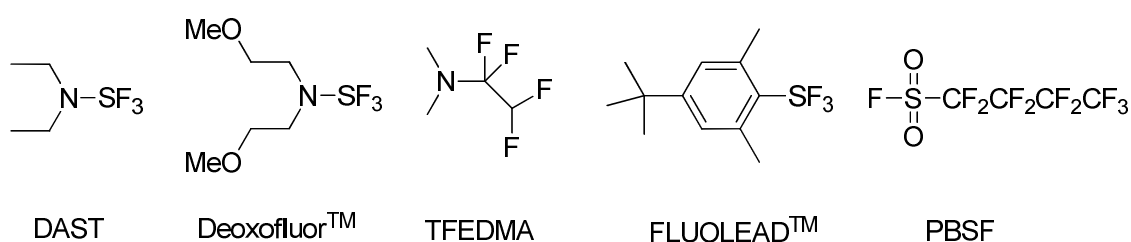
Figure 2.5. Dehydroxyfluorination reagents DAST, Deoxofluor[TM], TFEDMA, Fluolead[TM] and PBSF.

It was envisaged that starting materials **155a** and **155b** could be prepared in four steps following the synthetic route outlined in Scheme 2.18. Acetonide protection of D-mannitol **150** followed by oxidative cleavage of the resultant protected D-mannitol **151** would generate aldehyde **152**. Then an *anti* and a *syn* addition of aldehyde **152** to benzyl propargyl ether **153** would generate propargylic alcohols **154a** and **154b**, respectively. Reduction of propargylic alcohols **154a** (*anti*) and **154b** (*syn*) would furnish the desired substrates **155a** (*anti*) and **155b** (*syn*), respectively (Scheme 2.18).
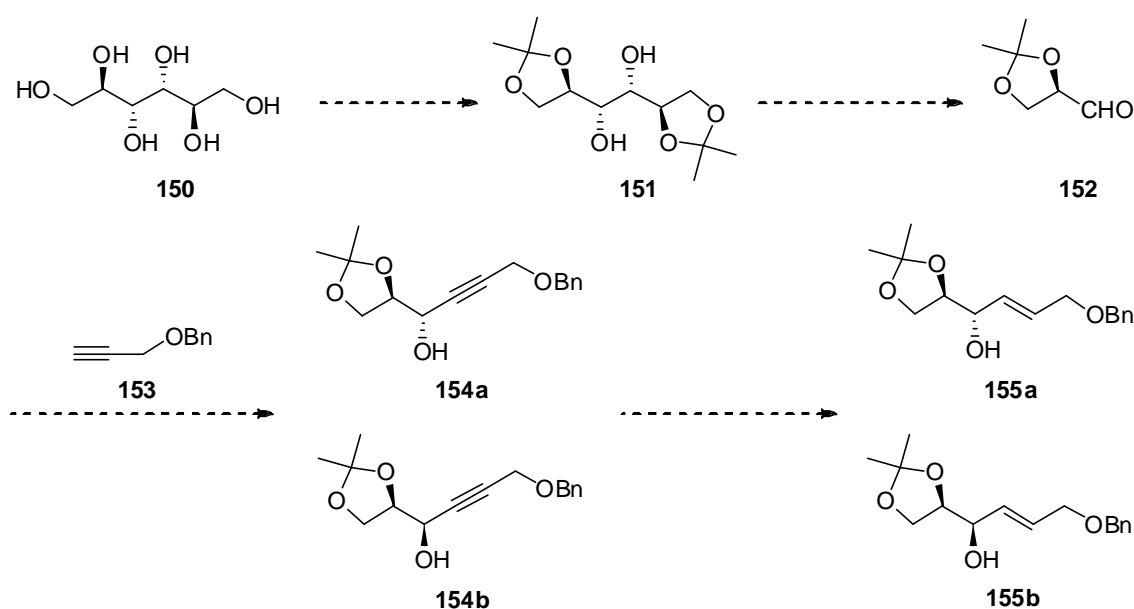
Scheme 2.18. Envisaged preparation of required substrates **155a** and **155b**.

2.3) Results and discussion:

2.3.1) Synthesis of 1,2:5,6-*di-O*-isopropylidene-D-mannitol 151:

1,2:5,6-*Di-O*-isopropylidene-D-mannitol **151** was prepared by reacting commercially available D-mannitol **150** with acetone and anhydrous zinc chloride (ZnCl$_2$) (Scheme 2.19),[19]

a method developed by Baer[20] and later optimised by Tipson and Cohen.[21] This procedure generated a complex mixture of mono-, di- and tri- acetals. Recrystallisation from a hot solution of CHCl$_3$/heptane gave **151** in 52% yield.
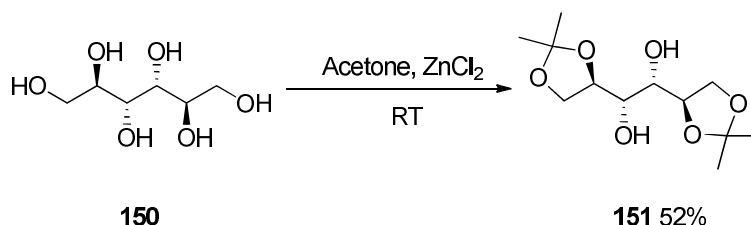
Scheme 2.19. Acetonide protection of D-mannitol **150** .[19-21]

Kuszmann *et al.*[19] reported that the acetonation procedures using 2-methoxypropene and *p*-toluenesulfonic acid in DMF, and the one using 2,2-dimethoxypropane, 1,2-dimethoxyethane and tin(II) chloride, give a more complex mixture of acetals than reported in the literature. Therefore these two methods were not attempted. Kuszmann *et al.*[19] also stated that that acetonation of D-mannitol **150** using acetone and zinc chloride (Scheme 2.19) is recommended because of easy isolation and high conversion to product **151**.

2.3.2) Preparation of protected glyceraldehyde 152:

Glycol cleavage of diol **151** using sodium metaperiodate (NaIO$_4$) in CH$_2$Cl$_2$ in the presence of NaHCO$_3$ (aq),[22,23] generated aldehyde **152** (Scheme 2.20) in 67% yield. The CH$_2$Cl$_2$ solvent was removed by distillation at atmospheric pressure, and aldehyde **152** was then purified by fractional distillation through a Vigreux column. The $[\alpha]_D$ of **152**, after distillation, was found to be consistent with literature values, and was a good indication that racemisation had not occurred during the distillation process.
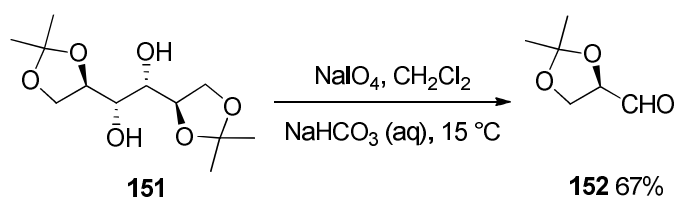
Scheme 2.20. Glycol cleavage of 151.[22]

Protected glyceraldehyde 152 is volatile and unstable and rapidly undergoes polymerisation at RT or lower.[22] However the polymer can be cracked upon redistillation. Furthermore it is reported that the enantiopurity of 152 is unaffected by repeated pyrolysis of the polymer and distillation.[22]

2.3.3) Preparation of benzyl propargyl ether 153:

Benzyl propargyl ether 153 was prepared in good yield starting from commercially available propargyl alcohol and benzyl bromide upon deprotonation of the alcohol with NaH in DMF (Scheme 2.21).[24]
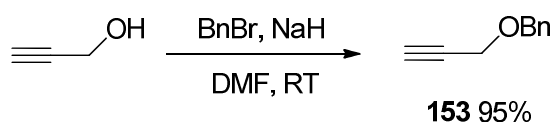
Scheme 2.21. Synthesis of benzyl propargyl ether 153.[24]

2.3.4) Preparation of propargylic alcohols 154a and 154b:

Mixtures of diastereoisomers 154a and 154b (Scheme 2.18) were prepared but with different diastereoisomeric biases. The *syn* addition of lithium acetylide derived from 153 to freshly prepared aldehyde 152 was first carried out under conditions planned to promote chelation-

control[25] as illustrated in Scheme 2.22. This generated **154b** as the major isomer, but with very low diastereoselectivity (9% de, determined by chiral GC-FID). The *syn* addition is consistent with a chelation transition state in which nucleophilic attack[26] occurs from the less hindered face as indicated by the arrow in Figure 2.6.
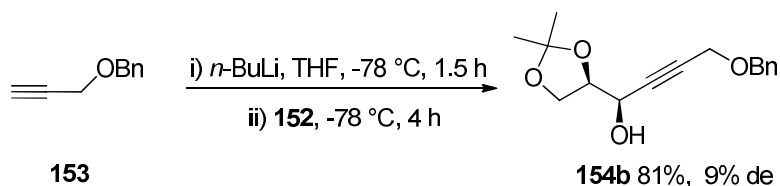
Scheme 2.22. *Syn* addition of lithium acetylide of **153** to freshly prepared aldehyde **152**.[25]
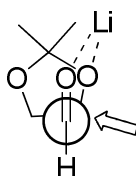
Figure 2.6. Chelation transition state leading preferentially to **154b**.[26]

Attempts to increase the diastereomeric excess (% de) of the *syn* adduct **154b** by following a *syn*-selective addition in the presence of anhydrous zinc bromide (ZnBr$_2$), described by Mead,[27] was also explored but without success (Scheme 2.23). Slow addition of a solution of *n*-BuLi in hexane *via* cannula, to a solution of **153** in dry diethyl ether at -78 °C, resulted in the formation of a precipitate. The solubility of *n*-BuLi was not improved even when the addition was performed at 0 °C and using a larger amount of diethyl ether. A lack of solubility of anhydrous ZnBr$_2$ in diethyl ether was also observed. Therefore *syn*-selective addition described by Mead[27] was not further attempted.
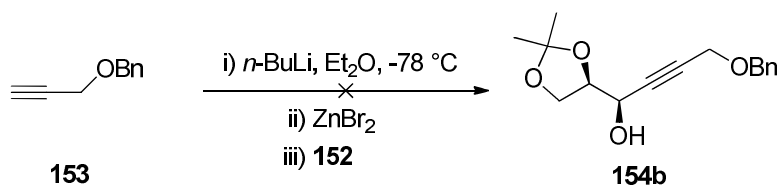
Scheme 2.23. Attempt to improve the % de of **154b** using ZnCl$_2$.[27]

An analogous reaction was carried out under non-chelation conditions using titanium tri-isopropoxychloride, to favour *anti*-selective addition[28] as illustrated in Scheme 2.24. This gave **154a** in a much higher diastereoisomeric excess (62% de, determined by chiral GC-FID). The *anti* addition is consistent with a non-chelation transition state in which nucleophilic attack[28] occurs from the less hindered face as indicated by the arrow in Figure 2.7.
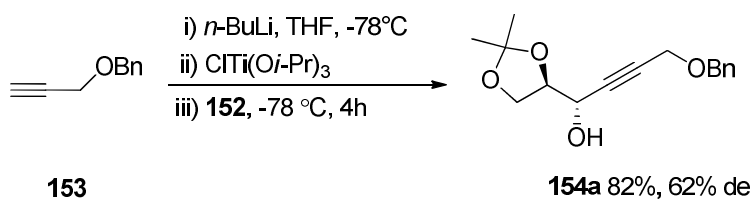
Scheme 2.24. *Anti* addition of lithium acetylide of **153** to freshly prepared aldehyde **152**.[28]
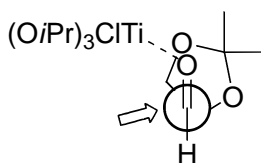
Figure 2.7. Non-chelation transition state leading preferentially to **154a**.[28]

The relative stereochemistry of diastereoisomers **154a** and **154b** was assigned by preparing the dinitrobenzoyl ester derivatives as illustrated in Scheme 2.25. Treatment of **154a** (62% de) with 3,5-dinitrobenzoyl chloride in pyridine generated a mixture of diastereoisomers **158** (**a** and **b**) as a crystalline solid. The esters were recrystallised from absolute ethanol, and the

relative stereochemistry of the major isomer **158a**, originating from **154a**, was determined by X-ray structure analysis (Figure 2.8). The corresponding X-ray structure revealed an *anti* relationship between the C-O bond of the ester group and the vicinal acetonide ether C-O bond in stereoisomer **158a**.
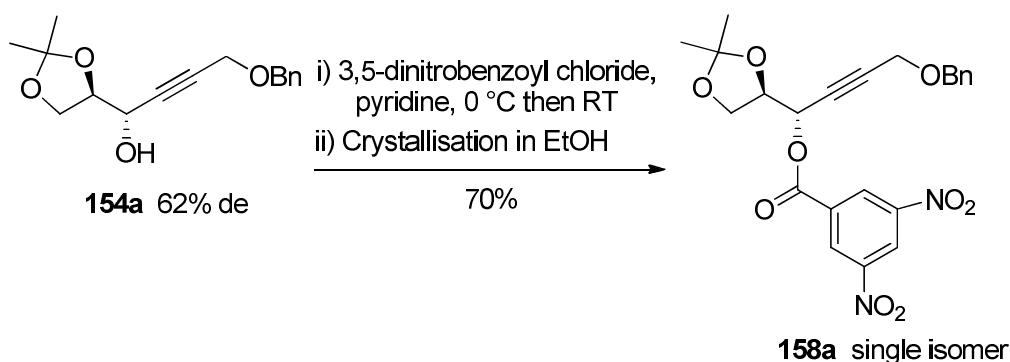
Scheme 2.25. Preparation of the dinitrobenzoyl ester derivative **158a** (single isomer).
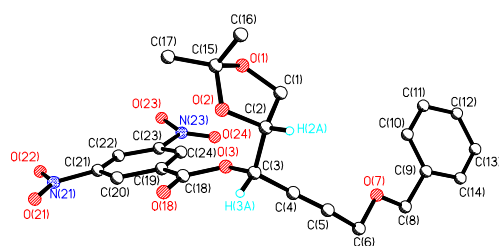
Figure 2.8. X-Ray structure of **158a**.

2.3.5) Preparation of allylic alcohols 155a and 155b:

The diastereoisomeric mixtures of **154a**/**154b** were then transformed separately by propargylic reduction to the corresponding allylic alcohols **155a**/**155b** using $LiAlH_4$[29] as illustrated in Scheme 2.26. These allylic alcohol reductions gave exclusively the *E*-olefins, as expected. Although after 2 h, t.l.c analysis indicated complete consumption of the starting

material, allylic alcohols **155a** and **155b** were obtained in only poor yield (respectively 55% and 45%) after purification by column chromatography.
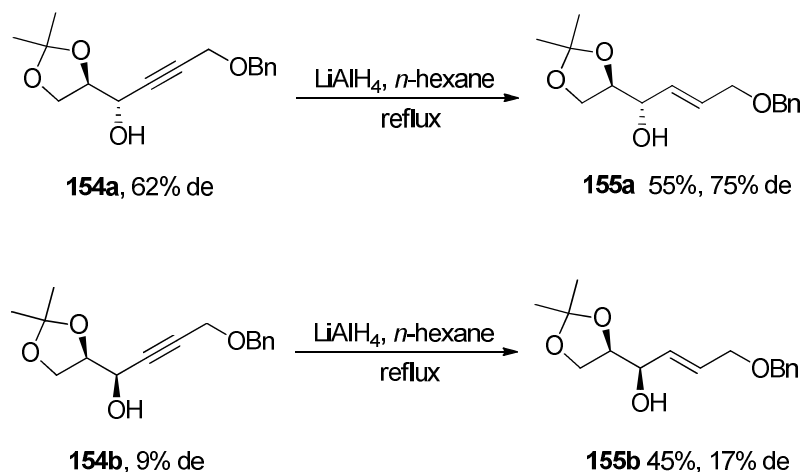
Scheme 2.26. Reduction of propargylic alcohols **154a** and **154b** by using LiAlH$_4$ in *n*-hexane.[29]

When reduction was initially performed by treating **154a/154b** with 2 equiv. of LiAlH$_4$ in THF, t.l.c analysis showed that the allylic alcohols were formed together with a large amount of an unidentified side-product. Replacement of THF with the less polar solvent hexane, and using only 1.3 equiv. of LiAlH$_4$, generated less side-product. Furthermore the yield of allylic alcohol formation was notably improved by replacing LiAlH$_4$ with Red-Al® (Figure 2.9).[30] Slow addition of 2 equiv. of Red-Al® (70% wt. in toluene) to a solution of **154a/154b** in THF at 0 °C generated **155a/155b** in 90-95% yield, and this became the method of choice.
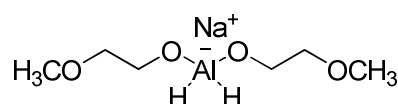
Figure 2.9. Structure of Red-Al®.[30]

2.3.6) Dehydroxyfluorination attempts of allylic alcohols 155a/155b:

With the allylic alcohol diastereomeric mixtures **155a**/**155b** in hand, the fluorination step was explored. Accordingly, dehydroxyfluorination was conducted by treating the product mixture **155a**/**155b** with 1.5 equiv. of Deoxofluor[TM] at RT for 1 h. The reaction was poorly regio- and stereo- selective as it generated a mixture of four fluorinated products. The ^{19}F{^{1}H}-NMR of the product mixture had four signals at -183.0, -183.4, -184.1 and -187.5 ppm (Figure 2.10).
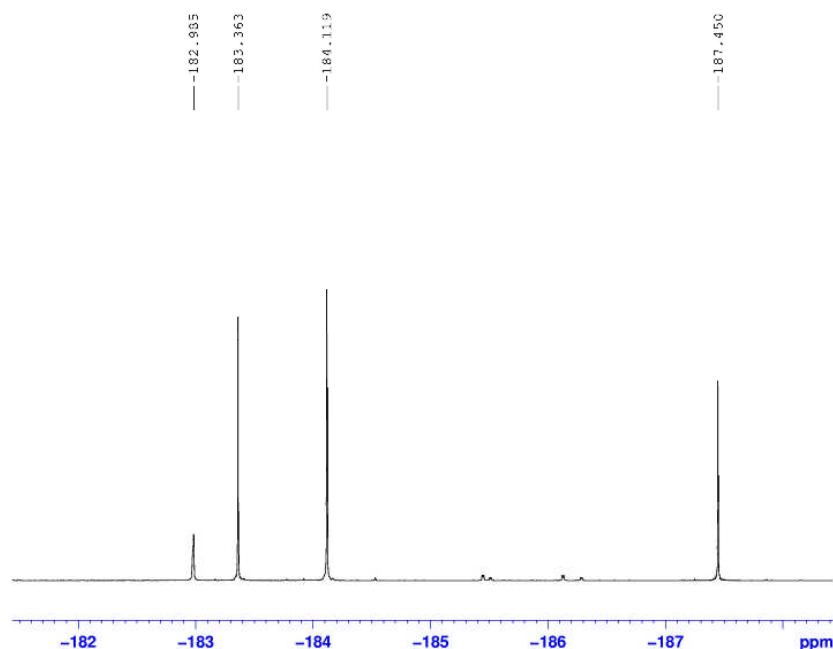
Figure 2.10. ^{19}F{^{1}H}-NMR spectrum of the product mixture after dehydroxyfluorination of **155a**/**155b** .

Identification of the individual fluorinated products was required. T.l.c analysis of the product mixture showed two adjacent spots of unequal intensity. Two rounds of column chromatography successfully separated these fractions from any unreacted starting material. Subsequent NMR analysis and mass spectrometry indicated that the minor fraction was **156a** generated by direct substitution of OH by F, whereas the major fraction contained both **157a**/**157b**, diastereoisomers generated by allylic substitution of OH by F. Diastereoisomer

156b, generated by direct substitution of OH by F, was also present in this major fraction (Scheme 2.27). Compounds **156b**, **157a** and **157b** could not be further separated by chromatography.

155a/155b

156a
minor fraction
(single isomer after
column chromatography)

156b   **157a**, **157b**

major fraction
(inseparable mixture after
column chromatography)
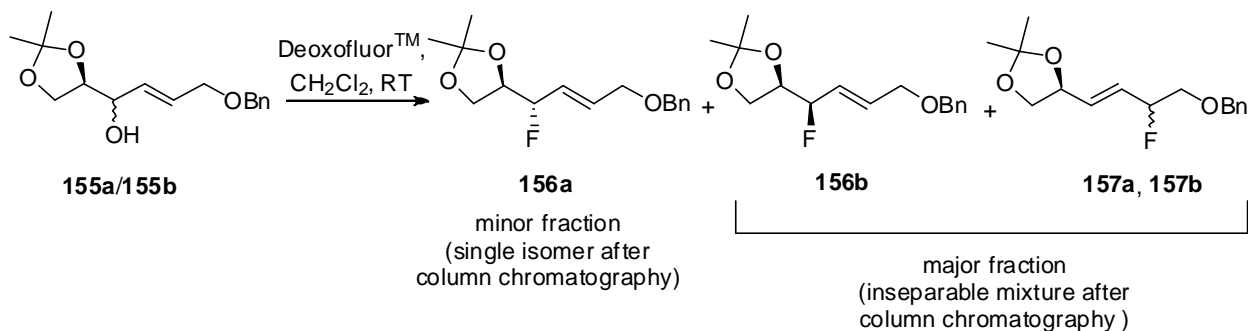
Scheme 2.27. Fluorination of allylic alcohols **155a**/**155b** gave **156a** and an inseparable mixture of isomers **156b**/**157a**/**157b**.

^{1}H-NMR analysis of **156a** (Figure 2.11) showed signals at 4.16 ppm and 4.88 ppm that were assigned to protons H^1 and H^2 respectively of **156a**. The ^{1}H- ^{1}H COSY spectrum (Figure 2.12) has dashed lines highlighting $^3J_{\text{H1-H2}}$ crosspeaks. This established that **156a** resulted from the direct substitution of OH by F. The ^{19}F{^{1}H}-NMR spectrum (Figure 2.13) of **156a** has a signal at -187.9 ppm corresponding to a single fluorine.
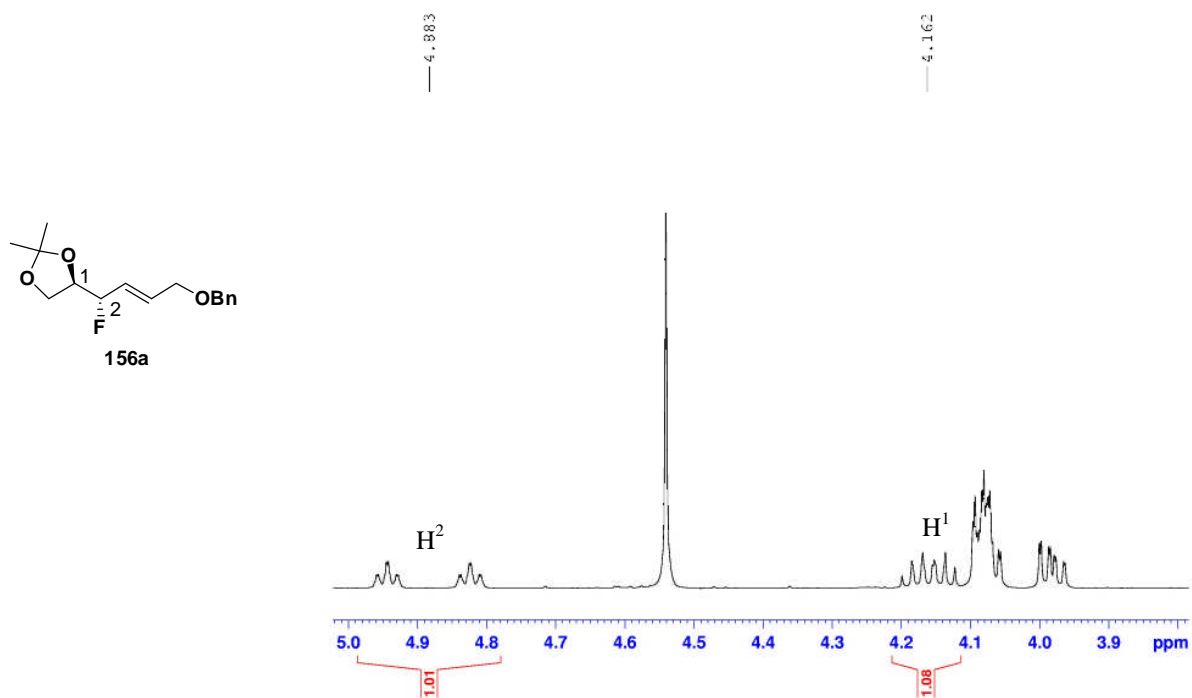
Figure 2.11. ^{1}H-NMR spectrum of **156a** highlighting H[1] and H[2] signals.
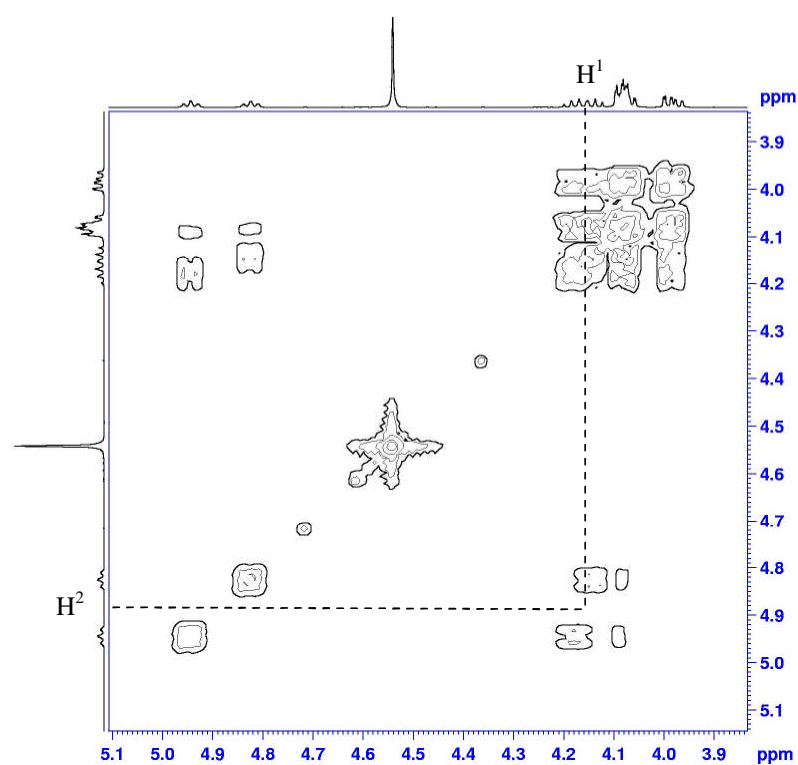
Figure 2.12. ^{1}H-^{1}H COSY-NMR spectrum of **156a** showing $^3J_{H1\text{-}H2}$ crosspeaks .
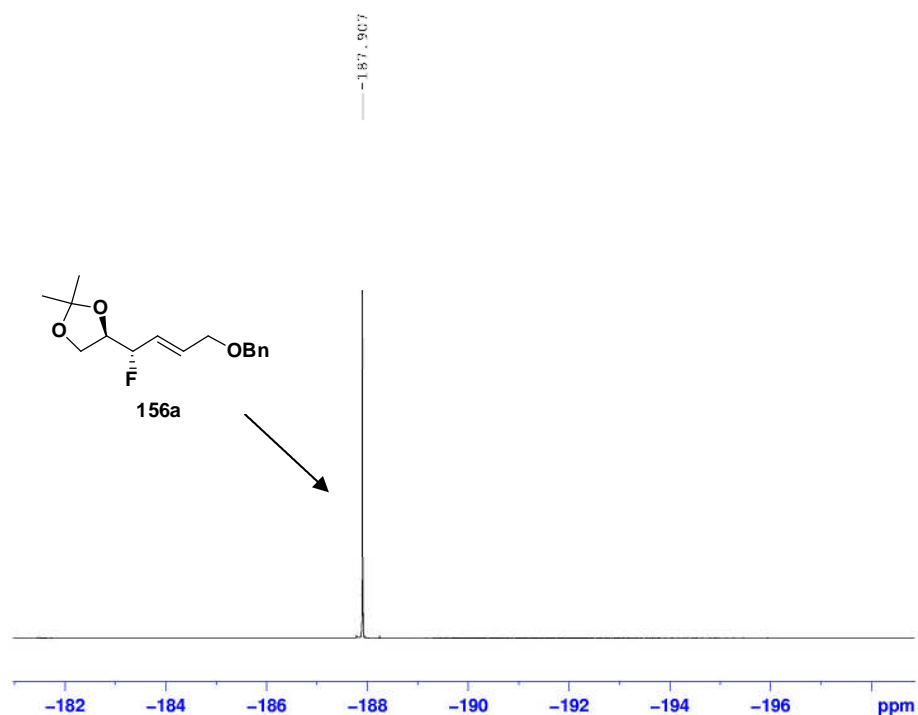
Figure 2.13. $^{19}F\{^1H\}$-NMR spectrum of **156a**.

The ^{1}H-NMR spectrum (Figure 2.14) of the major fraction is clearly more complex, and has signals at 5.12 ppm and 4.54 ppm that are assigned to protons H^4 and H^1 respectively in the product mixture of **157a**/**157b**. The signal at 4.87 ppm is assigned to proton $H^{2'}$ in product **156b**. The ^{1}H-^{1}H COSY spectrum (Figure 2.15) has dashed lines highlighting $^3J_{H1\text{-}H2}$, $^3J_{H3\text{-}H4}$ crosspeaks but significantly there are no crosspeaks between H^4 and H^1. This confirms that **157a/157b** are products resulting from the allylic substitution of OH by F.
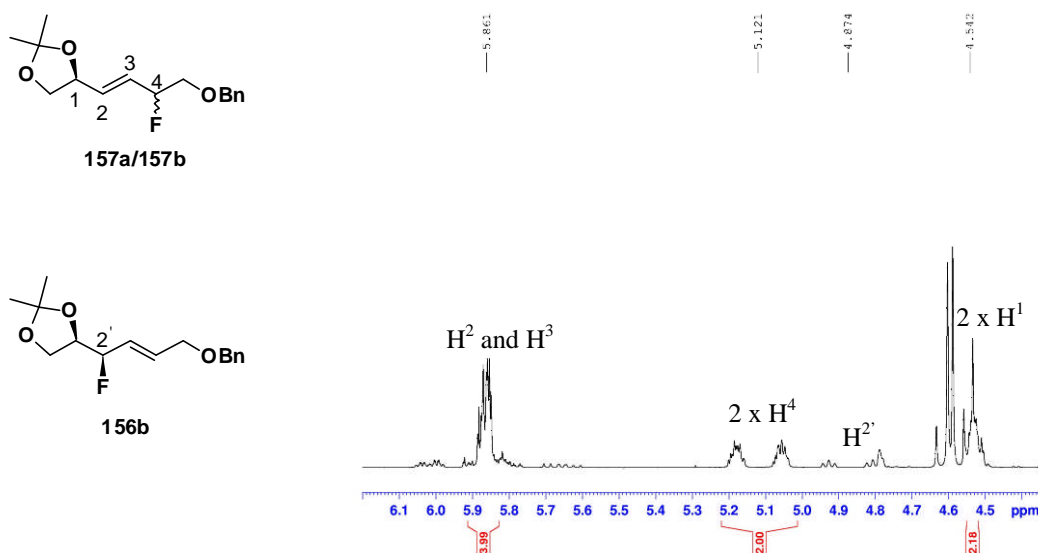
Figure 2.14. [superscript]1[/superscript]H-NMR spectrum of the inseparable mixture of **156b**/**157a**/**157b**.
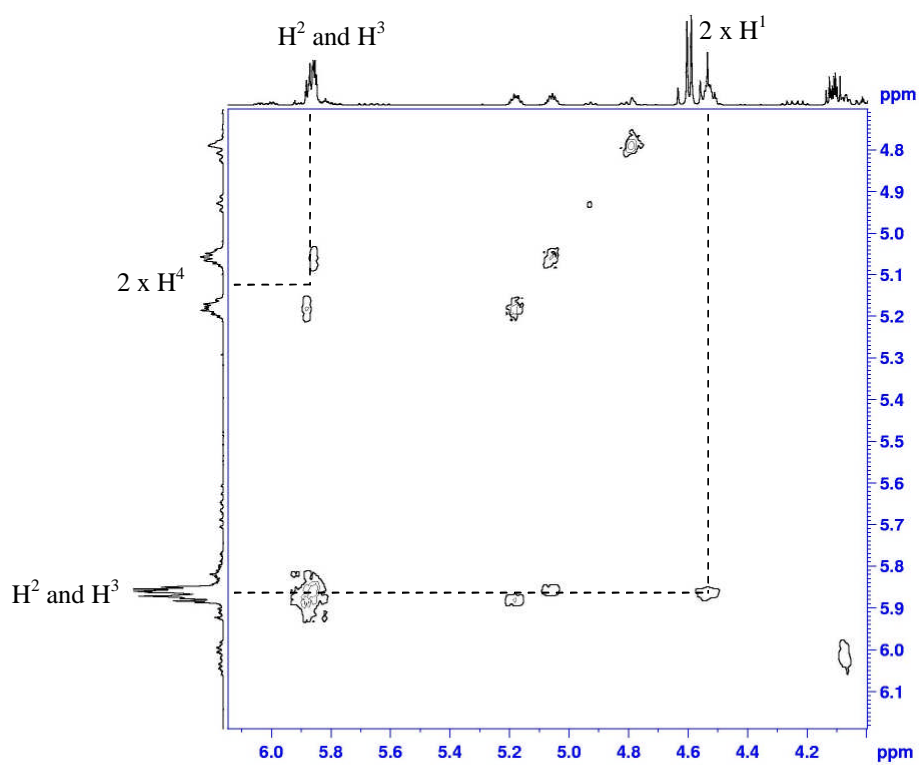
Figure 2.15. [superscript]1[/superscript]H-[superscript]1[/superscript]H COSY-NMR spectrum of the inseparable mixture of **156b**/**157a**/**157b**.

68

Analyisis of the ^{19}F-HMQC spectrum of the inseparable mixture **156b**/**157a**/**157b** (Figure 2.16) has dashed lines highlighting $^{2}J_{H4\text{-}F}$ and $^{2}J_{H2'\text{-}F}$ crosspeaks which allow individual assignment of the ^{19}F resonances to products **156b**, **157a** and **157b**. The ^{19}F{^{1}H}-NMR spectrum (Figure 2.17) of the minor fraction has signals at -183.0 ppm, -183.4 ppm and -184.1 ppm corresponding respectively to product **156b**, **157a** and **157b**.
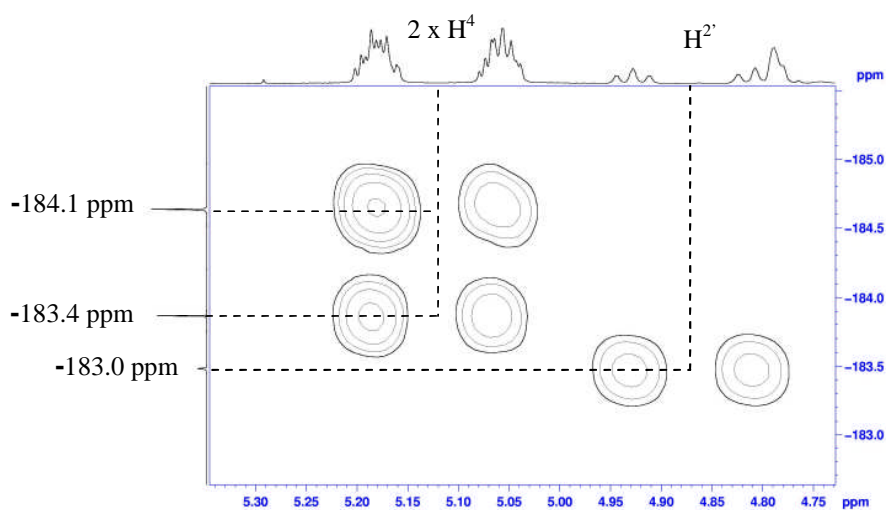
Figure 2.16. ^{19}F-HMQC spectrum of the inseparable mixture of **156b**/**157a**/**157b**.
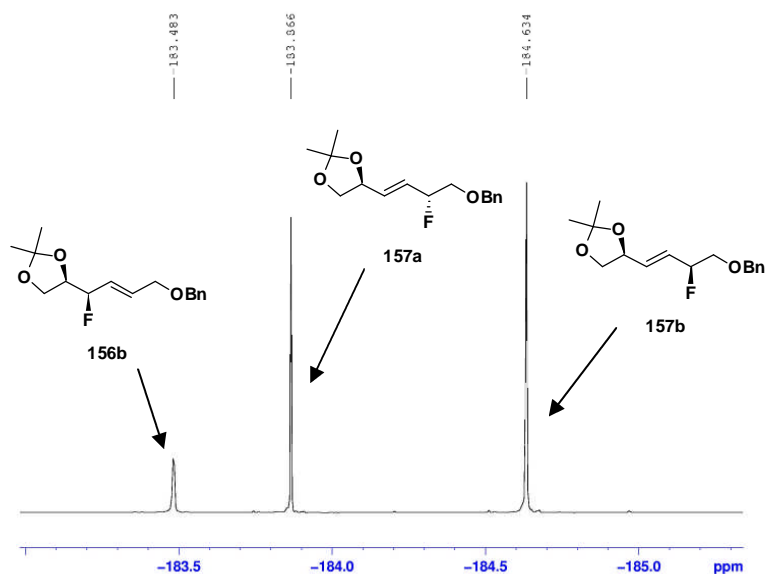
Figure 2.17. ^{19}F{^{1}H}-NMR spectrum of the inseparable mixture of **156a**/**157a**/**157b**.

The influence of the reagent (Figure 2.18) was investigated in the dehydroxyfluorination of **155a/155b.** The resultant ratios of products **156a**/**156b** and **157a**/**157b** were determined by ^{19}F-NMR in the product mixture and the results are summarised in Scheme 2.28 and Table 2.1. The consumption of starting material was followed by t.l.c. Reactions using Fluolead[TM] and TFEDMA were performed in polyethylene flasks as these reagents were found to etch the glass. Reactions employing Deoxofluor[TM] and DAST were conveniently carried out in standard laboratory glassware. Furthermore all of the reactions (see Paragraph 5.3, Chapter 5) were performed under anhydrous conditions to avoid the *in situ* generation of HF. All reactions gave very modest regio- and stereo- selectivity. A very low conversion was obtained at -78°C with DAST, Deoxofluor[TM] and TFEDMA, and conversion was only moderately improved at 0°C. Thus for these three reagents, warmer reactions temperatures were necessary (see conditions in Table 2.1). Although the yields were not determined, the reaction of Fluolead[TM] at 0 ºC proved efficient in terms of conversion, but gave a similar overall product profile to the other more established reagents that were investigated.
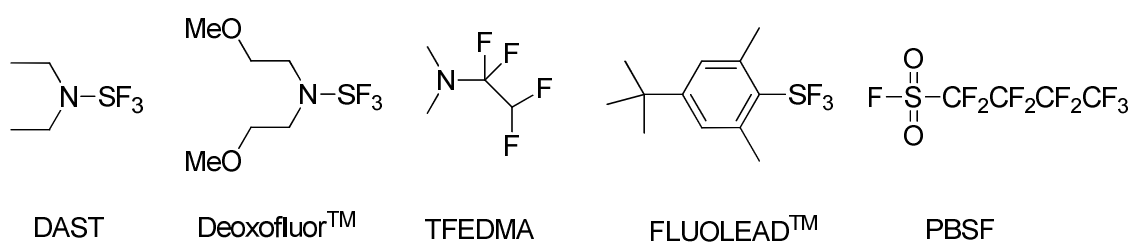
Figure 2.18. Dehydroxyfluorination reagents DAST, Deoxofluor[TM], TFEDMA, Fluolead[TM] and PBSF.
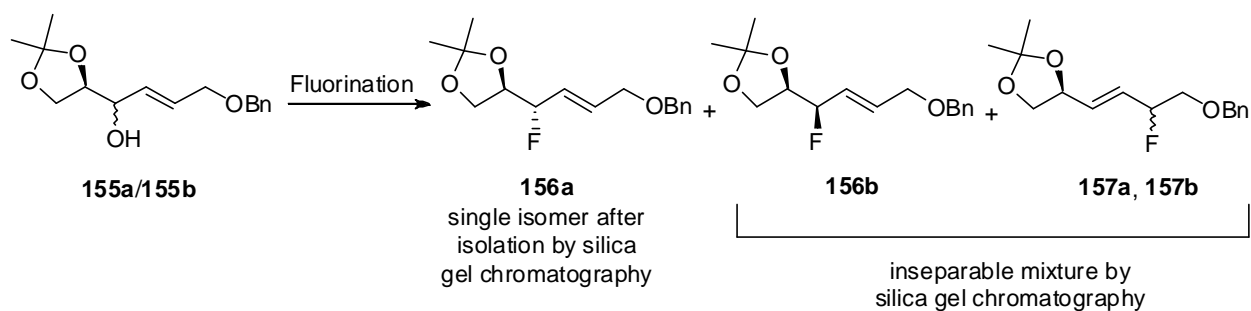
Scheme 2.28. Fluorination of allylic alcohol **155a/155b** gave **156a** and the inseparable mixture of isomers **156b/157a/157b**.

Fluorinating agent	Temp.	Major allylic alcohol substrate, de %	Ratio[a] 156a/156b/157a/157b	Yield, %[b]	
				156a	(156b/157a/157b)
TFEDMA	RT	**155a**, 75%	2.0/1.0/2.9/4.2	11	44
DAST	RT	**155a**, 75%	1.5/1.0/2.2/2.7	11	45
Deoxofluor[TM]	55 °C	**155a**, 75%	1.2/1.0/1.7/3.7	9	48
TFEDMA	RT	**155b**, 17%	2.5/1.0/3.7/3.9	13	46
DAST	RT	**155b**, 17%	1.5/1.0/2.1/2.2	12	44
Deoxofluor[TM]	55 °C	**155b**, 17%	1.5/1.0/2.6/2.7	10	44
Fluolead[TM]	0 °C[c]	**155a/155b** dr 1:1	1.9/1.0/2.6/2.8	ND[c]	ND[c]

[a] Ratio in the crude mixture determined by ^{19}F-NMR.

[b] Determined after two rounds of chromatography.

[c] ND-not determined. Product ratios determined by ^{19}F-NMR only, although the conversion was high.

Table 2.1 Influence of the dehydroxyfluorinating agent on direct or allylic fluorination of **155a**/**155b** in CH_2Cl_2 as a solvent.

The fluorination of **155a**/**155b** with 1.1 equiv. of perfluorobutansulfonyl fluoride (PBSF) in combination with Et$_3$N·3HF (1.1 equiv.) and 3.3 equiv. of Et$_3$N (3.3 equiv.)[18] was found to be very unreactive. T.l.c analysis indicated a very low conversion even after prolonged

heating and the use of a large excess of reagent. Therefore this reagent was not explored further. The relative stereochemistry of products **156a**, **156b**, **157a** and **157b** required to be assigned. The configuration of isomer **156a** was determined after conducting a Sharpless dihydroxylation.[31] Accordingly **156a** as a single stereoisomer was reacted with AD-mix-*β* in *t*-BuOH/H$_2$O (Scheme 2.29) to favour the formation of diol **159**. The reaction was stirred for 3 days at RT. ^{19}F{^{1}H}-NMR analysis of the product mixture showed the presence of three fluorinated products, together with a significant amount of unreacted starting material. The major fluorinated product was isolated by column chromatography as a white solid (single stereoisomer). Recrystallisation from diethyl ether afforded **159** as a crystalline compound suitable for X-ray structure analysis. The resultant structure (Figure 2.19) clearly shows that there is an *anti* relationship between the C-F bond and the vicinal acetonide ether C-O bond in stereoisomer **159**.
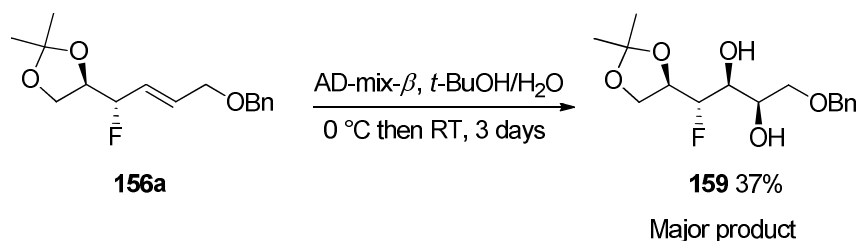
Scheme 2.29. Synthesis of **159** using a Sharpless dihydroxylation reaction.[31]
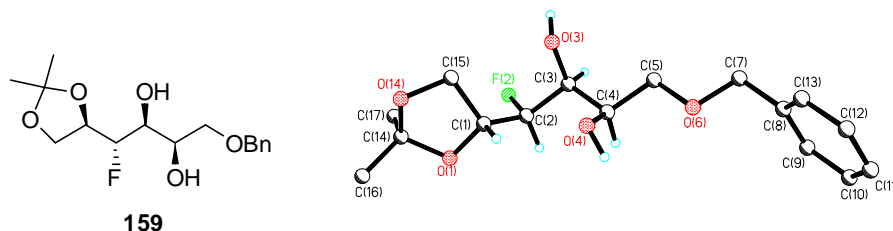
Figure 2.19. X-ray structure of **159** used to determine the relative stereochemistry of **156a**.

To complete the stereochemical analysis of the fluorination reaction of **155a**/**155b**, the diastereoisomer preference for the allylic substituted products **157a**/**157b** was also explored. A TFEDMA reaction on **155a** (75% de) generated a diastereoisomeric mixture of **156b**/**157a**/**157b** in the ratio 0.3/0.7/1.0 (determined by ^{19}F-NMR). The relative stereochemistry of **157a**/**157b** was determined after a Sharpless dihydroxylation[31] of the inseparable mixture of **156b**/**157a**/**157b**. Accordingly the mixture of **156b**/**157a**/**157b** was treated with AD-mix-β in t-BuOH/H$_2$O to favour the formation of a mixture of diols **160a**/**160b** (Scheme 2.30).
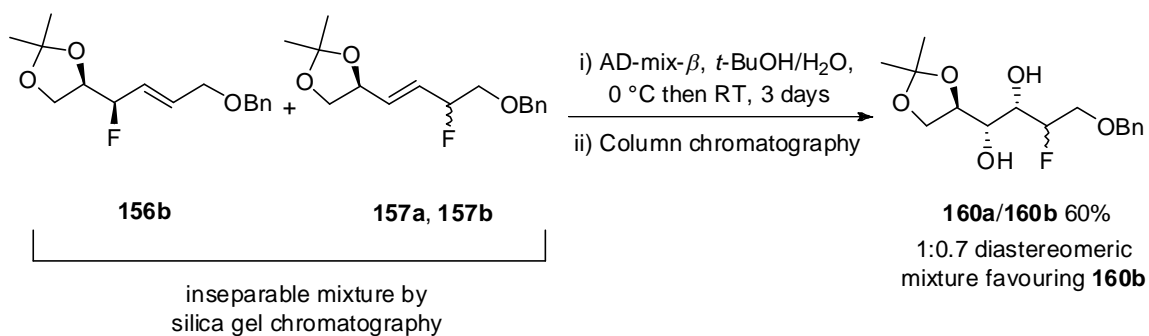
Scheme 2.30. Preparation of the mixture of diols **160a**/**160b**.

^{19}F{^{1}H}-NMR of the product mixture indicated that the Sharpless dihydroxylation had proceeded with high diastereoselectivity. Chromatography gave a 1:0.7 diastereoisomeric mixture of diols favouring **160b**.[32] Separation of the corresponding diol derived from **156b** was unsuccessful. The vicinal diols **160a** and **160b** were then converted to their corresponding cyclic sulfates using the Sharpless protocol (Scheme 2.31).[33] Thus **160b**/**160a** (dr 1:0.7) was treated with SOCl$_2$ and pyridine to generate a mixture of cyclic sulfites **161**. The resulting mixture of cyclic sulfites **161** was directly oxidised without isolation.

Oxidation used RuO_4 ($NaIO_4$ and catalytic amount of $RuCl_3$) in $MeCN$-H_2O generated the desired cyclic sulfates **162b** and **162a** in 1:0.7 diastereomeric ratio. The two diastereoisomers were successfully separated by flash chromatography (**162b** in 61% yield, **162a** in 27% yield).
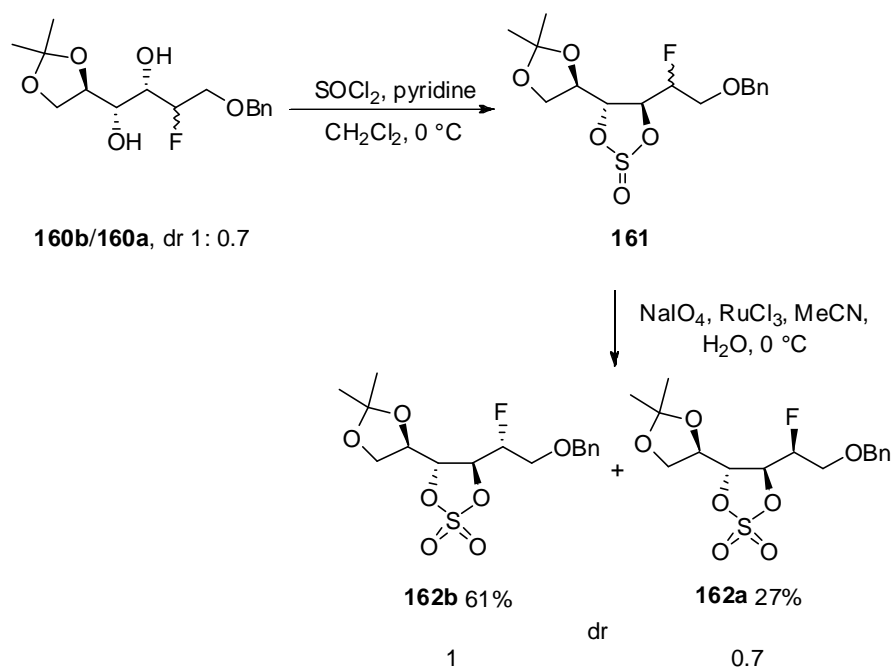
Scheme 2.31. Preparation of cyclic sulfates **162a** and **162b** by the Sharpless protocol.[33]

The minor isomer **162a** was crystallised in Et_2O and a suitable crystal was subjected to X-ray structure analysis. The corresponding X-ray derived structure is illustrated in Figure 2.20 and confirms the stereochemistry as shown. By inference the major isomer formed in the allylic fluorination reaction of **155a** (*de* 75%) is **157b** (Figure 2.21).
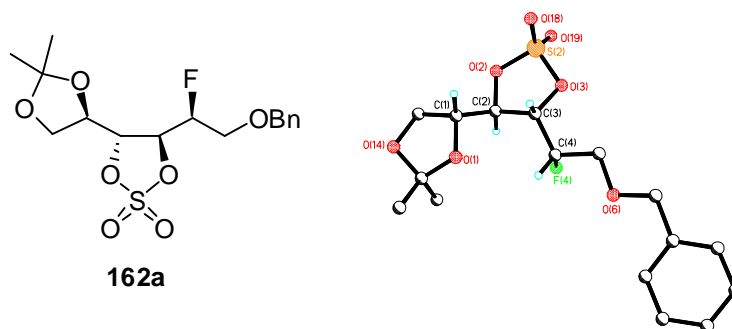
Figure 2.20. X-ray structure establishes the absolute configuration of **162a**.

74
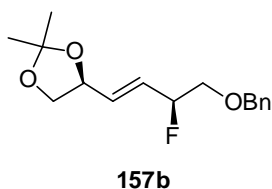
Figure 2.21. Structure of major isomer formed in the allylic fluorination reaction of **155a** (*de* 75%)

2.4) Conclusions:

In this Chapter the dehydroxyfluorination on substrate **155a**/**155b** was investigated with a range of reagents, which can proceed either by direct or allylic substitution. The stereochemical preference of direct substitution by fluoride and allylic fluorination were assessed by determining X-ray structures of suitable product derivatives. None of the reagents proved to be regio- or stereo- selective, however in all of the reactions the allylic fluorination products **157** (**a** and **b**) prevailed over the direct fluorination products **156** (**a** and **b**). In the case of direct substitution, the major isomer was **156a** for all of the reagents explored in spite of the stereochemical bias of both starting diastereoisomer mixtures of **155a**/**155b**. Furthermore **155a** (75% de) generates a fluorinated product with retention of configuration (**156a**), therefore an S_N1 pathway is proposed for the dehydroxyfluorination of **155a**/**155b**.

Most likely the reaction proceeds *via* a carbocation intermediate (shown in Scheme 2.32 for the reaction using TFEDMA), stabilised by transposition of the allylic double bond, which favours the formation of **157a**/**157b** over **156a**/**156b**. Furthermore, steric and electronic effects related to the acetonide and its ether oxygen induces fluoride attack to a specific face of the carbocation intermediate, favouring the formation of **156a** over **156b**. Allylic fluorination displayed a much reduced facial bias consistent with the proposed mechanistic pathway, thus the formation of **157b** is favoured over **157a**.
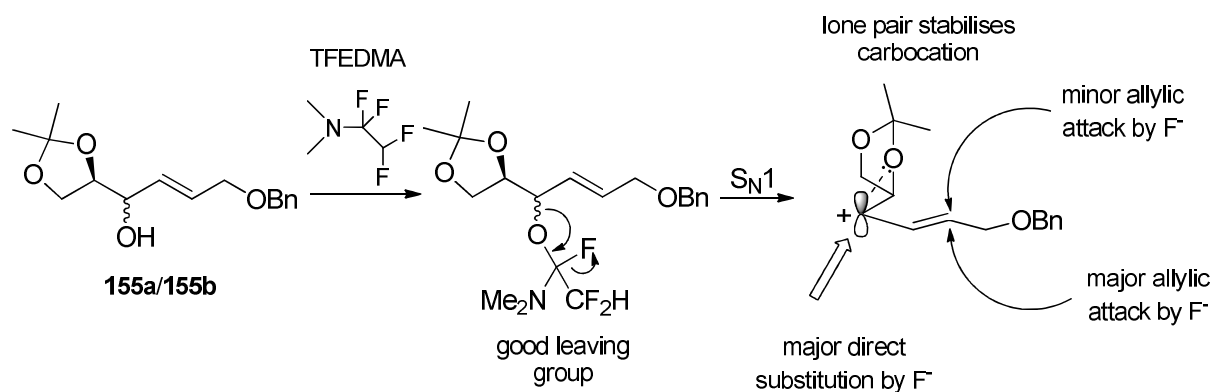
Scheme 2.32. Proposed mechanism for the dehydroxyfluorination of allylic alcohol **155a/155b**.

Product **156a** was used in the synthesis of trifluoro D-hexose glucose analogue **193** and trifluoro D-hexose altrose analogue **216** (Scheme 2.33), and this is discussed in Chapter 3.
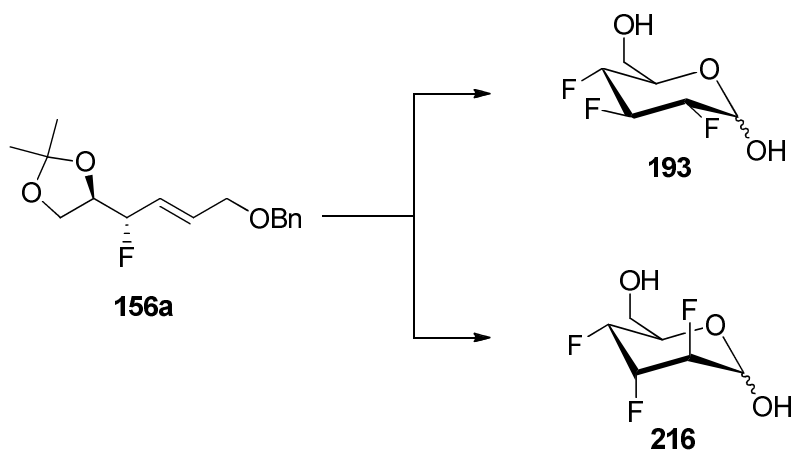
Scheme 2.33. Allylic fluoride **156a** is the key intermediate for the synthesis of trifluoro D-glucose analogue **193** and trifluoro D-altrose analogue **216**.

References Chapter 2

[1] M. C. Pacheco, S. Purser, V. Gouverneur, *Chem. Rev*., **108**, 1943-1981.

[2] S. Peleg, A. Ismail, M. R. Uskoković, Z. Avnur, *J. Cell. Biochem*., 2003, **88**, 267-273.

[3] A. Ismail, C. V. Nguyen, A. Ahene, J. C. Fleet, M. R. Uskoković, S. Peleg, *Mol. Endocrinol*., 2004, **18**, 874-887.

[4] Y. Matsamura, T. Nakano, T. Asai, Y. Morizawa, *ACS Symp. Ser*., 1996, **639**, 83-94.

[5] K. Yamamoto, T. Itoh, D. Abe, M. Shimizu, T. Kanda, T. Koyama, M. Nishikawa, T. Tamai, H. Ooizumi, S. Yamada, *Bioorg. Med. Chem. Lett*., 2005, **15**, 517-522.

[6] D. O'Hagan, *J. Fluorine Chem*., 2010, *in press*.

[7] J. Filmon, D. Grée, R. Grée, *J. Fluorine Chem*., 2001, **107**, 271-273.

[8] S. M. Graham, G. D. Prestwich, *J. Org. Chem*., 1994, **59**, 2956-2966.

[9] F. Dollé, P. Emond, S. Mavel, S. Demphel, F. Hinnen, Z. Mincheva, W. Saba, H. Valette, S. Chalon, C. Halldin, J. Helfenbein, J. Legaillard, J. -C. Madelmont, J. -B. Deloye, M. Bottlaender, D. Guilloteau, *Bioorg. Med. Chem*., 2006, **14**, 1115-1125.

[10] F. A. Davis, P. V. N. Kasu, G. Sundarababu, H. Qi, *J. Org. Chem*., 1997, **62**, 7546-7547.

[11] N. Minakawa, N. Kojima, A, Matsuda, *J. Org. Chem*., 1999, **64**, 7158-7172.

[12] L. Hunter, D. O'Hagan, A. M. Z. Slawin, *J. Am. Chem. Soc*., 2006, **128**, 16422-16423.

[13] W. J. Middleton, J. *Org. Chem*., 1975, **40**, 574-578.

[14] A. Boukerb, D. Grée, M. Laabassi, R. Grée, *J. Fluorine Chem*., 1998, **88**, 23-27.

[15] S. De Jonghe, I. V. Overmeire, S. Poulton, C. Hendrix, R. Busson, S. V. Calenbergh, D. De Keukeleire, S. Spiegel, P. Herdewijn, *Bioorg. Med. Chem. Lett*., 1999, **9**, 3175-3180.

[16] A. P. Kozikowsky, J. –P. Wu, *Tetrahedron Lett*., 1990, **31**, 4309-4312.

[17] F. Dollé, F. Hinnen, P. Emond, S. Mavel, Z. Mincheva, W. Saba, M. -A. Schöllhorn-Peyronneau, H. Valette, L. Garreau, S. Chalon, C. Halldin, J. Helfenbeim, J. Leigaillard, J. -

C. Madelmont, J. -B. Deloye, M. Bottlaender, D. Guilloteau, *J. Label. Compd. Radiopharm.*, 2006, **49**, 687-698.

[18] J. Yin, D. S. Zarkowsky, D. W. Thomas, M. M. Zhao, M. A. Huffman, *Org. Lett.*, 2004, **6**, 1465-1468.

[19] J. Kuszmann, Ě. Tomori, I. Meerwald, *Carbohydrate Res.*, 1984, **128**, 87-99.

[20] E. Baer, *J. Am. Chem. Soc.*, 1945, **67**, 338-339.

[21] R. S. Tipson, A. Cohen, *Carbohydr. Res.*, 1968, **7**, 232-243.

[22] C. R. Schmid, J. D. Bryant, M. Dowlatzedah, J. L. Phillips, D. E. Prather, R. D. Schantz, N. L. Sear, C. S. Vianco, *J. Org. Chem.*, 1991, **56**, 4056-4058.

[23] L. W. Hertel, C. S. Grossman, J. S. Kroin, *Synth. Commun.*, 1991, **21**, 151-154.

[24] D. Farran, A. M. Z. Slawin, P. Kirsch, D. O'Hagan, *J. Org. Chem.*, 2009, **74**, 7168-7171.

[25] J. Mulzer, A. Angermann, *Tetrahedron Lett.*, 1983, **24**, 2843-2846.

[26] E. K. Dolence, M. Adamczyk and D. S. Watt, *Tetrahedron Lett.*, 1985, **26**, 1189-1192.

[27] K. T. Mead, *Tetrahedron Lett.*, 1987, **28**, 1019-1022.

[28] B. M. Trost, Z. T. Ball, T. Jöge, *Angew. Chem. Int. Ed.*, 2003, **42**, 3415-3418.

[29] B. Grant, C. Djerassi, *J. Org. Chem.*, 1974, **39**, 968-970.

[30] N. Maezaky, M. Yano, Y. Hirose, Y. Itoh, T. Tanaka, *Tetrahedron*, 2006, **62**, 10361-10378.

[31] E. N. Jacobsen, I. Markŏ, W. S. Mungall, G. Schröder, K. B. Sharpless, *J. Am. Chem. Soc.*, 1988, **110**, 1968-1970.

[32] F. A. Davis, P. V. N. Kasu, G. Sundarababu, H. Qi, *J. Org. Chem.*, 1997, **62**, 7546-7547.

[33] Y. Gao, K. B. Sharpless, *J. Am. Chem. Soc.*, 1988, **110**, 7538-7539.

Chapter 3. Synthesis of trifluoro D-hexose sugar analogues and assessment of their erythrocyte transmembrane transport

3.1) Introduction:

3.1.1) Fluorosugars:

Over the last 15 years, the interest of the scientific community in the synthesis of fluorinated carbohydrates has increased steadily.[1,2] This is due to the possibility of modulating their physicochemical properties by the selective introduction of fluorine. The replacement of OH by fluorine in a sugar can alter the hydrophilic/lipophilic balance, change the adsorption, modify the hydrogen bonding capacity as well as affect the receptor binding ability of those sugars.[1] Furthermore a fluorine motif in a sugar offers a sensor to investigate carbohydrate metabolism and protein-carbohydrate interactions.[3,4,5] In particular ^{19}F is a NMR active nucleus[6] which allows generation of ^{19}F-NMR spectra without a background signal. Also, ^{18}F is positron-emitting isotope, and ^{18}F-labelled sugars are important compounds for positron emission tomography (PET) in the clinic.[7] Glycosyl fluorides are used as glycosyl donors in chemical and enzymatic glycosylation reactions, furthermore they can be important substrates or inhibitors in enzymatic reactions.[1]

This chapter focuses on deoxyfluoro sugar analogues obtained by fluorination of non-glycosydic positions.[1] The substitution of a single OH by fluorine in a sugar removes the hydrogen bonding donor capacity at that site because there is no hydrogen, but it retains the weak hydrogen bonding acceptor ability and the C-O/C-F polarity. Furthermore, the

substitution of OH (van der Waals radius around 1.57 Å) by F (van der Waals radius around 1.47 Å) has a negligible steric effect. Therefore monosubstituted deoxyfluoro sugars, such as the 2-deoxy-2-fluoro-D-glucose analogue **163** and 3-deoxy-3-fluoro-D-glucose analogue **164** (Figure 3.1), have become particularly attractive in assessing the influence of polarity versus hydrogen bonding ability in transport and binding studies.[8]
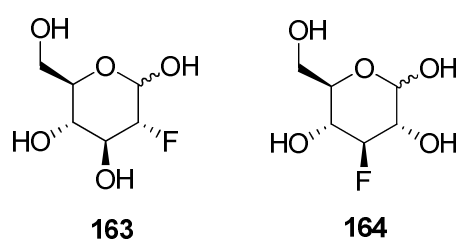
Figure 3.1. 2-Deoxy-2-fluoro-D-glucose analogue **163** and 3-deoxy-3-fluoro-D-glucose analogue **164**.[8]

Examination of the literature reveals that deoxyfluoro sugars with more than one fluorine are less common, for instance, there are only a few examples of deoxyfluoro hexoses with two fluorines replacing secondary alcohols eg. **165** and **166** (Figure 3.2).[9,10] Attention has focused on much more highly fluorinated sugar analogues, particularly on deoxyfluoro sugars containing an internal perfluoroalkylidene fragment (IPF).[1]

For instance DiMagno et al.[11] prepared the hexafluorohexose analogue **167** (Figure 3.2) to introduce the concept of "polar hydrophobicity",[12] which finds its fundamentals in the positive variation of entropy associated with the liberation of water by desolvation of a solute, occurring, for instance, when a hydrophobic molecule binds to a protein receptor. Thus, the replacement of hydrophilic OH groups with hydrophobic substituents such as CF_2 will increase the entropy of binding, as a hydrophobic molecule is more easily desolvated when transported to the receptor, increasing the molecular recognition of the transporter protein as a result. In parallel, advantageous electrostatic interactions occur in

proximity of the receptor, between the C-F bonds and polar charged centres of the protein. The transport of **167** across the red blood cell membranes was explored by ^{19}F-NMR and 2D ^{19}F EXSY-NMR.[11] This study has opened the way to the preparation of further IPF containing sugars. Linclau *et al.*[13,14] developed methodologies for the enantioselective synthesis of the tetrafluorinated ribose derivative **168** and for the synthesis of the tetrafluoropyranose analogue **169**, as well as the tetrafluorinated D-glucose analogue **170** and D-galactose analogue **171**[15] (Figure 3.2). Gouverneur *et al.*[16] have reported the synthesis of the tetrafluorofuranose derivative **172** (Figure 3.2) for incorporation into enantioenriched tetrafluorinated aryl-*C*-nucleosides.
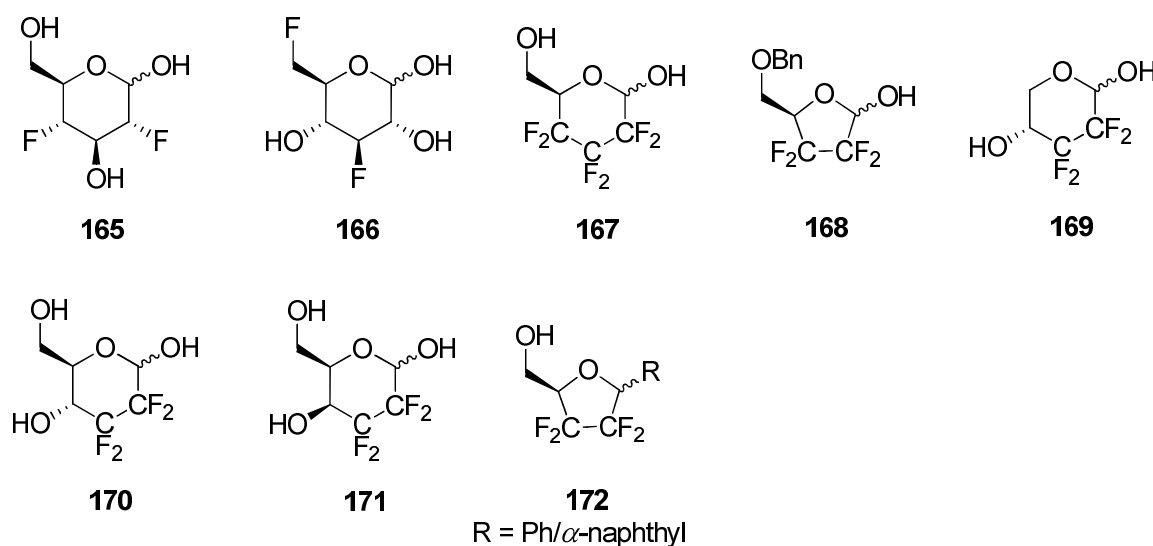
Figure 3.2. Some examples of relevant fluorinated carbohydrates analogues **165**-**167**, **169**-**172**, and derivative **168**.[9-15]

Interestingly, the synthetic methodologies adopted by DiMagno *et al.*,[11] Linclau *et. al.*,[13,15] and Gouverneur *et al.*[16] followed the building block approach,[1] which involves the preparation of a fluorinated non-sugar scaffold that can be transformed into a deoxyfluoro sugar. For example Linclau *et al.*[14] synthesised **169** in 5 steps starting from the fluorinated

scaffold **173** (Scheme 3.1). A Sharpless dihydroxylation of **173** generated **174**, which was then monofunctionalised by regioselective formation of the primary benzyl ether **175**. Formylation of **175** gave **176** and this was followed by lithiation to **177** *in situ*, *via* a bromine-lithium exchange, and subsequent anionic cyclisation furnishing **168**. Finally deprotection of the benzyl group of **168** generated the tetrafluoropyranose analogue **169**.
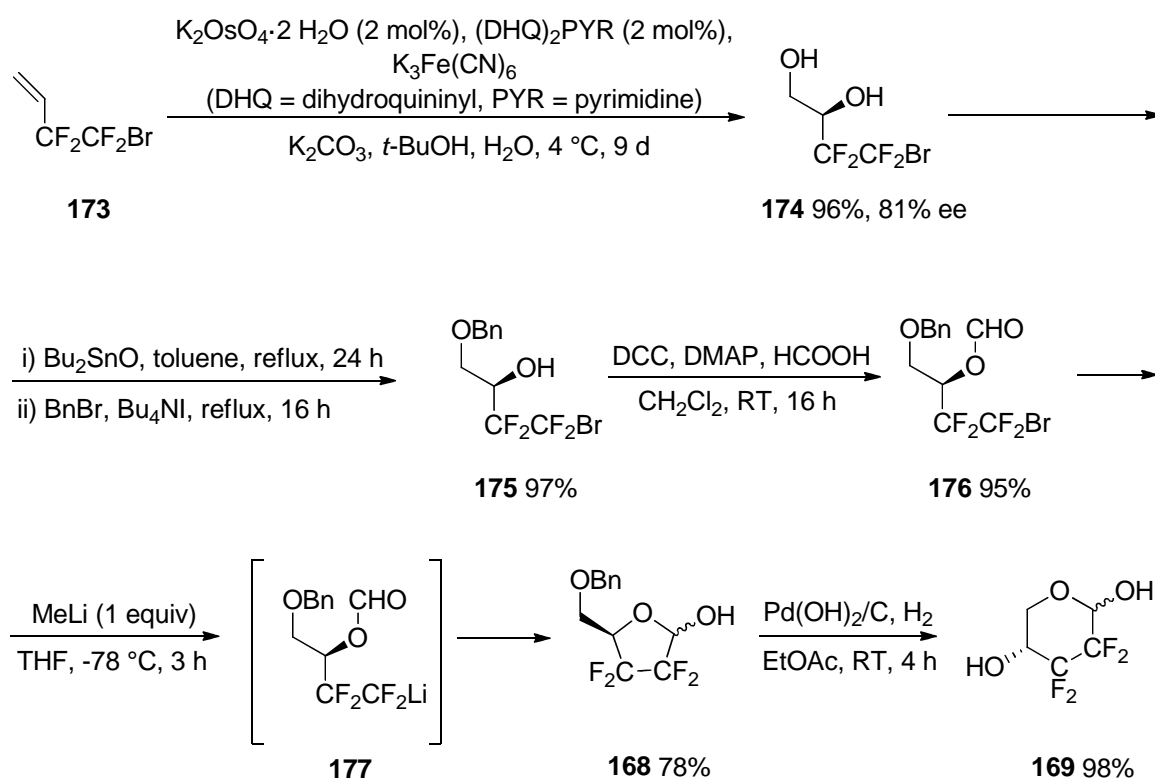
Scheme 3.1. Preparation of **169** *via* a building block approach.[1,14]

The synthesis of deoxyfluoro sugars from fluorinated building blocks differs from the more popular replacement of an OH group with fluorine directly on a carbohydrate precursor.[2] In this manner, Sarda *et al.*[17] reported the synthesis of diacetylated trifluoro D-galactose analogue **178** (Scheme 3.2) and D-glucose analogue **179** (Scheme 3.3). Compounds **178** and **179** are diastereoisomers that differ only in their configuration at C^4. Synthesis of **178** started from *p*-toluene-sulfonate **180** (Scheme 3.2). Treatment of **180**[18]

with sodium methoxide (NaOMe) generated epoxide **181.** Epoxide ring opening of **181** with KHF$_2$ in boiling ethylene glycol gave fluorohydrin **182** as the main product. Fluorohydrin **182** was then subjected to dehydroxyfluorination, which took place with retention of configuration, to give **183**. Debenzylation of **183** followed by dehydroxyfluorination, with an inversion of configuration afforded **185**. Treatment of **185** with a mixture of acetic anhydride (Ac$_2$O) and sulfuric acid (H$_2$SO$_4$) gave the diacetylated D-galactose **178** (Scheme 3.2).
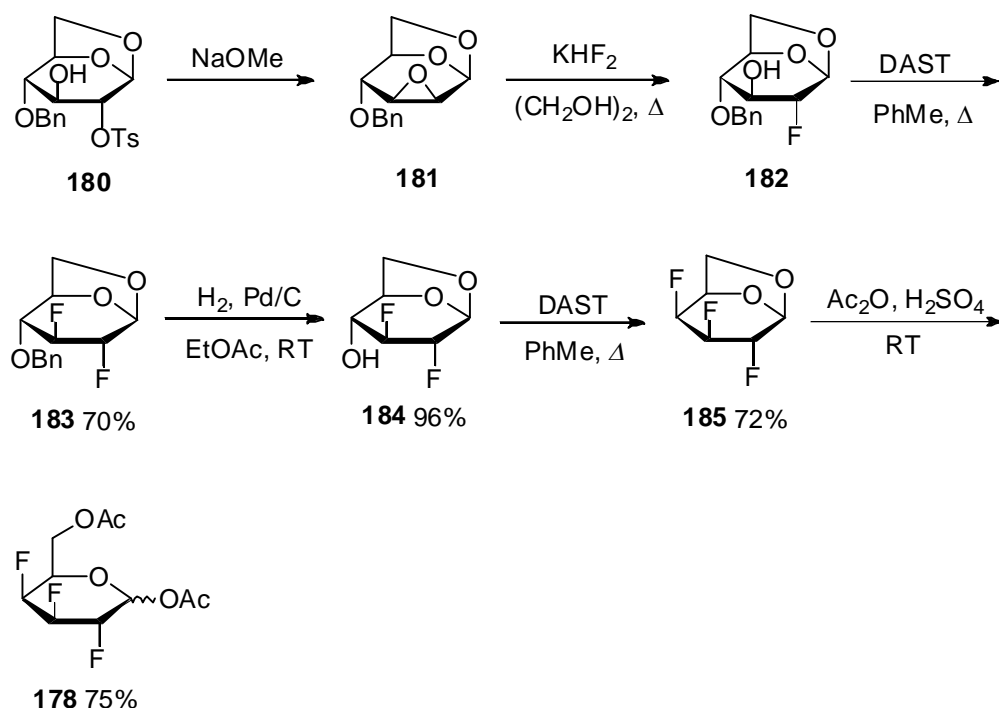
Scheme 3.2. Preparation of D-galactose trifluoro sugar precursor **178**.[17,18]

Synthesis of the diacetylated D-glucose analogue **179** was achieved starting from intermediate **184** (Scheme 3.3). The configuration at C^4 of **184** was inverted by preparing triflate **186**, followed by treatment with sodium benzoate (PhCO$_2$Na) which generated **187**. Methanolysis of ester **187** gave alcohol **188**. Dehydroxyfluorination of **188** took place with an inversion of configuration, to generate **189**, which was reacted with a

mixture of Ac_2O and H_2SO_4 to give **179** (Scheme 3.3). Sarda *et al.*[17] did not explain why dehydroxyfluorination using DAST occurred with an inversion of configuration in some cases and with a retention in other cases. Furthermore, the diacetylated analogues **178** and **179** were never hydrolysed to explore the physical or biological properties of the free carbohydrates.
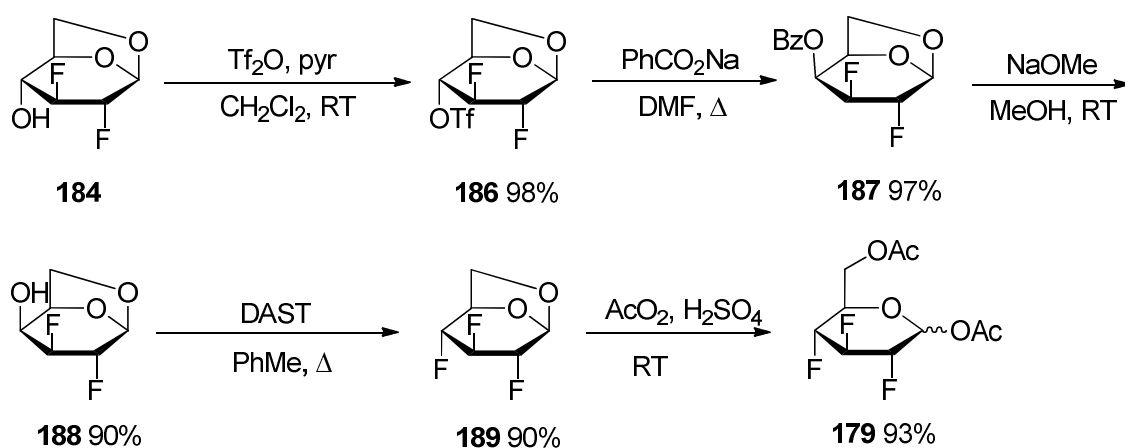
Scheme 3.3. Preparation of D-glucose trifluoro sugar precursor **179**.[17]

3.1.2) The Human Facilitative Glucose Transporter (Glut1):

Human erythrocytes (red blood cells) are recognised to have a transport capability for D-glucose across their cell membranes.[19] This is carried out by the Human Facilitative Glucose Transporter (Glut1), which is a protein of the glucose transporter facilitator family.[19] These proteins are not associated with ATP hydrolysis.[20] Their transport, through a process of facilitated diffusion is specific for the D-enantiomer of glucose. Thus D-glucose is transported depending on its chemical gradient inside or outside the cell.[20] Although no crystal structure of Glut1 has been obtained, two three-dimensional models

namely Glut1A and Glut1B have been predicted[19] based on the crystal structures of the two homologous proteins GlpT[21] and LacY[22], respectively.

Glut1 is a transmembrane protein composed of 492 residues[19] characterised by a channel across the protein connecting the intra- and extra- cellular environments. Glut1 is composed by twelve transmembrane helices divided into two 6-helical domains by a large intracellular loop between H6 and H7, as illustrated in Figure 3.3 (a). The extracellular side and the cytoplasmic view of the protein are shown in Figure 3.3 (b) and (c) respectively.[19] Key amino acid residues which line the walls of the channel have also been identified.
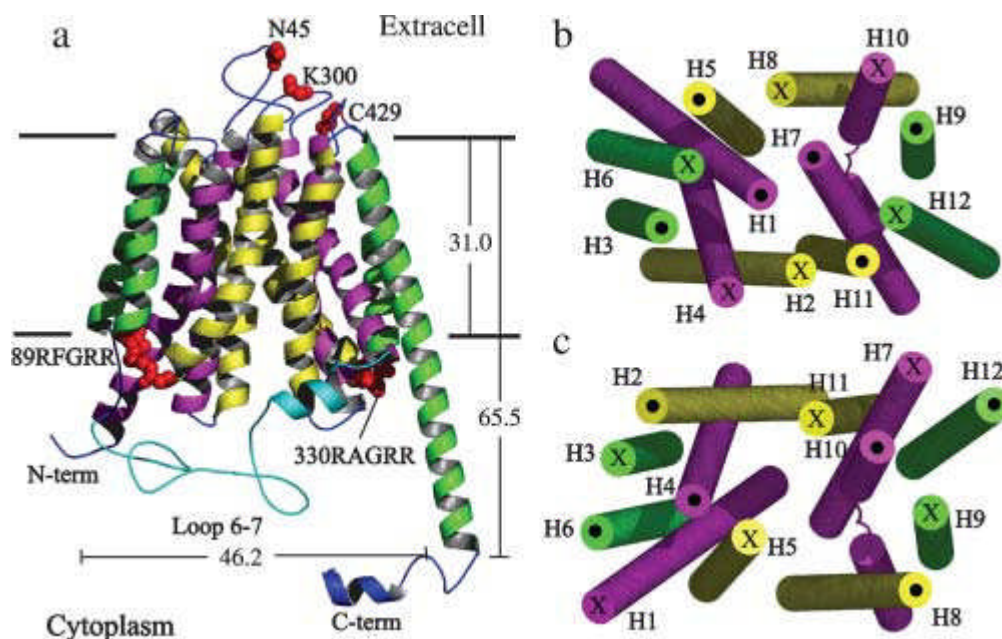
Figure 3.3. Representations of Glut1.[19] (a) Side view showing the relative positions of the helices; Glut 1 measures ~35.6 x 26.3 Å viewed from the top, and 46.2 x 27.2 Å from the bottom. Its height is ~61 Å. (b) View from the extracellular side showing the 12 transmembrane helices; (c) Cytoplasmic view. Reprinted from A. Salas-Burgos, P. Iserovich, F. Zuniga, J. C. Vera, J. Fischbarg, *Biophys. J.*, 2004, **87**, 2990-2999., Copyright 2004, with permission from Elsevier.

3.1.3) Erythrocyte transmembrane transport of fluorosugars:

Fluorosugars, such as the 3-deoxy-3-fluoro-D-glucose analogue **164** (Figure 3.1), have been studied with Glut1. G. J Riley and N. F. Taylor,[23] using an optical method developed by A. K. Sen and W. F. Widdas,[24] were the first to discover that **164** can cross the membrane of red blood cells *via* Glut1. The V_{max} of the transport of D-glucose, 3-deoxy-3-fluoro-D-glucose analogue **164** and 3-deoxy-D-glucose analogue **190** (Figure 3.4) were found to be very similar when Glut1 was saturated with each of these sugars.[23]

164   **190**
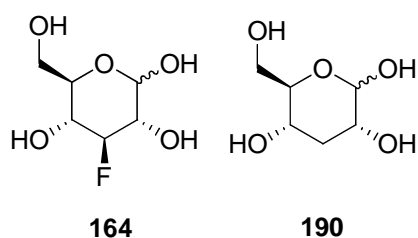
Figure 3.4. 3-deoxy-3-fluoro-D-glucose analogue **164** and 3 deoxy-D-glucose analogue **190**.[22]

Kuchel *et al.*[25] observed that the ^{19}F-NMR spectrum of **164** in a red blood cell suspension displayed four resonances, as a result of the intra- and extra- cellular populations of the α- and β- anomers. The intracellular resonances were broader and were found to be shifted downfielded compared to the extracellular signals. This experiment was consistent with previous work reported by R. E London and S. A. Gabel,[26] whereby the ^{19}F signals of trifluoroacetamide and trifluoroacetate were found to resolve intra- and extra- cellular when suspended in human red blood cells.

They suggested[27] that the chemical shift difference may be due to the different level of binding interactions between the intra- and extra- cellular enviroments, as well as high intracellular viscosity. Kuchel *et al.*[25] reported that the exchange rate of the α- and β-

anomers of **164** across red blood cell membranes can be determined by a ^{19}F-NMR spin-transfer technique. Furthermore, Kuchel *et al.*[25] revealed that the exchange of **164** across red blood cell membrane was reduced by glucose-transport inhibitors such as phloretin and cytochalasin B,[28,29] reinforcing Riley and Taylor's studies[30] whereby the transport of **164** involves Glut1 and is not simply due to diffusion. London *et al.*[8] described the erythrocyte transmembrane transport of the sugar analogues **163** and **164** (Figure 3.1) as well as the 4-deoxyfluoro-D-glucose **191** and 6-deoxyfluoro-D-glucose **192** (Figure 3.5) using a combination of 1D ^{19}F-NMR and 2D ^{19}F-NMR EXSY experiments. The 2D ^{19}F-NMR EXSY experiment detects correlations between the ^{19}F-NMR shifts of intra- and extra- cellular enviroments, the intensities of which correlates to the exchange rate across the membrane.

191   **192**
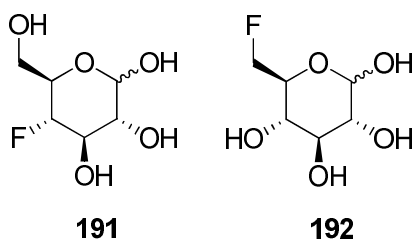
Figure 3.5 4-Deoxyfluoro glucose **191** and 6-deoxyfluoro glucose **192**.[8]

Although the presence of fluorine in sugars generally inhibits metabolism,[8] the ^{19}F-NMR spectrum of **164** showed, in addition to its intra- and extra- cellular resonances, extra signals corresponding to metabolites of **164**. One of these was identified as the 3-fluoro-3-deoxygluconate and/or its 6-phosphate ester (only intracellular), and also 3-fluorosorbitol (intra- and extra- cellular). Also the ^{19}F-NMR spectrum of **163** showed an additional signal corresponding to the 2-fluoro-2-deoxygluconate and/or its 6-phosphate.[8] The formation of these metabolites is slow, thus no interference with the transmembrane

study was observed. For each of the analogues **163**, **164**, **191** and **192** there were no cross-peaks associated with α/β anomer interconversion in the 2D ^{19}F-NMR EXSY spectrum. The efflux rate constants (k_{ef}) of **163**, **164**, **191** and **192** were determined either by 1D ^{19}F-NMR and 2D ^{19}F-NMR EXSY experiments, and the average values are shown in Table 3.1. The 2-deoxy-2-fluoro-D-glucose **163** and 3-deoxy-3-fluoro-D-glucose **164** were found to cross the erythrocyte membrane at similar rates to glucose, however 4-deoxyfluoro-D-glucose **191** and 6-deoxyfluoro-D-glucose **192** were found to be transported more slowly.[8] Furthermore the α-anomers were all more rapidly transported than the β-anomers,[8] similarly to D-glucose itself.[31] However the α- and β- anomers of **163** and **164** were transported at rates only slightly in favour of the α-anomer, whereas this difference was much bigger for **191** and **192**.

Analogue	k_{ef} (s^{-1})
163 (α-anomer)	1.29 ±0.31
163 (β-anomer)	1.21±0.22
164 (α-anomer)	1.35±0.32
164 (β-anomer)	1.04±0.23
191 (α-anomer)	0.77±0.16
191 (β-anomer)	0.30±0.09
192 (α-anomer)	0.72±0.21
192 (β-anomer)	0.44±0.20
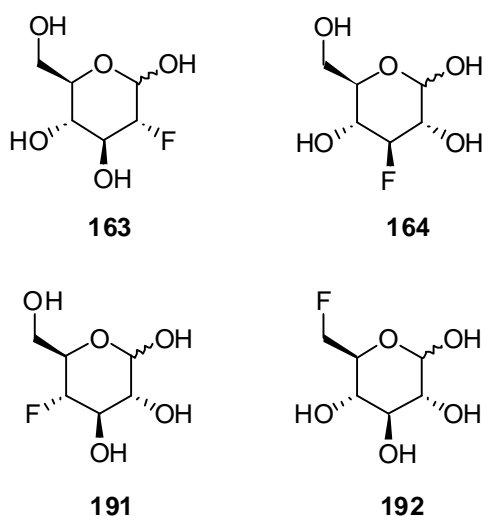
Table 3.1. Measured k_{ef} for the transport of **163**, **164**, **191** and **192** across the red blood cell membranes.[8]

This data suggest that the transport rates of monosubstituted deoxyfluoro sugar analogues across the red blood cell membranes are not dramatically affected by replacement of one OH by F at individual positions.[11] Conversely changing the configuration of a single

hydroxyl group on glucose has a dramatic impact on the tranport rates. For instance D-galactose is transported nearly 10 times slower than D-glucose across the red blood cell membrane.[32]

DiMagno *et al.*[11] carried out transmembrane transport studies of the highly fluorinated hexose analogue **167** (Figure 3.2) in red blood cells also by the use of 2D ^{19}F EXSY-NMR. It was found that **167** is transported 10 times faster than 3-deoxy-3-fluoro-D-glucose **164**,[11] most probably due to a higher affinity to the relevant membrane protein, and the *α*-anomer is more rapidly transported than the *β*-anomer.[11] No cross peaks associated with *α*/*β* anomer interconversion were observed, indicating that the rate of this phenomenon is slow. Also, there was no formation of metabolites observed. Replacement of OH by F can increase the lipophilicity of molecules,[33,34] and this can enhance the rate of transport across the membrane by simple diffusion. Thus, DiMagno *et al.*[11] performed a series of experiments to demonstrate that the improved transport of **167** compared to **164** across the red blood cell membranes was due to an increased binding to the Glut1 transporter, and not diffusion. For instance, when the potent glucose-transport inhibitor phloretin[28] was added, the exchange rate was reduced by a factor of three.

3.2) Aims and objectives:

The focus of this research was to explore a stereoselective synthesis to the trideoxy-trifluoro D-glucose analogue **193** (Figure 3.6). This would be the first example of a trifluorohexose in the literature.
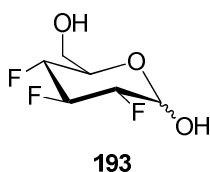
Figure 3.6. Trideoxy-trifluoro D-glucose analogue **193**.

It was envisaged that **193** could be prepared starting from intermediate **156a** (see preparation in Chapter 2) following the synthetic route outlined in Scheme 3.4. A key aspect of this approach involves the synthesis of the vicinal trifluoro motif **197**, which could then be converted to aldehyde **198** by oxidation. Acetonide cleavage of **198** would then generate **193** by an intramolecular cyclisation (Scheme 3.4). It was anticipated that this novel D-glucose analogue could be then explored for its ability to cross red blood cell membranes, in order to compare it with D-glucose. This could give some insight into the role of C-F bonds as C-OH mimics, and the importance of hydrogen bonding in the process.
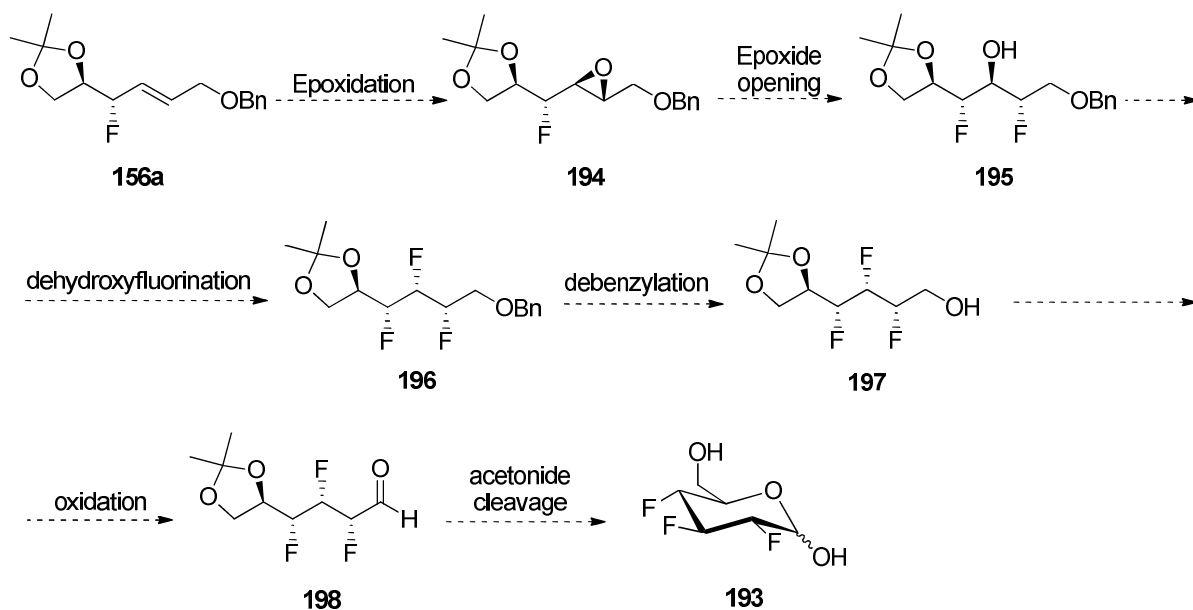
Scheme 3.4. Proposed route to the trifluorohexose **193**.

90

3.3) Results and discussion:

3.3.1) Synthesis of D-glucose analogue 193 and D-altrose analogue 216:

3.3.1.1) Introduction of the second fluorine:

The synthesis of allyl fluoride **156a** was discussed in Chapter 2. This was used as a starting point for the synthesis of **193** and **199**. Epoxidation of **156a** using *m*-CPBA[35] in CH$_2$Cl$_2$ generated an inseparable mixture of fluoro-epoxides **194a**/**194b** (dr 1:0.7, determined by ^{19}F-NMR) (Scheme 3.5).
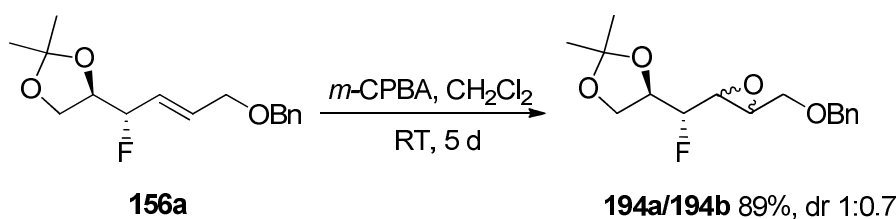
Scheme 3.5. Synthesis of epoxide isomers **194a**/**194b**.

With the diastereomeric mixture of fluoro-epoxides **194a**/**194b** in hand, an epoxide ring opening reaction was then explored. Initially the mixture of **194a**/**194b** was reacted with Et$_3$N·3HF (8.0 eq) in dry chloroform at RT. The reaction was slow and even after 3 days at 70 °C, t.l.c analysis of the product mixture still indicated the presence of unreacted starting material. ^{19}F{^{1}H}-NMR of the product mixture at this stage showed a complex pattern of fluorine signals (Figure 3.7), and clear identification of the individual fluorinated products was required.
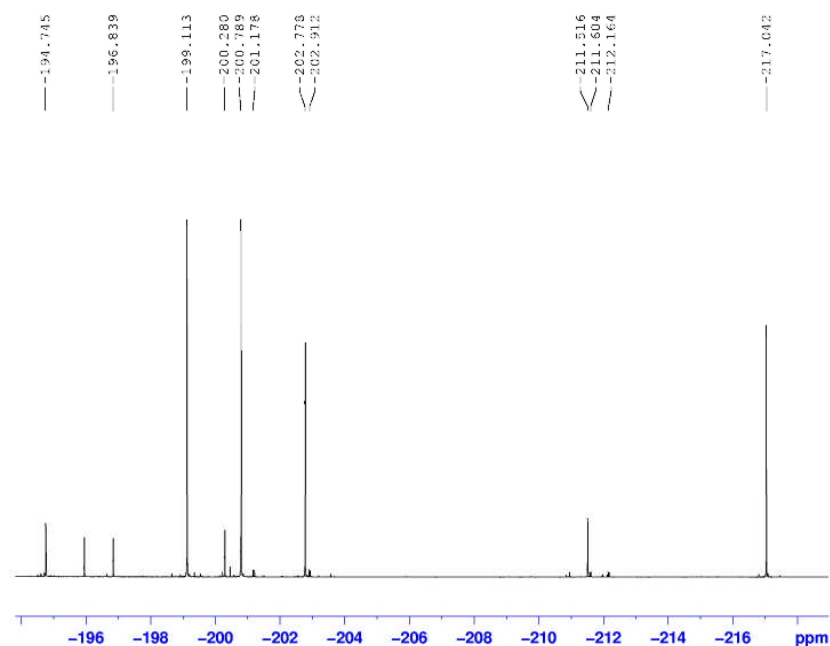
Figure 3.7. $^{19}F\{^1H\}$-NMR spectrum of the product mixture after epoxide ring opening of the inseparable mixture of **194a**/**194b**.

Chromatography successfully separated four fractions from unreacted starting material **194a**/**194b**. Subsequent structure analysis by NMR and mass spectrometry indicated that the two major components were **195a** and **195b** generated *via* an S_N2 pathway by fluoride ion attack at the less hindered β-position of the epoxide (Scheme 3.6 and Table 3.1). Compounds **195a** and **195b** could be separated by chromatography.

A minor component contained an inseparable mixture of diastereoisomers **199a**/**199b** (Scheme 3.6 and Table 3.1), which was presumably generated by fluoride attack at the more hindered position (α-position) of the epoxide. A fraction containing **200a**/**200b** (Scheme 3.6 and Table 3.1) was also isolated, which are products of acetonide cleavage. These could not be separated from each other by chromatography. Epoxide ring opening of **194a**/**194b** was also attempted by reaction with TBATF[36,37] and KHF$_2$,[36,37] however these attempts did not appreciably improve the outcome of the reaction. BF$_3$·Et$_2$O (33

mol%) in CH$_2$Cl$_2$ was also explored.[38] It proved to be very reactive even at low temperature (-78 °C), but it mainly resulted in the cleavage of the acetonide protecting group. Therefore Et$_3$N·3HF became the reagent of choice for the epoxide ring opening reaction of **194a**/**194b**. The reaction shown in Scheme 3.6 was therefore further developed and optimised. The goal was to reduce the cleavage of the acetonide protecting group (acid-labile) which generated side-products **200a** and **200b**, and also to shorten the reaction time.

The use of protic solvents was avoided as they diminish the nucleophilicity of fluoride ions. When epoxide ring opening of **194a**/**194b** was carried out with additional Et$_3$N, integration of the signals at -217.0 and -202.7 ppm (corresponding to **200a** and **200b,** see Table 3.2) in the ^{19}F{^{1}H}-NMR spectrum of the product mixture indicated a remarkable reduction of the acetonide cleavage side-reaction. Also, the reaction time was significantly reduced when performed under microwave (MW) irradiation.[39] Furthermore, a temperature gradient was found to be necessary to prevent the acetonide cleavage under MW conditions.
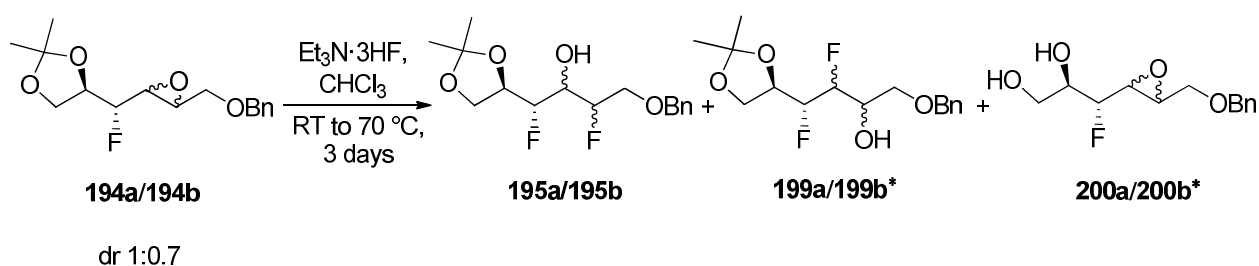
Scheme 3.6. Epoxide ring opening of **194a**/**194b** with Et$_3$N·3HF generated a complex mixture of products **195a**, **195b**, **199a**, **199b**, **200a** and **200b**.

*Probable structure based on partial purification/characterisation.

Table 3.2. ^{19}F-NMR chemical shifts (ppm) of products **194a**, **194b**, **199a**, **199b**, **200a** and **200b** and J_{F-F} coupling constants of products **195a**, **195b**, **199a** and **199b**.
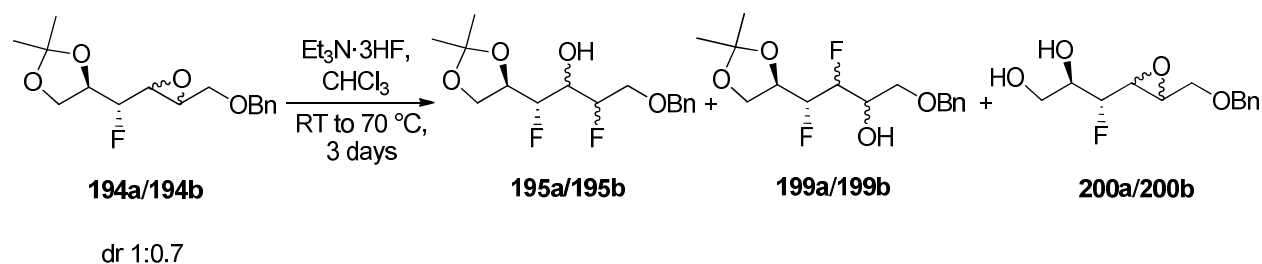
Product	^{19}F{^{1}H}-NMR chemical shifts (ppm)		J_{F-F} (Hz)
	F	F	J_{F-F}
194a	-199.1	-	-
194b	-200.8	-	-
195a	-196.8	-200.3	-
195b	-194.7	-211.5	3.0
199a	-211.6	-212.2	9.0
199b	-201.2	-202.9	12.0
200a	-217.0	-	-
200b	-202.8	-	-

The optimised method of choice for ring opening of **194a/194b** is illustrated in Scheme 3.7. Although fluorohydrins **195a** and **195b** were not crystalline materials, the stereoselectivity of this reaction was determined by X-ray crystallographic analysis of the final products **193** and **199**. Increasing the Et₃N (2.15 eq) (Scheme 3.7) required a longer reaction time (21 h under MW). Although t.l.c analysis of the product mixture showed high consumption of the starting material, the fluorohydrins **195a**, **195b**, **199a** and **199b** were obtained in low yields (Scheme 3.7). Furthermore, the ^{19}F{^{1}H}-NMR spectrum of the product mixture indicated that this reaction generated a mixture of isomers of **195a**:**195b**:**199a**:**199b** in a ratio of 0.7:1.0:0.2:0.3. This suggests that fluoride attack

preferentially occured at the less hindered *β*-position over the *α*-position. The reason for this is probably due to the strong electron-withdrawing effect of the vicinal fluorine, which strengthens the C_α-O epoxide bond and promotes fluoride ion attack at the *β*-position.[40]
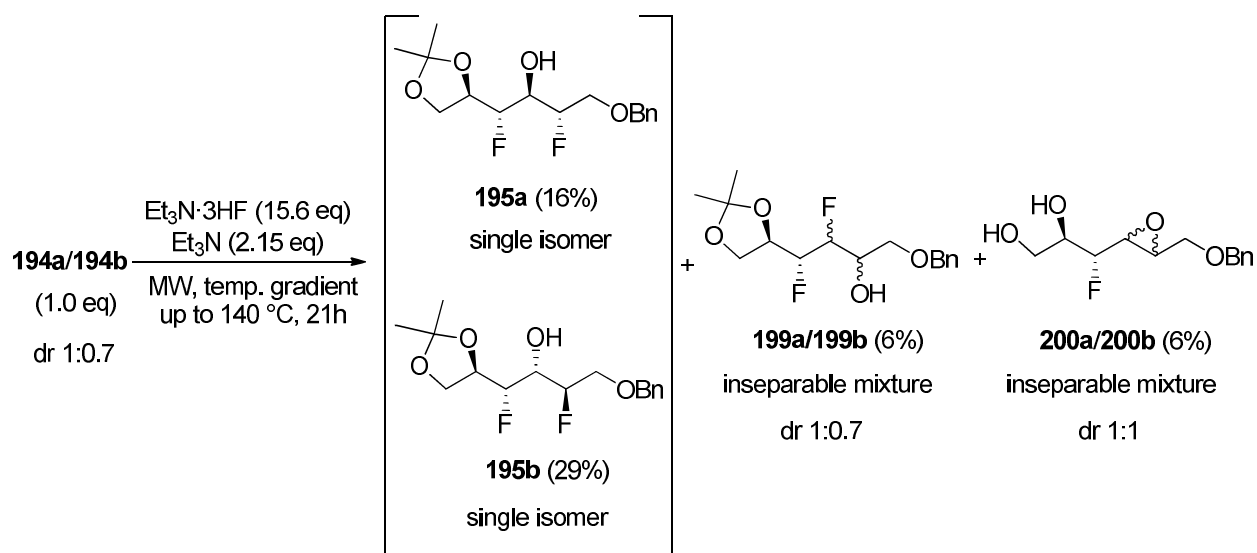
Scheme 3.7. Optimised conditions for epoxide ring opening. The yields (%) were recorded after two rounds of chromatography.

Epoxide ring opening of **194a/194b** proved to be even slower when carried out on a larger scale (1 g). A consistent cleavage of the acetonide protecting group occurred when the reaction was forced to go to completion by extending the reaction time. Therefore, these reactions were carried out repeatedly on a smaller scale (around 500 mg), and products were accumulated.

95

3.3.1.2) Introduction of the third fluorine:

Fluorohydrins **195a** and **195b** were used individually for their conversion to the corresponding trifluoro D-hexose analogues. Treatment of **195a** or **195b** with Deoxofluor[TM41] generated trifluoroacetal **196** (Scheme 3.8) and **201** (Scheme 3.9) respectively. After 14 h at RT, for dehydroxyfluorination of either **195a** and **195b**, the ^{19}F{^{1}H}-NMR spectrum of the product mixture showed complete consumption of the starting material and generation of the corresponding trifluoroacetal product as a single diastereoisomer.
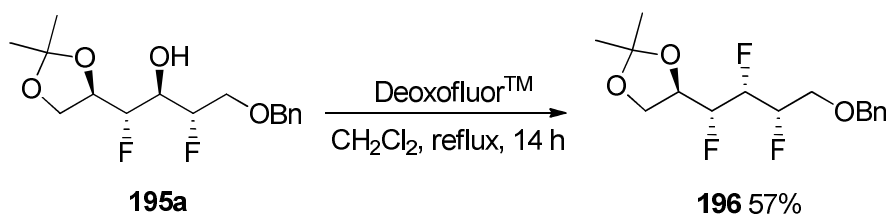
Scheme 3.8. Dehydroxyfluorination of **195a** generated **196**.
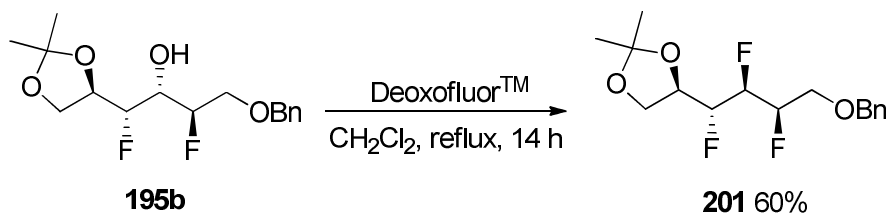
Scheme 3.9. Dehydroxyfluorination of **195b** generated **201**.

3.3.1.3) Debenzylation of trifluoroacetals 196 and 201:

The next step required the debenzylation of the trifluoroacetals **196** and **201**. Catalytic hydrogenolysis under a hydrogen atmosphere was initially attempted on both compounds **196** (Scheme 3.10) and **201** (Scheme 3.11). Different catalysts and a range of reaction

conditions were explored. Surprisingly the standard hydrogenation conditions for debenzylation failed, even under a hydrogen pressure of 15 atm. The results are summarised in Table 3.3. Starting material was recovered (entries 1 and 2 in Table 3.3) or was only partially consumed (entry 3 in Table 3.3). It was not clear why this approach failed, perhaps due to some sulfur residues from the preceding Deoxofluor™ reaction, however the origin of this remain unclear.
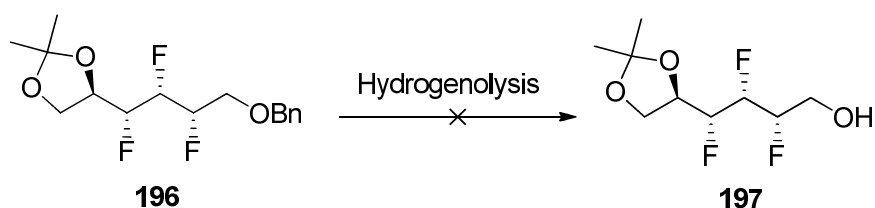
Scheme 3.10. Unsuccessful debenzylation reaction of **196** by hydrogenolysis, using the conditions reported in Table 3.3.
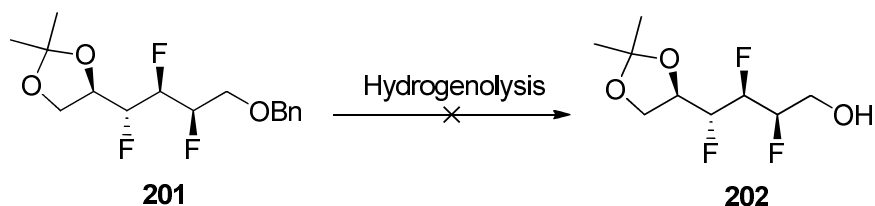
Scheme 3.11. Unsuccessful debenzylation reaction of **201** by hydrogenolysis, using the conditions reported in Table 3.3.

Entry	Catalyst	Solvent	Molar concentration (196 or 201)	Pressure (atm.)	Temp. (°C)	Time (h)
1	Pd/C (10 mol%)	MeOH	0.02	1	23	18
2	Pd(OH)$_2$ (10 mol%)	EtOAc	0.06	1	23	18
3	Pd/C (20 mol%)	THF	0.02	15	60	18

Table 3.3. Attempts at the debenzylation of **196** and **201** by catalytic hydrogenolysis.

When trifluoroacetal **196** was treated with BCl_3 (1M in CH_2Cl_2) at -78 °C, there was no reaction even after 2.5 h, however, increasing the reaction temperature to 0 °C resulted in a partial cleavage of both the benzyl and acetonide protecting groups. It was clear that a method to selectively deprotect the benzyl ether was necessary.

In the event, chemoselective deprotection of the benzyl ether was accomplished by a method described by Adinolfi *et al.*[42] Treatment of **196** (Scheme 3.12) and **201** (Scheme 3.13) with sodium bromate ($NaBrO_3$) and sodium dithionite ($Na_2S_2O_4$) under a two-phase solvent system ($EtOAc/H_2O$) generated **197** and **202** respectively. After 1 h at RT, for debenzylation of either **196** and **201**, the $^{19}F\{^{1}H\}$-NMR spectrum of the product mixture indicated complete consumption of the starting material and generation of the corresponding alcohol product as a single diastereoisomer.
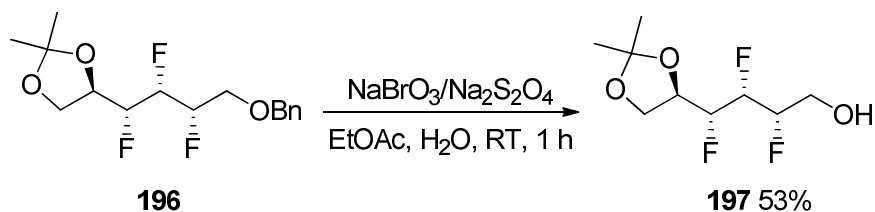
Scheme 3.12. Debenzylation reaction of **196**.
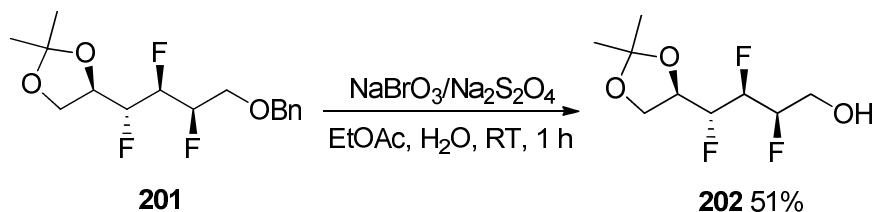
Scheme 3.13. Debenzylation reaction of **201**.

3.3.1.4) Oxidation and intramolecular cyclisation:

The final steps of the synthesis involved oxidation of trifluoroalcohol **197** to the correspondent aldehyde **198** using the Dess-Martin periodinane reagent[43] (Scheme 3.14). The resultant *α*-fluoroaldehyde **198** was unstable, thus it was not isolated and was immediately subjected to acetonide cleavage with anhydrous $SnCl_2$ in CH_2Cl_2.[44] This was followed by a spontaneous intramolecular cyclisation which generated the target D-glucose analogue **193**. ^{19}F-NMR indicated that **193** was generated as a mixture of anomers as expected (Scheme 3.14).
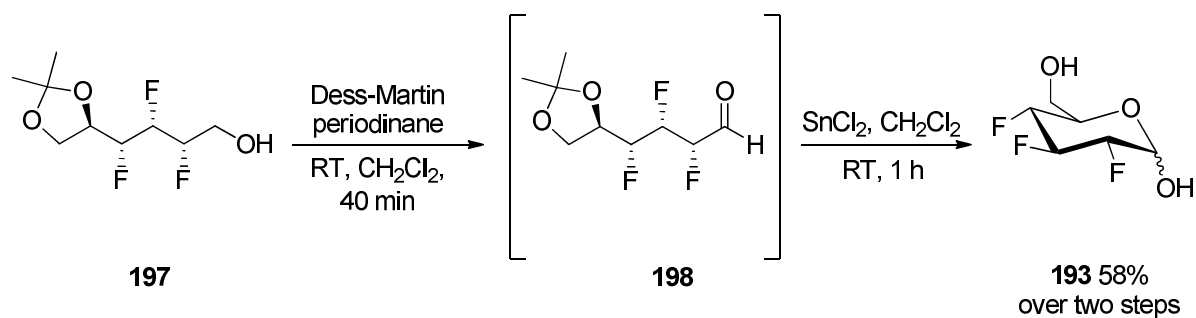
Scheme 3.14. Final steps for the preparation of the D-glucose analogue **193**.

The free sugar **193** is a white crystalline solid and a suitable crystal was subjected to X-ray structure analysis to confirm the relative and absolute stereochemistry. The resultant structure is shown in Figure 3.8. The stereochemistry is as anticipated and consistent with the expected configuration of each C-F bond forming reaction through the synthesis. The structure of the resultant *β*-anomer of **193** is shown in Figure 3.8.
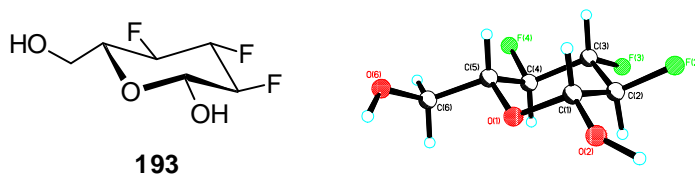
Figure 3.8. X-ray crystal structure of the D-glucose analogue **193** (*β*-anomer).

99

In a similar manner, trifluoroalcohol **202** was oxidised and subjected to acetonide cleavage to generate the target D-altrose analogue **216**, also as a mixture of anomers (Scheme 3.15).
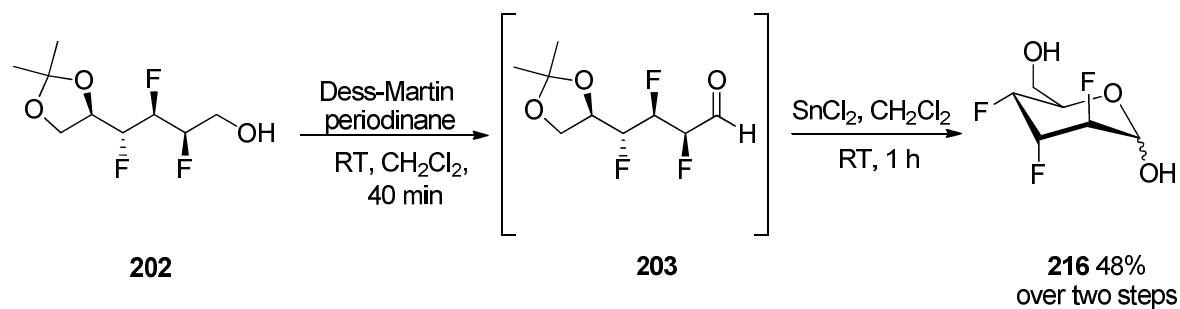
Scheme 3.15. Final steps for the preparation of the D-altrose analogue **216**.

Likewise a suitable crystal of hexose **216** was subjected to X-ray structure analysis and the resultant *β*-anomer is shown in Figure 3.9. Again, the structure confirms the expected stereochemistry, consistent with the anticipated stereochemical course of the various C-F bond forming reactions during the synthesis.
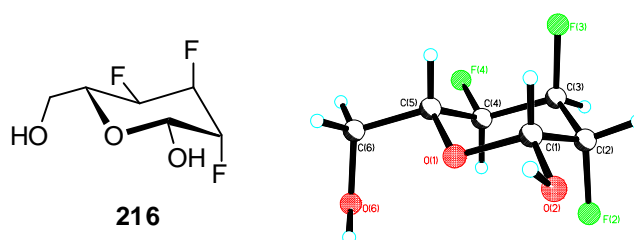
Figure 3.9. X-ray crystal structure of the D-altrose analogue **216** (*β*-anomer).

In both of the X-ray structures of the trifluorosugars **193** and **216**, the crystal packing revealed a partitioning of the oxygens/hydroxyls from the fluoromethylene residues, an intermolecular pattern most probably imposed by the stronger hydrogen bonding interactions between the oxygen atoms and hydroxyl groups. This can be seen in Figure 3.10 for the D-glucose analogue **193** where the shortest intermolecular O--H and F--H

interactions are 1.74 and 2.43 Å respectively, and in Figure 3.11 for the D-altrose analogue **216** where the shortest intermolecular O--H and F--H interactions are 1.82 and 2.42 Å respectively.
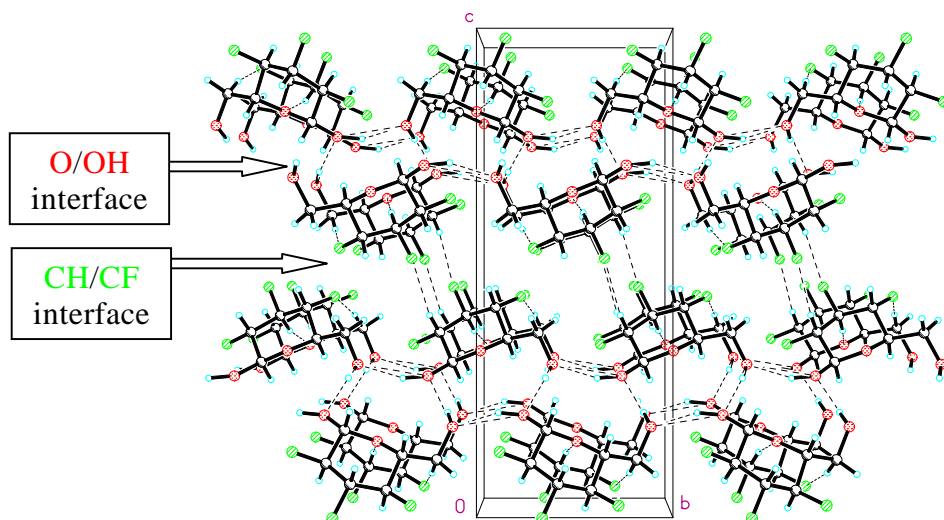
Figure 3.10. Molecular packing of analogue **193** (β-anomer).
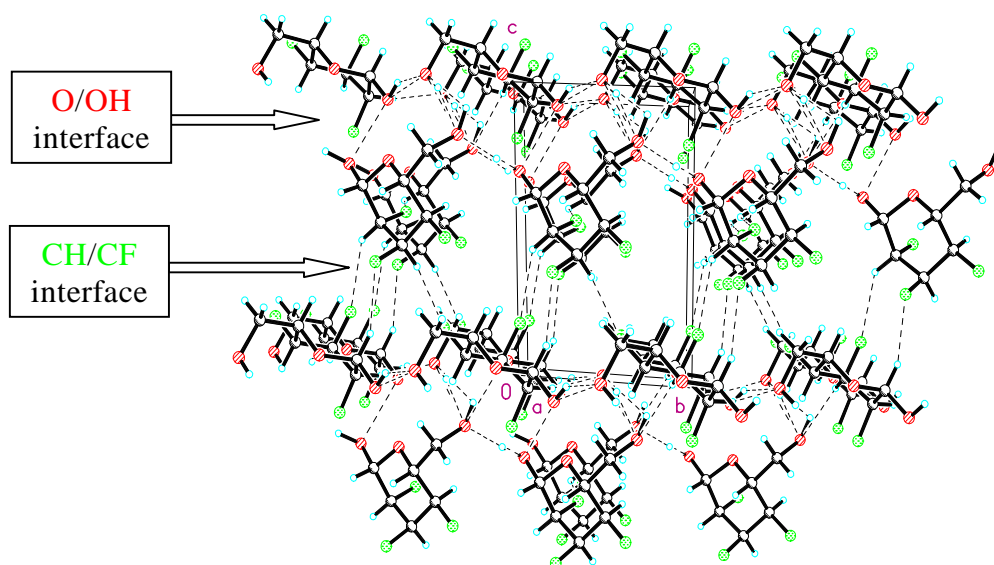
Figure 3.11. Molecular packing of analogue **216** (β-anomer).

*3.3.1.5) NMR analysis of D-glucose analogue **193** and D-altrose analogue **216**:*

NMR analysis provides ^{19}F chemical shifts as well as ^{19}F-^{1}H, ^{19}F-^{13}C and ^{19}F-^{19}F coupling constants as parameters to obtain structural information.[6] However, the presence of three vicinal fluorines in **193** and **216** generated a complex 1D spectrum. As a result, an unambigous assignment of all the ^{1}H, ^{13}C and ^{19}F signals was not possible due to extensive overlap of the NMR resonances. In these cases, carrying out 2D NMR analyses such as ^{1}H-^{19}F HMBC and ^{19}F-^{19}F COSY as well as 1D analysis such as $^{1}H\{^{19}F\}$-NMR, was essential to assist confident signal assignments.

In order to assign the specific anomers in the $CDCl_3$ solutions of **193** and **216**, a series of 1D and 2D NMR experiments was carried out. The ^{1}H-NMR spectrum of **193** (Figure 3.12) shows two doublet of doublets assigned to H^1 (*α* or *β*), one at 5.48 ppm displaying coupling constants of 3.7 and 3.1 Hz, and one at 4.91 ppm displaying coupling constants of 7.6 and 3.1 Hz. The $^{1}H\{^{19}F\}$-NMR spectrum of **193** in $CDCl_3$ allowed discrimination between the $^{3}J_{H-H}$ and $^{3}J_{H-F}$ coupling constants. The spectrum (Figure 3.13) shows two doublets at 5.48 ppm and 4.91 ppm displaying $^{3}J_{H-H}$ coupling constants of 3.7 and 7.6 Hz respectively. The larger $^{3}J_{H-H}$ coupling constant of 7.6 Hz is indicative of a *trans*-diaxial relationship between the protons H^1 and H^2, thus the signal at 4.91 ppm was assigned to the *β*-anomer. By inference, the signal at 5.48 ppm was assigned to the *α*-anomer. Integration of these signals indicated that the anomers were present in a ratio of 1:0.2 (*α*:*β*) (Figure 3.13).
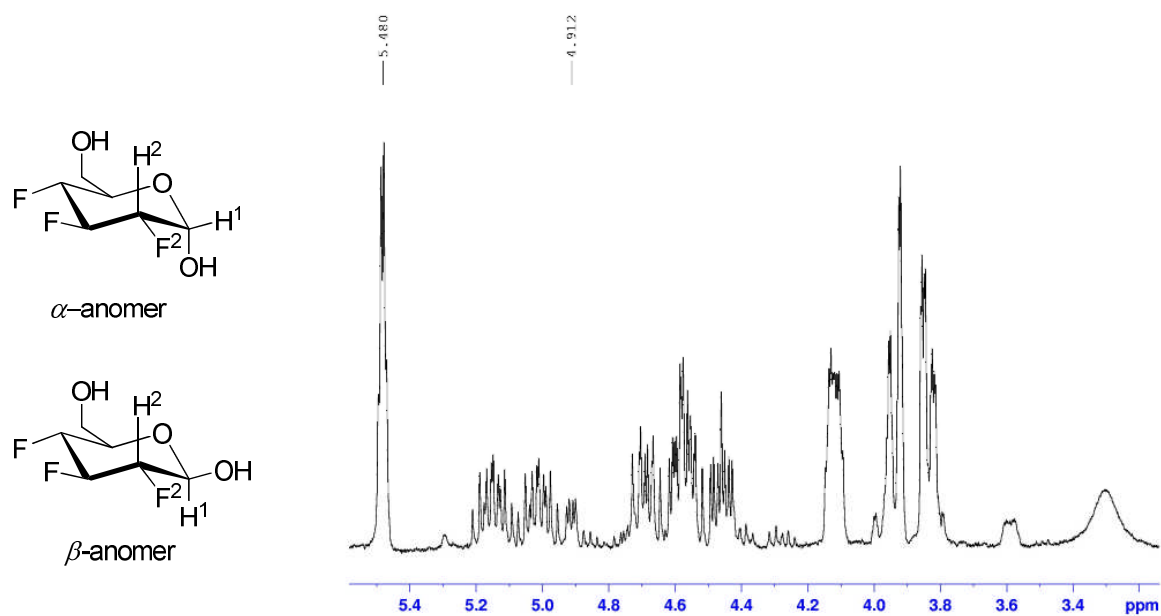
Figure 3.12. ^{1}H-NMR spectrum of **193** in CDCl$_3$.
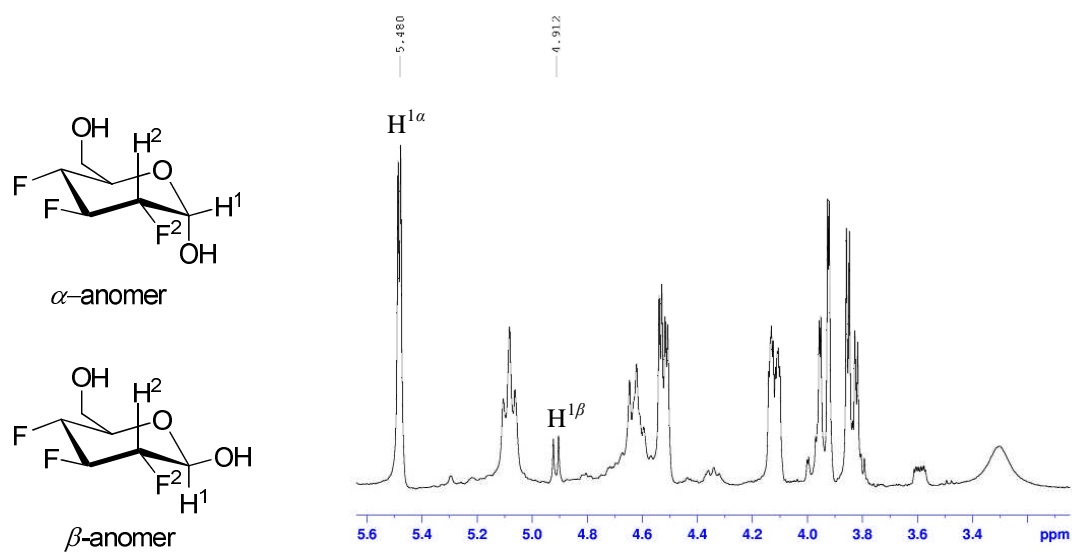
Figure 3.13. ^{1}H{^{19}F}-NMR spectrum of **193** in CDCl$_3$.

The ^{1}H,^{19}F-HMBC spectrum of **193** in CDCl$_3$ allowed an assignment of F$^{2\alpha}$ and F$^{2\beta}$. The spectrum (Figure 3.14) shows $^3J_{\text{H1}\alpha\text{-F2}\alpha}$ and $^3J_{\text{H1}\beta\text{-F2}\beta}$ crosspeaks which enabled an assignment of the doublet of doublets at -199.9 ppm and -200.5 ppm to F$^{2\alpha}$ and F$^{2\beta}$, respectively.

Figure 3.14. ^{1}H,^{19}F-HMBC spectrum of **193** in CDCl$_3$.

The ^{19}F{^{1}H}-NMR spectrum of **193** in CDCl$_3$ (Figure 3.15) allowed assignment of F$^{3\alpha}$/F$^{3\beta}$ and F$^{4\alpha}$/F$^{4\beta}$ to the corresponding signals. The spectrum shows six signals corresponding to the α- and β- anomers. The two doublet of doublets at -199.9 ppm and -200.5 ppm had previously been assigned to F$^{2\alpha}$ and F$^{2\beta}$, respectively (Figure 3.14). The signals at -195.8 ppm and -201.6 ppm are triplets whereas the signals at -201.2 ppm and -202.0 ppm are doublet of doublets (Figure 3.15). These two triplets arise due to the similar $^3J_{\text{F3-F2}}$ and $^3J_{\text{F3-F4}}$ coupling constants and are thus assigned to F^3 (α or β) (Figure 3.15). Furthermore integration of these signals gave a ratio of 1:0.2, corresponding to the ratio of the α- and β- anomers respectively (Figure 3.15). By inference, the doublet of doublets at -202.0

104

ppm was assigned to $F^{4\alpha}$ and the doublet of doublets at -201.2 ppm to $F^{4\beta}$ (Figure 3.15).
The anomeric ratio of **193** tends towards 1:1 by increasing the polarity of the solvent
(Figure 3.16), furthermore a significant change in the ^{19}F- chemical shifts are observed.
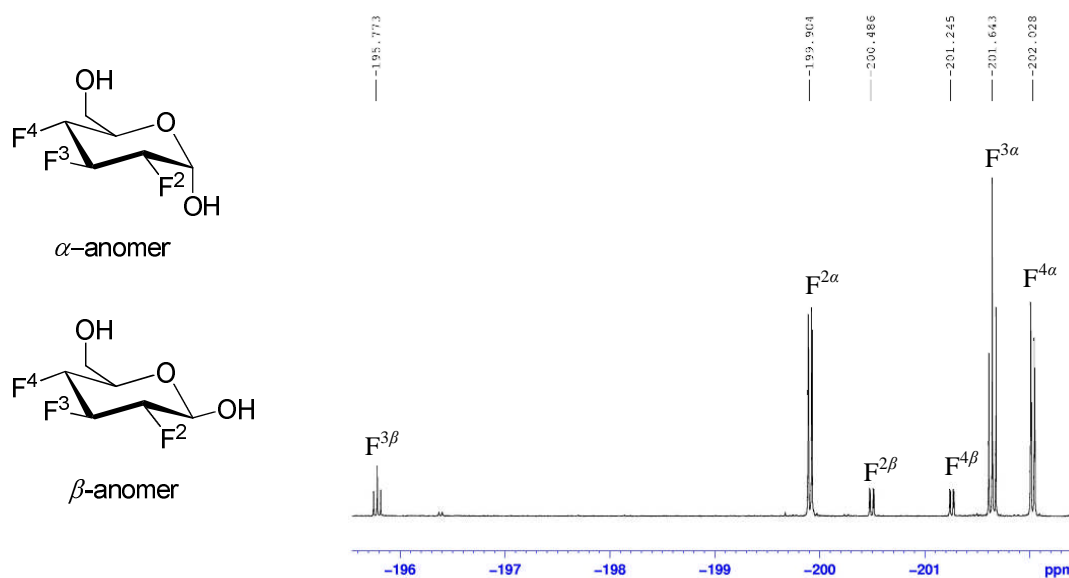
Figure 3.15. ^{19}F{^{1}H}-NMR spectrum of **193** in CDCl$_3$.
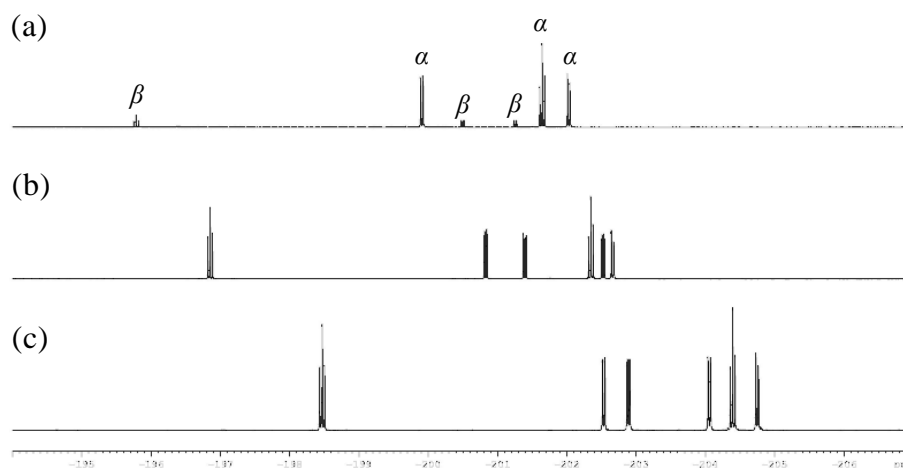
Figure 3.16. ^{19}F{^{1}H}-NMR showing the α/β anomer ratios of **193** in (a) CDCl$_3$ (α:β, 1:0.13); (b) CD$_3$CN (α:β, 1:1); (c) d_8-THF (α:β, 1:1).

105

The ^{1}H-NMR spectrum (Figure 3.17, section a) of **216** in CDCl$_3$ shows a doublet of doublets at 5.32 ppm, displaying both large and small coupling constants of 11.1 and 1.6 Hz, allowing assignment to H^1 (α or β). Although the accurate measurement of the coupling constants for the resonance at 5.19 ppm (assigned to the other anomeric proton H^1) was not achievable due to overlapping of signals, a large coupling constant of approximately 17 Hz was estimated. This coupling constant is lost in the ^{1}H{^{19}F}-NMR spectrum (Figure 3.17, section b), thus the larger coupling constant of 17 Hz is indicative of a *trans*-diaxial relationship between H$^{1\beta}$ and F$^{2\beta}$, whereas the smaller coupling constant (11.1 Hz) is indicative of an axial-equatorial relationship between H$^{1\alpha}$ and F$^{2\alpha}$. Thus the signals at 5.32 and 5.19 ppm were assigned to H$^{1\alpha}$ and H$^{1\beta}$, respectively. Also, the integration of these signals shows a ratio of 0.8:1 corresponding to the ratio of the α- and β- anomers respectively.
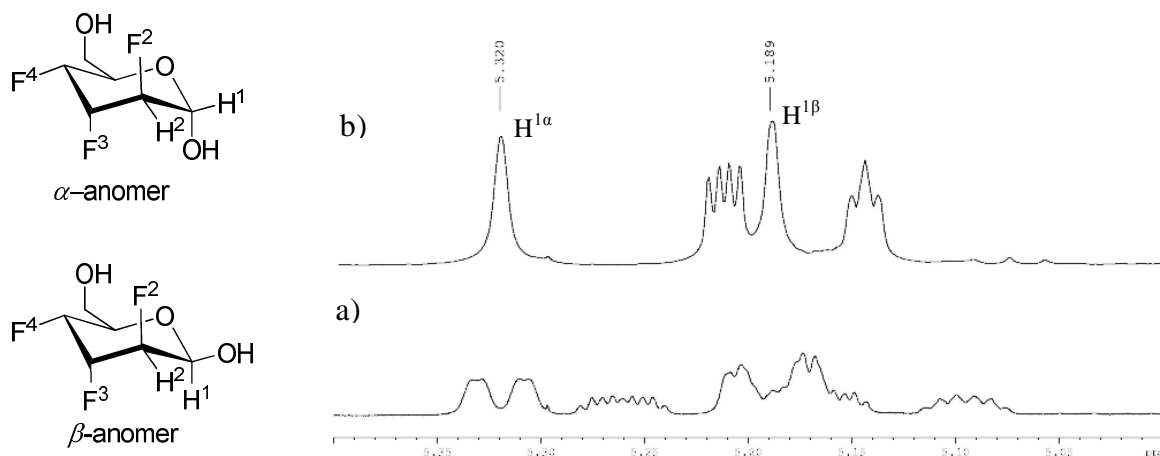
Figure 3.17. (a) ^{1}H and (b) ^{1}H{^{19}F}-NMR of **216** in CDCl$_3$.

A ^{19}F{^{1}H}-NMR spectrum of **216** in CDCl$_3$ was recorded (Figure 3.18) and showed six signals corresponding to the α- and β- anomers. Integration (α:β ratio of 0.8:1) enabled assignment of the resonances at -200.5, -209.7 and -213.8 ppm to the α-anomer, and of

106

the resonances at -213.4, -214.3 and -219.3 ppm to the β-anomer. However, an unambigous assignment of these resonances to the corresponding fluorines ($F^{1\alpha}$ and $F^{1\beta}$, $F^{2\alpha}$ and $F^{2\beta}$, $F^{3\alpha}$ and $F^{3\beta}$) by ^1H,^{19}F-HMBC was not possible.
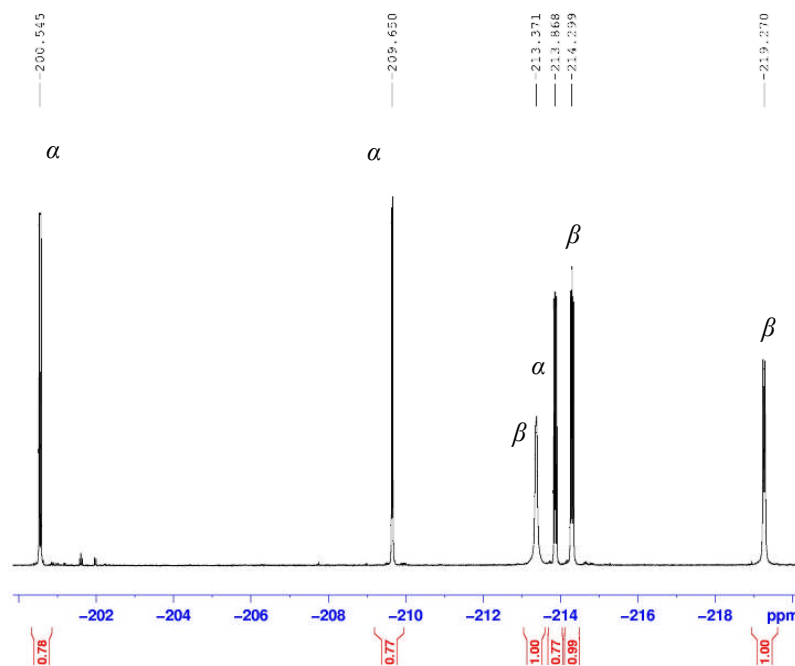
Figure 3.18. $^{19}F\{^1H\}$-NMR spectrum of **216** in CDCl$_3$.

3.3.2) Assessment of the erythrocyte transmembrane transport of D-glucose analogue 193 and D-altrose analogue 216:

The ability of the trifluoro D-hexose analogues **193** and **216** to cross erythrocyte membranes was evaluated. ^{19}F-NMR and 2D ^{19}F EXSY-NMR experiments were carried out to determine the efflux rate constants (k_{ef}) from human erythrocyte suspended in a D$_2$O buffer solution. Because of the different anomeric permeability across the erythrocyte membrane, the assignment of the specific anomers to **193** and **216** in a deuterated buffer (D$_2$O-Tris-HEPES) was first required. To achieve this, a series of 1D

107

and 2D NMR experiments was carried out. The ^{1}H{^{19}F}-NMR analysis of **193** in D_2O buffer allowed assignment of H^1 in each anomer. The spectrum (Figure 3.19) shows two doublets assigned to H^1 (α or β), one at 5.50 ppm displaying a $^3J_{\text{H-H}}$ coupling constant of 3.8 Hz, and one at 5.00 ppm displaying coupling constant of 8.2 Hz. The larger $^3J_{\text{H-H}}$ coupling constant is indicative of a *trans*-diaxial relationship between the H^1 and H^2 protons, thus the signals at 5.00 ppm and 5.50 ppm were assigned to the β- and α-anomers, respectively. Integration of these signals indicated that the anomers are present in 1:0.9 ratio (α:β).
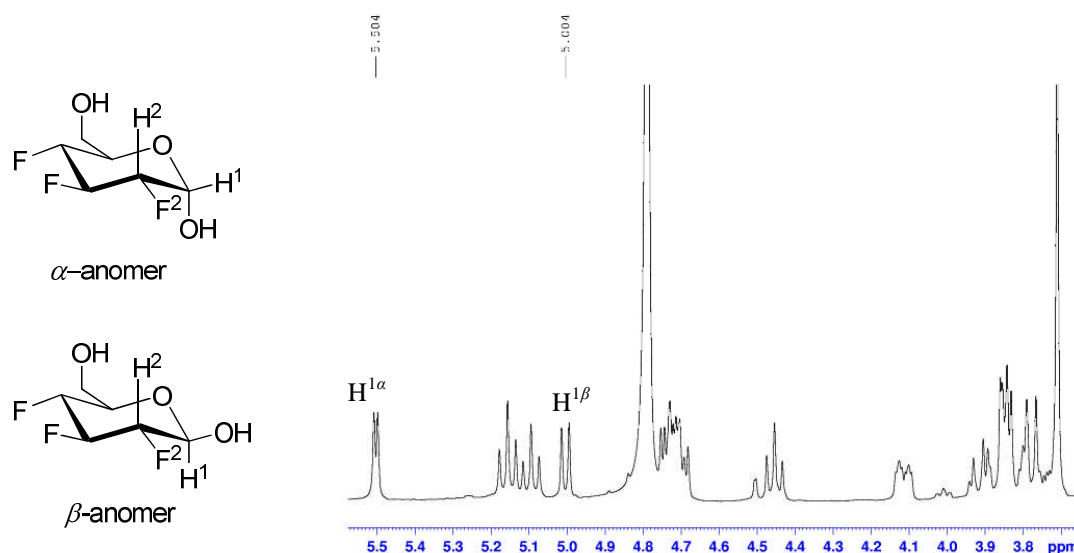
Figure 3.19. ^{1}H{^{19}F}-NMR spectrum of **193** in D_2O-Tris-HEPES buffer.

The ^{1}H,^{19}F-HMBC spectrum of **193** in D_2O-Tris-HEPES buffer in Figure 3.20 shows $^3J_{\text{H1}\alpha\text{-F2}}$ and $^3J_{\text{H1}\beta\text{-F2}}$ crosspeaks which enabled assignment of the doublets at -199.4 ppm and -200.7 ppm to F$^{2\alpha}$ and F$^{2\beta}$, respectively.

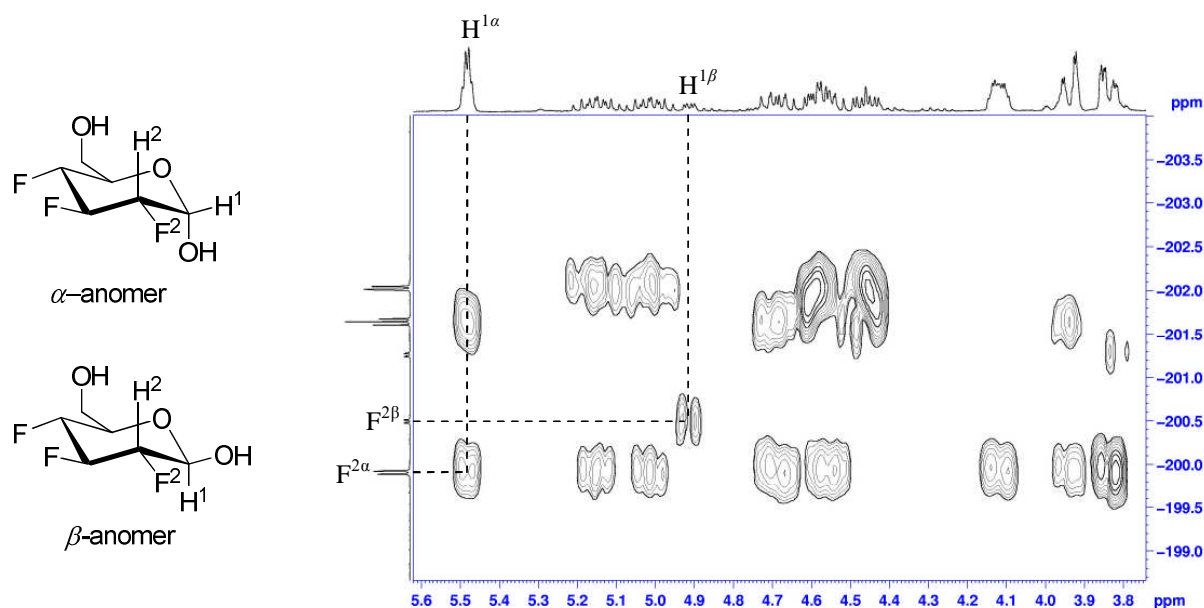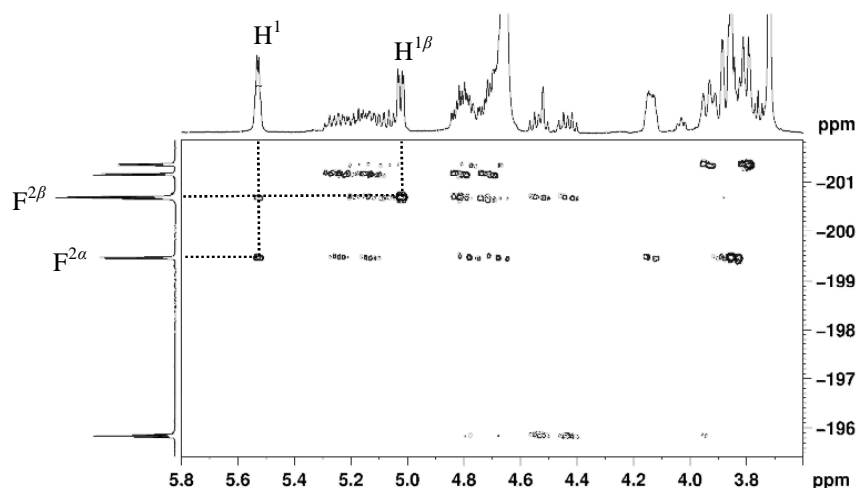**Figure 3.20.** $^1H,^{19}F$-HMBC spectrum of **193** in D_2O-Tris-HEPES recorded at 37 °C.

The use of ^1H-NMR (Figure 3.21, section a) and $^1H\{^{19}F\}$-NMR (Figure 3.21, section b) spectra to assign H^1 to the corresponding anomers (*α* or *β*) of **216** in D_2O-Tris-HEPES was not achievable, due to overlap of H^1 (*α* and *β*) and H^3 (Figure 3.21). To overcome this obstacle, the 1D gradient NOESY spectra was recorded in D_2O-Tris-HEPES buffer (Figure 3.22). The spectrum shows an NOE between H^5 (4.39 ppm) and a H^6 proton (Figure 3.22, section a), and also between H^5 (4.13 ppm) and both H^6 and H^1 protons (Figure 3.22, section b). This enabled assignment of the resonance at 4.39 ppm to $H^{5\alpha}$ and that at 4.13 ppm to $H^{5\beta}$.
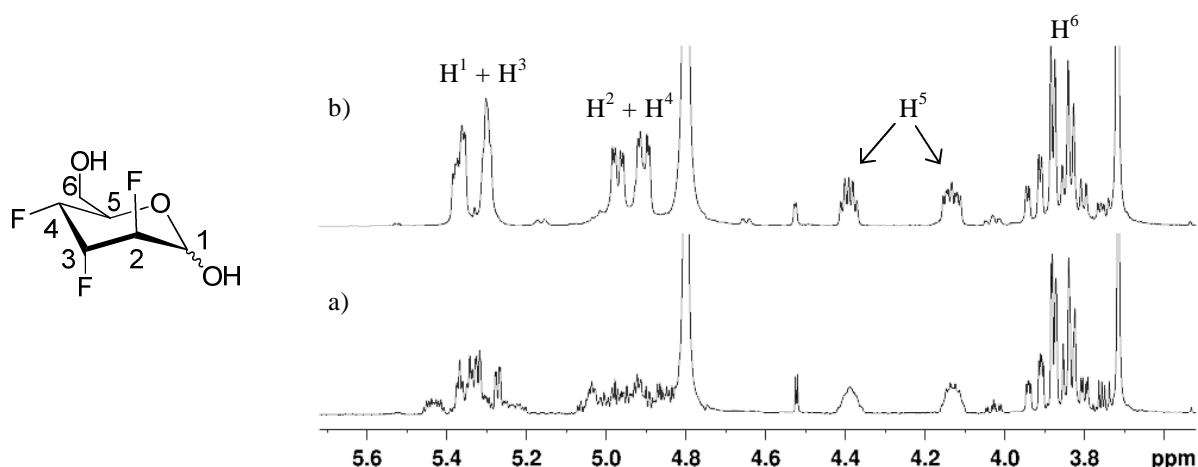
Figure 3.21. (a) ^1H-NMR and (b) $^1H\{^{19}F\}$-NMR spectra of **216** in D_2O-Tris-HEPES.
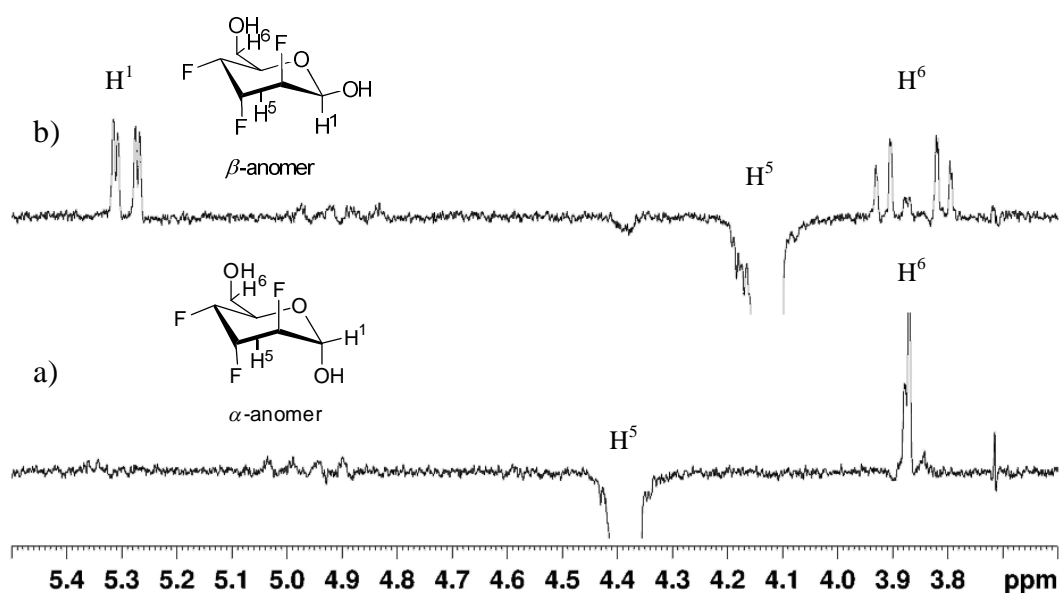
Figure 3.22. 1D gradient NOESY spectra of **216** in D_2O-Tris-HEPES: spectrum (a) shows NOE between H^5 at 4.39 ppm and H^6; spectrum (b) shows NOE between H^5 at 4.13 ppm and H^6 and H^1.

The $^1H,^{19}F$-HMBC spectrum of **216** in D_2O-Tris-HEPES buffer was recorded in order to assign F^2, F^3 and F^4 to the corresponding anomers. The spectrum (Figure 3.23) shows $^3J_{H5\alpha\text{-}F4\alpha,}$ $^4J_{H5\alpha\text{-}F3\alpha}$ crosspeaks which enabled an assignment of the signals at -212.0 ppm and -207.3 ppm to $F^{3\alpha}$ and $F^{4\alpha}$ respectively, and $^3J_{H5\beta\text{-}F4\beta}$ and $^4J_{H5\beta\text{-}F3\beta}$ (-214.3 ppm and -213.2 ppm) to $F^{3\beta}$ and $F^{4\beta}$ respectively. F^2 resonances (α and β) were assigned using $^{19}F,^{19}F$-COSY (not shown).
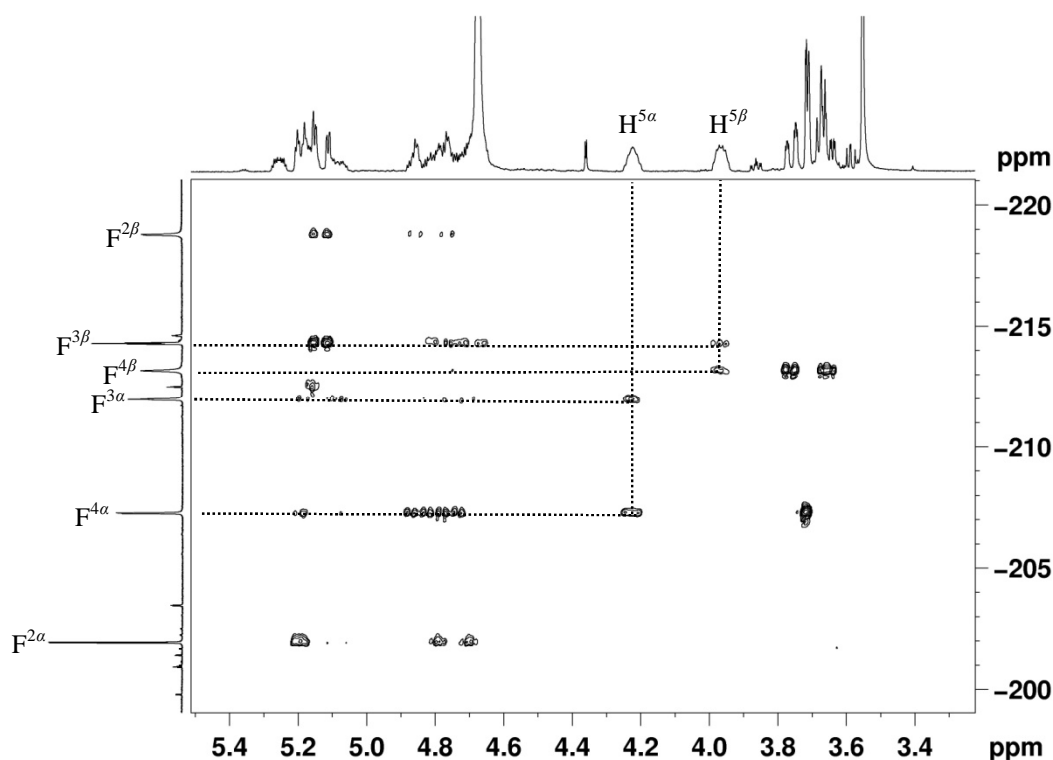
Figure 3.23. ^{1}H,^{19}F-HMBC spectrum of **216** in D_2O-Tris-HEPES buffer.

The next step of the erythrocyte transmembrane transport study required the preparation of a suspension of **193** and red blood cells in D_2O buffer. The experiment with **216** was performed in parallel. Human red blood cells were obtained from First Link (UK) Ltd. The human blood was centrifuged (4000 rpm, 5 min) and the plasma and supernatant were discarded. The cells were then washed four times in three volumes of saline buffer solution containing 123 mM NaCl, 15 mM Tris-HEPES and 5 mM ascorbic acid (previously filtered through sterile filters Nalgene 0.20 µm cellulose acetate membranes), and after each wash the supernatant was removed and the cells were collected by centrifugation. The red blood cells were then transferred to an Eppendorf tube and diluted with one volume of saline buffer and 20 mM of the trifluoroglucose analogue **193** (final hematocrit 0.5), carefully mixed and transferred into a WILMAD NMR tube with a J Joung valve. A sealed capillary tube containing D_2O was then introduced into the NMR

111

tube to provide a deuterium lock signal. Also a stream of carbon monoxide was bubbled through the cells for 3 minutes before sealing in order to eliminate any paramagnetic deoxyhemoglobin which can broaden the NMR resonances. The sample was sealed and was ready to be analysed by 2D ^{19}F EXSY-NMR spectroscopy. A control experiment consisted of the ^{1}F{^{1}H}-NMR spectra of **193** in D_2O-Tris-HEPES buffer, recorded at 37 °C. This showed six resonances (Figure 3.24, section a) corresponding to the α- and β-anomers as previously assigned.

The ^{19}F EXSY-NMR spectrum (consisting of two ^{19}F{^{1}H}-NMR spectra perpendicular to each other) of **193**, in the presence of erythrocytes suspended in the buffer at 37 °C showed twelve resonances corresponding to the intra- and extra- cellular populations of the α- and β- anomers (Figure 3.24, section b). All six resonances of the anomers of **193** were associated with broad downfield shifted resonances corresponding to the intracellular population of **193**. Furthermore the ^{19}F EXSY-NMR spectrum shows cross-peaks indicative of an exchange between the intra- and extra- cellular pools. Specifically, the intensities of the selected cross-peaks (Figure 3.24, section b) associated with $F^{2\alpha}$ (signal at -199.3 ppm) and $F^{3\beta}$ (signal at -195.7 ppm) are proportional to the exchange rates of the α- and β- anomers between the intra- and extra- cellular enviroments. The efflux rate constants (k_{ef}) (Table 3.3) were calculated importing the quantified EXSY data into EXSY CALC software (Mestrelab Research).
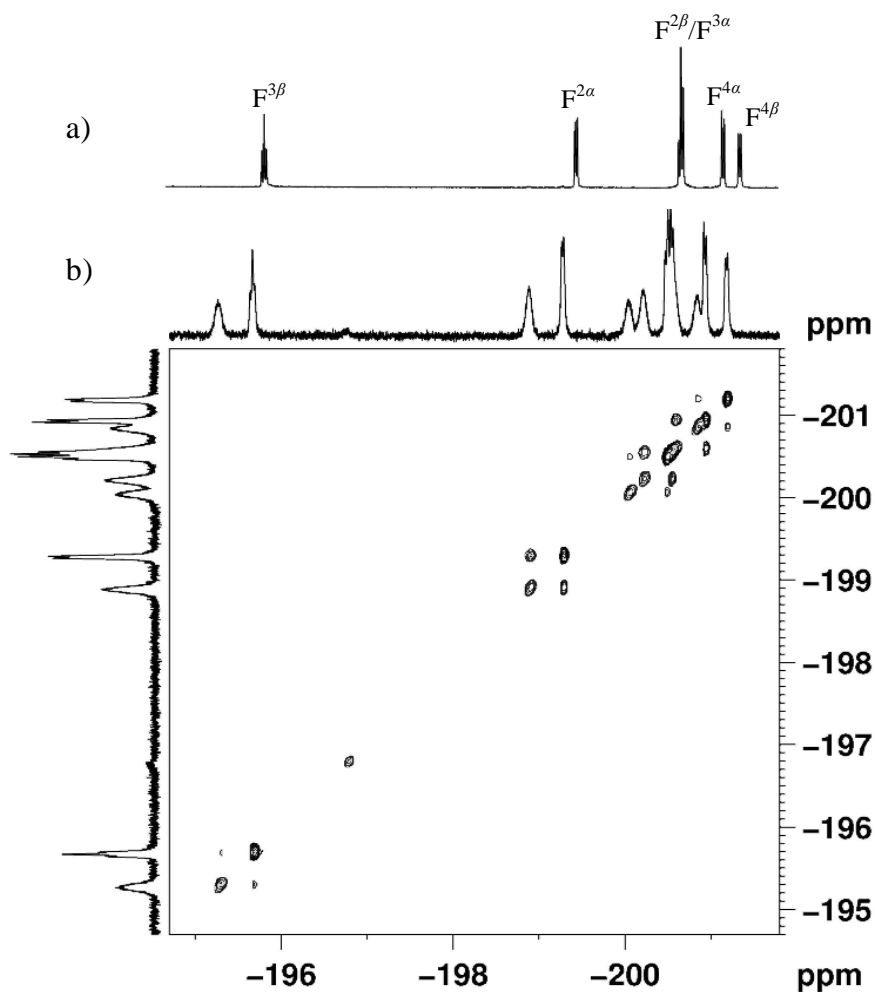
Figure 3.24 (a) ^{19}F{^{1}H}-NMR spectrum (470.4 MHz) (control experiment) of **193** in D$_2$O-Tris-HEPES buffer (b) ^{19}F EXSY-NMR spectrum of **193** in the presence of erythrocytes suspended in the buffer at 37 °C.

Over time a new metabolite appeared (Figure 3.25). Although the identification of this metabolite was not successful, it is apparent from the ^{19}F{^{1}H}-NMR spectrum that the metabolite is generated as a single diastereoisomer, and this might be indicative of an oxidation at the anomeric position to generate **204** (Figure 3.26). The formation of this metabolite was very slow, and did not interfere with the determination of the exchange rates of **193**.

113
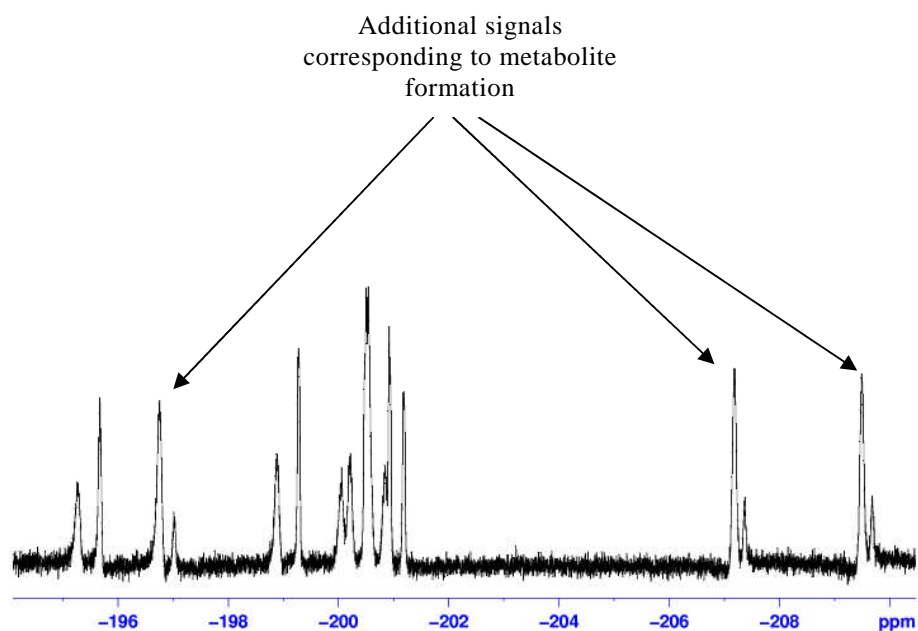
Figure 3.25. $^{19}F\{^{1}H\}$-NMR spectrum (470.4 MHz) of **193** in the presence of erythrocytes suspended in D$_2$O-Tris-HEPES buffer at 37 °C, showed additional signals corresponding to metabolite formation.

204
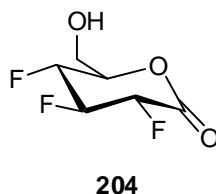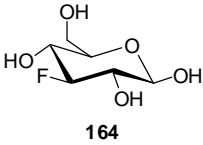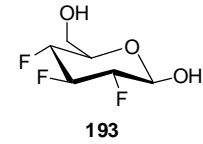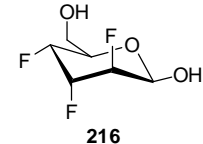
Figure 3.26. Putative metabolite generated by oxidation of **193** at the anomeric position.

London *et al.*[8] evaluated the human erythrocyte transmembrane transport of the 3-deoxy-3-fluoro-D-glucose **164**, and showed transport ability similar to that of the D-glucose. The corresponding k_{ef} is reported in Table 3.4. This experiment was now repeated, and the resulting k_{ef} (Table 3.4) found to be in good agreement with the literature.[8] The D-glucose **193** and D-altrose **216** analogues cross the human erythtrocyte membrane less efficiently when compared to **164**, but **193** was transported better (~70% efficiency) than **216**.

114

Furthermore, for **193** there is a marked preference for transport of the α-anomer over the β-anomer. Conversely, for **216**, transport is slow and there is no obvious preference for a particular anomer.

	k_{ef} [s^{-1}]	
	α-anomer	β-anomer
164 (3-F-D-glucose)[a]	1.35±0.32	1.04±0.23
164 (3-F-D-glucose)[b]	1.38±0.02	1.01±0.08
193 (D-glucose)[b]	0.97±0.21	0.22±0.07
216 (D-altrose)[b]	0.33±0.07	0.40±0.05

[a]Data from the literature.[8]

[b]Data reproduced in this work.

Table 3.4. Efflux rate constants for **164**, **193** and **216** across erythrocyte cell membranes measured by 2D ^{19}F EXSY-NMR. The values reported are averages from different ^{19}F resonances and mixing times. Errors are standard deviations.

3.4) Conclusion:

Two fully deprotected trifluoro D-hexose analogues **193** and **216** (Figure 3.27), were successfully synthesised and characterised.
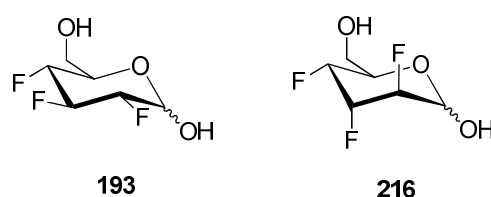
Figure 3.27. D-glucose analogue **193** and D-altrose analogue **216**.

115

Transmembrane studies provided efflux rate constants (k_{ef}), indicating that the Glut1 transmembrane protein can recognise and selectively transport these analogues. The study suggested, that Glut1 can recognise the stereogenicity associated with the C-F bonds, and favours the glucose over the altrose analogue as expected. This raises the possibility that recognition occurs through dipolar interactions rather than hydrogen bonding. Furthermore, a clear distinction between the transport of the *α*- and *β*- anomers of **193** was observed, similar to the 3-deoxy-3-fluoro-D-glucose analogue **164** and also D-glucose itself.

References Chapter 3

[1] M. Hein, R. Miethchen, *Adv. Org. Synth.*, 2006, **2**, 381-429.

[2] K. Dax, M. Albert, J. Ortner, B. J. Paul, *Carbohydrate Res.*, 2000, **327**, 47-86.

[3] I. P. Street, C. R. Armstrong, S. G. Withers, *Biochemistry*, 1986, **25**, 6021-6027.

[4] L. L. Lairson, B. Henrissat, G. J. Davies, S. G. Withers, *Ann. Rev. Biochem.*, 2008, **77**, 521-555.

[5] S. A. Allman, H. H. Jensen, B. Vijayakrishnan, J. A. Garnett, E. Leon, Y. Liu, D. C. Anthony, N. R. Sibson, T. Feizi, S. Matthews, B. G. Davis, *ChemBioChem*, 2009, **10**, 2522-2529.

[6] M. Michalik, M. Hein, M. Frank, *Carbohydr. Res.*, 2000, **327**, 185-218.

[7] L. Cai, S. Lu, V. W. Pike, *Eur. J. Org. Chem.*, 2008, **17**, 2853-2873.

[8] T. M. O'Connell, S. A. Gabel, R. E. London, *Biochemistry*, 1994, **33**, 10985-10992.

[9] S. G. Withers, M. D. Percival, I. P. Street, *Carbohydrate Res.*, 1989, **187**, 43-66.

[10] (a) J. Pakák, J. Podešva, Z. Točik, M. Černý, *Collect. Czech. Chem. Commun.*, 1972, **37**, 2589-2599.

[11] H. W. Kim, P. Rossi, R. K. Shoemaker, S. G. DiMagno, *J. Am. Chem. Soc.*, 1998, **120**, 9082-9083.

[12] J. C. Biffinger, H. W. Kim, S. G. DiMagno, *ChemBioChem.*, 2004, **5**, 622-627.

[13] A. J. Boydell, V. Vinader, B. Linclau, *Angew. Chem. Int. Ed.*, 2004, **43**, 5677-5679.

[14] B. Linclau, A. J. Boydell, R. S. Timofte, K. J. Brown, V. Vinader, A. C. Weymouth-Wilson, *Org. Biomol. Chem.*, 2009, **7**, 803-814.

[15] R. S. Timofte, B. Linclau, *Org. Lett.*, 2008, **10**, 3673-3676.

[16] L. Bonnac, S. E. Lee, G. T. Giuffredi, L. M. Elphick, A. A. Anderson, E. S. Child, D. J.

Mann, V. Gouverneur, *Org. Biomol. Chem.*, 2010, **8**, 1445-1454.

[17] (a) P. Sarda, F. C. Escribano, R. J. Alves, A. Olesker, G. Lukacs, *J. Carbohydr. Chem.*, 1989, **8**, 115-123; (b) J. Pakák, Z. Točik, M. Černý, *Chem. Commun.*, 1969, 77.

[18] M. Černý, L. Kalvoda, J. Pakák, *Collect. Czech. Chem. Comm.*, 1968, **33**, 1143-1155.

[19] A. Salas-Burgos, P. Iserovich, F. Zuniga, J. C. Vera, J. Fischbarg, *Biophys. J.*, 2004, **87**, 2990-2999.

[20] G. W. Gould, G. D. Holman, *Biochem. J.*, 1993, **295**, 329-341.

[21] Y. Huang, M. J. Lemieux, J. Song, M. Auer, D. N. Wang, *Science*, 2003, **301**, 616-620.

[22] J. Abramson, I. Smirnova, V. Kasho, G. Verner, H. R. Kaback, S. Iwata, *Science*, 2003, **301**, 610-615.

[23] G. J. Riley, N. F. Taylor, *Biochem. J.*, 1973, **135**, 773-777.

[24] A, K. Sen, W. F. Widdas, *J. Physiol.*, 1962, **160**, 392-403.

[25] J. R. Potts, A. M. Hounslow, P. W. Kuchel, *Biochem. J.*, 1990, **266**, 925-928.

[26] R. E. London, S. A. Gabel, *Biochemistry*, 1989, **28**, 2378-2382.

[27] R. E. London, S. A. Gabel, *Biophys. J.*, 1995, **69**, 1814-1818.

[28] P. G. LeFevre, *Symp. Soc. Exp. Biol.*, 1954, **8**, 118-135.

[29] R. Bloch, *Biochemistry*, 1973, **12**, 4799-4801.

[30] G. J. Riley, N. F. Taylor, *Biochem. J.*, 1973, **135**, 773-777.

[31] J. R. Appleman, G. E. Lienhard, *Biochemistry*, 1989, **28**, 8221-8227.

[32] G. J. Riley, N. F. Taylor, *Biochem. J.*, 1973, **135**, 773-777.

[33] A. Leo, *J. Chem. Soc., Perkin Trans*, 1983, **2**, 825-838.

[34] F. M. Menger, U. V. Venkataram, *J. Am. Chem. Soc.*, 1986, **108**, 2980-2984.

[35] M. Fujita, H. Ishizuka, K. Ogura, *Tetrahedron Lett.*, 1991, **32**, 6355-6358.

[36] D. Albanese, D. Landini, M. Penso, *Tetrahedron Lett.*, 1993, **33**, 7295-7300.

[37] D. Albanese, D. Landini, M. Penso, *Tetrahedron Lett.*, 1992, **48**, 4163-4170.

[38] G. Islas-González, C. Puigjaner, A. Vidal-Ferran, A. Moyano, A. Rieira, M. A. Pericás, *Tetrahedron Lett.*, 2004, **45**, 6337-6341.

[39] T. Inagaky, T. Fukuhara, S. Hara, *Synthesis*, 2003, **8**, 1157-1159.

[40] V. Brunet, PhD thesis, "*Synthesis Studies to Single Stereoisomers of the Vicinal Trifluoroalkane Motif*", University of St. Andrews, 2009.

[41] G. S. Lai, G. P. Pez, R. J. Pesaresi, F. M. Prozonic, H. Cheng, *J. Org. Chem.*, 1999, **64**, 7048-7054.

[42] M. Adinolfi, G. Barone, L. Guariniello, A. Iadonisi, *Tetrahedron Lett.*, 1999, **40**, 8439-8441.

[43] F. A. Davis, V. Srirajan, D. D. Titus, *J. Org. Chem.*, 1999, **64**, 6931-6934.

[44] X. –H. Xu, Z. – W. You, X. Zhang, F. – L. Qing, *J. Fluorine Chem.*, 2007, **128**, 535-539.

Chapter 4. Stereospecific dehydroxyfluorination of enantiopure benzylic alcohols with TMS-amine additives

4.1) Introduction:

4.1.1) Strategies in stereospecific nucleophilic fluorination of alcohols:

Over the last 20 years a large number of reagents have been developed for the incorporation of stereogenic C-F bonds into organic molecules, and in this context, catalytic asymmetric fluorinations have attracted a lot of attention.[1] The stereospecific conversion of an enantiomerically pure alcohol to its corresponding fluoride, with high stereointegrity, can also be very attractive, due to the relative easy of access to enantiopure alcohols as starting materials. S_N2 reactions are required, however, there are frequently side-reactions associated with such dehydroxyfluorinations; for instance, the fluorination (Scheme 4.1) can follow an S_N1 reaction course (racemisation), or proceed with retention of configuration (anchimeric assistance), as well as generate elimination or rearrangement products.[2] The outcome depends on the nature of the alcohol, the reaction conditions (temperature and solvent) and the type of dehydroxyfluorinating reagent used (nature of the leaving group).[2]

120
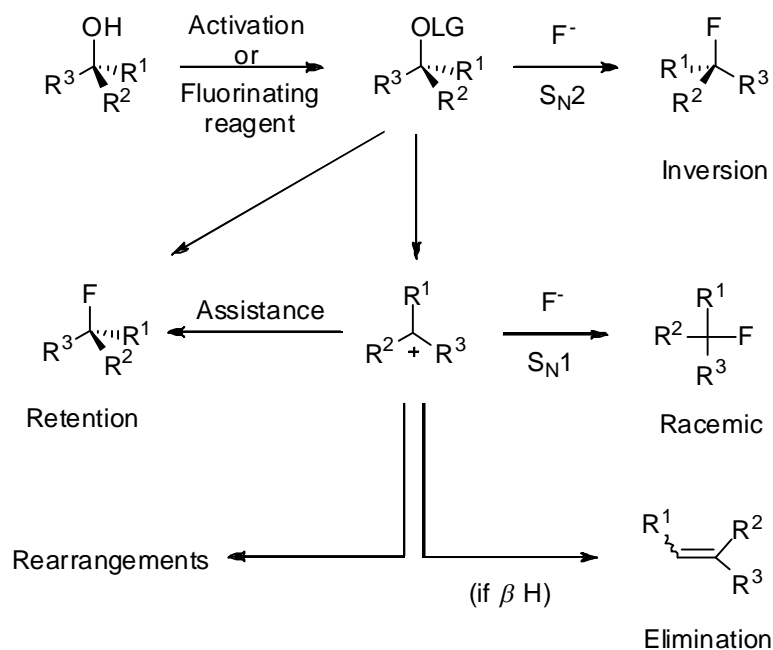
Scheme 4.1. The dehydroxyfluorination reaction of an enantiopure alcohol can follow different reaction pathways.[2]

Particularly, the stereospecific conversion of an enantiomerically pure benzylic alcohol to the corresponding benzylic fluoride with high stereochemical integrity (S_N2 reaction) is a major challenge, due to competing S_N1 reactions. Such reactions can be achieved either by nucleophilic fluorination of e.g. tosylates or mesylates, or by a direct dehydroxyfluorination of the alcohol (see Paragraph 1.5.1, Chapter 1). For instance, the tosylate derivative (*R*)-**205** of (*R*)-2-octanol has been subjected to nucleophilic fluorination, by the use of several nucleophilic sources of fluoride under different conditions, to generate (*S*)-2-fluorooctane **206** and 1-octene (Table 4.1).[3,4,5] The best % ee (100%) was obtained by reaction of (*R*)-**205** with the methyl *tri-n*-butylfluorophosphorane (*n*-Bu$_3$PMeF), although the yield was low. Tetrabutylammonium fluoride (TBAF) generated (*S*)-**206** in 54% yield and 96% ee.

(R)-**205**   (S)-**206**
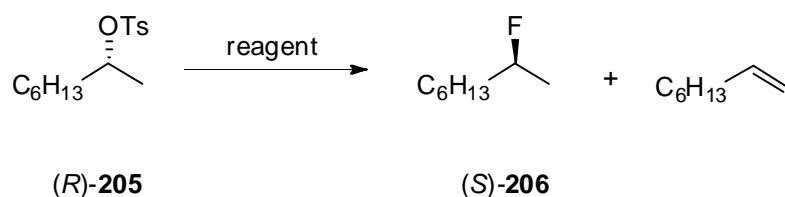
Reagent	(S)-**206**[a]	1-octene[a]	(S)-**206**[b]	$[\alpha]_D^{20}$	% ee of (S)-**206**
KF	50	50	31	13.5	91
n-Bu$_3$PMeF	40	60	15	14.8	100
TBAF	58	33	54	14.2	96

[a] Ratios by GC; [b] Isolated yields.

Table 4.1. Nucleophilic fluorination of the tosylate (R)-**205** by the use of several nucleophilic sources of fluoride.[2-5]

A systematic study was carried out exploring nucleophilic fluorination of a series of sulfonates (R)-**207** by reaction with metal fluorides (MF) such as cesium (CsF) or potassium fluoride (KF) in different solvents (Table 4.2). This generated (S)-**208**, and alcohol (R)-**209** as a side-product (Table 4.2).[6] Yields of this reaction were higher using CsF instead of KF. Furthermore, the presence of R^1 electron withdrawing groups proved necessary to favour the formation of **208** over the generation of side-product alcohol (R)-**209**.

Due to the low solubility of (R)-**207** with R^1 = CN and R^1 = CO$_2$Et in polar solvents, which results in lower yields, the use of N-methylformamide (MFA) is preferred over DMF or formamide (FA). In most of the fluorination reactions attempted,[6] product (S)-**208** was generated with high stereospecificity (S$_N$2 mechanism), in spite of the fact that an S$_N$1 mechanism is generally favoured for a benzylic substrate.[6]
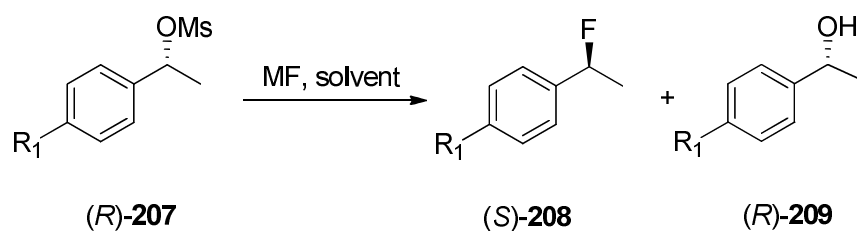
R[1]	MF (equiv.)	solvent	T (°C)	Time (h)	Yield of (S)-208 (%)	% ee of (S)-208
CN	CsF (4)	MFA	60	4	81	96.0
CN	CsF(4)	DMF	60	4	60	ND[a]
CO$_2$Et	CsF(4)	MFA	60	1	46	73.0
NO$_2$	CsF(2)	MFA	100	0.5	73	ND[a]
NO$_2$	CsF(8)	MFA	100	0.5	75	91.4
NO$_2$	CsF(16)	FA	60	1	62	ND[a]
NO$_2$	KF(8)	FA	60	8	25	ND[a]

Table 4.2. Selected examples of nucleophilic fluorinations of the mesylate (R)-**207**.[6]

[a] Not detemined.

When the mesylate derivative (S)-**210** was treated with 4 equiv. of CsF in MFA, only the formation of racemic-**211** was observed (Scheme 4.2).[6] The racemisation process is most likely due to α-deprotonation by basic fluoride (also favoured by the presence of the electron withdrawing ester function), as the ^{1}H-NMR analysis showed disappearance of the benzylic proton signal of (S)-**210** in d_7-DMF/D$_2$O after addition of CsF.

Scheme 4.2. Nucleophilic fluorination of the mesylate (S)-**210** with CsF gave a racemic product.[6]

An alternative strategy involves direct dehydroxyfluorination of alcohols (see chapter 1). Several examples are reported in the literature.[2] For instance, direct dehydroxyfluorination of (R)-2-octanol **212** was carried out by the use of the Yarovensko's reagent (ClCHFCF$_2$NEt$_2$), DAST and phenyltetrafluorophosphorane (PhPF$_4$), which generated (S)-**206** and octene (Table 4.3[2,3]). It is interesting to compare these results with those reported in Table 4.1. The best dehydroxyfluorination reagent in terms of stereospecificity was DAST, although the yield was low due to substantial elimination to generate octene.

Table 4.3. Examples of dehydroxyfluorination reactions of (R)-**212**.[3]
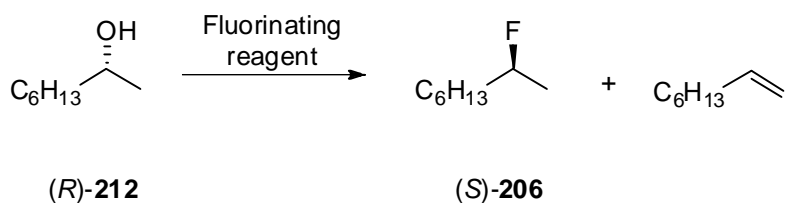
Reagent	(S)-206 (%)	1-octene (%)	Isolated yield of (S)-206 (%)	% ee of (S)-206
ClCHFCF$_2$NEt$_2$	78	22	40	88
DAST	48	52	23	98
PhPF$_4$	58	42	11	69

(R)-1-Phenylethanol **213** reacts with N,N-diethyl-1,1,2,3,3,3-hexafluoropropaneamine (Ishikawa's reagent) to generate (1-fluoroethyl)benzene **214**. Oxidation by the action of RuCl$_3$/KIO$_4$ (Scheme 4.5) generated carboxylic acid **215**.[7] The acid was then derivatised by coupling to (R)-methyl mandelate in N,N'-dicyclohexylcarbodiimide (DCC) and 4-dimethylaminopyridine (DMAP) to generate ester **217** (Scheme 4.3). ^{1}H-NMR analysis

revealed product **217** in 55% de, presumably in favour of the diastereoisomer with the inverted configuration. Thus at least a 55% ee was assigned to the enantiopurity of 2-fluorobenzene **214**.
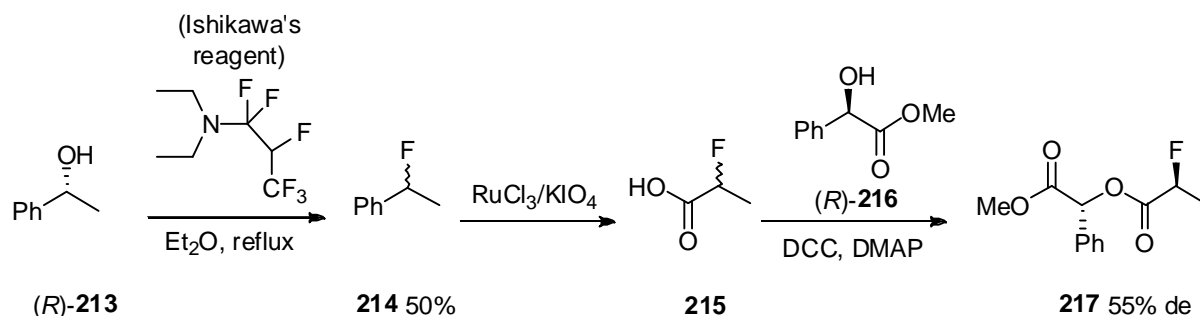
Scheme 4.3. Dehydroxyfluorination of (*R*)-**213** and subsequent derivatisation to **217**.[7]

The dehydroxyfluorination reaction of (*R*)-ethyl mandelate **218** with the Ishikawa's reagent generated ethyl 2-fluoro-2-phenylacetate **211** in 66% yield (Scheme 4.4).[8] Reduction of **211** with LiAlH$_4$ generated alcohol **220**, which was then coupled with the Mosher reagent (*R*)-α-methoxy-α-trifluoromethylphenylacetic acid (*R*)-MPTA **221**, to give the corresponding ester **222** in 74% de, presumably in favour of the inverted product. Thus, at least a 74% ee was assigned to the enantiopurity of **211**.
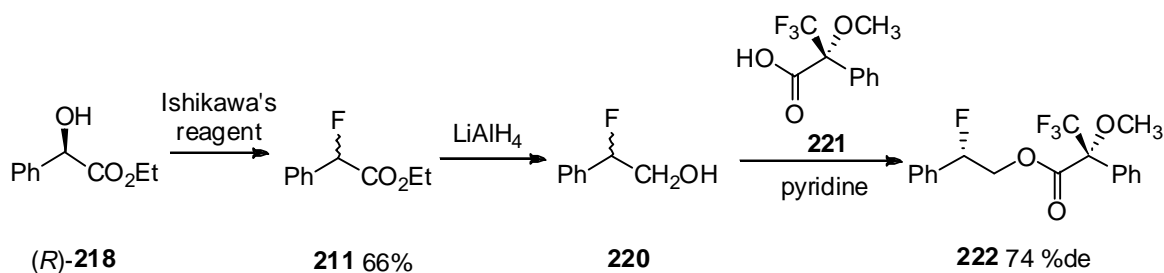
Scheme 4.4. Fluorination of (*R*)-**218** and subsequent derivatisation to **222**.[8]

4.1.2) Bio's TMS-amine additive approach:

In 2008, in a medicinal chemistry program aimed at the preparation of a *N*-methyl-D-aspartate (NMDA) antagonist analogue, Bio *et al.*[9] investigated the stereospecificity of the DAST- and Deoxofluor^{TM}-mediated dehydroxyfluorination reactions of two *ortho*-fluorobenzylic alcohols (*S*)-**223a** and (*S*)-**223b** (Table 4.4). For instance reaction of (*S*)-**223a** with Deoxofluor^{TM} (Entry 1, Table 4.4) and DAST (Entry 2, Table 4.4) in CH_2Cl_2 generated (*R*)-**224a** in 50% ee and 38% ee respectively, with configurational inversion.

A considerable improvement in the stereospecificity of this reaction was achieved when alcohol (*S*)-**223a** was added to a solution of DAST and *N*-(trimethylsilyl)diethylamine **225** (Figure 4.1) in CH_2Cl_2, to provide (*S*)-**224a** in 99% ee (Entry 3, Table 4.4). However this also gave a substantial amount of elimination product. Replacement of DAST and additive **225** with Deoxofluor^{TM} and *N*-(trimethylsilyl)morpholine **226** (Figure 4.1) significantly reduced the elimination side-reaction, allowing the reaction to be performed at 0 °C instead of -70 °C, with negligible loss of stereospecificity (Entry 4, Table 4.4).[9]

(S)-223a R = Cbz
(S)-223b R = Boc

(R)-224a R = Cbz
(R)-224b R = Boc
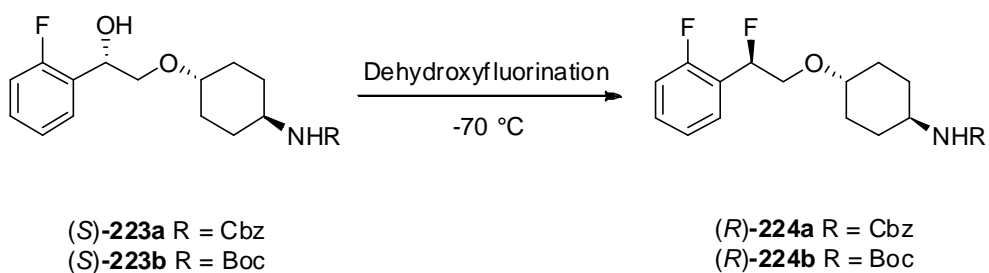
Entry	Solvent	Fluorinating reagent (equiv.)	Additive	% ee of (R)-224a or (R)-224b
1	CH$_2$Cl$_2$	Deoxofluor^{TM}	none	50
2	CH$_2$Cl$_2$	DAST	none	38
3	CH$_2$Cl$_2$	DAST	**225**	99
4	toluene^a	Deoxofluor^{TM}	**226**	96

^{a} Reaction performed at 0 °C.

Table 4.4. Stereospecificity of dehydroxyfluorination reactions of (S)-**223a** and (S)-**223b** under various conditions.

N-(trimethylsilyl)diethylamine

225

N-(trimethylsilyl)morpholine

226
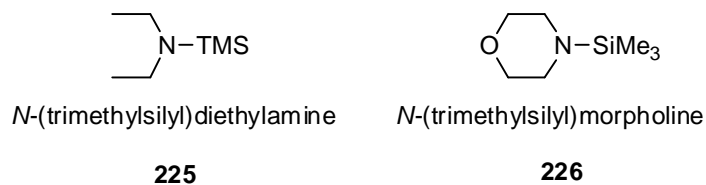
Figure 4.1. Additives **225** and **226**.

4.2) Aims and objectives:

Encouraged by the results obtained by Bio *et al.*,[9] it became an objective to apply this methodology to the benzylic dehydroxyfluorination reaction of more challenging substrates, such as benzylic alcohols without fluorine at the *ortho*-aryl position. The presence of the *ortho* fluorine destabilises the benzylic carbocation intermediate, and promotes inversion (S_N2). It was envisaged that benzylic alcohol substrates (*R*)-1-phenylethanol **213** and methyl (*R*)-(-)-mandelate **227** (Figure 4.2) would present more challenging substrates as they are more prone to S_N1 reaction courses. In this study, Bio's methodology[9] is applied to benzylic dehydroxyfluorination reactions of (*R*)-**213** (Scheme 4.5) and (*R*)-**227** (Scheme 4.6), to generate (*S*)-(1-fluoroethyl)benzene **214** and (*S*)-methyl 2-fluoro-2-phenylacetate **228** respectively.

(*R*)-**213**   (*R*)-**227**
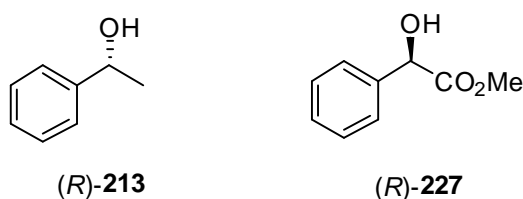
Figure 4.2. Benzylic alcohol substrates (*R*)-**213** and (*R*)-**227**.

Fluorinating reagent /
TMS-amine additive

(*R*)-**213**   (*S*)-**214**
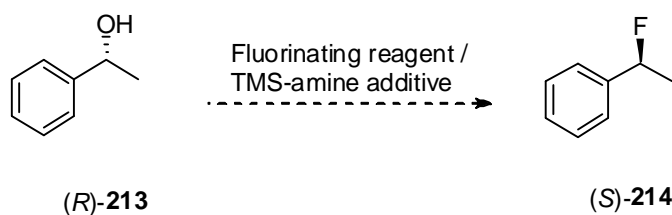
Scheme 4.5 Envisaged stereospecific benzylic dehydroxyfluorination of (*R*)-**213**.
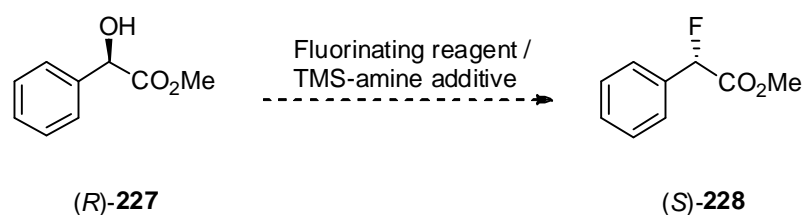
Scheme 4.6 Envisaged stereospecific benzylic dehydroxyfluorination of (*R*)-**227**.

Without any TMS amine, reactions of (*R*)-**213** and (*R*)-**227** with 1.1 equiv. of DAST in CH$_2$Cl$_2$ gave the corresponding benzylic fluorides in 7% ee and 8% ee respectively, thus there was considerable room for improvement.

4.3) Results and discussion:

4.3.1) Stereospecific benzylic dehydroxyfluorination of (*R*)-213:

To provide a framework for this study, the dehydroxyfluorination reaction of alcohol (*R*)-**213** was explored with four dehydroxyfluorination reagents (see Paragraph 5.4, Chapter 5): Fluolead^{TM}, TFEDMA, Deoxofluor^{TM} and DAST (Figure 4.3). At the beginning of this study, an analytical method to determine the enantiopurity of the fluorinated product **213** was necessary. Attempts to determine the enantiomeric ratios by ^{19}F-NMR analysis with the chiral adducting reagent (+)-methyl D-lactate and by ^{1}H-NMR analysis with lanthanide shift reagents proved unsuccessful. Also an assessment of the enantiomeric purities by chiral HPLC also failed, as separation of the enantiomers could not be achieved, despite exploring a range of different columns and conditions. Separation of the enantiomers of **214** by chiral GC

was successful (Figure 4.4). Therefore, the % ee's of benzylic fluoride **214** were determined

by chiral-phase GC-MS, directly on the product mixture (see Paragraph 5.5, Chapter 5).
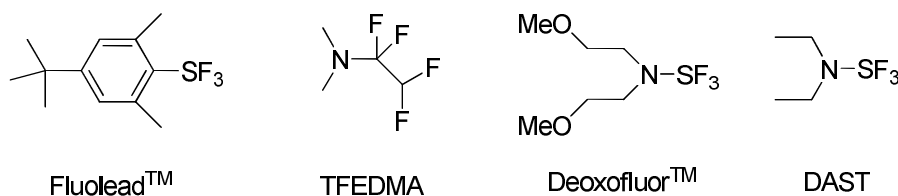
Figure 4.3. Dehydroxyfluorination reagents employed in this study.
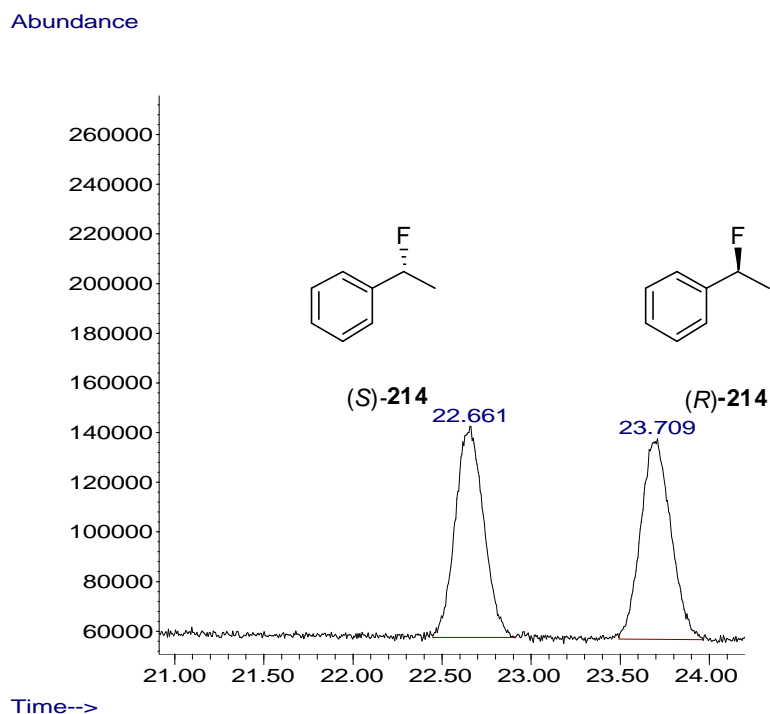
Figure 4.4. Chiral-phase GC chromatogram of racemic-**214**: temperature-gradient oven (80 °C for 30 min), 250 °C injector temperature, 100:1 split ratio, 0.9 ml/min flow, He carrier gas, Betadex[TM] 120 fused silica capillary column (30 m x 0.25 mm i.d., 0.25 µm film thickness), MS (EI) detection.

Treatment of (*R*)-**213** with 1.1 equiv. of each fluorinating reagent in CH_2Cl_2, either at -78°C or RT, led to product **214** of very low enantiopurity (Table 4.5). Deoxofluor[TM] proved to be the best reagent in terms of stereospecificity (Entry 3, Table 4.5). When the reaction with (*R*)-

213 was carried out at -78 °C, there was no improvement of % ee. This was the case for all four dehydroxyfluorination reagents.

(R)-**213**
1.0 equiv., 0.20 M
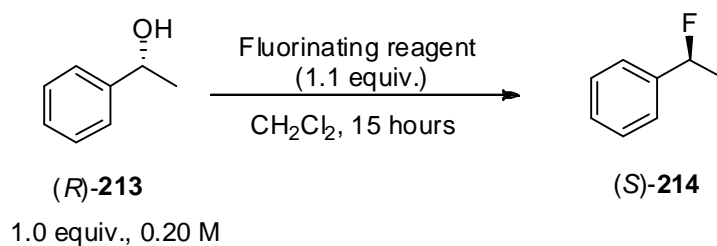
(S)-**214**

Entry	Fluorinating reagent (1.1 equiv.)	% ee of (S)-214 (-78 °C)	% ee of (S)-214 (RT)
1	Fluolead^{TM}	0	0
2	TFEDMA	3	0
3	Deoxofluor^{TM}	13	13
4	DAST	7	7

Table 4.5. Stereospecificity of dehydroxyfluorination reactions of (R)-**213**.

The next stage of the study involved exploring the use of the TMS-amine additives **226** and **229** (Figure 4.5) to assess if they could be added to improve the enantiopurity of product **214**.

N-(trimethylsilyl)morpholine

226

N-(trimethylsilyl)pyrrolidine

229
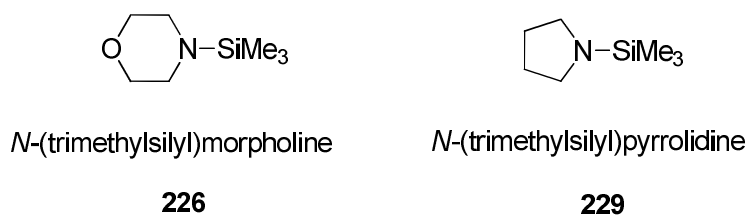
Figure 4.5. TMS-amine additives **226** and **229** used in this study.

Reactions were performed either at -78 °C or RT by addition of a solution of (R)-**213** in CH$_2$Cl$_2$ to a solution of a 1.1 equiv. of a preformed 1:1 fluorination reagent:TMS-amine adduct in CH$_2$Cl$_2$ (Table 4.6). Moderate to good % ee's (52-74) were obtained in all cases.

131

No significant difference was observed for the enantiopurity of the products either at -78 °C or RT. Fluorination of (*R*)-**213** with TFEDMA and either additives **226** or **229** proceeded with very low conversion (Entries 3 and 4, Table 4.6), thus TFEDMA was not explored further. Also fluorination of (*R*)-**213** with Fluolead™ and either **226** or **229** gave a very low conversion at -78 °C. However t.l.c analysis indicated a good conversion to product **214** when the reaction was performed at RT (Entries 1 and 2, Table 4.6). The best outcome in terms of enantiopurity was generated by the reaction of (*R*)-**213** with 1.1 equiv. of a 1:1 DAST:**226** adduct (Entry 7, Table 4.6).
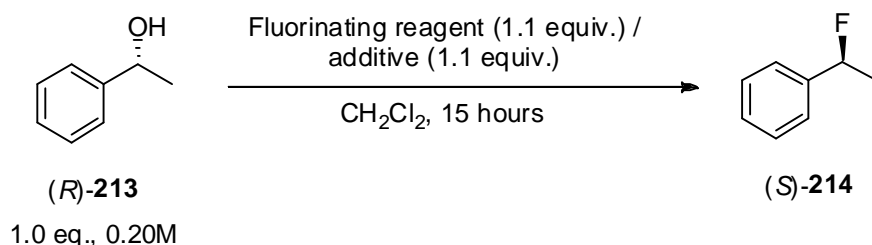
Entry	Fluorinating reagent (1.1 equiv.)	Additive (1.1 equiv.)	% ee of (*S*)-214 (-78 °C)	% ee of (*S*)-214 (RT)
1	Fluolead™	**226**	Low conversion	57
2	Fluolead™	**229**	Low conversion	56
3	TFEDMA	**226**	Low conversion	Low conversion
4	TFEDMA	**229**	Low conversion	Low conversion
5	Deoxofluor™	**226**	56	58
6	Deoxofluor™	**229**	65	66
7	DAST	**226**	72	74
8	DAST	**229**	52	54

Table 4.6. Enantiomeric purity of (*S*)-**214** under various conditions.

The effect of varying the number of equiv. of additive was then investigated. The resulting % ee's, and selected % conversions determined by GC-FID using *n*-decane as an internal standard (see Paragraph 5.5, Chapter 5) are shown in Table 4.7. Changing the

reaction solvent from CH$_2$Cl$_2$ to toluene did not significantly improve the % ee (Entry 5, Table 4.7), however CH$_2$Cl$_2$ was preferred due to its higher volatility which simplifies isolation and purification of products. Generally a substantial improvement of % ee occurs by addition of 3.3 equiv. of a preformed 1:1 fluorinating reagent:TMS-amine adduct of either **226** or **229**. The most significant improvement was made by addition of 3.3 equiv. of a preformed 1:1 DAST:**226**. The reaction improved from an almost racemic product (Entry 4, Table 4.5) to generate (*S*)-**214** in 95% ee with an excellent conversion (Entry 7, Table 4.7). Reaction with Fluolead^{TM} under similar conditions gave a product (*S*)-**214** in 92% ee, however the conversion (34%) was modest (Entry 1, Table 4.7).

(*R*)-**213**
1.0 eq., 0.20M
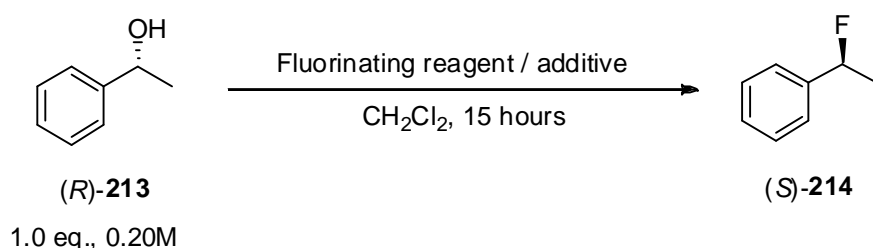
(*S*)-**214**

Entry	Fluorinating reagent (equiv.)	Additive (equiv.)	% ee of (*S*)-214 (% conv.)
1	Fluolead^{TM} (3.3)	**226** (3.3)	92 (34)
2	Fluolead^{TM} (3.3)	**229** (3.3)	85
3	Deoxofluor^{TM} (3.3)	**226** (3.3)	84 (96)
4	Deoxofluor^{TM} (3.3)	**229** (3.3)	59
5	DAST (1.1)^a	**226** (1.1)	75
6	DAST (2.2)	**226** (2.2)	83
7	DAST (3.3)	**226** (3.3)	95 (92)
8	DAST (4.4)	**226** (4.4)	93
9	DAST (8.8)	**226** (8.8)	93
10	DAST (3.3)	**229** (3.3)	69

^{a} Reaction performed in toluene.

Table 4.7. The stereospecificity of dehydroxyfluorination of (*R*)-**213** under various conditions.

The enantiopurity of (*S*)-**214** could not be further improved by the addition of more than 3.3 equiv. (Entries 8 and 9, Table 4.7). A rationale for the improved stereospecificity using 3.3 eq of adduct is illustrated in Scheme 4.7. Reaction of the first equiv. of 1:1 fluorinating reagent:TMS-amine adduct with the alcohol generates one equiv. of HF, which may catalize the S_N1 process (1). The addition of a second equiv. of adduct will buffer the HF as hydrogen bifluoride (HF_2^-), which is a weak nucleophile (2). The addition of a third equiv. would then generate a free fluoride ion (F^-), which is a better nucleophile than hydrogen bifluoride, and as a result the S_N2 mechanism predominates over the S_N1 mechanism (3).
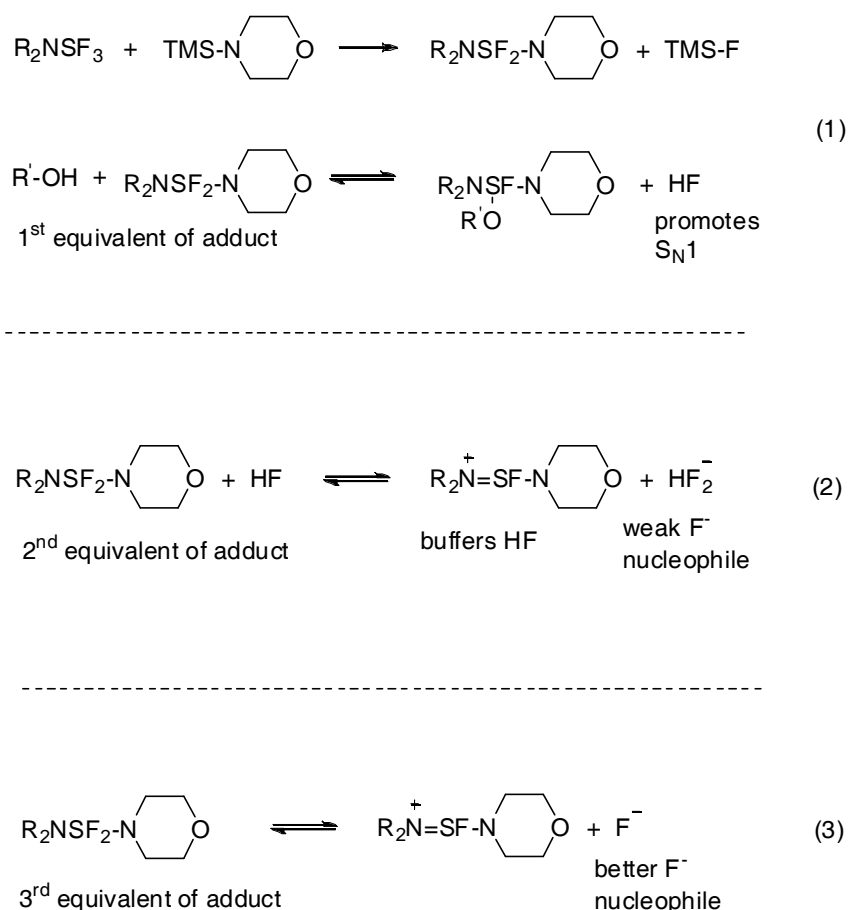
Scheme 4.7. Rationale for the improved stereospecificity at three equiv. of a preformed 1:1 fluorinating reagent:TMS-amine adduct.

134

4.3.2) Stereospecific benzylic dehydroxyfluorination of (*R*)-227:

Separation of the enantiomers of **228** by chiral GC was successful (Figure 4.6). Thus, the %

ee's of benzylic fluoride **228** were determined by chiral-phase GC-MS, directly on the

product mixture (see Paragraph 5.5, Chapter 5).
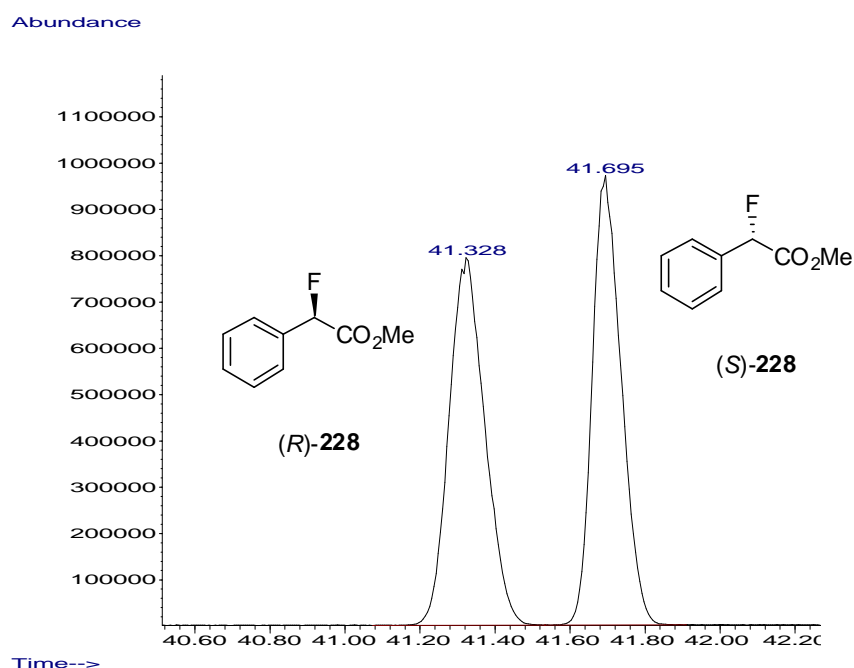
Figure 4.6. Chiral-phase GC chromatogram of racemic-**228**: temperature-gradient oven (start at 110 °C

held for 40 min, then gradient at 20 °C/min to 150 °C held for 15 min), 250 °C injector temperature, 100:1

split ratio, 0.9 ml/min flow, He carrier gas, Betadex[TM] 120 fused silica capillary column (30 m x 0.25 mm

i.d., 0.25 µm film thickness), MS (EI) detection.

Dehydroxyfluorination of (*R*)-**227** with 1.1 equiv. of each fluorinating reagent in CH_2Cl_2

either at -78 °C or RT, similarly to that of (*R*)-**213**, generated product **228** of low

enantiopurity (Table 4.8). Reactions performed at -78 °C did improve the % ee to some

extent over those at RT (Table 4.8). Product conversion was low even after extended reaction

135

times, and particularly with the reaction of (R)-**227** with TFEDMA (Entry 2, Table 4.8). Accordingly reactions with TFEDMA were not further attempted.

Table 4.8. Stereospecificity of dehydroxyfluorination reactions of (R)-**227**.
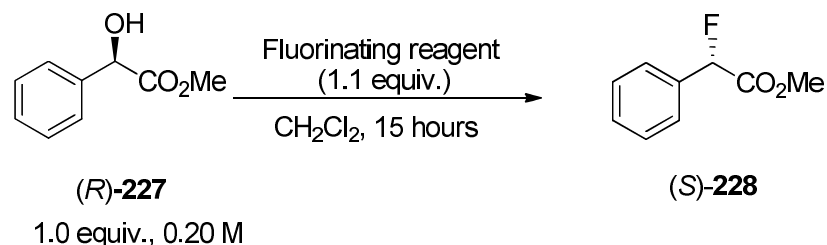
Entry	Fluorinating reagent (1.1 equiv.)	% ee of (S)-228 (-78 °C)	% ee of (S)-228 (RT)
1	Fluolead^{TM}	40	3
2	TFEDMA	low conversion	12
3	Deoxofluor^{TM}	48	25
4	DAST	19	8

Fluorinations of (R)-**227** with 1.1 equiv. of fluorinating reagent:TMS-amine adduct are shown in Table 4.9. The selected % conversion were determined by GC-FID, using *n*-decane as an internal standard (see Paragraph 5.5.2, Chapter 5). Although the reaction time was extended to 24 h to enhance conversion, Fluolead^{TM} was found to be unreactive at -78 °C in combination with either **226** or **229** (Entries 1 and 2, Table 4.9). Furthermore Fluolead^{TM} gave rise to higher % ee's when **229** is used as an additive at RT (Entry 2, Table 4.9). It is clear that there is a major improvement in the stereospecificity (up to 99% ee) for Deoxofluor^{TM} (Entries 3 and 4, Table 4.9) and DAST (Entries 5 and 6, Table 4.9) with the addition of either **226** or **229**. However, using **226** as an additive, DeoxoFluor^{TM} (Entry 3, Table 4.9) gave a better conversion than DAST (Entry 5, Table 4.9).

Reaction scheme:

OH
Ph—CH(CO₂Me) (R)-**227**
1.0 eq., 0.20M

Fluorinating reagent (1.1 equiv.) /
additive (1.1 equiv.)
————————————————→
CH₂Cl₂, 24 hours

F
Ph—CH(CO₂Me) (S)-**228**
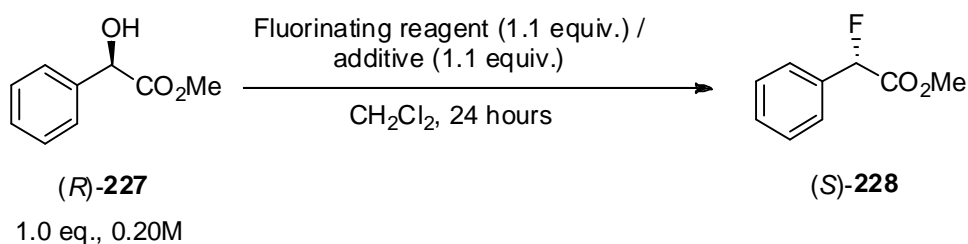
Entry	Fluorinating reagent (1.1 equiv.)	Additive (1.1 equiv.)	% ee of (*S*)-**228** (-78 °C)	% ee of (*S*)-**228**, RT (% conv.)
1	Fluolead™	**226**	Low conversion	64
2	Fluolead™	**229**	Low conversion	89
3	Deoxofluor™	**226**	98	99 (51)
4	Deoxofluor™	**229**	97	98
5	DAST	**226**	99	99 (31)
6	DAST	**229**	98	98

Table 4.9. Enantiomeric purity of (*S*)-**228** under various conditions.

TMS-pyrrolidine **229** proved to be the best additive in combination with 3.3 equiv. of Fluolead™ (Entry 2, Table 4.10). Increasing the equiv. of adduct again did not further improve the stereospecificity in the reactions with Deoxofluor™ (Entries 3 and 4, Table 4.10) and DAST (Entries 5, 6 and 7, Table 4.10).
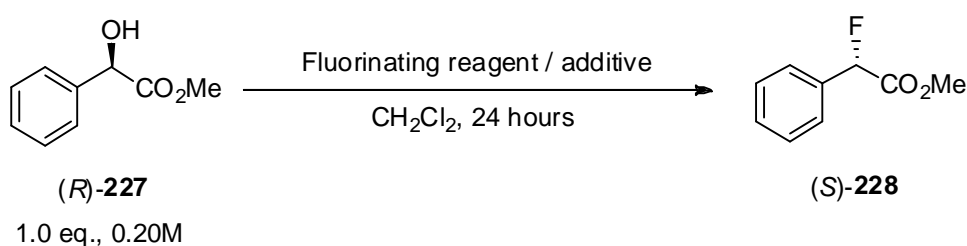
Entry	Fluorinating reagent (equiv.)	Additive (equiv.)	% ee of (*S*)-228 (% conv.)
1	Fluolead^{TM} (3.3)	**226** (3.3)	87 (20)
2	Fluolead^{TM} (3.3)	**229** (3.3)	94
3	Deoxofluor^{TM} (3.3)	**226** (3.3)	98
4	Deoxofluor^{TM} (4.4)	**226** (4.4)	98
5	DAST (2.2)	**226** (2.2)	98
6	DAST (3.3)	**226** (3.3)	97
7	DAST (4.4)	**226** (4.4)	97

Table 4.10. The stereospecificity of dehydroxyfluorination reactions of (*R*)-**227** under various conditions.

4.4) Conclusion:

The stereospecific conversion of an enantiomerically pure benzyl alcohol to the corresponding organic fluoride is a considerable challenge, due to a competing S_N1 reaction course. The methodology developed by Bio *et al.*[9] has successfully been applied to achieve the highly stereospecific benzylic dehydroxyfluorinations of (*R*)-**213** and (*R*)-**227**, using additives **226** and **229**. Addition of one equiv. of a preformed 1:1 fluorinating reagent:TMS-amine adduct noticeably improved the % ee for the dehydroxyfluorination of both substrates (*R*)-**213** and (*R*)-**227**. However, the best result for substrate (*R*)-**213**, the more challenging in terms of suppressing the S_N1 pathway, was obtained using three equiv. of the adduct. Benzylic fluorides (*S*)-**214** and (*S*)-**228** of up to 95% ee and 99% ee, respectively, were prepared by the method. The dehydroxyfluorination of (*R*)-**227**

proceeded with the higher stereointegrity (S_N2 mechanism) compared to (*R*)-**213**, presumably due to the electron withdrawing effect of the ester function which suppresses the formation of a benzylic carbocation relative to a methyl group. However, in the case of (*R*)-**227**, reaction conversions were significantly lower, due to the electron-withdrawing nature of the ester group.

References Chapter 4

[1] V. Brunet, D. O'Hagan, *Angew. Chem. Int. Ed.*, 2008, **47**, 1179-1182.

[2] V. A. Soloshonok, "*Enantiocontrolled synthesis of fluoro-organic compounds*", Wiley, 1999.

[3] J. Leroy, E. Hebert, C. Wakselman, *J. Org. Chem.*, 1979, **44**, 3406-3408.

[4] S. Colonna, A. Re, G. Gelbard, E. Cesarotti, *J. Chem. Soc., Perkin Trans. 1*, 1979, 2248-2252.

[5] D. P. Cox, J. Terpinsky, W. Alwrynowicz, *J. Org. Chem.*, 1984, **49**, 3216-3219.

[6] E. Fritz-Langhals, *Tetrahedron: Asymmetry*, 1994, **5**, 981-986.

[7] D. O'Hagan, *J. Fluorine Chem.*, 1989, **43**, 371-377.

[8] S. Watanabe, T. Fujita, Y. Usui, T. Kitazume, *J. Fluorine Chem.*, 1986, **31**, 247-253.

[9] M. M. Bio, M. Waters, G. Javadi, Z. J. Song, F. Zhang, D. Thomas, *Synthesis*, 2008, 891-896.

Chapter 5. Experimental section

5.1) General Procedures:

5.1.1) Reagents and solvents:

All reagents were obtained from commercial sources and were used without further purification unless otherwise stated. Dry CH_2Cl_2, ether, THF, hexane and toluene were obtained from the Solvent Purification System MB SPS-800. Chloroform was dried with K_2CO_3, refluxed with Na_2SO_4, distilled and stored under N_2 prior to use. Acetone was dried with $CaSO_4$, refluxed with $CaSO_4$, distilled and stored under N_2 prior to use.

5.1.2) Reaction conditions:

All moisture sensitive reactions were carried out under a positive pressure of argon or nitrogen in oven-dried glassware (160 °C). Na_2SO_4 or $MgSO_4$ were used as a drying agents. Room temperature (RT) refers to 20 °C. Reaction temperatures of 0 °C were obtained in an ice/water bath. Reaction temperatures below 0 °C were obtained using either a bath-cooling apparatus LP Technology RP-100-CD or an acetone-dry ice bath. Reaction reflux conditions were obtained using an oil bath equipped with a contact thermometer. All microwave-assisted reactions were performed under sealed vessels (vial size 25 mL) on a Biotage Initiator 2.0 under various temperature gradient conditions, the reaction was monitored by t.l.c. Solvent evaporations were carried out under reduced pressure on a Büchi rotary evaporator.

5.1.3) Purification techniques and t.l.c:

Column chromatography was performed using silica gel 60 (40–63 micron). Thin layer chromatography (t.l.c) was carried out using Macherey-Nagel Polygram Sil G/UV254 plastic plates; visualisation was achieved by inspection under UV light (255 nm) or by the staining with a solution of basic potassium permanganate or phosphomolybdic acid.

5.1.4) Nuclear magnetic resonance spectroscopy (NMR):

NMR spectra were recorded on a Bruker AV-300 (^{1}H, 300 MHz; ^{13}C, 75 MHz; ^{19}F, 282 MHz) spectrometer, a Bruker AV-400 (^{1}H, 400 MHz; ^{13}C, 100 MHz; ^{19}F, 376 MHz) spectrometer or a Bruker AV-500 (^{1}H, 500 MHz; ^{19}F, 470 MHz) spectrometer. ^{1}H and ^{13}C NMR spectra were calibrated using the residual solvent shift from the deuterated solvent. ^{19}F NMR spectra were referenced to $CFCl_3$ as the external standard. Chemical shifts are reported in parts per million (ppm) and coupling constants (*J*) are given in Hertz (Hz). The abbreviations for the multiplicity of the proton, carbon and fluorine signals are as follows: s singlet, d doublet, dd doublet doublets, ddd doublet of doublet of doublets, dddd doublet of doublet of doublet of doublets, t triplet, dt double of triplets, td triplet of doublets, q quartet, dq double of quartets, m multiplet, app. apparent and br s broad singlet. When necessary, resonances were assigned using two-dimensional experiments (COSY, TOCSY, HMBC, HSQC, NOESY).

5.1.5) Mass spectrometry:

High and low resolution mass analyses (*m/z*) were carried out by Mrs Caroline Horsburgh, and spectra were recorded on a Micromass LCT TOF mass spectrometer using ES ionization in +ve ion mode. Where this method was inadequate, CI or EI were used using a Micromass GCT TOF instrument.

5.1.6) Melting point analyses:

Melting points were determined in Pyrex capillaries using a Gallenkamp Griffin MPA350.BM2.5 melting point apparatus and are uncorrected.

5.1.7) Infrared spectrosopy (IR), polarimetric and X-ray diffraction analyses:

IR spectra were recorded on a Nicolet Avatar 360 FT-IR from a thin film (either neat or combined with nujol) supported between NaCl plates. Optical rotations $[\alpha]_D$ are given in 10^{-1} deg cm^2 g^{-1} and were measured using a Perkin Elmer Model 341 polarimeter. Single X-ray diffraction analyses were carried out by Professor Alexandra M. Z. Slawin at the University of St Andrews.

5.1.8) Gas Chromatography:

5.1.8.1) GC-MS:

Low resolution GC-MS analyses were carried out using an Agilent 6890 gas chromatograph coupled to a 5973N mass selective detector in EI mode, with helium as a carrier gas. Automatic injections using a 7683 series injector were made into both non-chiral and chiral columns. Chiral separations were achieved with a Supelco Betadex[TM] 120 fused silica capillary chiral column (30 m x 0.25 mm i.d., 0.25 µm film thickness). Conditions for the chiral separation of product **214**: oven 80 °C held for 30 min, 250 °C injector temperature, 0.9 mL/min flow. Conditions for the chiral separation of product **228**: oven start at 110 °C held for 40 min, then gradient at 20 °C/min to 150 °C), 250 °C injector temperature, 100:1 split ratio, 0.9 mL/min flow.

5.1.8.2) GC-FID:

GC-FID analyses were carried out using an Agilent 6890 equipped with a flame ionisation detector, with helium as a carrier gas. Automatic injections using a 6890 series injection were made into both non-chiral and chiral columns. Non-chiral separations for products **214**, **228** and internal standard *n*-decane were carried out with a Hewlett Packard 1 column (30 m x 0.25 mm i.d, 0.25 µm film thickness): oven start at 50 °C held for 4 min, then gradient at 20 °C/min to 130 °C held for 2 min, then gradient at 20 °C/min to 280 °C, 250 °C injector temperature, 100:1 split ratio, 1.0 mL/min flow. Chiral separations for products **154a**, **154b**, **155a** and **155b** were carried out with a Supelco Betadex[TM] 225 fused silica capillary chiral column (60 m x 0.25 mm i.d., 0.25 mm film thickness): oven start at 40 °C held for 15 min,

then gradient at 0.9 °C/min to 230 °C, 250 °C injector temperature, 100:1 split ratio, 0.9 mL/min flow.

5.1.9) 2D ^{19}F EXSY- NMR spectroscopy:

Human blood was purchased from First Link (UK) Ltd. 3-Deoxy-3-fluoro-D-glucose **164** was purchased from Apollo Scientific Limited. The human blood was spun down (4000 rpm, 5 min) and the plasma and buffy coat were discarded. The cells were washed four times in 3 volumes of saline buffer solution containing 123 mM NaCl, 15 mM Tris-HEPES and 5 mM ascorbic acid (the saline buffer solutions were filtered through sterile filters Nalgene 0.20 µm cellulose acetate membranes before use). After each wash the supernatant was removed and the cells were collected by centrifugation. The red blood cells were then transferred to an Eppendorf tube and diluted with one volume of saline buffer containing 123 mM NaCl, 15 mM Tris-HEPES, 5 mM ascorbic acid and 20 mM of fluorinated sugar (final hematocrit 0.5), carefully mixed and transferred into a WILMAD NMR tube with J Joung valve. A sealed capillary tube containing D_2O was then introduced into the NMR tube to provide deuterium signal for the NMR lock. A stream of carbon monoxide was bubbled through the cells for 3 min before sealing. Immediately after that the sample was sealed and analysed by NMR.

2D ^{19}F spectra were recorded using Bruker AVANCE 500 MHz spectrometer equipped with double resonances ^{19}F SEF probe at 310 K. The spectra were acquired using NOESYPH sequence which was adjusted by adding ^{1}H decoupling for directly detected dimension and the ^{1}H 180° refocusing pulse in the middle of t_1 evolution period to achieve decoupling in the F1 dimension. Each spectrum was digitised using 1024 points in F2 dimension and 256 points in F1 dimension which was later zero-filled to 1024 points. 8 scans were accumulated for each increment with interscan delay 2s. Sine squared window multiplication was used for

all the spectra. Every sample was analysed using at least three different mixing times ranging from 0 to 800 ms. The program EXSY CALC (Mestrelab Research) was used to analyse integral intensities of crosspeaks according to a full relaxation matrix analysis.[1]

5.2) Protocols:

((Prop-2-ynyloxy)methyl)benzene 153:[2]

153
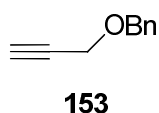
Propargyl alcohol (9.0 mL, 154.6 mmol) was added in portions to a suspension of NaH (60% in mineral oil, 6.80 g, 170.1 mmol) in DMF (150 mL) at 0 °C. After 30 min, benzyl bromide (20.2 mL, 170.1 mmol) was added and the resultant mixture was stirred at RT overnight. The mixture was then diluted with EtOAc (300 mL), washed by HCl (1N) (300 mL), and dried over MgSO$_4$. The EtOAc extract was concentrated *in vacuo*. The product was purified over silica gel (8:1 hex:EtOAc → 5:1) to give pure **153** (20.79 g, 95%) as a colourless oil.

δ_H (400 MHz, CDCl$_3$) 7.42–7.27 (m, 5H), 4.63 (s, 2H), 4.19 (d, J = 2.4 Hz, 2H), 2.49 (t, J = 2.4 Hz, 1H).[2]

(1*S*,2*S*)-1,2-Bis((*R*)-2,2-dimethyl-1,3-dioxolan-4-yl)ethane-1,2-diol 151:[3,4]

151
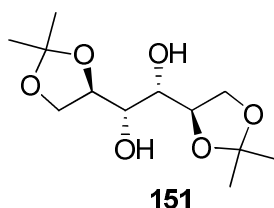
Anhydrous $ZnCl_2$ (65.6 g, 0.48 mol) was dissolved in dry acetone (410 mL, 5.5 mol). The solution was cooled to RT and dry D-Mannitol (41.7 g, 0.229 mol) was added and the solution stirred for 22 h. Then the reaction was poured into a vigorously stirred (ultra-turax mixer), and extensively cooled suspension of K_2CO_3 (66 g) in water (66 mL). The precipitated salts were filtered off with suction and washed three times with $CHCl_3$. The acetonic filtrates were combined and evaporated *in vacuo* to give a white solid (46.8 g). The product was recrystallised from a hot mixture of $CHCl_3$/heptane (10:1) to give **151** (31.2 g, 52%) as a white crystalline solid.

Mp = 119–120 °C, lit.[5] mp = 120–121 °C; δ_H (300 MHz, $CDCl_3$) 4.24–4.15 (m, 2H), 4.12 (dd, *J* = 8.4, 6.3 Hz, 2H), 3.97 (dd, *J* = 8.4, 5.5 Hz, 2H), 3.79–3.71 (m, 2H), 2.60 (d, *J* = 6.7 Hz, 2OH), 1.41 (s, 6H), 1.36 (s, 6H); δ_C (75 MHz, $CDCl_3$) 109.5 (2 x C), 76.4 (2 x CH), 71.4 (2 x CH), 66.9 (2 x CH_2), 26.8 (2 x CH_3), 25.3 (2 x CH_3); **MS** (ESI, +ve) *m/z* 285.08 [M+Na]$^+$ (100).

(*R*)-2,2-Dimethyl-1,3-dioxolane-4-carbaldehyde 152:[6]
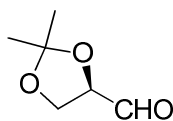
152

Sat. aqueous $NaHCO_3$ (2 mL) was added to a stirred solution of 1,2:5,6-*di-O*-isopropylidene-D-mannitol **151** (3.3 g, 13 mmol) in CH_2Cl_2 (30 mL) while maintaining the temperature at 15 °C. Sodium metaperiodate (5.3 g, 25 mmol) was then added over a 20 min period with vigorous stirring and the reaction was allowed to proceed for 4 h at 15 °C. The solution was then decanted and the remaining solid was stirred with additional CH_2Cl_2 (10 mL) for 5 min and it was again decanted from the solid. The organic solutions were combined and concentrated *in vacuo* and then distilled under reduced pressure (67–72 °C, 30 mmHg) giving the aldehyde **152** as a colourless oil (1.46 g, 67%).

$[\alpha]_D$ + 76.2° (c 1.3, benzene), lit.[7] $[\alpha]_D$ + 73.1° (c 1.3, benzene); δ_H (300 MHz, $CDCl_3$) 9.63 (d, J = 1.9 Hz, 1H), 4.31 (ddd, J = 7.3, 4.8, 1.9 Hz, 1H), 4.10 (dd, J = 8.8, 7.3 Hz, 1H), 4.02 (dd, J = 8.8, 4.8 Hz, 1H), 1.41 (s, 3H), 1.34 (s, 3H); δ_C (75 MHz, $CDCl_3$) 201.8 (CHO), 111.2 (C), 79.8 (CH), 65.5 (CH_2), 26.2 (CH_3), 25.1 (CH_3); **MS** (CI+) *m/z* 131.07 $[M+H]^+$ (100); **HRMS** (CI+) $C_6H_{10}O_3H^+$ requires *m/z* 131.0708, found 131.0704.

(*R*)-4-(Benzyloxy)-1-((*R*)-2,2-dimethyl-1,3-dioxolan-4-yl)but-2-yn-1-ol 154b:[8]

154b
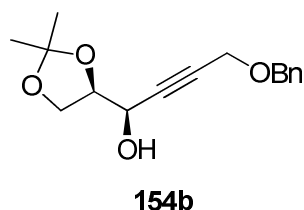
*n*BuLi (1.6 M in *n*-hexane, 9.6 mL, 15.4 mmol) was added to a stirred solution of benzyl propargyl ether **153** (2.3 mL, 15.4 mmol) in dry THF (19 mL) at -78 °C. After stirring at -78 °C for 1.5 h , a solution of **152** (1.0 g, 7.7 mmol) in THF (8 mL) was added dropwise to the mixture and the reaction stirred for 4 h at -78 °C. The reaction was then poured into sat. aqueous NH_4Cl (50 mL) at -78 °C. Water (70 mL) was added and the reaction was extracted into Et_2O (3 x 110 mL). The Et_2O extract was successively washed with water and brine, then dried ($MgSO_4$) and concentrated *in vacuo*. The product was purified over silica (9:1 hex:EtOAc → 3:1) to give the desired alcohol **154b** (1.723 g, 81%, mixture favouring the *syn* diastereoisomer) as a clear oil. Chiral-phase **GC-FID** analysis of the product, t_R = 226.0 min for the minor *anti* diastereoisomer and t_R = 226.6 min for the major *syn* diastereoisomer, indicated that the de was 9%.

Data for major diastereoisomer: δ_H (400 MHz, CDCl$_3$) 7.38–7.26 (m, 5H), 4.58 (s, 2H), 4.37 (dt, *J* = 8.8, 1.7 Hz, 1H), 4.28–3.86 (m, 5H), 2.70 (br s, OH), 1.46 (s, 3H), 1.38 (s, 3H); δ_C (100 MHz, CDCl$_3$) 137.3 (C) 128.6 (2 x CH), 128.2 (2 x CH), 128.0 (CH), 110.6 (C), 83.9 (C), 82.3 (C), 78.7 (CH), 71.8 (CH), 66.2 (CH$_2$), 64.3 (CH), 57.4 (CH$_2$), 26.9 (CH$_3$), 25.3 (CH$_3$); **MS** (ESI, +ve) *m/z* 299.11 [M+Na]$^+$ (55), 259 [M+H-H$_2$O]$^+$ (100); **HRMS** (ES+) C$_{16}$H$_{20}$O$_4$Na$^+$ requires *m/z* 299.1260, found 299.1259.

(S)-4-(Benzyloxy)-1-((R)-2,2-dimethyl-1,3-dioxolan-4-yl)but-2-yn-1-ol 154a:[9]

154a
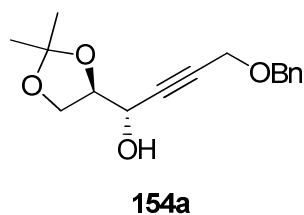
n-BuLi (1.6 M in *n*-hexane, 13.9 mL, 22.2 mmol) was added dropwise to a solution of benzyl propargyl ether **153** (3.3 mL, 22.2 mmol) in THF (21.0 mL) at -78 °C. After 30 min, ClTi(O*i*-Pr)$_3$ (1M in *n*-hexane, 41.0 mL, 22.2 mmol) was added and the flask warmed to -60 °C. To maintain solubility, additional THF (41 mL) was added and the solution was stirred for 90 min prior to re-cooling to -78 °C. Compound **152** (1.44 g, 11.1 mmol) was then added in one portion and the mixture stirred for 4 h prior to quenching with sat. NH$_4$Cl (70 mL) at -78 °C. Water (100 mL) was added and the reaction was extracted into Et$_2$O (3 x 150 mL). The product was purified over silica gel (9:1 hex:EtOAc → 3:1) to give the desired alcohol **154b** (2.52 g, 82%, mixture favouring the *anti* diastereoisomer) as a clear oil. Chiral-phase **GC-FID** analysis of the product, t_R = 226.0 min for the major *anti* diastereoisomer and t_R = 226.6 min for the minor *syn* diastereoisomer, indicated that the de was 62%.

Data for major diastereoisomer: δ_H (400 MHz, CDCl$_3$) 7.38–7.26 (m, 5H), 4.58 (s, 2H), 4.52 (dt, *J* = 4.4, 1.7 Hz, 1H), 4.28–3.86 (m, 5H), 2.56 (br s, OH), 1.47 (s, 3H), 1.38 (s, 3H); δ_C (100 MHz, CDCl$_3$) 137.4 (C), 128.6 (2 x CH), 128.2 (2 x CH), 128.0 (CH), 110.3 (C), 83.9 (C), 82.4 (C), 77.9 (CH), 71.8 (CH), 65.4 (CH$_2$), 62.7 (CH), 57.4 (CH$_2$), 26.5 (CH$_3$), 25.2 (CH$_3$); **MS** (ESI, +ve) *m/z* 299.11 [M+Na]$^+$ (55), 259 [M+H-H$_2$O]$^+$ (100); **HRMS** (ES+) C$_{16}$H$_{20}$O$_4$Na$^+$ requires *m/z* 299.1260, found 299.1259.

(S)-4-(Benzyloxy)-1-((R)-2,2-dimethyl-1,3-dioxolan-4-yl)but-2-ynyl 3,5-dinitrobenzoate 158a:

158a
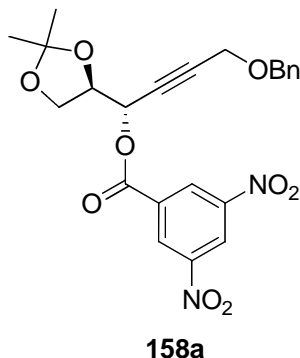
3,5-Dinitrobenzoyl chloride (0.48 g, 2.0 mmol) was added to a solution of alcohol **154a** (0.515 g, 1.8 mmol, de 62%) in dry pyridine (29 mL) at 0 °C. After stirring for 16 h at RT the reaction was poured into ice-water and extracted into Et$_2$O (3 x 70 mL). The product was purified over silica gel (9:1 hex:EtOAc → 5:1) to give **158a** which was recrystallised from absolute ethanol (0.59 g, 70%).

Mp 86–88 °C (from EtOH); **[α]$_D$** + 38.8 (c 0.5, CHCl$_3$); **ν_{max}** (NaCl)/cm^{-1} 2923, 1764, 1629, 1545, 1459, 1345, 1273, 1153, 1074, 721; **δ_H** (400 MHz, CDCl$_3$) 9.25 (t, 1H, J = 2.1 Hz), 9.21 (d, 2H, J = 2.1 Hz), 7.39–7.27 (m, 5H), 5.88–5.83 (m, 1H), 4.58 (s, 2H), 4.55–4.46 (m, 1H), 4.27–4.15 (m, 4H), 1.38 (s, 3H), 1.39 (s, 3H); **δ_C** (100 MHz, CDCl$_3$,) 161.6 (C), 148.9 (2 x C), 137.2 (C), 133.4 (C), 130.1–127.9 (7 x CH), 122.9 (CH), 111.0 (C), 84.9 (C), 79.6 (C), 76.3 (CH), 72.1 (CH$_2$), 66.6 (CH), 65.6 (CH$_2$), 57.3 (CH$_2$), 26.5 (CH$_3$), 25.0 (CH$_3$); **MS** (ESI, +ve) *m/z* 493.06 [M+Na]$^+$ (100); **HRMS** (ESI, +ve) C$_{23}$H$_{22}$N$_2$O$_9$Na$^+$ requires *m/z* 493.1223, found 493.1218.

(_R_,_E_)-4-(Benzyloxy)-1-((_R_)-2,2-dimethyl-1,3-dioxolan-4-yl)but-2-en-1-ol 155b:[10]

155b
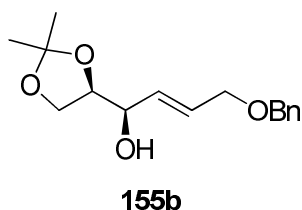
A solution of **154b** (1.62 g, 5.9 mmol, 9% de) in _n_-hexane (6.5 mL) was added to a suspension of LiAlH$_4$ (0.3 g, 7.6 mmol) in _n_-hexane (13 mL) at 0 °C. The reaction was heated under reflux for 2 h and was then quenched by dropwise addition of water (10 mL). The mixture was filtered and the resultant precipitate was washed with Et$_2$0 (3 x 75 mL). The combined organics were dried (MgSO$_4$) and the product purified over silica gel (9:1 hex:EtOAc → 3:1) to give alcohol **155b** (0.73 g, 45%, mixture favouring the _syn_ diastereoisomer) as a clear oil. Chiral-phase **GC-FID** analysis of the product, t_R = 221.5 min for the major _syn_ diastereoisomer and t_R = 222.0 min for the minor _anti_ diastereoisomer, indicated that the de was 17%.

Alternative procedure: Red-Al® (70% w/v in toluene, 3.4 mL, 11.8 mmol) was added slowly to a solution of **154b** (1.62 g, 5.9 mmol, 9% de, _syn_ favour) in THF (6.5 mL) at 0 °C. After stirring for 1 h at 0 °C, the reaction was quenched with sat. aqueous Rochelle salt and extracted into Et$_2$O (3 x 30 mL). The combined organics were dried (MgSO$_4$) and the product purified over silica gel (9:1 hex:EtOAc → 3:1) to give alcohol **155b** (1.46 g, 90%, 17% de, _syn_ favour) as a clear oil.

Data for major diasteroisomer: δ_H (400 MHz, CDCl$_3$) 7.38–7.26 (m, 5H), 5.98–5.89 (m, 1H), 5.78–5.67 (m, 1H), 4.51 (s, 2H), 4.13–3.82 (m 5H), 3.81–3.71 (m, 1H), 2.25 (br s, OH), 1.45 (s, 3H), 1.36 (s, 3H); δ_C (100 MHz, CDCl$_3$) 138.2 (C), 130.5 (CH), 130.4 (CH),

128.5 (2 x CH), 127.8 (3 x CH), 110.0 (C), 78.8 (CH), 73.4 (CH), 72.4 (CH$_2$), 69.9 (CH$_2$), 66.0 (CH$_2$), 26.9 (CH$_3$), 25.4 (CH$_3$); **MS** (ESI, +ve) *m/z* 301.08 [M+Na]$^+$ (100); **HRMS** (ES+) C$_{16}$H$_{22}$O$_4$Na$^+$ requires *m/z* 301.1416, found 301.1421.

(*S*,*E*)-4-(Benzyloxy)-1-((*R*)-2,2-dimethyl-1,3-dioxolan-4-yl)but-2-en-1-ol 155a:[10]
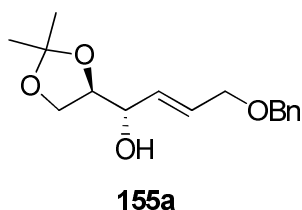

155a

A solution of **154a** (2.43 g, 8.8 mmol, 62% de) in *n*-hexane (10 mL) was added to a suspension of LiAlH$_4$ (0.45 g, 11.9 mmol) in *n*-hexane (20 mL) at 0 °C. The reaction was heated under reflux for 2 h and was quenched by dropwise addition of water (15 mL). The mixture was filtered and the precipitate washed with Et$_2$O (3 x 100 mL). The combined organics were dried (MgSO$_4$) and evaporated and the product purified over silica gel (9:1 hex:EtOAc → 3:1) to give alcohol **155a** (1.35 g, 55%, mixture favouring the *anti* diastereoisomer) as a clear oil. Chiral-phase **GC-FID** analysis of the product, t_R = 221.5 min for the minor *syn* diastereoisomer and t_R = 222.0 min for the major *anti* diastereoisomer, indicated that the de was 75%.

Alternative procedure: Red-Al® (70% wt in toluene, 3.4 mL, 11.8 mmol) was added slowly to a solution of **154a** (1.62 g, 5.9 mmol, 62% de, *anti* favour) in THF (6.5 mL) at 0 °C. After stirring for 1 h at 0 °C, the reaction was quenched with sat. aqueous Rochelle salt and extracted into Et$_2$O (3 x 30 mL). The combined organics were dried (MgSO$_4$) and the product purified over silica gel (9:1 hex:EtOAc → 3:1) to give alcohol **155a** (1.51 g, 93%, 75% de, *anti* favour) as a clear oil.

Data for major diastereoisomer: δ_H (400 MHz, CDCl$_3$) 7.38–7.26 (m, 5H), 5.98–5.89 (m, 1H), 5.78–5.67 (m, 1H), 4.51 (s, 2H), 4.33–4.27 (m 1H), 4.13–4.07 (m, 1H), 4.05–4.02 (m, 2H), 3.99–3.87 (m, 2H), 2.25 (br s, OH), 1.44 (s, 3H), 1.36 (s, 3H); δ_C (100 MHz,

CDCl$_3$,) 138.2 (C), 130.4 (CH), 129.4 (CH), 128.5 (2 x CH), 127.9 (2 x CH), 127.8 (CH), 109.5 (C), 78.2 (CH), 71.3 (CH), 72.4 (CH$_2$), 70.1 (CH$_2$), 64.9 (CH$_2$), 26.5 (CH$_3$), 25.2 (CH$_3$); **MS** (ESI, +ve) *m/z* 301.08 [M+Na]$^+$ (100); **HRMS** (ES+) C$_{16}$H$_{22}$O$_4$Na$^+$ requires *m/z* 301.1416, found 301.1421.

(R)-4-((S,E)-4-(Benzyloxy)-1-fluorobut-2-enyl)-2,2-dimethyl-1,3-dioxolane 156a and the inseparable mixture of (R)-4-((R,E)-4-(benzyloxy)-1-fluorobut-2-enyl)-2,2-dimethyl-1,3-dioxolane 156b, (S)-4-((R,E)-4-(benzyloxy)-3-fluorobut-1-enyl)-2,2-dimethyl-1,3-dioxolane 157a and (S)-4-((S,E)-4-(benzyloxy)-3-fluorobut-1-enyl)-2,2-dimethyl-1,3-dioxolane 157b:[11]

156a   156b   157a   157b
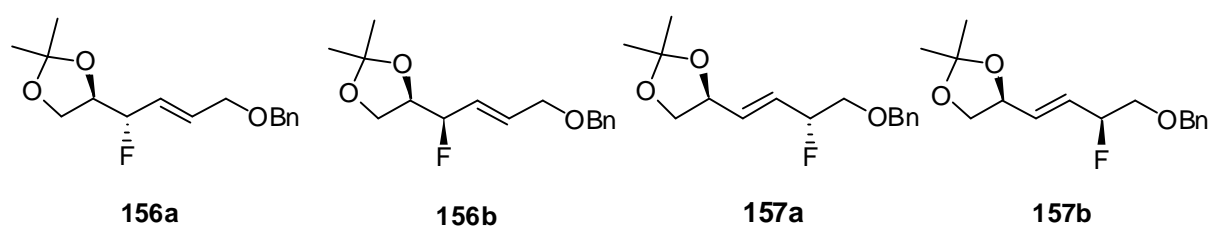
A solution of allylic alcohol **155a** (1.39 g, 5 mmol, 17% de) in CH_2Cl_2 (10 mL) was added to a solution of TFEDMA (0.66 mL, 5.5 mmol) in CH_2Cl_2 (10 mL) at 0 °C in a polythene vessel. After addition the reaction was stirred for 1 h at RT. The reaction was then worked up by adding sat. aqueous $NaHCO_3$ solution and the product was extracted into CH_2Cl_2 (3 x 150 mL). The product was purified over silica gel (6:1→3:1 hex:EtOAc) to give **156a** (0.18 g, 13%, single stereoisomer) and the inseparable mixture of isomers **156b/157a/157b** (0.64 g, 46%, ratio 0.3/0.7/1.0) as clear oils.

Data for 156a: $[\alpha]_D$ -7.6 (c 1.0, $CHCl_3$), ν_{max} (NaCl)/cm^{-1} 1215, 1115, 1071, 972; δ_H (300 MHz, $CDCl_3$) 7.37–7.27 (m, 5H), 6.00 (m, 1H), 5.84 (m, 1H), 4.88 (dm, J = 47.9 Hz, 1H), 4.54 (s, 2H), 4.15 (m, 1H), 4.10 – 4.04 (m, 3H), 3.98 (ddd, J = 8.7, 5.5, 1.1 Hz, 1H), 1.43 (s, 3H), 1.36 (s, 3H); δ_C (75 MHz, $CDCl_3$) 132.1 (d, J = 11.6 Hz, CH), 138.3 (C), 128.8 (2 x CH), 128.1 (2 x CH), 127.7 (CH), 127.0 (d, J = 18.6 Hz, CH), 120.0 (CH), 109.9 (C), 91.9 (d. J = 173.0 Hz, CH), 76.9 (d, J = 27.7 Hz, CH), 72.8 (CH_2), 69.9 (CH_2), 65.8 (d. J = 4.2 Hz, CH_2), 26.8 (CH_3), 25.6 (CH_3); δ_F (282 MHz, $CDCl_3$) -187.5 (dm, J = 47.9 Hz, 1F);

$\delta_{\text{F\{H\}}}$ (282 MHz, CDCl$_3$) -187.5 (s, 1F); **MS** (ESI, +ve) m/z 303.07 [M+Na]$^+$ (100); **HRMS** (ESI, +ve) C$_{16}$H$_{21}$FO$_3$Na$^+$ requires m/z 303.1372, found 303.1378.

Data for inseparable mixture of isomers 156b/157a/157b: δ_{H} (400 MHz, CDCl$_3$) 7.39–7.26 (m, 15H), 6.06–5.59 (m, 6H), 5.22–4.76 (m, 3H), 4.64–3.52 (m, 21H), 1.36–1.47 (m, 18H); δ_{C} (100 MHz, CDCl$_3$) 138.1 (C), 137.8 (2 x C), 133.2 (d, J = 11.2 Hz, CH), 132.1 (d, J = 10.7 Hz, CH), 131.7 (d, J = 10.6 Hz, CH), 128.7–127.7 (17 x CH), 125.8 (d, J = 18.9 Hz, CH), 110.4 (C), 109.7 (2 x C), 92.8 (d, J = 173.6 Hz, CH), 91.6 (d, J = 172.5 Hz, CH), 91.4 (d, J = 172.8 Hz, CH), 76.1–76.0 (3 x CH), 72.6 (3 x CH$_2$), 72.1 (d, J = 23.1 Hz, CH$_2$), 72.0 (d, J = 22.6 Hz, CH$_2$), 69.5 (CH$_2$), 69.4 (2 x CH$_2$), 65.2 (d, J = 5.4 Hz, CH$_2$), 26.7–25.4 (6 x CH$_3$). **MS** (ESI, +ve) m/z 303.04 [M+Na]$^+$ (100); **HRMS** (ESI, +ve) C$_{16}$H$_{21}$FO$_3$Na$^+$ requires m/z 303.1372, found 303.1375.

Data for 156b: δ_{F} (282 MHz, CDCl$_3$) -183.48 (dm, J = 48.3 Hz, 1F); $\delta_{\text{F\{H\}}}$ (282 MHz, CDCl$_3$) -183.0 (s, 1F).

Data for 157a: δ_{F} (282 MHz, CDCl$_3$) -183.4 (m, 1F); $\delta_{\text{F\{H\}}}$ (282 MHz, CDCl$_3$) -183.4 (s, 1F).

Data for 157b: δ_{F} (282 MHz, CDCl$_3$) -184.1 (m, 1F); $\delta_{\text{F\{H\}}}$ (282 MHz, CDCl$_3$) -184.1 (s, 1F).

(1S,2S,3R)-4-(Benzyloxy)-1-((R)-2,2-dimethyl-1,3-dioxolan-4-yl)-1-fluorobutane-2,3-diol 159:[12]

159
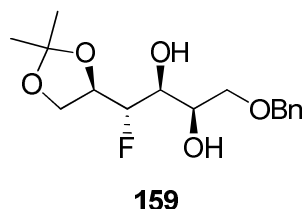
Methanesulfonamide (0.04 g, 0.4 mmol) was added to a solution of *AD*-mix-*β* (0.60 g) in *tert*-butyl- alcohol (2.3 mL) and water (2.3 mL). A solution of **156a** (0.12 g, 0.4 mmol) in *tert*-butyl- alcohol (2.3 mL) was then added and the resultant mixture was stirred at 0 °C for 1 h and then at RT for 3 d. Solid Na_2SO_3 (0.66 g) was added and the mixture stirred for 30 min. The product was then extracted into Et_2O (3 x 20 mL) and the combined organic layers were washed with 2M KOH (20 mL) and concentrated. The product was purified over silica gel (9:1 hex:EtOAc → 4:1) and **159** was recrystallised from Et_2O (0.05 g, 37%).

Mp 94–96 °C (from Et_2O); **[*α*]$_D$** +1.9° (c 0.6, $CHCl_3$); ν_{max} (NaCl)/cm^{-1} 3456, 2727, 1700, 1265, 1225, 1161, 1138, 1115, 1054, 725; δ_H (400 MHz, $CDCl_3$) 7.40–7.27 (m, 5H), 4.58 (s, 2H), 4.57–4.44 (dm, *J* = 46.0 Hz, 1H), 4.44–4.37 (m, 1H), 4.14 (ddd, *J* = 8.7, 6.5, 6.2 Hz, 1H), 4.06 (ddd, *J* = 8.7, 5.5, 5.3 Hz, 1H), 4.03–3.95 (m, 1H), 3.90 (dddd, *J* = 11.2, 6.1, 4.7, 1.7 Hz, 1H), 3.65 (d, *J* = 5.3 Hz, 2H), 3.08 (d, *J* = 4.7 Hz, 1H), 2.88 (d, *J* = 5.9 Hz, 1H), 1.44 (s, 3H), 1.37 (s, 3H); δ_C (100 MHz, $CDCl_3$) 137.7 (C), 128.7 (2 x CH), 128.1 (CH), 128.0 (2 x CH), 110.2 (C), 91.2 (d, *J* = 176.8 Hz, CH), 74.3 (d, *J* = 27.3 Hz, CH), 73.8 (CH_2), 72.2 (CH_2), 71.6 (d, *J* = 23.3 Hz, CH), 68.4 (d, *J* = 5.4 Hz, CH), 65.9 (d. *J* = 4.7 Hz, CH_2), 26.5 (CH_3), 25.3 (CH_3); δ_F (376 MHz, $CDCl_3$) -198.4 (ddd, *J* = 46.0, 13.0, 11.2 Hz, 1F); $\delta_{F\{H\}}$ (376 MHz, $CDCl_3$) -198.4 (s, 1F); **MS** (ESI, +ve) *m/z* 337.19 [M+Na]$^+$ (100); **HRMS** (ESI, +ve) $C_{16}H_{23}FO_5Na^+$ requires *m/z* 337.1427, found 337.1431.

(1*S*,2*S*,3*R*)-4-(Benzyloxy)-1-((*R*)-2,2-dimethyl-1,3-dioxolan-4-yl)-3-fluorobutane-1,2-diol 160a/160b:[12]

160a/160b
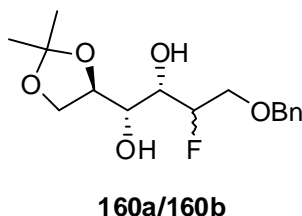
Methanesulfonamide (0.20 g, 2.2 mmol) was added to a solution of *AD*-mix-*β* (3.01 g) in *tert*-butyl- alcohol (11.5 mL) and water (11.5 mL). A solution of **156b**/**157a**/**157b** (0.60 g, 2.2 mmol, ratio 0.3:0.7:1) in *tert*-butyl- alcohol (11.5 mL) was then added and the resultant mixture was stirred at 0 °C for 1 h and then at RT for 3 d. Solid Na_2SO_3 (3.31 g) was added and the mixture stirred for 30 min. The product was then extracted into Et_2O (3 x 100 mL) and the combined organic layers were washed with 2M KOH (100 mL) and concentrated. The product was purified over silica gel (9:1 hex:EtOAc → 4:1) to give the desired diols **160a/160b** as a solid (0.41 g, 60%, dr 1:0.7).

$δ_H$ (300 MHz, $CDCl_3$) 7.42–7.27 (m, 10H), 4.63–4.57 (m, 4H), 4.22–2.45 (m, 20H), 1.42–1.38 (m, 12H); $δ_C$ (100 MHz, $CDCl_3$) 137.4 (C), 137.3 (C), 128.0 (4 x CH), 128.7 (2 x CH), 128.2 (4 x CH), 109.5 (C), 109.4 (C), 93.6 (d, *J* = 174.7 Hz, CH), 90.8 (d, *J* = 174.6 Hz, CH), 76.1 (CH), 75.6 (CH), 74.0 (2 x CH_2), 71.6 (d, *J* = 3.8 Hz, CH), 70.4 (d, *J* = 3.6 Hz, CH), 69.8 (d, *J* = 21.0 Hz, CH), 69.6 (d, *J* = 24.7 Hz, CH), 69.4 (d, *J* = 22.9 Hz, CH_2), 69.2 (d, *J* = 22.7 Hz, CH_2), 67.1 (CH_2), 66.8 (CH_2), 26.9 (CH_3), 26.8 (CH_3), 25.4 (CH_3), 25.3 (CH_3); $δ_F$ (282 MHz, $CDCl_3$) -194.4 (m, 1F), -200.8 (m, 1F); $δ_{F\{H\}}$ (282 MHz, $CDCl_3$) -194.4 (s, 1F), -200.8 (s, 1F); **MS** (ESI, +ve) *m/z* 337.11 [M+Na]$^+$ (100); **HRMS** (ESI, +ve) $C_{16}H_{23}FO_5Na^+$ requires *m/z* 337.1427, found 337.1425.

(1*R*,2*R*,3*S*)-4-(benzyloxy)-1-((*S*)-2,2-dimethyl-1,3-dioxolan-4-yl)-3-fluorobutane-[1,3,2]dioxolane 2,2-dioxide 162a and (1*R*,2*R*,3*S*)-4-(Benzyloxy)-1-((*R*)-2,2-dimethyl-1,3-dioxolan-4-yl)-3-fluorobutane [1,3,2]dioxolane 2,2-dioxide 162b:[13]

162a   162b
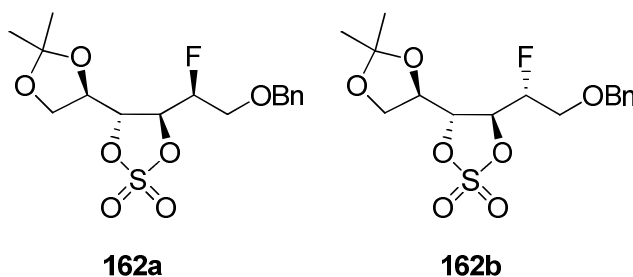
Thionyl chloride (0.13 mL, 1.7 mmol) was added to a solution of **160a/160b** (0.45 g, 1.4 mmol, dr 1:0.7) in CH_2Cl_2 (65 mL) and pyridine (0.17 mL, 2.1 mmol) and the mixture was stirred at 0 °C for 30 min. Saturated $CuSO_4$ (aq) (35 mL) was then added and the product extracted into CH_2Cl_2 (3 x 70 mL). The organics were dried ($MgSO_4$) and concentrated and then dissolved in CH_3CN (50 mL). The solution was cooled to 0 °C and then $NaIO_4$ (0.76 g, 3.5 mmol), $RuCl_3\cdot3H_2O$ (1 mol%) and H_2O (35 mL) were added and the heterogenous mixture was stirred vigorously at 0 °C for 3 h. Et_2O (140 mL) was then added and the organic layer was washed with 5% aqueous $NaHCO_3$ (50 mL) and dried ($MgSO_4$). The product was purified over silica gel (9:1 hex:EtOAc → 4:1) to give a solid which was then recrystallised from Et_2O to provide **162a** as a white crystalline solid (0.14 g, 27%), and **162b** (0.32 g, 61%) as a clear oil.

  Data for 162a: Mp 38–40 °C; **[*α*]$_D$** +30.5 (c 0.63, CHCl$_3$); **ν$_{max}$** (NaCl)/cm^{-1} 3090, 3066, 3033, 2990, 1881, 1812, 1734, 1606, 1396, 1261, 1213, 1061, 986, 953, 833; **δ$_H$** (400 MHz, CDCl$_3$) 7.42–7.27 (m, 5H), 5.07–4.76 (m, 3H), 4.62 (d, *J* = 11.8 Hz, 1H), 4.58 (d, *J* = 11.8 Hz, 1H), 4.37 (m, 1H), 4.19 (dd, *J* = 9.6, 6.0 Hz, 1H), 4.07 (d, *J* = 9.6, 3.1 Hz, 1H),

3.89–3.67 (m, 2H), 1.44 (s, 3H), 1.35 (s, 3H); δ_C (100 MHz, CDCl$_3$) 137.1 (C), 128.8 (2 x CH), 128.4 (CH), 128.1 (2 x CH), 111.3 (C), 88.1 (d, J = 184.3 Hz, CH), 82.7 (d, J = 18.7 Hz, CH), 79.5 (d, J = 5.4 Hz, CH), 74.8 (CH), 74.1 (CH$_2$), 67.1 (CH$_2$), 67.5 (d, J = 27.6 Hz, CH$_2$), 26.9 (CH$_3$), 24.9 (CH$_3$); δ_F (376 MHz, CDCl$_3$) -206.9 (dddd, J = 45.8, 24.6, 18.2, 11.8 Hz, 1F); $\delta_{F\{H\}}$ (376 MHz, CDCl$_3$) -206.9 (s, 1F); **MS** (ESI, +ve) m/z 399.09 [M+Na]$^+$ (100); **HRMS** (ESI, +ve) C$_{16}$H$_{21}$O$_7$FSNa$^+$ requires m/z 399.0888, found 399.0886.

Data for 162b: $[\alpha]_D$ +23.1 (c 1.9, CHCl$_3$); ν_{max} (NaCl)/cm^{-1} 3090, 3066, 3033, 2990, 1881, 1812, 1734, 1606, 1396, 1261, 1213, 1061, 986, 953, 833; δ_H (400 MHz, CDCl$_3$) 7.42–7.28 (m, 5H), 5.16 (ddd, J = 11.0, 6.2, 4.0 Hz, 1H), 4.94 (ddt, J = 46.0, 6.2, 4.1 Hz), 4.83–4.76 (m, 1H), 4.63 (d, J = 11.9 Hz, 1H), 4.57 (d, J = 11.9 Hz, 1H), 4.43 (ddd, J = 9.5, 6.2, 3.4 Hz, 1H), 4.18 (dd, J = 9.5, 6.2 Hz, 1H), 4.03 (dd, J = 9.5, 3.4 Hz, 1H), 3.84 (ddd, J = 18.0, 11.5, 4.1 Hz, 1H), 3.79 (ddd, J = 27.0, 11.5, 4.1 Hz, 1H), 1.42 (s, 3H), 1.35 (s, 3H); δ_C (100 MHz, CDCl$_3$) 137.1 (C), 128.7 (2 x CH), 128.3 (CH), 127.9 (2 x CH), 111.2 (C), 89.0 (d, J = 179.6, CH), 81.1 (d, J = 4.1 Hz, CH), 80.2 (d, J = 29.0 Hz, CH), 74.0 (CH$_2$), 73.8 (CH), 67.1 (d, J = 22.6 Hz, CH$_2$), 66.4 (CH$_2$), 26.7 (CH$_3$), 24.9 (CH$_3$); δ_F (376 MHz, CDCl$_3$) -198.4 (dddd, J = 46.0, 27.0, 18.0, 11.0 Hz, 1F); $\delta_{F\{H\}}$ (376 MHz, CDCl$_3$) -198.4 (s, 1F); **MS** (ESI, +ve) m/z 399.11 [M+Na]$^+$ (100); **HRMS** (ESI, +ve) C$_{16}$H$_{21}$O$_7$FSNa$^+$ requires m/z 399.0888, found 399.0890.

(R)-4-((R)-(3-(Benzyloxymethyl)oxiran-2-yl)fluoromethyl)-2,2-dimethyl-1,3-dioxolane 194a/194b:[14]
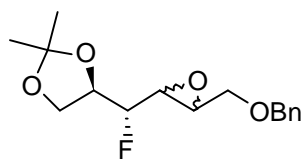
194a/194b

m-CPBA (4.99 g, 15.1 mmol) was added to a solution of **156a** (2.11 g, 7.5 mmol) in CH$_2$Cl$_2$ (38 mL) at 0 °C. After 1 min the ice/water bath was removed and the solution was stirred for 5 d at RT. The resultant solution was then stirred with a mixture of 10% (w/v) aqueous Na$_2$SO$_3$ (50 mL) for 15 min and was then washed with sat. aqueous NaHCO$_3$ (50 mL). The organic layer was dried over Na$_2$SO$_4$ and the product purified over silica gel (9:1→3:1 hex:EtOAc) to give the inseparable mixture **194a/194b** (2.00 g, 89%, dr 1:0.7) as a clear oil.

Data for the diastereomeric mixture: δ_H (400.13 MHz, CDCl$_3$) 7.42–7.26 (m, 10H), 4.65–4.17 (m, 8H), 4.16–4.08 (m, 2H), 4.06–3.98 (m, 2H), 3.85–3.75 (m, 2H), 3.60–3.46 (m, 2H), 3.38–3.12 (m, 4H), 1.44 (s, 3H), 1.42 (s, 3H), 1.36 (m, 6H); **MS** (ESI, +ve) *m/z* 319.02 [M+Na]$^+$ (100); **HRMS** (ESI, +ve) C$_{16}$H$_{21}$FO$_4$Na$^+$ requires *m/z* 319.1322, found 319.1331. **Data for major diastereoisomer*: δ_C** (100 MHz, CDCl$_3$) 137.9 (C), 128.6 (2 x CH), 128.0 (CH), 127.9 (2 x CH), 110.1 (C), 90.8 (d, *J* = 180.1 Hz, CH), 74.26 (d, *J* = 29.0 Hz, CH), 73.5 (CH$_2$), 69.4 (CH$_2$), 66.1 (d, *J* = 2.8 Hz, CH), 54.4–53.3 (m, 2 x CH), 26.7 (CH$_3$), 25.2 (CH$_3$); **δ_F** (376 MHz, CDCl$_3$) -201.3 (dm, *J* = 47.7 Hz, 1F); **$\delta_{F\{H\}}$** (376 MHz, CDCl$_3$) -201.3 (s, 1F). **Data for minor diastereoisomer**: **δ_C** (100 MHz, CDCl$_3$) 137.8 (C), 128.6 (2 x CH), 128.0 (CH), 127.9 (2 x CH), 110.3 (C), 90.2 (d, *J* = 178.1 Hz, CH), 74.3 (d, *J* = 25.7 Hz, CH), 73.5 (CH$_2$), 69.2 (CH$_2$), 65.7 (d, *J* = 4.8 Hz, CH), 54.4–53.3 (m, 2 x CH), 26.6 (CH$_3$), 25.3 (CH$_3$); **δ_F** (376 MHz, CDCl$_3$) -199.6 (dt, *J* = 48.0, 12.7 Hz, 1F); **$\delta_{F\{H\}}$** (376 MHz, CDCl$_3$) -199.6 (s, 1F).

(1S,2R,3R)-4-(Benzyloxy)-1-((R)-2,2-dimethyl-1,3-dioxolan-4-yl)-1,3-difluorobutan-2-ol 195a and (1S,2S,3S)-4-(benzyloxy)-1-((R)-2,2-dimethyl-1,3-dioxolan-4-yl)-1,3-difluorobutan-2-ol 195b, (4R)-1-(Benzyloxy)-4-((R)-2,2-dimethyl-1,3-dioxolan-4-yl)-3,4-difluorobutan-2-ol 199a/199b, (2R,3R)-3-(3-((benzyloxy)methyl)oxiran-2-yl)-3-fluoropropane-1,2-diol 200a/200b:[15]
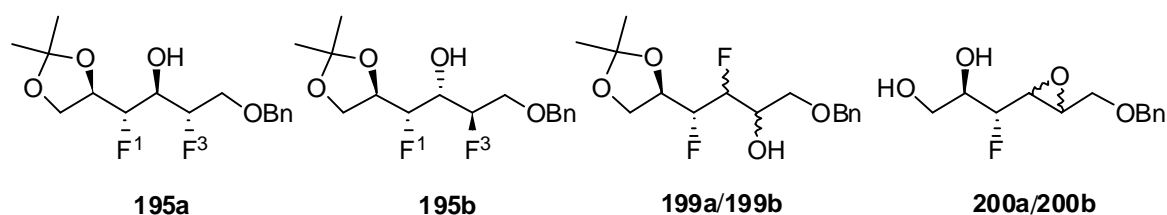
A solution of **194a/194b** (0.46 g, 1.6 mmol, dr 1:0.7) in dry CHCl$_3$ (5.2 mL) was introduced in a microwave reaction glass vessel under an atmosphere of argon. Et$_3$N·3HF (2.06 mL, 12.5 mmol) and dry Et$_3$N (0.47 mL, 3.4 mmol) were then added and the reaction was stirred for 2 h at 120 °C under microwave irradiation. After cooling, further Et$_3$N·3HF (2.06 mL, 12.5 mmol) was added and the reaction was stirred for 3 h at 100 °C, for 12 h at 120 °C, for 3 h at 130 °C and for 3 h at 140 °C under microwave irradiation. After cooling the reaction was concentrated onto silica and subjected to flash chromatography over silica gel (9:1→4:1 hexane/ethyl acetate) to give separately products **195a** (0.08 g, 16%) and **195b** (0.14 g, 29%) as clear oils, and side-products **199a/199b**[*] (0.03 g, 6%, dr 1:0.7) and **200a/200b*** (0.03 g, 6%, dr 1:1) as yellow oils.

[*]Probable structure based on partial purification/characterisation.

     Data for 195a: $[\alpha]_D^{22}$ -6.23 (c 1.25 in CHCl$_3$); ν_{max} (NaCl)/cm^{-1} 3445, 3086, 3058, 3025, 2980, 2936, 1497, 1455, 1410, 1373, 1256, 1217, 1150, 1102, 1063, 845, 738, 699; δ_H (400 MHz, CDCl$_3$) 7.42–7.26 (m, 5H), 4.83 (dm, J = 46.4 Hz, 1H), 4.68–4.49 (m, 3H), 4.48–

4.35 (m, 1H), 4.33–4.17 (m, 1H), 4.17–4.09 (m, 1H), 4.09–4.02 (m, 1H), 3.91–3.87 (m, 1H), 3.84–3.77 (m, 1H), 2.83 (d, J = 4.9 Hz, OH), 1.44 (s, 3H), 1.36 (s, 3H); δ_C (100 MHz, CDCl$_3$) 137.5 (C), 128.7 (2 x CH), 128.2 (CH), 128.0 (2 x CH), 110.1 (C), 91.7 (dd, J = 176.3, 3.6 Hz, CH), 90.6 (dd, J = 175.2, 6.2 Hz, CH), 73.9 (CH$_2$), 73.8 (d, J = 29.2 Hz, CH), 70.9 (dd, J = 24.1, 22.2 Hz, CH), 69.3 (d, J = 21.7 Hz, CH$_2$), 66.2 (d, J = 4.4 Hz, CH$_2$), 26.7 (CH$_3$), 25.3 (CH$_3$); δ_F (376 MHz, CDCl$_3$) -196.8 (dddd, J = 46.4, 27.2, 24.7, 9.4 Hz, F[3]), -200.3 (ddd, J = 46.5, 14.0, 12.6, F[1]); $\delta_{F\{H\}}$ (376 MHz, CDCl$_3$) -196.8 (s, F[3]), -200.3 (s, F[1]); **MS** (ESI, +ve) m/z 339.07 [M+Na]$^+$ (100); **HRMS** (ESI, +ve) C$_{16}$H$_{22}$F$_2$O$_4$Na$^+$ requires m/z 339.1384, found 339.1389.

Data for 195b: [α]$_D^{22}$ -8.3 (c 1.25 in CHCl$_3$); ν_{max} (NaCl)/cm^{-1} 3440, 3087, 3070, 3025, 2986, 2930, 1455, 1373, 1256, 1217, 1069, 842, 738, 699; δ_H (400 MHz, CDCl$_3$) 7.42–7.26 (m, 5H), 4.82–4.48 (m, 4H), 4.46–4.33 (m, 1H), 4.23–4.00 (m, 3H), 3.94–3.78 (m, 2H), 2.54 (d, J = 6.2 Hz, OH), 1.42 (s, 3H), 1.37 (s, 3H); δ_C (100 MHz, CDCl$_3$) 137.5 (C), 128.7 (2 x CH), 128.1 (CH), 128.0 (2 x CH), 110.0 (C), 90.5 (dd, J = 178.1, 2.6 Hz, CH), 89.8 (dd, J = 176.3, 3.7 Hz, CH), 73.9 (CH$_2$), 73.0 (d, J = 29.8 Hz, CH), 69.4 (d, J = 21.0 Hz, CH$_2$), 68.5 (dd, J = 25.9, 17.6 Hz, CH), 66.5 (d, J = 2.7 Hz, CH$_2$), 26.9 (CH$_3$), 25.2 (CH$_3$); δ_F (376 MHz, CDCl$_3$) -194.7 (dm, J = 46.8 Hz, F$_3$), -211.5 (dm, J = 46.6 Hz, F$_1$); $\delta_{F\{H\}}$ (376 MHz, CDCl$_3$) -194.7 (d, J = 3.0 Hz, F$_3$), -211.5 (d, J = 3.0 Hz, F$_1$); **MS** (ESI, +ve) m/z 339.05 [M+Na]$^+$ (100); **HRMS** (ESI, +ve) C$_{16}$H$_{22}$F$_2$O$_4$Na$^+$ requires m/z 339.1384, found 339.1394.

Data for 199a/199b: δ_H (400 MHz, CDCl$_3$) 7.42–7.26 (m, 10H), 5.16–3.05 (m, 22H), 1.48–1.32 (m, 12H); δ_F (376 MHz, CDCl$_3$) -201.2 (dm, J = 46.5 Hz, F), -202.9 (m, F), -211.6 (m, F), -212.2 (m, F); $\delta_{F\{H\}}$ (376 MHz, CDCl$_3$) -201.2 (d, J = 12.0 Hz, F), -202.9 (d, J = 12.0 Hz, F), -211.6 (d, J = 9.0 Hz, F), -212.2 (d, J = 9.0 Hz, F); **MS** (ESI, +ve) m/z 339.09 [M+Na]$^+$ (100); **HRMS** (ESI, +ve) C$_{16}$H$_{22}$F$_2$O$_4$Na$^+$ requires m/z 339.1384, found 339.1390.

Data for 200a/200b: δ_F (376 MHz, CDCl$_3$) -217.0 (m, F), -202.8 (m, F); $\delta_{F\{H\}}$ (376 MHz, CDCl$_3$) -217.0 (s, F), -202.8 (s, F); **MS** (ESI, +ve) *m/z* 279.03 [M+Na]$^+$ (100); **HRMS** (ESI, +ve) C$_{13}$H$_{17}$FO$_4$Na$^+$ requires *m/z* 279.1009, found 279.1000.

(*R*)-4-((1*R*,2*R*,3*S*)-4-(Benzyloxy)-1,2,3-trifluorobutyl)-2,2-dimethyl-1,3-dioxolane 196:[16]
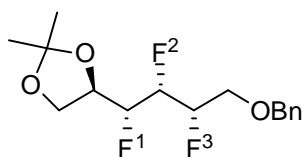
196

Deoxofluor[TM] (1.34 mL, 3.2 mmol) was added to a solution of **195a** (0.40 g, 1.3 mmol) in dry CH_2Cl_2 (25 mL) at 0 ºC. After addition the mixture was heated at reflux (oil bath temperature 70 °C) for 14 h. The reaction was allowed to cool to RT, concentrated onto silica and subjected to flash chromatography over silica gel (9:1→5:1 hexane/ethyl acetate) to give **196** (0.23 g, 57%) as a yellow oil.

ν_{max} (NaCl)/cm^{-1} 3033, 2989, 2941, 2868, 1497, 1452, 1382, 1371, 1250, 1216, 1150, 1119, 1071, 839, 741, 699; δ_H (400 MHz, CDCl$_3$) 7.43–7.27 (m, 5H), 5.18–4.76 (m, 2H), 4.66–4.50 (m, 3H), 4.41–4.30 (m, 1H), 4.23–4.01 (m, 2H), 3.95–3.70 (m, 2H), 1.37 (s, 3H), 1.36 (s, 3H); δ_C (100 MHz, CDCl$_3$) 137.3 (C), 128.6 (2 x CH), 128.2 (CH), 127.9 (2 x CH), 110.1 (C), 88.5–98.2 (m, 3 x CH), 74.0 (CH$_2$), 72.5 (dd, *J* = 29.1, 5.0 Hz, CH), 68.5 (dd, *J* = 21.7, 8.0 Hz, CH$_2$), 66.1 (m, CH) 26.8 (CH$_3$), 25.2 (CH$_3$); δ_F (376 MHz, CDCl$_3$) -198.3 (dm, *J* = 47.3 Hz, F^3), -209.4 (dm, *J* = 46.7 Hz, F^1), -214.2 (dm, *J* = 47.1 Hz, F^2); $\delta_{F\{H\}}$ (376 MHz, CDCl$_3$) -198.3 (d, *J* = 14.2 Hz, F^3), -209.4 (d, *J* = 9.9 Hz, F^1), -214.2 (dd, *J* = 14.2, 9.9 Hz, F^2); **MS** (ESI, +ve) *m/z* 340.98 [M+Na]$^+$ (100); **HRMS** (ESI, +ve) C$_{16}$H$_{21}$F$_3$O$_3$Na$^+$ requires *m/z* 341.1340, found 341.1334.

(2*S*,3*R*,4*R*)-4-((*R*)-2,2-Dimethyl-1,3-dioxolan-4-yl)-2,3,4-trifluorobutan-1-ol 197:[17]
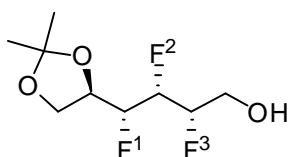
197

A solution of NaBrO$_3$ (0.1 g, 0.6 mmol) in water (2.1 mL) was added to a solution of **196** (0.07 g, 0.2 mmol) in ethyl acetate (2.9 mL). This mixture was stirred at RT for 10 min and a solution of Na$_2$S$_2$O$_4$ (0.11 g, 0.5 mmol) in water (4.3 mL) was added dropwise over 20 min at RT. The mixture was stirred for 1 h at RT. The mixture was then diluted with EtOAc and the organic phase was washed with aq. Na$_2$S$_2$O$_3$. The product was purified over silica gel (9:1→5:1 hexane/ethyl acetate) to give **197** (0.03 g, 53%) as a clear oil.

$[\alpha]_D^{22}$ -20.1 (c 0.57 in CHCl$_3$); ν_{max} (NaCl)/cm^{-1} 3434, 2986, 2958, 2936, 2896, 1634, 1457, 1385, 1373, 1256, 1222, 1150, 1113, 1066, 1049, 987, 945, 917, 842, 870, 786, 766, 708, 666); δ_H (400 MHz, CDCl$_3$) 5.13–4.73 (m, 2H), 4.60 (dm, *J* = 46.7 Hz, 1H), 4.45–4.31 (m, 1H), 4.22–3.79 (m, 4H), 1.91 (t, *J* = 6.3 Hz, OH), 1.43 (s, 3H), 1.37 (s, 3H); δ_C (100 MHz, CDCl$_3$) 110.2 (C), 93.3–88.2 (m, 3 x CH), 72.5 (dd, *J* = 29.0 Hz, 4.9, CH), 66.1 (m, CH), 61.7 (dd, *J* = 21.9, 8.1 Hz, CH$_2$) 26.9 (CH$_3$), 25.2 (CH$_3$); δ_F (376 MHz, CDCl$_3$) -202.0 (dm, *J* = 47.4 Hz, F^3), -209.4 (dm, *J* = 46.7 Hz, F^1), -215.0 (dm, *J* = 46.5 Hz, F^2); $\delta_{F\{H\}}$ (376 MHz, CDCl$_3$) -202.0 (d, *J* = 14.3 Hz, F^3), -209.4 (d, *J* = 9.6 Hz, F^1), -215.0 (dd, *J* = 14.3, 9.6 Hz, F^2); **MS** (ESI, +ve) *m/z* 251.03 [M+Na]$^+$ (100); **HRMS** (ESI, +ve) C$_9$H$_{15}$F$_3$O$_3$Na$^+$ requires *m/z* 251.0871, found 251.0872.

(2*S*,3*S*,4*R*)-4-((*R*)-2,2-Dimethyl-1,3-dioxolan-4-yl)-2,3,4-trifluorobutanal 198:[18]
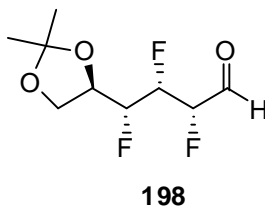
198

A solution of Dess-Martin periodinane reagent (0.13 g, 0.3 mmol) in dry CH_2Cl_2 (1.1 mL) was placed in an oven-dried round-bottom flask and stirred at RT for 5 min. Then a solution of **197** (0.04 g, 0.2 mmol) in dry CH_2Cl_2 (1.1 mL) was added. After stirring for 40 min at RT, a mixture of hexane/ethyl acetate (9:1, 5 mL) was added and the resultant suspension was quickly filtered through a silica plug (2.5 cm) by flushing with 9:1 hexane/ethyl acetate (125 mL). This provided aldehyde **198** (0.04 g) as a yellow oil which was used in the next reaction without further purification due to its instability.

δ_F (282 MHz, CDCl$_3$) -204.3 (dd, *J* = 11.1, 4.8 Hz, 1F), -212.5 (dd, *J* = 12.8, 11.1 Hz, 1F), -213.5 (dd, *J* = 12.8, 4.8 Hz, 1F).

2,3,4-Trideoxy-2,3,4-trifluoro D-glucose 193:[19]

193
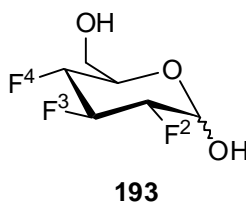
A mixture of **198** (0.04 g, 0.2 mmol) and anhydrous tin(II) chloride (0.06 g, 0.3 mmol) were stirred in dry CH_2Cl_2 (3.9 mL) at RT for 1 h. The undissolved tin(II) chloride was removed by filtration. Silica gel (1 g) was added to the filtrate. The resultant suspension was evaporated to dryness and purified over silica gel (9:1→1:9 hexane/ethyl acetate) to give **193** (0.02 g, 58%, as a mixture of α- and β- anomers) as a transparent oil. The product was recrystallised from $CHCl_3$. The relative stereochemistry of the β-anomer was determined by X-ray structure analysis. The anomeric ratio was α/β: 1:0.13 determined by $^{19}F\{^1H\}$-NMR (376 MHz, $CDCl_3$), and α/β: 1:0.2 determined by $^1H\{^{19}F\}$-NMR (400 MHz, $CDCl_3$).

Data for the anomeric mixture: $[\alpha]_D^{22}$ +40.1 (c 1.15 in d_8-THF, 1:1 anomeric ratio); δ_H (400 MHz, $CDCl_3$) 5.56–4.78 (m, 4H), 4.77–4.21 (m, 4H), 4.20–3.26 (m, 6H), 3.30 (br s, OH), 1.78 (br s, OH); **MS** (ESI, +ve) m/z 208.99 [M+Na]$^+$ (100); **HRMS** (ESI, +ve) $C_6H_9F_3O_3Na^+$ requires m/z 209.0401, found 209.0405. **Data for α-anomer:** δ_C (100 MHz, $CDCl_3$) 91.5–89.2 (m, 3 x CH), 90.5 (dd, J = 21.1, 9.7 Hz, CH), 88.0 (ddd, J = 192.8, 16.7, 8.1 Hz, CH), 86.6 (ddd, J = 186.0, 18.4, 7.7 Hz, CH), 68.7 (dd, J = 24.3, 6.3 Hz, CH), 60.9 (CH$_2$); δ_F (376 MHz, $CDCl_3$) -199.9 (dm, J = 51.0 Hz, 1F^2), -201.6 (dm, J = 55.0 Hz, 1F^3), -202.0 (dm, J = 49.6, 1F^4); $\delta_{F\{H\}}$ (376 MHz, $CDCl_3$) -199.9 (dd, J = 12.7, 2.0 Hz, 1F^2), -201.6 (dd, J = 13.2, 12.7 Hz, 1F^3), -202.0 (dd, J = 13.2, 2.0 Hz, 1F^4). **Data for β-anomer:** **Mp** 103–105 °C (from $CHCl_3$); δ_F (376 MHz, $CDCl_3$) -195.8 (dm, J = 52.8 Hz, 1F^3), -200.5 (dm, J = 50.9 Hz, 1F^2), -201.2 (dm, J = 50.4 Hz, 1F^4); $\delta_{F\{H\}}$ (376 MHz, $CDCl_3$) -195.8 (dd, J = 13.2, 12.7 Hz, 1F^3), -200.5 (dd, J = 13.2, 2.8 Hz, 1F^2), -201.2 (dd, J = 12.7, 2.8 Hz, 1F^4).

(*R*)-4-((1*R*,2*S*,3*R*)-4-(Benzyloxy)-1,2,3-trifluorobutyl)-2,2-dimethyl-1,3-dioxolane 201:[16]
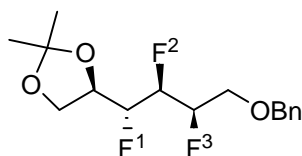

201

Deoxofluor^{TM} (1.34 mL, 3.2 mmol) was added to a solution of **195b** (0.40 g, 1.3 mmol)   in dry CH$_2$Cl$_2$ (25 mL) at 0 ℃. After addition the mixture was heated at reflux (oil bath temperature 70 °C) for 14 h. The reaction was allowed to cool to RT, concentrated onto silica and subjected to flash chromatography over silica gel (9:1→5:1 hexane/ethyl acetate) to give **201** (0.24 g, 60%) as a yellow oil.

ν_{max} (NaCl)/cm^{-1} 3089, 3058, 3025, 2986, 2930, 2874, 1497, 1455, 1379, 1370, 1259, 1214, 1147, 1108, 1066, 845, 744; δ_H (400 MHz, CDCl$_3$) 7.43–7.27 (m, 5H), 5.06–4.52 (m, 5H), 4.48–4.36 (m, 1H), 4.15–4.05 (m, 1H), 4.05–3.95 (m, 1H), 3.84–3.72 (m, 2H), 1.39 (s, 3H), 1.36 (s, 3H); δ_C (100 MHz, CDCl$_3$) 137.4 (C), 128.7 (2 x CH), 128.2 (CH), 128.0 (2 x CH), 110.1 (C), 91.1–87.8 (m, 3 x CH), 73.8 (CH$_2$), 73.4 (dd, J = 25.1, 3.7 Hz, CH), 67.6 (dd, J = 25.2, 7.0 Hz, CH$_2$), 65.3 (dd, J = 5.7, 2.9 Hz, CH$_2$) 26.2 (CH$_3$), 25.3 (CH$_3$); δ_F (376 MHz, CDCl$_3$) -201.3 (dm, J = 45.9 Hz, F^1), -203.3 (dm, J = 47.8 Hz, F^3), -213.6 (dm, J = 47.1 Hz, F^2); $\delta_{F\{H\}}$ (376 MHz, CDCl$_3$) -201.3 (dd, J = 13.0, 5.7 Hz, F^1), -203.3 (dd, J = 10.7, 5.7 Hz, F^3), -213.6 (dd, J = 13.0, 10.7 Hz, F^2); **MS** (ESI, +ve) *m/z* 341.07 [M+Na]$^+$ (100); **HRMS** (ESI, +ve) C$_{16}$H$_{21}$F$_3$O$_3$Na$^+$ requires *m/z* 341.1340, found 341.1344.

(2R,3S,4R)-4-((R)-2,2-Dimethyl-1,3-dioxolan-4-yl)-2,3,4-trifluorobutan-1-ol 202:[17]

202
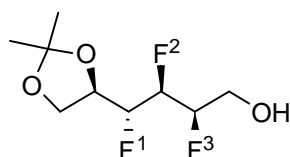
A solution of NaBrO$_3$ (0.1 g, 0.6 mmol) in water (2.1 mL) was added to a solution of **201** (0.07 g, 0.2 mmol) in ethyl acetate (2.9 mL). This mixture was stirred for 10 min at RT and a solution of Na$_2$S$_2$O$_4$ (0.11 g, 0.5 mmol) in water (4.3 mL) was added dropwise over 20 min at RT. The mixture was stirred for 1 h at RT. The mixture was then diluted with EtOAc and the organic phase was washed with aq. Na$_2$S$_2$O$_3$. The product was purified over silica gel (9:1→5:1 hexane/ethyl acetate) to give **202** (0.02 g, 51%) as a clear oil.

$[\alpha]_D^{22}$ -4.4 (c 0.39 in CHCl$_3$); ν_{max} (NaCl)/cm^{-1} 3446, 2986, 2930, 2891, 1636, 1483, 1457, 1382, 1376, 1258, 1211, 1152, 1063, 848); δ_H (400 MHz, CDCl$_3$) 5.03–4.64 (m, 3H), 4.52–4.36 (dq, J = 15.4, 5.9 Hz, 1H), 4.18–4.10 (m, 1H) , 4.07–4.00 (m, 1H) 3.99–3.84 (m, 2H), 1.97 (t, J = 6.4 Hz, OH), 1.44 (s, 3H), 1.37 (s, 3H); δ_C (100 MHz, CDCl$_3$) 110.3 (C), 92.0–87.8 (m, 3 x CH), 73.4 (dd, J = 25.3, 4.1 Hz, CH), 65.4 (dd, J = 5.7, 2.9 Hz, CH$_2$), 61.3 (dd, J = 24.4, 7.2 Hz, CH$_2$), 26.3 (CH$_3$), 25.2 (CH$_3$); δ_F (376 MHz, CDCl$_3$) -201.3 (dm, J = 45.5 Hz, F^1), -205.4 (m, F^3), -212.8 (dm, J = 47.0 Hz, F^2); $\delta_{F\{H\}}$ (376 MHz, CDCl$_3$) -201.3 (dd, J = 12.7, 5.9 Hz, F^1), -205.4 (dd, J = 10.9, 5.9 Hz, F^3), -212.8 (dd, J = 12.7, 10.9 Hz, F^2); **MS** (ESI, +ve) m/z 251.00 [M+Na]$^+$ (100); **HRMS** (ESI, +ve) C$_9$H$_{15}$F$_3$O$_3$Na$^+$ requires m/z 251.0871, found 251.0877.

(2*R*,3*R*,4*R*)-4-((*R*)-2,2-Dimethyl-1,3-dioxolan-4-yl)-2,3,4-trifluorobutanal 203:[18]
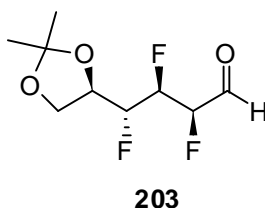
203

A solution of Dess-Martin periodinane reagent (0.13 g, 0.3 mmol) in dry CH_2Cl_2 (1.1 mL) was placed in an oven-dried round-bottom flask and stirred at RT for 5 min. Then a solution of **202** (0.04 g, 0.2 mmol) in dry CH_2Cl_2 (1.1 mL) was added. After stirring for 40 min, a mixture of hexane/ethyl acetate (9:1, 5 mL) was added and the resultant suspension was quickly filtered through a silica plug (2.5 cm) by flushing with 9:1 hexane/ethyl acetate (125 mL). This provided aldehyde **203** (0.04 g) as a yellow oil which was used in the next reaction without further purification due to its instability.

δ_F (282 MHz, CDCl$_3$) -201.5 (dd, J = 13.4, 7.6 Hz, 1F), -210.7 (dd, J = 10.1, 13.4 Hz, 1F), -217.0 (dd, J = 10.1, 7.6 Hz, 1F).

2,3,4-Trideoxy-2,3,4-trifluoro D-altrose 216:[19]

216
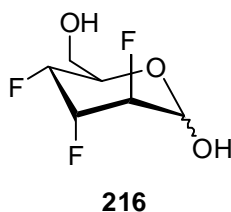
A mixture of **203** (0.04 g, 0.2 mmol) and anhydrous tin(II) chloride (0.06 g, 0.3 mmol) were stirred in dry CH_2Cl_2 (3.9 mL) at RT for 1 h. The undissolved tin(II) chloride was removed by filtration. Silica gel (1 g) was added to the filtrate. The resultant suspension was evaporated to dryness and purified over silica gel (9:1→1:9 hexane/ethyl acetate) to give **216** (0.01 g, 48%, as a mixture of *α*- and *β*- anomers) as a transparent oil. The product was recrystallised from $CHCl_3$. The relative stereochemistry of the *β*-anomer was determined by X-ray structure analysis. The anomeric ratio was *α*/*β*: 0.8:1 determined by $^{19}F\{^1H\}$-NMR (376 MHz, $CDCl_3$) and $^1H\{^{19}F\}$-NMR (400 MHz, $CDCl_3$).

Data for the anomeric mixture: δ_H (400 MHz, $CDCl_3$) 5.51–5.02 (m, 4H), 5.00–4.59 (m, 4H), 4.51–4.33 (m, 1H), 4.09–3.76 (m, 5H), 2.84 (br s, OH); **MS** (ESI, +ve) *m/z* 208.98 [M+Na]$^+$ (100); **HRMS** (ESI, +ve) $C_6H_9F_3O_3Na^+$ requires *m/z* 209.0401, found 209.0403. **Data for *β*-anomer: Mp** 78–80 °C (from $CHCl_3$); δ_C (100 MHz, $CDCl_3$) 91.4 (d, *J* = 17.4 Hz, CH), 88.5–81.8 (m, 3 x CH), 72.2 (dd, *J* = 25.0, 2.8 Hz, CH), 61.4 (CH_2); δ_F (376 MHz, $CDCl_3$) -213.4 (dm, *J* = 44.4 Hz, 1F), -214.3 (dm, *J* = 48.8 Hz, 1F), -219.3 (dt, *J* = 46.5, 17.3 Hz, 1F); $\delta_{F\{H\}}$ (376 MHz, $CDCl_3$) -213.4 (d, *J* = 11.7 Hz, 1F), -214.3 (dd, *J* = 17.3, 11.7 Hz, 1F), -219.3 (d, *J* = 17.3 Hz, 1F). **Data for *α*-anomer:** δ_C (100 MHz, $CDCl_3$) 91.9 (d, *J* = 32.1 Hz , CH), 88.5–81.8 (m, CH), 66.1 (dd, *J* = 24.6, 2.8 Hz, CH), 61.5 (CH_2); δ_F (376 MHz, $CDCl_3$) -200.5 (dm, *J* = 44.2 Hz, 1F), -209.7 (dm, *J* = 45.4 Hz, 1F), -213.9 (dm, *J* =

48.7 Hz, 1F); $\delta_{\mathbf{F\{H\}}}$ (376 MHz, CDCl$_3$) -200.5 (dd, J = 17.7, 2.1 Hz, 1F), -209.7 (dd, J = 11.1, 2.1 Hz, 1F), -213.9 (dd, J = 17.7, 11.1 Hz, 1F).

**(*S*)-(1-Fluoroethyl)benzene (*S*)-214 (95% ee):[20]**
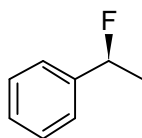
(*S*)-**214**

N-(Trimethylsilyl)morpholine **226** (neat, 447 µl, 2.5 mmol) was added dropwise to a solution of DAST (312 µl, 2.4 mmol) in dry CH_2Cl_2 (0.96 mL) at -78 °C, and was stirred at RT for 2.5 h. The reaction was further cooled to -78 °C and a solution of (*R*)-**213** (90 µl, 0.7 mmol) in dry CH_2Cl_2 (2.24 mL) was slowly added *via* cannula. The reaction was stirred at RT for 15 h. The mixture was then slowly poured over sat. aqueous $NaHCO_3$ solution (15 mL). The organic layer was separated and the aqueous extracted into CH_2Cl_2 (3 x 1.5 mL). The combined organic layers were dried over anhydrous $MgSO_4$ and the solvent was evaporated under reduced pressure. The residue was purified over silica gel (100% pentane) to afford (*S*)-**214** (65 mg, 71% yield) as a colourless oil. Chiral-phase GC/MS (EI) analysis of the product, t_R = 20.3 min for the major (*S*)-enantiomer and t_R = 21.3 min for the minor (*R*)-enantiomer, indicated that the ee was 95%.

$[\alpha]_D^{22}$ +35.6 (c 1.0, $CHCl_3$); ν_{max} (NaCl)/cm^{-1} 3083, 3064, 3034, 2980, 2926, 1451, 1211, 1063; δ_H (300 MHz, $CDCl_3$) 7.43–7.29 (m, 5H), 5.64 (dq, *J* = 47.6, 6.4 Hz, 1H), 1.65 (dd, *J* = 23.9, 6.4 Hz, 3H); δ_C (75 MHz, $CDCl_3$) 141.7 (d, *J* = 20.0 Hz, C), 128.6 (CH), 128.3 (d, *J* = 1.9 Hz, 2 x CH), 125.3 (d, *J* = 6.7 Hz, 2 x CH), 91.1 (d, *J* = 167.4 Hz, CH), 23.1 (d, *J* = 25.3 Hz, CH_3); δ_F (282 MHz, $CDCl_3$) -167.5 (dq, *J* = 47.6, 23.9 Hz, 1F); $\delta_{F\{H\}}$ (282 MHz, $CDCl_3$) -167.5 (s, 1F); **GC/MS** (EI, +ve) *m/z* 124 [M]$^+$, 109 [M-CH$_3$]$^+$; **HRMS** (EI, +ve) C_8H_9F requires *m/z* 124.0688, found 124.0689.

(S)-Methyl 2-fluoro-2-phenylacetate (S)-228:[20]
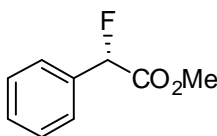
(S)-**228**

N-(Trimethylsilyl)morpholine **226** (neat, 298 µl, 1.7 mmol) was added dropwise to a solution of Deoxofluor[TM] (50% in THF, 690 µl, 1.6 mmol) in dry CH_2Cl_2 (2.20 mL) at -78 °C. The resultant solution was stirred at RT for 2.5 h. The reaction was further cooled to -78 °C and a solution of methyl (*R*)-**227** (248 mg, 1.5 mmol) in dry CH_2Cl_2 (4.48 mL) was slowly added *via* cannula. The reaction was stirred at RT for 24 h. The mixture was then slowly poured over sat. aqueous $NaHCO_3$ solution (30 mL). The organic layer was separated and the aqueous extracted into CH_2Cl_2 (3 x 3.0 mL). The combined organic layers were dried over anhydrous $MgSO_4$ and the solvent was evaporated under reduced pressure. The residue was purified over silica gel (9:1 hexane:EtOAc → 4:1) to afford (*S*)-**228** (48 mg, 19% yield) as a colourless oil. Chiral-phase GC/MS (EI-SIM) analysis of the product, t_R = 42.2 min for the minor (*R*)-enantiomer and t_R = 42.5 min for the major (*S*)-enantiomer, indicated that the ee was 99%.

$[\alpha]_D^{22}$ +117.5 (*c* 1.4, CDCl$_3$); ν_{max} (NaCl)/cm^{-1} 3083, 3062, 3027, 2972, 2937, 2877, 1761, 1714, 1448, 1350, 1091; δ_H (400 MHz, CDCl$_3$) 7.51–7.36 (m, 5H), 5.80 (d, *J* = 47.5 Hz, 1H), 3.78 (s, 3H); δ_C (75 MHz, CDCl$_3$) 169.1 (d, *J* = 27.7 Hz, C), 134.3 (d, *J* = 20.6 Hz, C), 129.8 (d, *J* = 2.1 Hz, 2 x CH), 128.9 (CH), 126.8 (d, *J* = 6.1 Hz, 2 x CH), 89.4 (d, *J* = 185.6 Hz, CH), 52.7 (s, CH$_3$); δ_F (282 MHz, CDCl$_3$) -180.3 (d, *J* = 47.5 Hz, 1F); $\delta_{F\{H\}}$ (282

MHz, CDCl$_3$) -180.3 (s, 1F); **GC/MS** (EI-SIM, +ve) m/z 168 [M]$^+$; **HRMS** (ESI, +ve)

C$_9$H$_9$FO$_2$Na$^+$ requires m/z 191.0484, found 191.0482.

5.3) General procedures for dehydroxyfluorination of allylic alcohol 155a/155b:

5.3.1) Dehydroxyfluorination with TFEDMA:[21]

A solution of allylic alcohol **155a/155b** (5.0 mmol) in CH_2Cl_2 (10 mL) was added to a solution of TFEDMA (5.5 mmol) in CH_2Cl_2 (10 mL) at 0 °C placed in a polythene vessel. After addition the reaction was brought to RT and stirred for 1 h and the progress of the reaction was monitored by t.l.c. The reaction was worked up by adding sat. aqueous $NaHCO_3$ solution and the product was extracted into CH_2Cl_2 (3 x 150 mL). Purification by chromatography (6:1 hex:EtOAc → 3:1) gave **156a** and an inseparable mixture of isomers **156b/157a/157b**. Stereoisomer ratios (determined by ^{19}F-NMR) and yields (after isolation by column chromatography) are given in Table 2.1, Chapter 2.

5.3.2) Dehydroxyfluorination with Deoxofluor[TM]:[22]

A solution of Deoxofluor[TM] (7.5 mmol, 50% in THF) was added to a solution of **155a/155b** (5.0 mmol) in CH_2Cl_2 (20 mL) at 0 ℃ placed in a round-bottom flask (standard glassware). After addition the reaction was heated to 55 °C for 3.5 h and the progress of the reaction was monitored by t.l.c. The reaction was allowed to cool to RT and was then worked up by adding sat. aqueous $NaHCO_3$ solution. The product was extracted into CH_2Cl_2 (3 x 150 mL) and was purified over silica gel eluting with a hexane/ethyl acetate gradient (6:1 hex:EtOAc → 3:1). This gave **156a** and an inseparable mixture of isomers **156b/157a/157b**. Stereoisomer ratios

(determined by ^{19}F-NMR) and yields (after isolation by column chromatography) are given in Table 2.1, Chapter 2.

5.3.3) Dehydroxyfluorination with DAST:[23]

DAST^{TM} (neat, 7.5 mmol) was added to a solution of **155a/155b** (5.0 mmol) in dry CH$_2$Cl$_2$ (20 mL) at 0 ºC placed in a round-bottom flask (standard glassware). After addition the reaction was brought to RT and stirred for 4.5 h and the progress of the reaction was monitored by t.l.c. The reaction was worked up by adding sat. aqueous NaHCO$_3$ solution and the product was extracted into CH$_2$Cl$_2$ (3 x 150 mL) and purified over silica gel (hexane/ethyl acetate gradient (6:1 hex:EtOAc → 3:1). This gave **156a** and an inseparable mixture of isomers **156b/157a/157b**. Stereoisomer ratios (determined by ^{19}F-NMR) and yields (after isolation by column chromatography) are given in Table 2.1, Chapter 2.

5.3.4) Dehydroxyfluorination with Fluolead^{TM}:[24]

A solution of allylic alcohol **155a**/**155b** (1.1 mmol) in dry CH$_2$Cl$_2$ (2.2 mL) was added to a solution of Fluolead^{TM} (1.2 mmol) in dry CH$_2$Cl$_2$ (2.2 mL) at 0 °C placed in a polyethylene vessel. After addition the reaction was stirred at 0 °C for 40 min. The progress of the reaction was monitored by t.l.c. The reaction was worked up by slowly adding sat. aqueous NaHCO$_3$ solution and the product was extracted into CH$_2$Cl$_2$ (3 x 20 mL). Evaporation of solvents *in vacuo* gave a product that was analysed directly by ^{19}F NMR spectroscopy. Stereoisomer ratios (determined by ^{19}F-NMR) of **156a**/**156b**/**157a**/**157b** are given in Table 2.1, Chapter 2.

5.4) General procedures for dehydroxyfluorination of alcohols 213 and 227:

5.4.1) Dehydroxyfluorination without additive:

A solution of alcohol **213** or **227** (0.7 mmol, 1.0 equiv.) in dry CH_2Cl_2 (2.2 mL) was slowly added *via* cannula to a solution of dehydroxyfluorination reagent (1.1, 2.2 or 3.3 equiv.) in CH_2Cl_2 (1.4 mL) at -78 °C[a] placed in a round-bottom flask[b]. The solution was then allowed to warm to RT and stirred for 15 h. The mixture was slowly poured over sat. aqueous $NaHCO_3$ solution (30 mL). The organic phase was separated and washed with water (10 mL), dried over $MgSO_4$ and analysed by chiral GC-MS (see Paragraph 5.5).

[a] For reactions performed using Fluolead[TM], addition of alcohol was performed at -20 °C.

[b] Reaction using Fluolead[TM] and TFEDMA were performed in a polyethylene vessel.

5.4.2) Dehydroxyfluorination with additive:[20]

Neat additive **226** or **229** (1.1, 2.2 or 3.3 equiv.) was added dropwise to a solution of dehydroxyfluorination reagent (1.1, 2.2 or 3.3 equiv.) in dry CH_2Cl_2 (1.4 mL) at -78 °C[a] placed in a round-bottom flask[b]. The solution was then allowed to warm to RT, stirred for 2.5 h and further cooled to -78 °C. A solution of alcohol **213** or **227** (0.7 mmol, 1.0 equiv.) in dry CH_2Cl_2 (2.2 mL) was slowly added *via* cannula at -78 °C. The solution was allowed to warm to RT and stirred for 15 h. The mixture was slowly poured over sat. aqueous $NaHCO_3$ solution (30 mL). The organic phase was separated and washed with water (10 mL), dried over $MgSO_4$ and analysed by chiral GC-MS (see Paragraph 5.5.1).

[a] For reactions performed using Fluolead[TM], addition of alcohol was performed at -20 °C.

[b] Reaction using Fluolead[TM] and TFEDMA were performed in a polyethylene vessel.

5.5 GC analyses for determination of the enantiopurities and the % conversions of products 214 and 228:

5.5.1) GC analyses for determination of the enantiopurities:

Analyses were run using a Betadex^{TM} 120 fused silica capillary column (30 m x 0.25 mm i. D., 0.25 μm film thickness). Different temperature gradients were used for the chiral separation of racemic-**214** and racemic-**228**. The GC chromatogram of racemic-**214** is presented . It has two peaks of the same area at 22.66 and 23.71 min. The MS (EI) spectra of the peak at 22.66 min (Figure 5.2) and of the peak at 23.71 min (Figure 5.3) show identical fragmentation patterns for **214** (m/z = 124 [M]$^+$, 109 [M-CH$_3$]$^+$), consistent with each peak belonging to enantiomers of **214**.

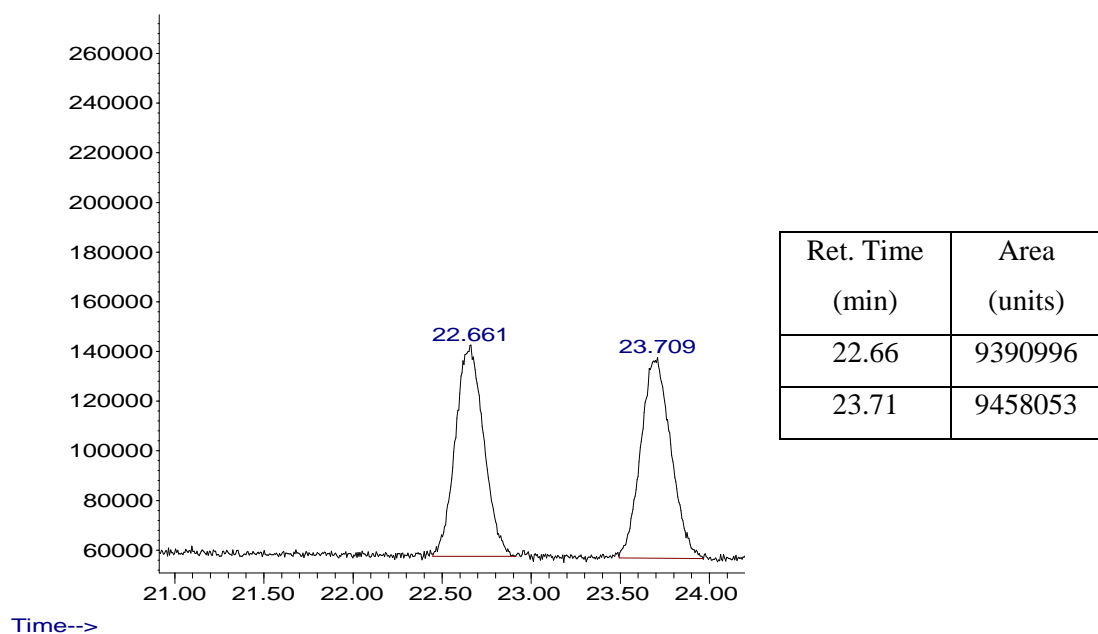| Ret. Time (min)	Area (units)
22.66	9390996
23.71	9458053

Figure 5.1. Chiral-phase GC chromatogram of racemic-**214**: temperature-gradient oven (80 °C held for 30 min), 250 °C injector temperature, 100:1 split ratio, 0.9 mL/min flow, He carrier gas, Betadex^{TM} 120 fused silica capillary column (30 m x 0.25 mm i.d., 0.25 μm film thickness), MS (EI) detection.
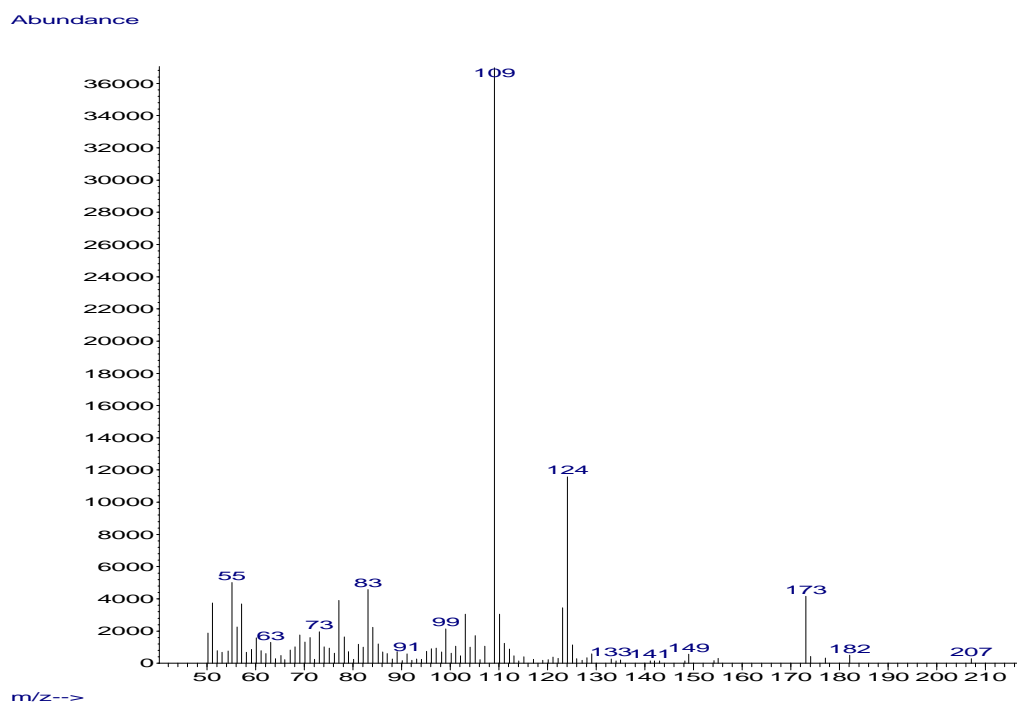
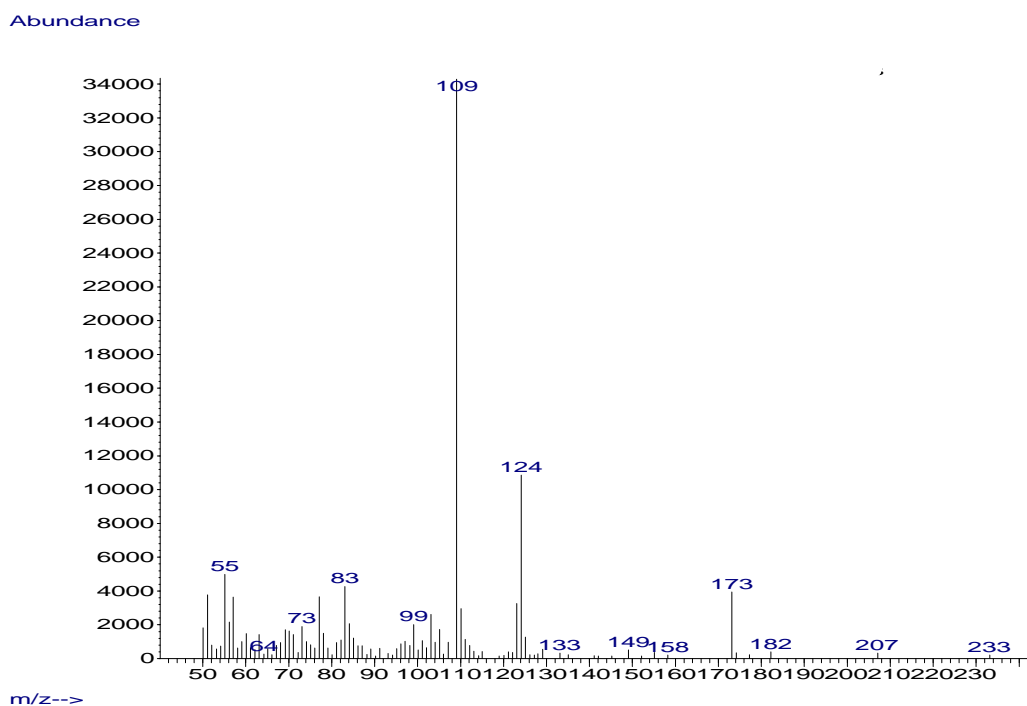**Figure 5.2.** GC/MS (EI) spectrum of racemic-**214**, scan at 22.66 min.


Figure 5.3. GC/MS (EI) spectrum of racemic-**214**, scan at 23.70 min.

Chiral-phase GC-MS allowed determination of the enantiomeric ratios of **214** prepared in this study. GC/MS (EI) analysis of (*S*)-**214** (95% ee, Entry 7 in Table 4.7, Chapter 4) allowed the

individual (*R* or *S*) enantiomers of each peak to be assigned. The GC chromatogram of (*S*)-**214** (95% ee) is presented in Figure 5.4 and shows a major peak at 20.27 min which corresponds to the (*S*) enantiomer, and a minor peak at 21.30 min corresponding to the (*R*) enantiomer. The MS (EI) spectra for each peak are shown in Figures 5.5 and 5.6. In each case they display a fragmentation pattern consistent with **214** (m/z = 124 [M]$^+$, 109 [M-CH$_3$]$^+$).

Ret. Time (min)	Area (units)
20.27	59566830
21.30	1545765
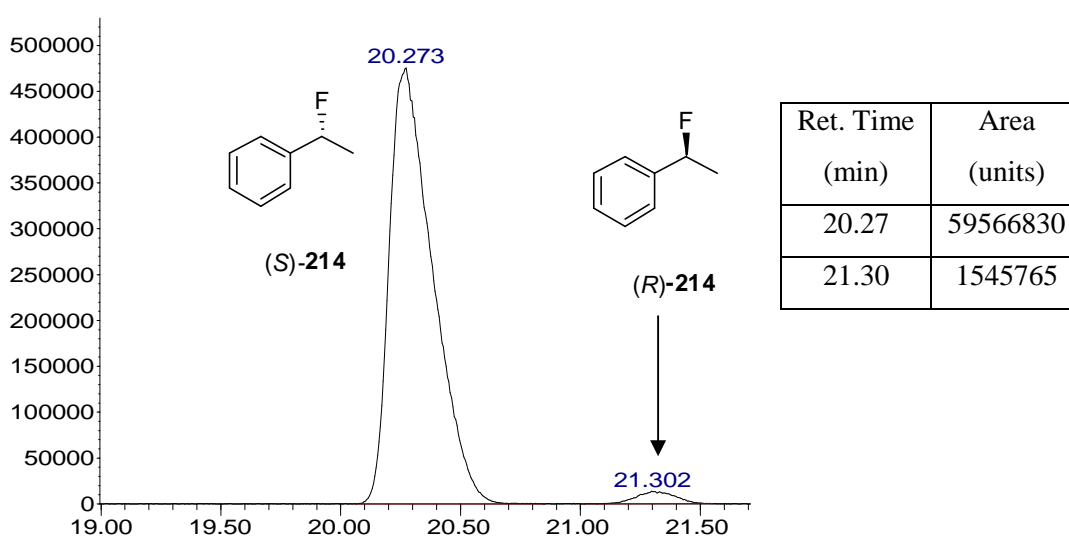
Figure 5.4. Chiral-phase GC chromatogram of (*S*)-**214** (95% ee): temperature-gradient oven (80 °C held for 30 min), 250 °C injector temperature, 100:1 split ratio, 0.9 mL/min flow, He carrier gas, Betadex^{TM} 120 fused silica capillary column (30 m x 0.25 mm i.d., 0.25 µm film thickness), MS (EI) detection.
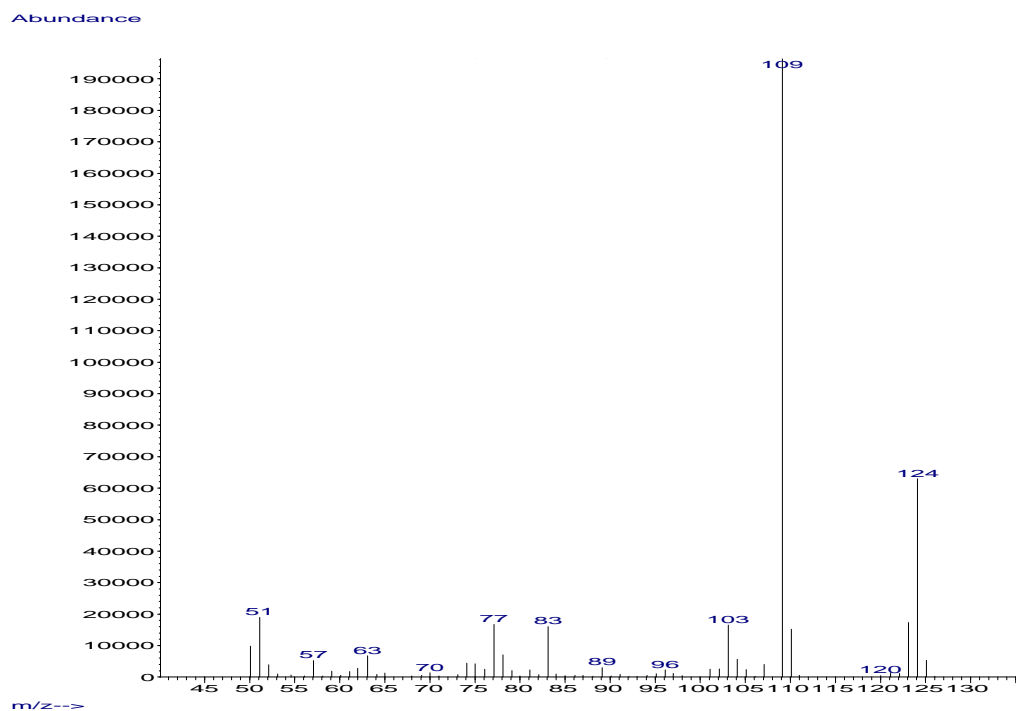
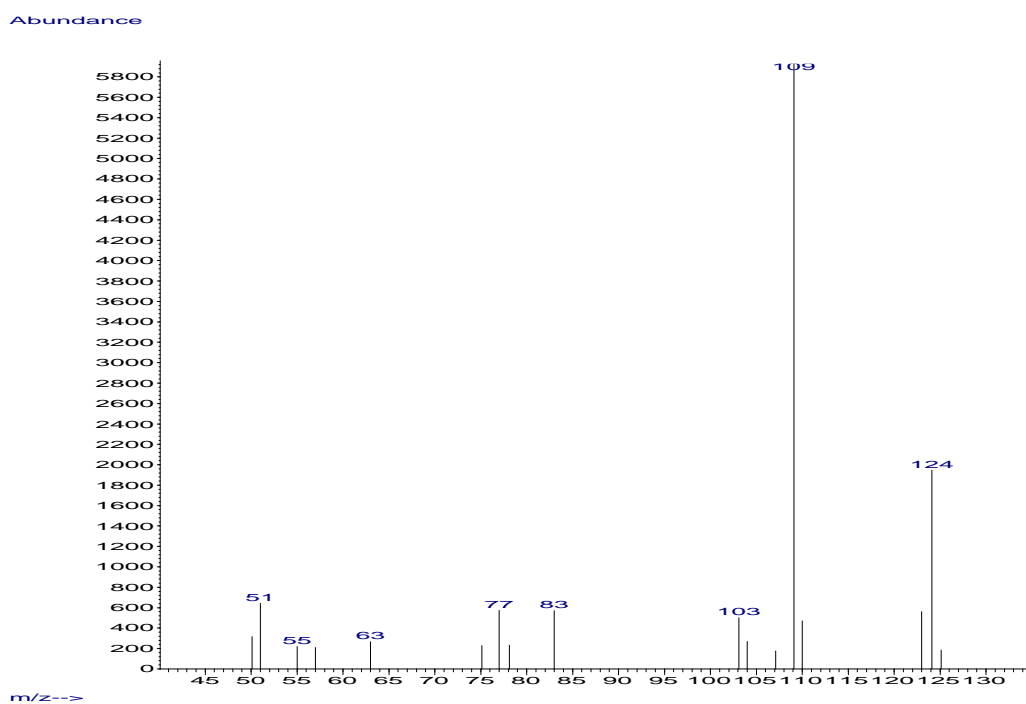**Figure 5.5.** GC/MS (EI) spectrum of (*S*)-**214**, scan at 20.28 min.

Figure 5.6. GC/MS (EI) spectrum of (*R*)-**214**, scan at 21.30 min.

A similar procedure was adopted for product **228**. The GC chromatogram of racemic-**228** is

presented in Figure 5.7 and has two peaks of the same area at 41.33 and 41.70 min. The MS

(EI) spectra of the peaks at 41.33 min (Figure 5.8) and 41.70 min (Figure 5.9) show the same expected fragmentation pattern for **228** (m/z = 168 [M]$^+$, 109 [M-CH$_3$]$^+$), indicating that they belong to the enantiomers of **228**.

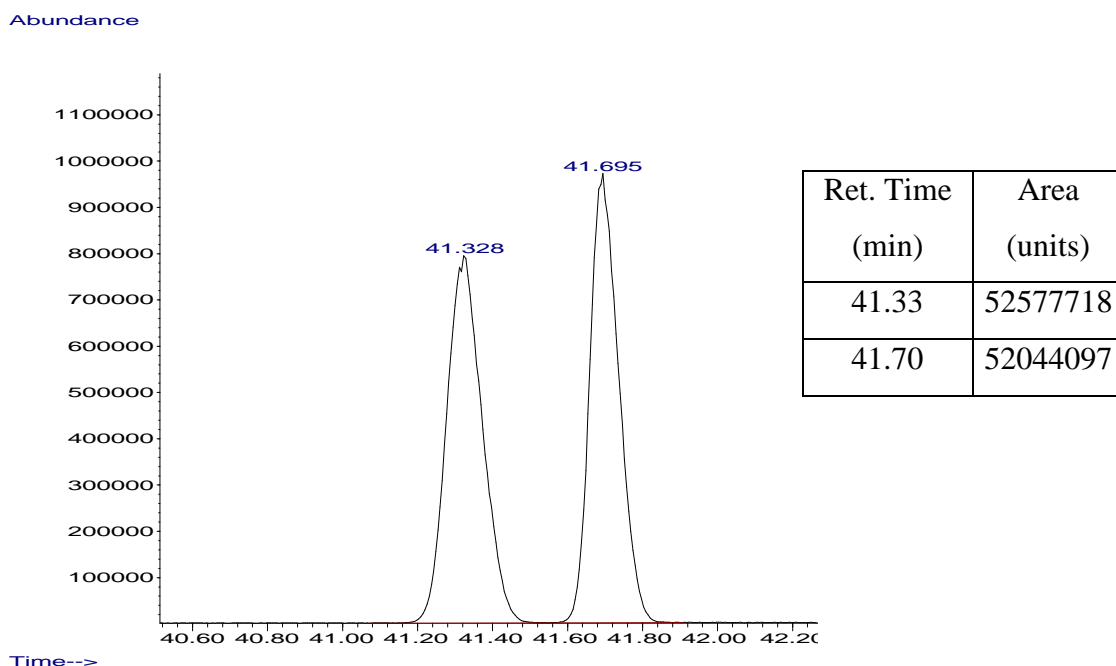| Ret. Time (min)	Area (units)
41.33	52577718
41.70	52044097

Figure 5.7. Chiral-phase GC chromatogram of racemic-**228**: temperature-gradient oven (start at 110 °C held for 40 min, then gradient at 20 °C/min to 150 °C held for 15 min), 250 °C injector temperature, 100:1 split ratio, 0.9 mL/min flow, He carrier gas, Betadex^{TM} 120 fused silica capillary column (30 m x 0.25 mm i.d., 0.25 µm film thickness), MS (EI) detection.
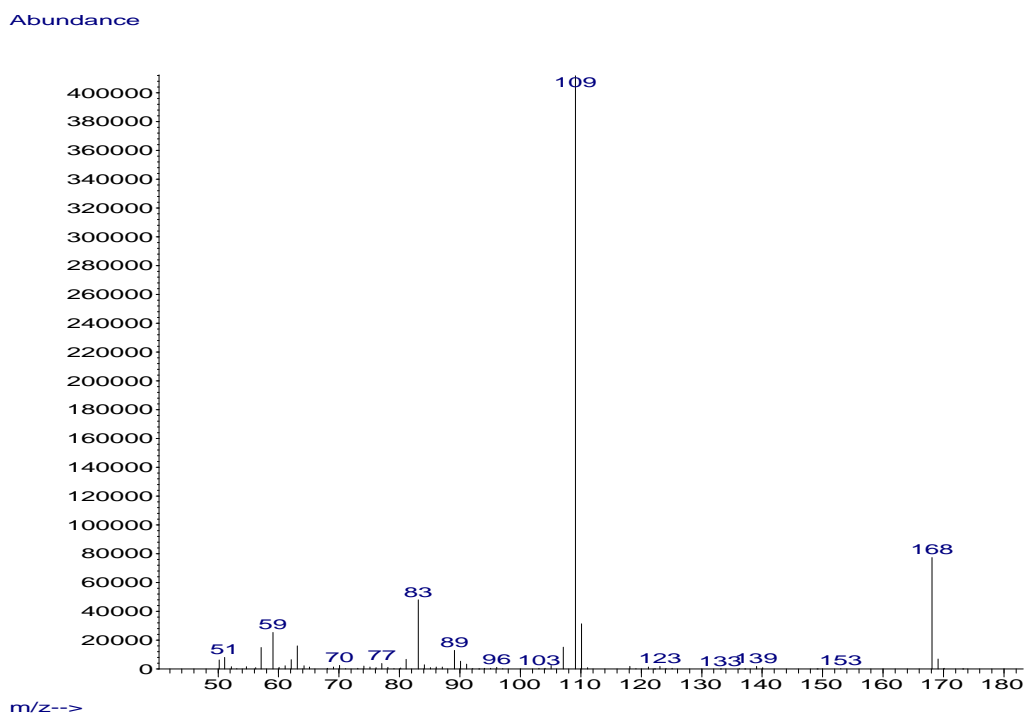
Figure 5.8. GC/MS (EI) spectrum of racemic-**228**, scan at 41.33 min.
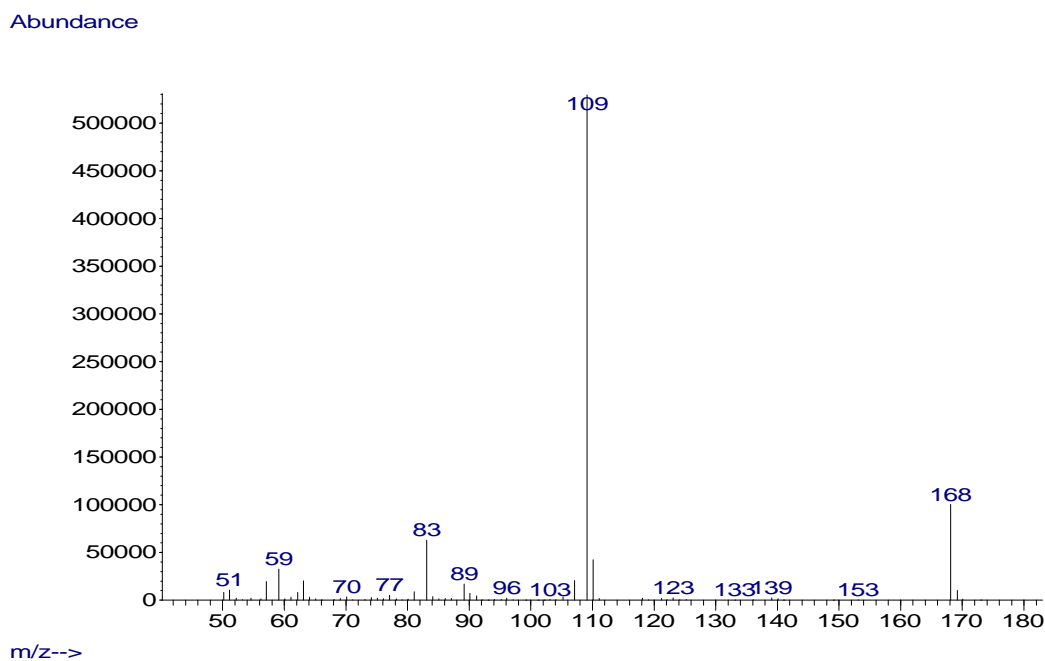
Figure 5.9. GC/MS (EI) spectrum of racemic-**228**, scan at 41.70 min.

Chiral-phase GC/MS (EI) analysis of (*S*)-**228** (99% ee, Entry 3, Table 4.9, Chapter 4) allowed the individual (*R* or *S*) enantiomers of each peak to be assigned. The GC chromatogram of (*S*)-**228** (99% ee) is presented in Figure 5.10 and shows a small peak at 42.20 min which

186

corresponds to the (*R*) enantiomer, and the main peak at 42.45 min which corresponds to the

(*S*) enantiomer. The MS (EI-SIM) spectra for the peak at 42.20 min and the peak at 42.45 min

are shown in Figure 5.11 and Figure 5.12 respectively. In each case they display the same

expected fragmentation pattern consistent with **228** ($m/z = 168$ $[M]^+$).
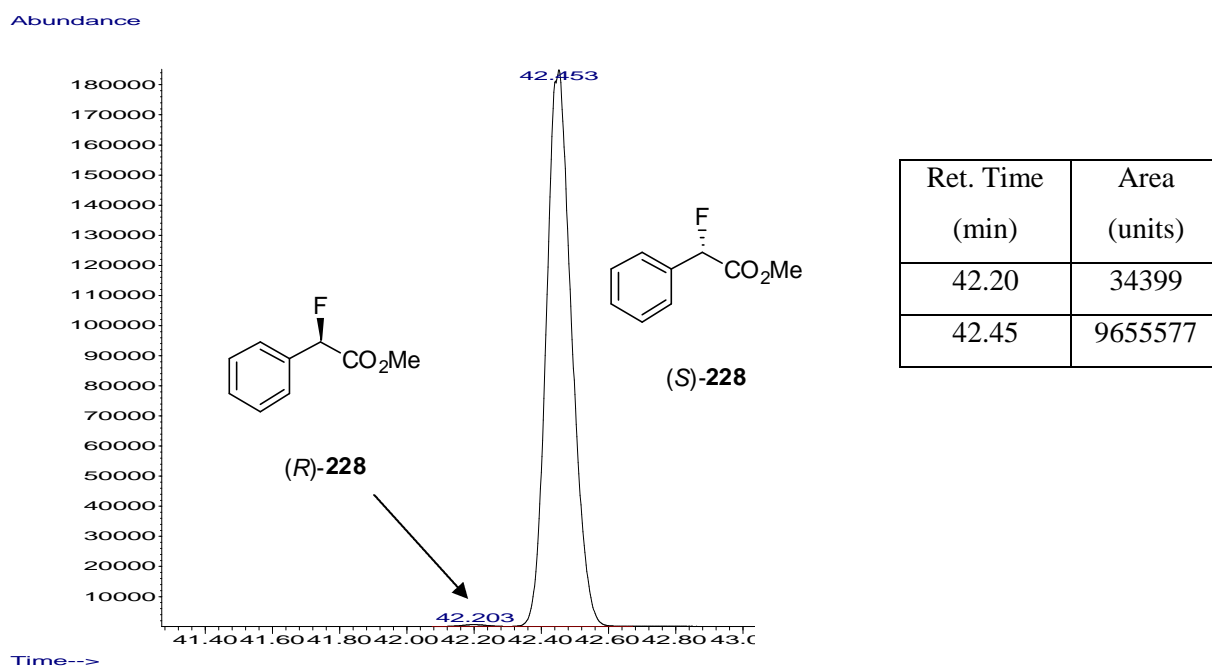
Figure 5.10. Chiral-phase GC chromatogram of (*S*)-**228** (99% ee): temperature-gradient oven (start at 110 °C

held for 40 min, then gradient at 20 °C/min to 150 °C held for 15 min), 250 °C injector temperature, 100:1 split

ratio, 0.9 mL/min flow, He carrier gas, Betadex^{TM} 120 fused silica capillary column (30 m x 0.25 mm i.d., 0.25

µm film thickness), MS (EI-SIM) detection.

187

Figure 5.11. GC/MS (EI-SIM) spectrum of (*R*)-**228**, scan at 42.20 min.

Figure 5.12. GC/MS (EI-SIM) spectrum of (*R*)-**228**, scan at 42.45 min.

5.5.2) GC analyses for determination of the % conversions:

In this study, the reaction conversions were determined by GC-FID using *n*-decane as an internal standard. GC-FID analyses 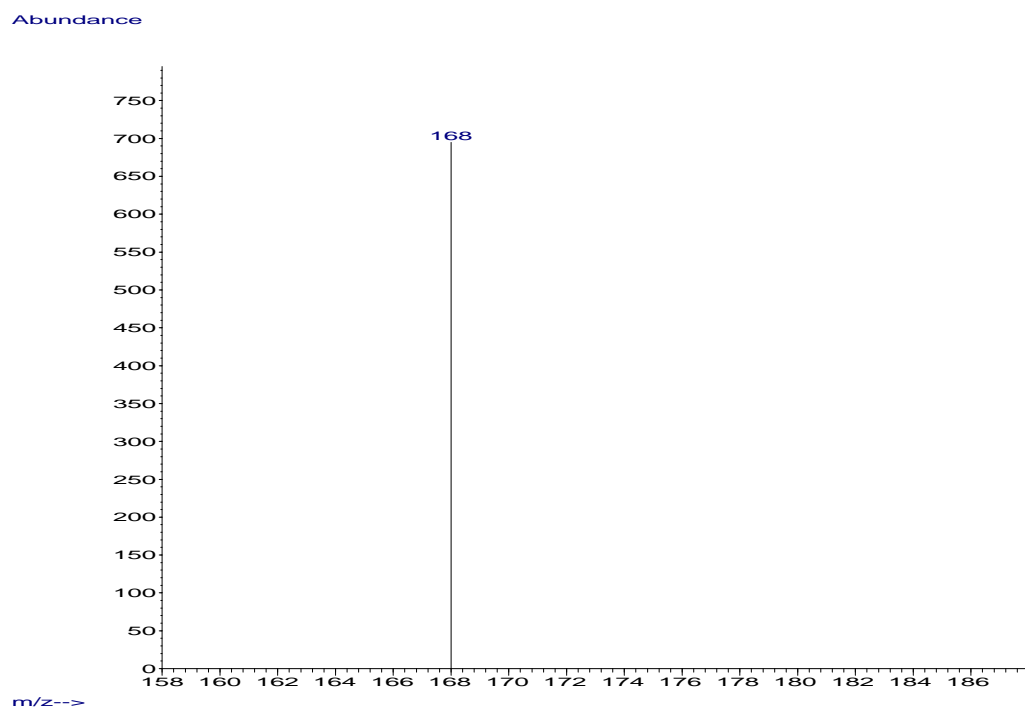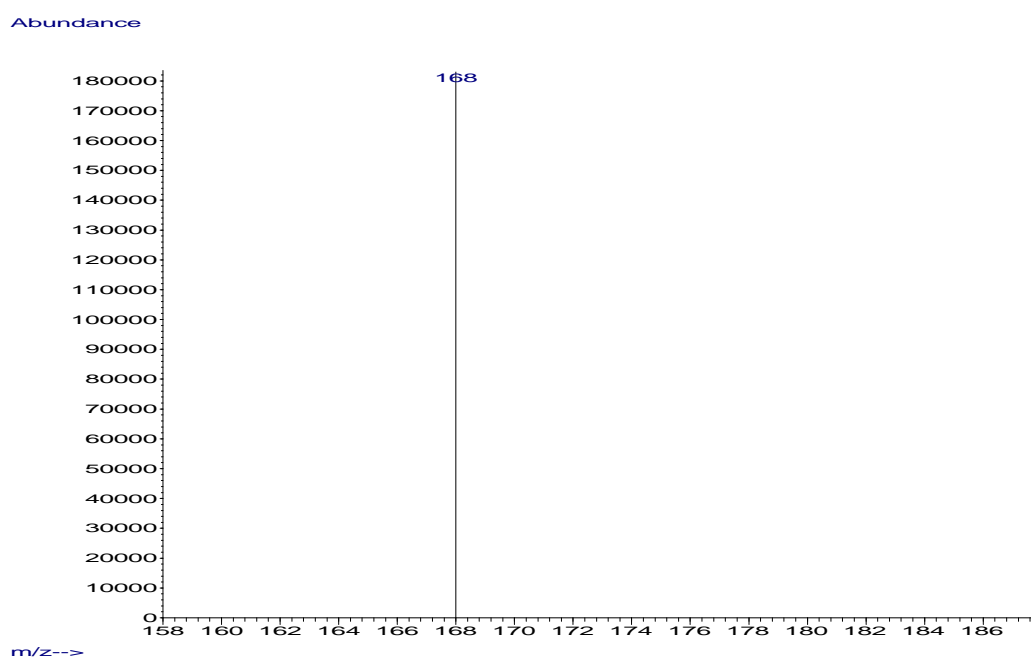were run on a Hewlett Packard 1 column (30 m x 0.25 mm i.d, 0.25 µm film thickness). *n*-Decane was chosen as an internal standard as it does not react or overlap with the other components of the reaction. In addition, its low volatility allows for more accurate results. Two calibration curves for the two analytes (*S*)-**214** and (*S*)-**228** were generated by GC-FID analyses of solutions containing a constant concentration of *n*-decane. The amounts of analyte (number of mmol) were varied, covering the range of levels expected. The two calibration curves, one for (*S*)-**214** (Figure 5.13) and the other for (*S*)-**228** (Figure 5.14) were constructed by plotting the ratio of the area of the analyte to the area of the internal standard (y axis) against the number of mmol (no. mmol) of the analytes (x axis).
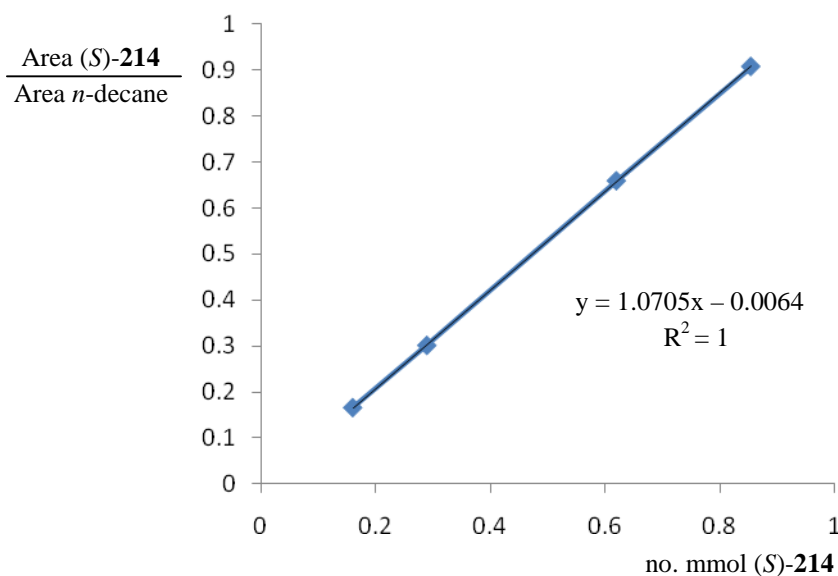

Figure 5.13. Calibration curve for analyte (*S*)-**214**.

189
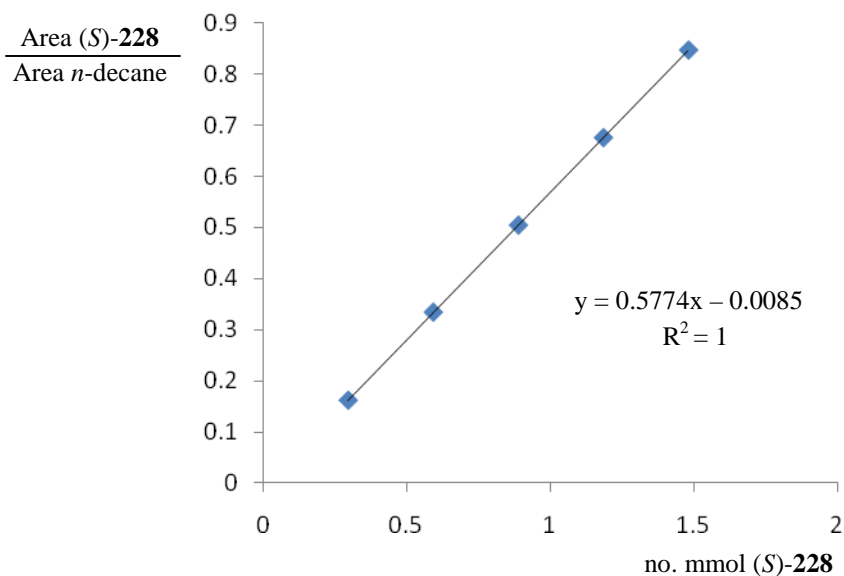
Figure 5.14. Calibration curve for analyte (*S*)-**228**.

A known quantity of *n*-decane, similar to that of the starting material, was added to the reaction vessel immediately before the reaction quench. This was followed by extraction with a known volume of CH_2Cl_2, which had been previously established to guarantee quantitative extraction of the product. GC-FID analysis of the sample containing the unknown amount of analyte to be determined, allowed the ratio of the analyte area to that of the internal standard area to be calculated. The corresponding no. mmol of product formed was then determined from the graph, which allowed determination of the % conversion. For example GC-FID analysis (Figure 5.15) of the product mixture containing the amount of (*S*)-**214** to be determined (Entry 7, Table 4.7, Chapter 4), provided the following areas:

Area (*S*)-**214** = 110486801 (units)

Area *n*-decane = 152916682 (units)

Ret. Time (min)	Area
7.21	110486801
8.55	152916682

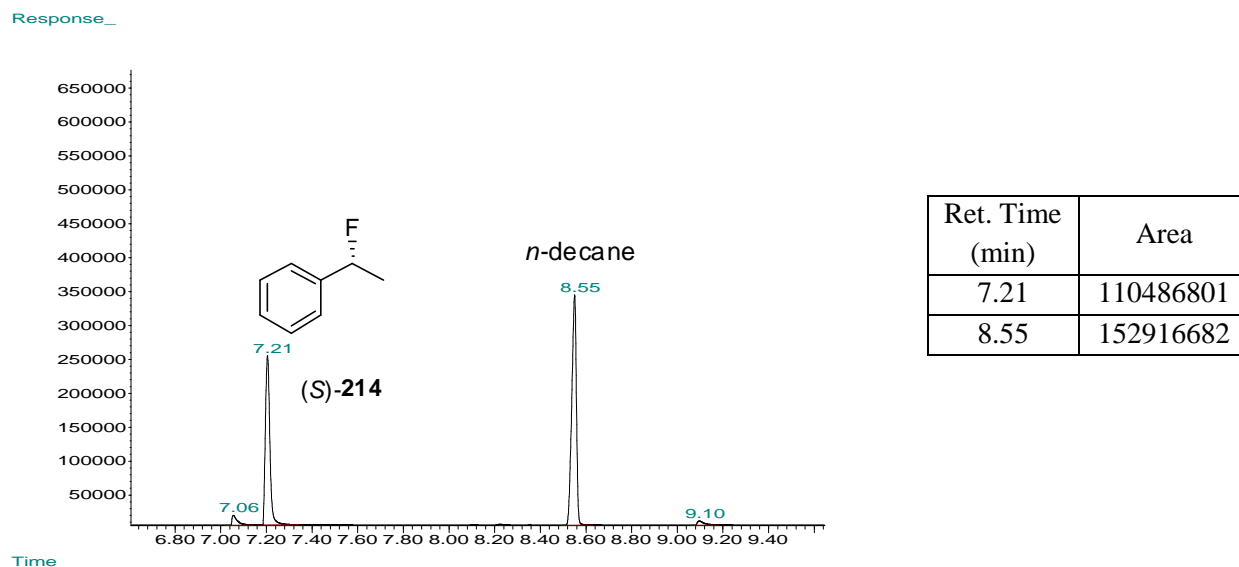**Figure 5.15.** Gas chromatogram (GC-FID) of the quenched reaction mixture of (*S*)-**214** (95% ee): temperature-gradient oven (start at 50 °C held for 4 min, then gradient at 20 °C/min to 130 °C held for 2 min, then gradient at 20 °C/min to 280 °C), 250 °C injector temperature, 100:1 split ratio, 1.0 mL/min flow He carrier gas, Hewlett Packard 1 column (30 m x 0.25 mm i.d, 0.25 µm film thickness.

This allowed the ratio (y) of the (*S*)-**214** area to *n*-decane area to be determined: y = 110486801 / 152916682 = 0.723. The corresponding no. mmol of (*S*)-**214** formed is determined from the calibration curve (Figure 5.13): x = 0.723 + 0.0064 / 1.0705 = 0.68 mmol. Considering that the mmol of alcohol starting material (*R*)-**213** are 0.74, the conversion is calculated as follows: % conversion = 0.68 / 0.74 · 100 = 92%

GC-FID analysis (Figure 5.16) of the product mixture containing the amount of (*S*)-**228** to be determined (Entry 3, Table 4.9, Chapter 4), provided the following areas:

Area (*S*)-**228** = 130338322 (units)

Area *n*-decane = 306942672 (units)
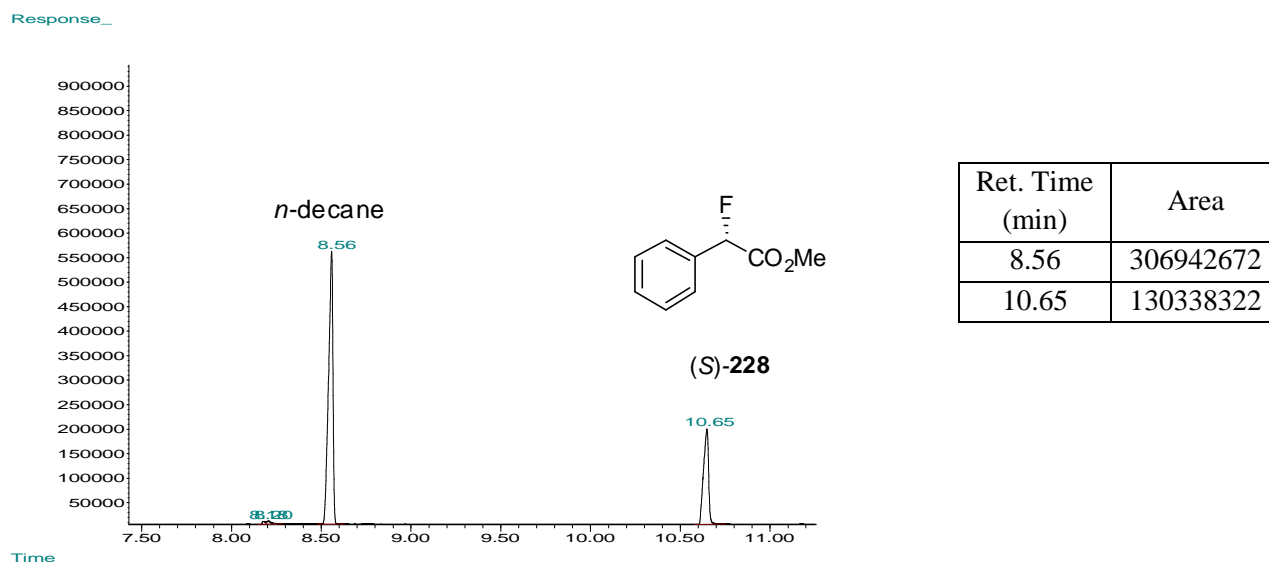
Figure 5.16. Gas chromatogram (GC-FID) of the quenched reaction mixture of (*S*)-**228** (99% ee): temperature-gradient oven (start at 50 °C held for 4 min, then gradient at 20 °C/min to 130 °C held for 2 min, then gradient at 20 °C/min to 280 °C), 250 °C injector temperature, 100:1 split ratio, 1.0 mL/min flow, He carrier gas, Hewlett Packard 1 column (30 m x 0.25 mm i.d, 0.25 µm film thickness).

This allowed the ratio (y) of the (*S*)-**228** area to *n*-decane area to be determined: y = 130338322 / 306942672 = 0.425. The corresponding no. mmol of (*S*)-**228** formed is determined from the calibration curve (Figure 5.14): x = 0.425 + 0.0085 / 0.5774 = 0.75 mmol. Considering that the mmol of alcohol starting material (*R*)-**227** are 1.48, the conversion is calculated as follows: % conversion = 0.74 / 1.48 · 100 = 51%

5.6) X-ray crystallographic data

Table 1. Crystal data and structure refinement for sbdh5: 158a

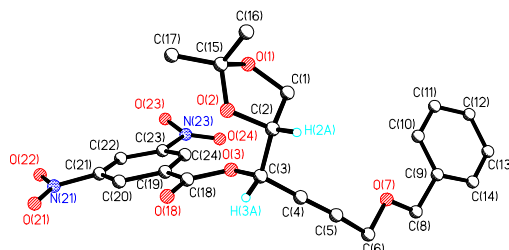|	
Identification code	sbdh5
Empirical formula	C23 H22 N2 O9
Formula weight	470.43
Temperature	173(2) K
Wavelength	1.54178 Å
Crystal system	Monoclinic
Space group	P2(1)
Unit cell dimensions	a = 11.1345(5) Å α= 90°.
	b = 11.5467(5) Å β= 98.261(2)°.
	c = 17.7582(7) Å γ = 90°.
Volume	2259.42(17) Å^3
Z	4
Density (calculated)	1.383 Mg/m^3
Absorption coefficient	0.914 mm^{-1}
F(000)	984
Crystal size	0.250 x 0.200 x 0.030 mm^3
Theta range for data collection	4.01 to 67.97°.
Index ranges	-13<=h<=13, -13<=k<=13, -21<=l<=21
Reflections collected	25733
Independent reflections	7204 [R(int) = 0.0327]
Completeness to theta = 67.00°	93.5 %
Absorption correction	Multiscan
Max. and min. transmission	1.0000 and 0.9148
Refinement method	Full-matrix least-squares on F^2
Data / restraints / parameters	7204 / 32 / 591
Goodness-of-fit on F^2	2.976
Final R indices [I>2sigma(I)]	R1 = 0.1662, wR2 = 0.5312
R indices (all data)	R1 = 0.1718, wR2 = 0.5446
Absolute structure parameter	0.00
Extinction coefficient	0.0051(18)
Largest diff. peak and hole	1.883 and -0.887 e.Å^{-3}
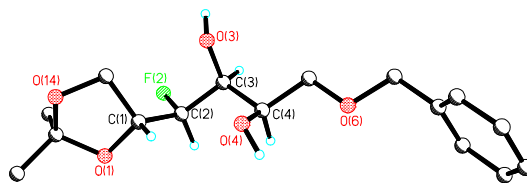
Table 1. Crystal data and structure refinement for sbdh4: 159

|	
Identification code	sbdh4
Empirical formula	C16 H23 F O5
Formula weight	314.34
Temperature	173(2) K
Wavelength	1.54178 Å
Crystal system	Monoclinic
Space group	P2(1)
Unit cell dimensions	a = 8.0621(9) Å α= 90°.
	b = 5.9382(6) Å β= 91.350(4)°.
	c = 16.5465(17) Å γ = 90°.
Volume	791.93(14) Å^3
Z	2
Density (calculated)	1.318 Mg/m^3
Absorption coefficient	0.877 mm^{-1}
F(000)	336
Crystal size	0.200 x 0.200 x 0.080 mm^3
Theta range for data collection	5.35 to 66.90°.
Index ranges	-8<=h<=8, -6<=k<=7, -19<=l<=19
Reflections collected	9882
Independent reflections	2573 [R(int) = 0.0332]
Completeness to theta = 66.50°	93.0 %
Absorption correction	Multiscan
Max. and min. transmission	1.0000 and 0.9285
Refinement method	Full-matrix least-squares on F^2
Data / restraints / parameters	2573 / 3 / 208
Goodness-of-fit on F^2	1.058
Final R indices [I>2sigma(I)]	R1 = 0.0296, wR2 = 0.0754
R indices (all data)	R1 = 0.0298, wR2 = 0.0755
Absolute structure parameter	0.03(12)
Largest diff. peak and hole	0.117 and -0.148 e.Å^{-3}
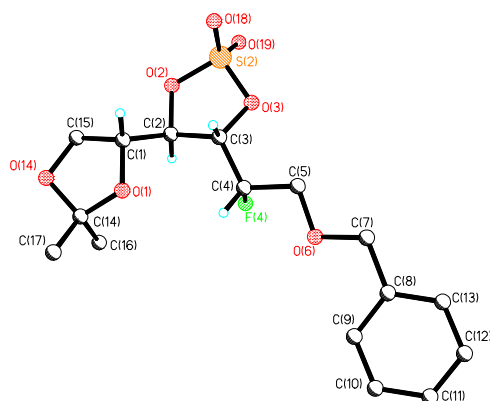
Table 1. Crystal data and structure refinement for sbdh10: 162a

|	
Identification code	sbdh10
Empirical formula	C16 H21 F O7 S
Formula weight	376.39
Temperature	93(2) K
Wavelength	0.71073 Å
Crystal system	Monoclinic
Space group	P2(1)
Unit cell dimensions	a = 10.727(4) Å α= 90°.
	b = 6.988(3) Å β= 98.075(17)°.
	c = 11.271(4) Å γ = 90°.
Volume	836.5(5) Å^3
Z	2
Density (calculated)	1.494 Mg/m^3
Absorption coefficient	0.241 mm^{-1}
F(000)	396
Crystal size	0.150 x 0.100 x 0.030 mm^3
Theta range for data collection	3.44 to 25.35°.
Index ranges	-11<=h<=12, -6<=k<=8, -9<=l<=13
Reflections collected	4600
Independent reflections	2505 [R(int) = 0.0539]
Completeness to theta = 25.00°	97.1 %
Absorption correction	Multiscan
Max. and min. transmission	1.0000 and 0.9515
Refinement method	Full-matrix least-squares on F^2
Data / restraints / parameters	2505 / 1 / 227
Goodness-of-fit on F^2	1.097
Final R indices [I>2sigma(I)]	R1 = 0.0538, wR2 = 0.1175
R indices (all data)	R1 = 0.0608, wR2 = 0.1216
Absolute structure parameter	0.12(14)
Largest diff. peak and hole	0.259 and -0.406 e.Å^{-3}
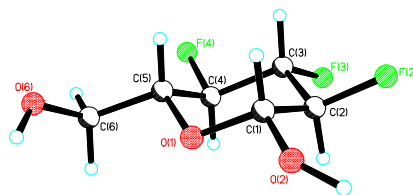
Table 1. Crystal data and structure refinement for sbdh11: 193

|	
Identification code	sbdh11
Empirical formula	C6 H9 F3 O3
Formula weight	186.13
Temperature	173(2) K
Wavelength	1.54178 Å
Crystal system	Orthorhombic
Space group	P2(1)2(1)2(1)
Unit cell dimensions	a = 5.507(3) Å α= 90°.
	b = 7.525(4) Å β= 90°.
	c = 18.773(9) Å γ = 90°.
Volume	777.9(7) Å^3
Z	4
Density (calculated)	1.589 Mg/m^3
Absorption coefficient	1.518 mm^{-1}
F(000)	384
Crystal size	0.100 x 0.100 x 0.010 mm^3
Theta range for data collection	6.34 to 66.27°.
Index ranges	-6<=h<=6, -8<=k<=8, -20<=l<=21
Reflections collected	4650
Independent reflections	1101 [R(int) = 0.1393]
Completeness to theta = 66.27°	85.4 %
Absorption correction	Multiscan
Max. and min. transmission	1.0000 and 0.8871
Refinement method	Full-matrix least-squares on F^2
Data / restraints / parameters	1101 / 2 / 118
Goodness-of-fit on F^2	1.152
Final R indices [I>2sigma(I)]	R1 = 0.1567, wR2 = 0.3500
R indices (all data)	R1 = 0.1892, wR2 = 0.3752
Absolute structure parameter	-1.1(16)
Largest diff. peak and hole	0.438 and -0.369 e.Å^{-3}

196
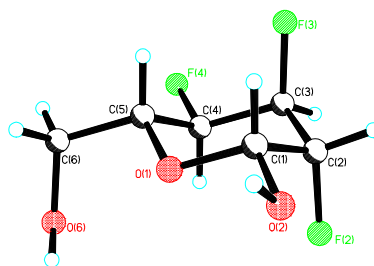
Table 1. Crystal data and structure refinement for SBDH13: 216

Identification code	sbdh13
Empirical formula	C6 H9 F3 O3
Formula weight	186.13
Temperature	93(2) K
Wavelength	0.71073 Å
Crystal system	Triclinic
Space group	P1
Unit cell dimensions	a = 6.373(5) Å α= 88.89(7)°.
	b = 6.623(9) Å β= 72.96(6)°.
	c = 10.220(8) Å γ = 75.90(5)°.
Volume	399.4(7) Å^3
Z	2
Density (calculated)	1.548 Mg/m^3
Absorption coefficient	0.164 mm^{-1}
F(000)	192
Crystal size	0.15 x 0.15 x 0.03 mm^3
Theta range for data collection	3.18 to 25.33°.
Index ranges	-6<=h<=7, -7<=k<=7, -12<=l<=12
Reflections collected	3843
Independent reflections	2297 [R(int) = 0.0235]
Completeness to theta = 25.00°	98.0 %
Absorption correction	Multiscan
Max. and min. transmission	1.000 and 0.930
Refinement method	Full-matrix least-squares on F^2
Data / restraints / parameters	2297 / 3 / 217
Goodness-of-fit on F^2	1.157
Final R indices [I>2sigma(I)]	R1 = 0.0345, wR2 = 0.0982
R indices (all data)	R1 = 0.0345, wR2 = 0.0983
Absolute structure parameter	-0.3(6)
Largest diff. peak and hole	0.347 and -0.349 e.Å^{-3}

197

References Chapter 5

[1] C. L. Perrin, T. J. Dwyer, *Chem. Rev.* 1990, **90***,* 935-967.

[2] D. Farran, A. M. Z. Slawin, P. Kirsch, D. O'Hagan, *J. Org. Chem.*, 2009, **74**, 7168-7171.

[3] J. Kuszmann, Ė. Tomori, I. Meerwald, *Carbohydrate Res.*, 1984, **128**, 87-99.

[4] R. S. Tipson, A. Cohen, *Carbohydr. Res.*, 1968, **7**, 232-243.

[5] R. S. Tipson, A. Cohen, *Carbohydr. Res.*, 1968, **7**, 232-243.

[6] C. R. Schmid, J. D. Bryant, M. Dowlatzedah, J. L. Phillips, D. E. Prather, R. D. Schantz, N. L. Sear, C. S. Vianco, *J. Org. Chem.*, 1991, **56**, 4056-4058.

[7] C. R. Schmid, J. D. Bryant, M. Dowlatzedah, J. L. Phillips, D. E. Prather, R. D. Schantz, N. L. Sear, C. S. Vianco, *J. Org. Chem.*, 1991, **56**, 4056-4058.

[8] J. Mulzer, A. Angermann*, Tetrahedron Lett.*, 1983, **24**, 2843-2846.

[9] B. M. Trost, Z. T. Ball, T. Jöge, *Angew. Chem. Int. Ed.*, 2003, **42**, 3415-3418.

[10] B. Grant, C. Djerassi, *J. Org. Chem.*, 1974, **39**, 968-970.

[11] V. A. Petrov, S. Swearingen, W. Hong, W. C. Petersen, *J. Fluorine Chem.*, 2001, **109**, 25-31.

[12] E. N. Jacobsen, I. Markǒ, W. S. Mungall, G. Schröder, K. B. Sharpless, *J. Am. Chem. Soc.*, 1988, **110**, 1968-1970.

[13] Y. Gao, K. B. Sharpless, *J. Am. Chem. Soc.*, 1988, **110**, 7538-7539.

[14] M. Fujita, H. Ishizuka, K. Ogura, *Tetrahedron Lett.*, 1991, **32**, 6355-6358.

[15] T. Inagaky, T. Fukuhara, S. Hara, *Synthesis*, 2003, **8**, 1157-1159

[16] G. S. Lai, G. P. Pez, R. J. Pesaresi, F. M. Prozonic, H. Cheng, *J. Org. Chem.*, 1999, **64**, 7048-7054.

[17] M. Adinolfi, G. Barone, L. Guariniello, A. Iadonisi, *Tetrahedron Lett.*, 1999, **40**, 8439-

8441.

[18] F. A. Davis, V. Srirajan, D. D. Titus, *J. Org. Chem.*, 1999, **64**, 6931-6934.

[19] X. –H. Xu, Z. – W. You, X. Zhang, F. – L. Qing, *J. Fluorine Chem.*, 2007, **128**, 535-539.

[20] M. M. Bio, M. Waters, G. Javadi, Z. J. Song, F. Zhang, D. Thomas, *Synthesis*, 2008, 891-896.

[21] V. A. Petrov, S. Swearingen, W. Hong, W. C. Petersen, *J. Fluorine Chem.*, 2001, **109**, 25-31.

[22] S. Lal, G. P. Pez, R. J. Pesaresi, F. M. Prozonic, H. Cheng, *J. Org. Chem.*, 1999, **64**, 7048-7054.

[23] W. J. Middleton, *J. Org. Chem.*, 1975, **40**, 574-578.

[24] (a) T. Umemoto, Y. Xu, *US patent* 7,265,247 (IM&T Research Inc.) Feb 2008 (b) T. Umemoto, R. P. Singh, *US patent* 20080039660 (IM&T Research Inc.) Feb 2008.

Appendix

Conferences attended:

- *2-3 September 2009, 10th RSC Fluorine Subject Meeting, Durham (UK):* Oral presentation.

- *11-15 July 2010, Perugia Fluorine Days, Perugia (Italy):* Poster presentation.

- *17-18 September 2009, 9th RSC Fluorine Subject Meeting, Southampton (UK):* Oral presentation.

- *16-20 August 2009, 238th ACS National Meeting, Washington DC (USA):* Poster presentation.

- *11-12 September 2008, 8th RSC Fluorine Subject Group Postgraduate Meeting, Newcastle (UK):* Poster presentation.

- *7-8 April 2008, Drugs from Natural Products IV, Cambridge (UK):* Visitor.

List of publications:

- S. Bresciani, A. M. Z. Slawin, D. O'Hagan*,* A regio- and stereo- isomeric study of allylic alcohol fluorination with a range of reagents, *J. Fluorine Chem.,* 2009*,* **130**, 537-543.

- S. Bresciani, T. Lebl, A. M. Z. Slawin, D. O'Hagan*,* Fluorosugars: synthesis of the 2,3,4-trideoxy-2,3,4-trifluoro hexose analogues of D-glucose and D-altrose and assessment of their erythrocyte transmembrane transport, *Chem. Commun.,* 2010, **46**, 5434-5436.

- S. Bresciani, D. O'Hagan*,* Stereospecific benzylic dehydroxyfluorination reactions using Bio's TMS-amine additive approach with challenging substrates, *Tetrahedron Lett*., 2010, **51**, 5795-5797.